The cell and molecular biological characterization of cell-cell junctions in mammalian heart valves

Inaugural Dissertation

for the degree of
Doctor rerum naturalium (Dr. rer. nat.)

submitted to the
Combined Faculties for the Natural Sciences and for Mathematics
of the Ruperto-Carola University of Heidelberg, Germany

presented by

Dipl.- Biol. Mareike Barth

born 01.03.1982 in Groß-Gerau, Germany

April 2011

This work has been carried out in the laboratory of Prof. emer. Dr. Werner W. Franke in the Helmholtz Group for Cell Biology at the German Cancer Research Center (DKFZ), Heidelberg, Germany.

Referees: Prof. emer. Dr. Werner W. Franke
Prof. Dr. Thomas W. Holstein

Oral examination: 16.06.2011

Parts of this work have been published in:

Barth M, Schumacher H, Kuhn C, Akhyari P, Lichtenberg A, Franke WW. (2009). Cordial connections: molecular ensembles and structures of adhering junctions connecting interstitial cells of cardiac valves in situ and in cell culture. Cell Tissue Res. 337(1):63-77.

Further co-authorships:

Moll R, Sievers E, Hämmerling B, Schmidt A, Barth M, Kuhn C, Grund C, Hofmann I, Franke WW. (2009). Endothelial and virgultar cell formations in the mammalian lymph node sinus: endothelial differentiation morphotypes characterized by a special kind of junction (complexus adhaerens). Cell Tissue Res. 335(1):109-41.

Franke WW, Rickelt S, Barth M, Pieperhoff S. (2009). The junctions that don't fit the scheme: special symmetrical cell-cell junctions of their own kind. Cell Tissue Res. 338(1):1-17.

Pieperhoff S, Borrmann C, Grund C, Barth M, Rizzo S, Franke WW. (2010). The area composita of adhering junctions connecting heart muscle cells of vertebrates. VII. The different types of lateral junctions between the special cardiomyocytes of the conduction system of ovine and bovine hearts. Eur J Cell Biol. 89(5):365-78.

Pieperhoff S, Barth M, Rickelt S, Franke WW. (2010). Desmosomal molecules in and out of adhering junctions: normal and diseased States of epidermal, cardiac and mesenchymally derived cells. Dermatol Res Pract. 2010:139167.

Gwanmesia P, Ziegler H, Eurich R, Barth M, Kamiya H, Karck M, Lichtenberg A, Akhyari P. (2010). Opposite effects of transforming growth factor-β1 and vascular endothelial growth factor on the degeneration of aortic valvular interstitial cell are modified by the extracellular matrix protein fibronectin: implications for heart valve engineering. Tissue Eng Part A. 16(12):3737-46.

Dedicated to my family

Abbreviations

α	alpha
Ab(s)	antibody (antibodies)
AJ(s)	adherens junction(s)
AMV	avian myeloblastosis virus
ARVCF	“armadillo repeat gene deleted in the Velo-Cardio-Facial syndrome”
AV(s)	aortic heart valve(s)
β	beta
bFGF	basic fibroblast grwoth factor
ca.	circa
cDNA	complementary DNA
cm	centimeter
DAPI	4', 6-diamidino-2-phenylindole
DNA	deoxyribonucleic acid
dNTP	deoxyribonucleoside triphosphate
DTT	dithiothreitol
ECM	extracellular matrix
EDTA	ethylenediaminetetraacetic acid
e.g.	for example
EGF	epidermal growth factor
EMT	epithelial-mesenchymal transition
etc.	et cetera
FACS	fluorescence-activated cell sorting
FCS	fetal calf serum
g	gram
GAGs	glycosaminoglycans
GFAP	glial filament acidic protein
γ	gamma
GJ(s)	gap junction(s)
gp	guinea pig
h	hour
HEPES	2-(4-(2-hydroxyethyl)-1-piperazinyl)-ethane sulfonic acid
Hg	mercury
HH	Hamburger-Hamilton stages (chronological stages in chick development)
HRP	horseradish peroxidase
H_20	double distilled water
ID(s)	intercalated disk(s)

IF(s)	intermediate-sized filament(s)
IgG	immunoglobulin G
INF-γ	interferon gamma
IP(s)	immunoprecipitation(s)
kDa	kilodalton
kV	kilovolt
L	liter
m	mouse
M	molar
mA	milliampere
mAb(s)	monoclonal antibody/antibodies
mg	milligram
mcl	monoclonal
min	minute
mL	milliliter
mm	millimeter
mM	millimolar
MSC(s)	mesenchymal stem cell(s)
MV(s)	mitral heart valve(s)
MW	molecular weight
NCS	newborn calf serum
nm	nanometer
PAGE	polyacrylamide gel electrophoresis
PBS	phosphate buffered saline
pcl	polyclonal
PCR	polymerase chain reaction
PDGF-BB	platelet-derived growth factor BB
pmol	picomol
PV(s)	pulmonary heart valve(s)
PVDF	polyvinyliden fluoride
rb	rabbit
RNA	ribonucleic acid
rpm	rounds per minute
RT	room temperature
SDS	sodium dodecyl sulfate
sec	second
siRNA	small interference RNA
sn	supernatant
TGF-β1	transforming growth factor beta 1

TJ(s)	tight junction(s)
TNF-α	tumor necrosis factor alpha
TV(s)	tricuspid heart valve(s)
U	unit
V	volt
VEGF	vascular endothelial growth factor
VIC(s)	valvular interstitial cell(s)
v/v	volume per volume
w/v	weight per volume
%	percentage
µg	microgram
µL	microliter
µm	micrometer
10X	ten times
2D	two-dimensional
3D	three-dimensional
°C	degree Celsius

Summary

In view of the large proportion of cardiac cells represented by interstitial mesenchymal cells, in particular in the valves, of the frequency and importance of valve surgery, notably replacements, and of the numerous “tissue engineering” projects to provide artificial valve structures it is actually surprising to see how limited the cell and molecular biological knowledge of valvular interstitial cells (VICs) still is. Surprisingly, the molecular components of the special adherens junctions (AJs) of VICs have not yet been elucidated to a satisfying degree. Therefore, the AJs of adult and fetal VICs of human and animal (bovine, ovine and porcine) heart valves have been studied *in situ* and cell culture preparations, using light and electron microscopy, including immunolocalization techniques, protein as well as glycoprotein analysis by SDS-PAGE, followed by identification of the separated molecules using immunoblotting.

In my thesis I could show that adult mammalian VICs *in situ* possess cell-cell adhering junctions only of the *puncta adhaerentia* AJ-type, comprising N-cadherin and cadherin-11 as constitutive transmembrane glycoproteins, anchored in cytoplasmic plaques containing α- and β-catenin, plakoglobin, proteins p120 and p0071 which are accompanied by actin-binding proteins such as afadin, vinculin, α-actinin and proteins ZO-1-3.

In two-dimensional (2D) cell cultures of adult mammalian VICs of different species, this rather simple molecular AJ ensemble was surprisingly found to be modified by the acquisition of the desmosomal plaque protein plakophilin-2, in the total absence of desmosomal structures and other desmosomal proteins. In three-dimensional (3D) culture constructs mimicking a native valve matrix environment, it could be shown that AJ-plakophilin-2 gradually decreased or was even lost but was able to re-assemble when VICs were re-isolated from 3D constructs and grown in 2D culture again.

Human and porcine fetal VICs *in situ* also presented plakophilin-2 in their AJs, showing that the phenomenon of plakophilin-2 acquisition is not an artefact of cell culture conditions. Primary cultures of porcine fetal VICs also revealed adventitious plakophilin-2. Even more surprisingly fetal endothelial cells of the endocardium – but only those located at the valves and not those at the myocardium – also displayed the addition of this desmosomal protein to their AJ plaques, whereas those of other regions of fetal vascular endothelia remained negative for this protein.

Again unexpectedly, pathologically altered cells of adult heart valves, showing an elevated proliferative activity, did not present plakophilin-2 in their AJs. Such as fetal VICs showed only relatively low proliferative activity, these findings may lead to the hypothesis

that the acquisition of plakophilin-2 might be rather the result of a general activation- than a proliferation-induced event. Correspondingly, an alternative concept for early valvulogenesis is proposed, differering from the presently prevailing “epithelial- (here better: endothelial-) mesenchymal-transition” (EMT) hypothesis, which is based on the assumption of an *ab initio* presence of mesenchymal cells of the VIC type, even in the early heart tube “anlage”.

The advent of a single desmosome-typical protein, plakophilin-2, in VICs of fetal heart valves and in culture is not an isolated phenomenon as it fits in phenomena observed in recently identified forms of plakophilin-2-containing AJs (*coniunctiones adhaerentes*) found in other mesenchymal cells such as bone marrow-derived stem cells, malignantly transformed mesenchymal cell lines and certain soft tissue tumors. It is obvious that a more detailed characterization of VICs, notably their AJs, will be needed to provide a safe basis for replacement valve surgery using structures formed by cells grown in valvular cell cultures *in vitro*.

Zusammenfassung

In Anbetracht des hohen Anteils mesenchymaler Interstitialzellen an der Gesamtmenge der Zellen des Herzens, besonders in Klappen, der Häufigkeit und Wichtigkeit von Herzklappen-Operationen, vor allem auch von Klappenersatz-Eingriffen, und der zahlreichen „Tissue Engineering"-Projekte zur Herstellung artifizieller Herzklappenkonstrukte, ist es sehr erstaunlich zu sehen, wie begrenzt der zell- und molekularbiologische Wissensstand über valvuläre Interstitialzellen (VICs) immer noch ist. Überraschenderweise sind besonders die molekularen Komponenten der speziellen Adhärenz-Verbindungen (AJs) der VICs weitgehend unbekannt geblieben. Daher wurden die AJs adulter und fötaler VICs sowohl aus humanen und tierischen (Rind, Schaf und Schwein) Herzklappen *in situ* und in Zellkulturansätzen mit licht- und elektronenmikroskopischen Methoden, vor allem auch Immunlokalisierungstechniken, sowie durch Protein- und Glykoprotein-Analysen in der Polyacrylamid-Gelelektrophorese und anschließender Identifizierung der aufgetrennten Moleküle durch Antikörper-Bindung, untersucht.

In der vorliegenden Arbeit konnte ich zeigen, dass die VICs adulter Säuger *in situ* ausschließlich AJ-Verbindungen des *puncta adhaerentia*-Typs besitzen. Darin sind die konstitutiven Transmembran-Glykoproteine N-Cadherin und Cadherin-11 in zyto-plasmatischen „Plaques" verankert, die α- und β-Catenin, Plakoglobin, die Proteine p120 und p0071 sowie eine Reihe von Aktin-bindenden Proteinen wie Afadin, Vinculin, α-Aktinin und die Proteine ZO-1-3 enthalten bzw. enthalten können.

In zwei-dimensionalen Zellkulturen adulter Säuger-VICs verschiedener Spezies ist dieses relativ einfache AJ-Molekül-Ensemble überraschenderweise durch das Hinzukommen des desmosomalen Plaque-Leitproteins Plakophilin-2, verändert, wobei jedoch desmosomale Strukturen und andere desmosomen-spezifische Moleküle fehlen. In drei-dimensionalen Kulturen, welche die natürliche Matrix-Umgebung der Herzklappe imitieren, konnte dann gezeigt werden, dass sich darin die Menge an AJ-Plakophilin-2 allmählich verringert oder sogar ganz verschwinden kann, dann aber in aus solchen Konstrukten wiedergewonnenen Zellkulturen wieder nachgewiesen werden kann.

In menschlichen wie auch in vom Schwein stammenden fötalen VICs konnte *in situ* ebenfalls Plakophilin-2 als Bestandteil ihrer AJs nachgewiesen werden, was beweist, dass es sich bei dem Phänomen der Plakophilin-2-Akquisition nicht um einen Zellkultur-Artefakt handelt. Noch überraschender war jedoch die Entdeckung, dass fötale Endothelzellen de Endokards – allerdings nur solche im Bereich von Klappen, aber nicht solche, die an das

Myokard grenzen – ebenfalls Plakophilin-2 enthielten, wobei dieses Protein in den AJs der Endothelien anderer Blutgefäße nicht vorkam.

Unerwartet war dann wiederum die Beobachtung, dass Zellen pathologisch veränderter Herzklappen mit erhöhter Zellproliferation kein Plakophilin-2 in ihren AJs aufwiesen. Da auch fötale VICs nur noch eine relativ geringe Teilungsaktivität aufweisen, führen diese Befunde zur Vermutung, dass das Hinzukommen von Plakophilin-2 in AJs eher das Ergebnis eines allgemeinen Aktivierungs- als das eines Proliferations-Prozesses an sich ist. In diesem Zusammenhang sollte man – alternativ zur bisherigen Hypothese der „Epithelial- (hier eher zutreffend: Endothelial-) Mesenchymalen-Transition“ (EMT) – das Konzept einer *ab initio* Präsenz des VIC-Zelltyps schon in der frühen Entwicklung der Herzklappe in Erwägung ziehen.

Das isolierte Auftreten eines einzelnen desmosomen-spezifischen Proteins, Plakophilin-2, in den AJs fötaler VICs *in situ* sowie auch in Zellkultur gehaltener VICs ist übrigens kein isoliertes Phänomen, sondern wurde jüngst ebenfalls in anderen mesenchymalen Zellen wie z.B. in Kulturen von „Stammzellen“ aus dem Knochenmark, tumorös transformierten mesenchymalen Zellkulturen sowie in bestimmten Weichteil-Tumoren gefunden und als neuartige, Plakophilin-2-haltige Adhärenzverbindung (*coniunctio adhaerens*) beschrieben. Diese Beobachtungen machen deutlich, dass gerade als Basis für die Erforschung und Herstellung von Klappenersatz-Konstrukten, die auf in Kultur gewachsenen VICs oder ähnlichen Zelltypen basieren, eine detaillierte Charakterisierung der Zellen, besonders ihrer Zell-Zell-Verbindungen, erforderlich ist.

1 Introduction

Cell-cell junctions are obviously essential for the development and the architectonic stabilization of complex tissues and thus of complex organisms such as all multicellular organisms, particularly metazoa. Correspondingly, the components of these junctional structures are evolutionarily rather old. Already among the unicellular colonial flagellates, the choanoflagellates express several genes encoding multidomain proteins with motifs highly similar to some of the metazoan cadherins, the so-called protocadherins (King et al., 2003). The parazoan sponges also contain a range of cell-cell adhesion molecules as well as extracellular matrix (ECM) adhesion molecules (Nichols et al., 2006). And one of the lowest metazoans, the diploblastic fresh-water polyp *Hydra*, develops epithelioid layers, the cells of which already are connected by junctional complexes comprising adhering junction molecules highly conserved throughout the entire metazoan evolution (Hobmayer et al., 1996, 2000; for further references see, e.g., Halbleib and Nelson, 2006; Franke, 2009). Higher metazoans, including already some cnidaria, are not only capable of building up two-layered systems like *Hydra* but also develop a third cell layer, the evolutionary precursor of the mesoderm. Clearly, at the molecular level, there is remarkable homology of cell-cell connecting junctional proteins, both in evolution and ontogenesis (see, e.g., Bryant, 1997, and the reviews mentioned afore).

1.1 Cell-cell junctions of vertebrates

In principle, the types of cell-cell junctions occurring in metazoans can be subdivided into four major categories: 1) desmosomes, 2) adherens junctions (AJs), 3) tight junctions (TJs) and 4) gap junctions (GJs). The ultrastructural organizations and the molecular ensembles of these four major kinds of junctions have been elucidated over the last half century (Farquhar and Palade, 1963; Campbell and Campbell, 1971; Staehelin, 1974; for recent review anthologies see, e.g., Edelman and Thierry, 1985; Edelman et al., 1990; Behrens and Nelson, 2004; La Flamme and Kowalczyk, 2008; Nelson and Fuchs, 2010; for schematic presentations of the diverse subtypes of adhering junctions see Tsukita et al., 2001; Matter and Balda, 2003; Franke, 2009; Franke et al., 2009), including changes of such structures that are related to diverse diseases.

1.1.1 Desmosomes (*maculae adhaerentes*)

Desmosomes occur in epithelial tissues and cell cultures, in meningothelial cells, in dendritic reticulum cells of the thymus and lymph follicles, and in cardiomyocytes. In the electron microscope, they reveal a typical subarchitecture comprised of a 20-30 nm wide membrane-to-membrane structure between the two plasma membrane lipid bilayers, representing the so-called *desmogloea.* The latter is often characterized by a dense midline-structure and a periodically cross-striated structure ("ladder") extending from the midline to the plasma membrane bilayers (Schwarz et al., 1990). This intercellular structure is built by an electron-dense plaque on the cytoplasmic side of the desmosomal structure of about 15-30 nm thickness, which provides the anchorage plate of intermediate-sized filaments (IFs) in many cell types.

Extensive studies using biochemical methods as well as immunofluorescence and immunoelectron microscopy have revealed the molecular components of desmosomes. The first characterized desmosomal plaque proteins, the desmoplakins, consist of a near-amino-terminal plakin domain, a central coiled-coil domain and a carboxy-terminal, plakin-repeat domain. Desmoplakin I and II are major splice variants originating from the same gene (Franke et al., 1981, 1982a, b; Cowin and Garrod, 1983; Müller and Franke, 1983; Cowin et al., 1984a, b, 1985; Green et al., 1988, 1990; Virata et al., 1992) and very recently another splice variant, desmoplakin Ia, has been added (Cabral et al., 2010). The two other components building the desmosomal plaque had originally been described as desmosomal "band five" and "band six" proteins (Franke et al., 1983b; Kapprell et al., 1985) but were later defined as plakoglobin (Cowin et al., 1986; Franke et al., 1987a, c, 1989, 1992; Kapprell et al., 1987; Fouquet et al., 1992) and members of the plakophilin group (Kapprell et al., 1988; Heid et al., 1994; Schmidt et al., 1994).

In the early 1990s it was recognized that plakoglobin is a homolog to the *armadillo* protein encoded by the *Drosophila melanogaster* segment polarity gene (Peifer and Wieschaus, 1990; McCrea et al., 1991; Peifer et al., 1992, 1994). Furthermore, the large *armadillo* multigene family includes several other desmosomal and AJ proteins such as the plakophilins. Here the three subforms, plakophilins 1-3, are synthesized in different tissue patterns: Plakophilin-1 is restricted to suprabasal layers of stratified epithelia (Kapprell et al., 1988; Schäfer et al., 1993; Hatzfeld et al., 1994; Heid et al., 1994; Schmidt et al., 1994) and exists in two splice variants, plakophilin-1a and plakophilin-1b (Schmidt et al., 1994, 1997). Both subforms can also be detected in the nucleoplasm of desmosome-forming as well as non-desmosome-forming cells (Schmidt et al., 1997). On the other hand, plakophilin-2 is the most widespread form and occurs in simple epithelia,

in complex epithelia and often also in the basal cell layer of multistratified epithelia, in meningothelia as well as in specific non-epithelial desmosomes and desmosome-related junctions such as the AJ-related junctions (*areae compositae*) of the intercalated disks (IDs) of cardiac tissue and the dendritic reticulum cells of lymphatic germinal centers (Kartenbeck et al., 1984; Mertens et al., 1996, 1999; Akat et al., 2003, 2008; Moll et al., 2009). This protein also exists in two splice variants and often occurrs in karyoplasmic particles as well as in the desmosomal plaque (Mertens et al., 1996, 2001). The third subform, plakophilin-3, often accompanies plakophilin-2 (Bonné et al., 1999, 2003; Schmidt et al., 1999) but is absent in specific cell types such as hepatocytes and cardiomyocytes (Schmidt et al., 1999; Borrmann et al., 2000; Borrmann, 2002). For discussions of functions and protein evolution it is remarkable that several *armadillo* proteins such as plakoglobin, plakophilins and also the AJ proteins β-catenin and p120 are not only located in cell-cell junctions but are often also found in the nucleus of desmosome-containing as well as desmosome-lacking cells (Mertens et al., 1996, 2001; Schmidt et al., 1997; Klymkowsky, 1999; for reviews see Godsel et al., 2004; Bass-Zubek et al., 2009; McCrea et al., 2009).

Moreover, the two desmosomal glycoprotein groups, the desmogleins (Dsg) and desmocollins (Dsc), show high amino acid sequence homology to the classic cadherins like N- and E-cadherin which are typical transmembrane glycoproteins in AJs. Dsg and Dsc molecules have been also found to exist in different subforms (Dsg 1-4, Dsc 1-3), synthesized as cell type- and cell layer-specific glycoproteins (Gorbsky and Steinberg, 1981; Cohen et al., 1983; Giudice et al., 1984; Gorbsky et al., 1985; Kapprell et al., 1985; Parrish et al., 1986, 1990; Schmelz et al., 1986a, b; Steinberg et al., 1987; Holton et al., 1990; Collins et al., 1991; Koch et al., 1991a, b, 1992; Buxton et al., 1993; King et al., 1993a, b, 1995, 1997; Koch and Franke, 1994; Troyanovsky et al., 1994). Dsg2 and Dsc2 occur in one-layered epithelia, cardiomyocytes, reticulum cells of lymphatic tissues, in meningothelia and often also in the basal layer of stratified epithelia (Schäfer et al., 1994, 1996; Nuber et al., 1995, 1996). Dsg1 and Dsc1, often in combination with Dsg3 and Dsc3, can be found in the more differentiated, suprabasal cell layers of stratified epithelia, and Dsg4 only occurs in the cells in the topmost cell strata of the epidermis (for reviews see Godsel et al., 2004; Bazzi et al., 2006; Schmidt and Koch, 2008). Dsg and Dsc molecules seem to appear always together as pairs, probably as cis-heterodimers (Figure 1; see, e.g., Troyanovsky et al., 1993; Witcher et al., 1996; Troyanovsky, 2005). However, recent findings have shown that Dsg2 can also occur “alone”, i.e. as a cell surface molecule without a Dsc-partner, for example in cultures of melanocytes and

melanoma cell lines as well as in certain melanomas *in situ* (Schmitt et al., 2007; Rickelt et al., 2008; for cell culture model experiments see also Köser et al., 2003).

Depending on the type of IF anchored to the desmosomal plaque structure, several cell type- or tissue-type specific desmosomes can be distinguished. In normal epithelia the desmosomes anchor keratin IFs (Achtstätter et al., 1989), in meningothelia and in dendritic reticulum cells they anchor vimentin IFs (Kartenbeck et al., 1984; Schmelz and Franke, 1993) and in cardiomyocytes desmin-containing IFs (Kartenbeck et al., 1983).

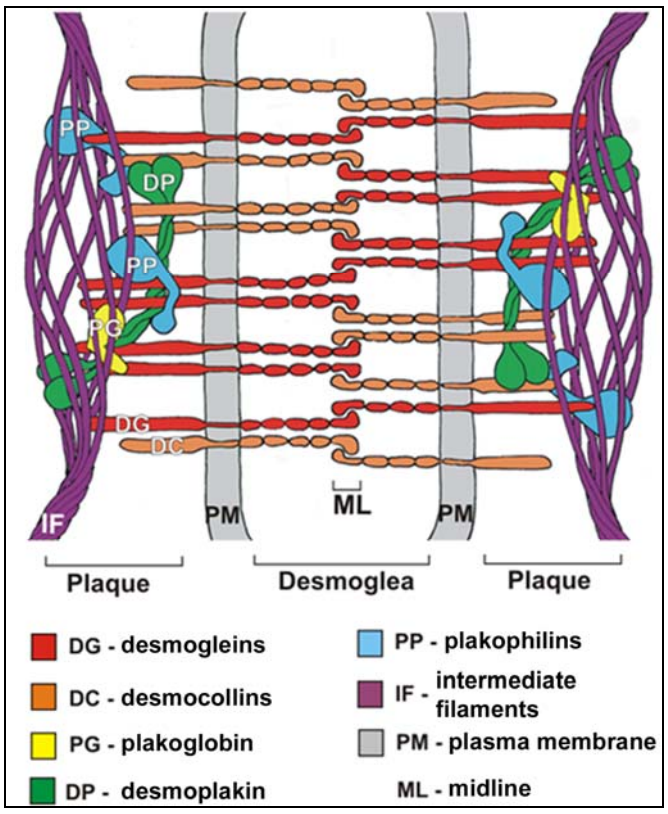

Figure 1: Schematic hypothetical model of the molecular organization of the desmosomal structure with transmembrane glycoproteins and plaque-building cytoplasmic proteins (cf. Leube et al., 2003).

1.1.2 Adherens junctions (*zonulae adhaerentes, fasciae adhaerentes and puncta adhaerentia*)

At the electron microscopic level, AJs appear as two triple-layered membranes with an intermembrane distance of about 20 nm from each other and in association with a cytoplasmic plaque at which bundles of microfilaments are anchored. This junction type can extend from ca. 0.2 µm to more than 2 µm in diameter or axis length (Farquhar and Palade, 1963; Staehelin, 1974; for recent reviews see Franke, 2009).

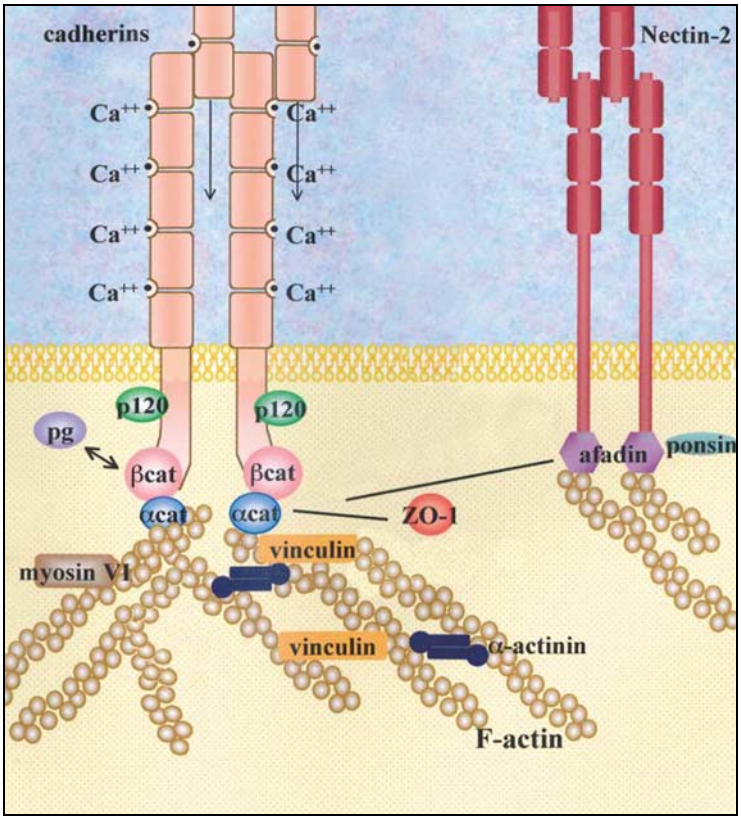

Figure 2: Schematic hypothetical presentation of AJ structures. Shown is the cadherin-catenin system (left hand side) as well as the nectin-afadin-ponsin system (right hand side). Both structures are linked to the actin cytoskeleton of the cell and can also be superimposed or "mixed" (modified from Perez-Moreno et al., 2003). Abbreviations: pg, plakoglobin; p120, protein p120; αcat, α-catenin; βcat, β-catenin.

The identification and characterization of proteins of the AJ ensemble were originally advanced by embryologists recognizing that cell-cell adhesion plays a fundamental role during development. The term "cadherin" has been based on the finding that Ca^{2+}-ions are generally essential in this specific kind of cell-cell adhesion and

embryogenesis (e.g., Steinberg, 1958; Takeichi, 1977, 1995; Yoshida and Takeichi, 1982; Yoshida-Noro et al., 1984; Duguay et al., 2003; Foty and Steinberg, 2005). Several groups have identified a series of cadherin-type cell-cell adhesion glycoproteins, firstly described as uvomorulin (Vestweber and Kemler, 1984, 1985; Ringwald et al., 1987), L-CAM (Edelman et al., 1983; Cunningham et al., 1984), A-CAM (Geiger et al., 1985a, b) or cell-CAM (Damsky et al., 1983, 1985). These proteins then have been identified as the same glycoprotein, namely E-cadherin ("Epithelial-cadherin"; Yoshida and Takeichi, 1982; Gallin et al., 1983, 1987; Imhof et al., 1983; Yoshida-Noro et al., 1984; Behrens et al., 1985; Bussemakers et al., 1993).

Subsequently, other AJ glycoproteins were identified and characterized such as N-cadherin ("Neuronal-cadherin"; Hatta and Takeichi, 1986; Nose and Takeichi, 1986; Hatta et al., 1987), P-cadherin ("Placental-cadherin"; Nose and Takeichi, 1986; Nose et al., 1987), M-cadherin ("Muscle-cadherin"; Donalies et al., 1991; Hollnagel et al., 2002; for the occurrence of M-cadherin together with N-cadherin see Rose et al., 1995) and VE-cadherin ("Vascular Endothelium-cadherin"; Lampugnani et al., 1995; Dejana, 1996; Dejana et al., 2000). Another transmembrane glycoprotein, cadherin-11, was first described as OB-cadherin ("Osteoblast-cadherin"; Okazaki et al., 1994) as it was assumed to selectively occur in osteoblastic cells. Subsequently, cadherin-11 gene expression was also demonstrated in a diversity of other mesenchymal and mesenchymally derived tissues (Hoffmann and Balling, 1995; Kimura et al., 1995). Other cadherins like T-cadherin ("Truncated cadherin"; Ranscht and Dours-Zimmermann, 1991; Angst et al., 2001), LI-cadherin ("Liver-Intestine-cadherin"; Berndorff et al., 1994; Gessner and Tauber, 2000) and R-cadherin ("Retinal-cadherin"; Inuzuka et al., 1991) do not contribute to the AJ structure but are present at the plasma membrane (for reviews see, e.g., Goossens and van Roy, 2005; Cavallaro et al., 2006; Berx and van Roy, 2009; Hulpiau and van Roy, 2009).

After the finding that plakoglobin can occur in both, desmosomes and AJs (Cowin et al. 1986; for amino acid sequence of plakoglobin see Franke et al., 1989), related proteins of the larger *armadillo* protein family (Peifer and Wieschaus, 1990; McCrea et al., 1991; Peifer et al., 1992, 1994), have been identified in AJ plaques such as β-catenin (Ozawa et al., 1989, 1990a, b), protein p120 (Reynolds et al., 1994, 1996a, b; Aghib and McCrea, 1995; Shibamoto et al., 1995; for reviews see Anastasiadis and Reynolds, 2000; McCrea et al., 2009), protein ARVCF (Sirotkin et al., 1997a, b; Mariner et al., 1999, 2000; Walter et al., 2008), protein p0071 (Hatzfeld and Nachtsheim, 1996; Hatzfeld, 1999; Hofmann et al., 2008, 2009) and neurojungin (Paffenholz and Franke, 1997; Lu et al.,

1999; Paffenholz et al., 1999). Such proteins are able to bind vinculin-related linker-proteins, in particular α-catenin which occurs in three different cell type-specific subforms: α-E-, α-N- and α-T-catenin (Herrenknecht et al., 1991; Nagafuchi et al., 1991; Hirano et al., 1992; Rimm et al., 1994, 1995; Uchida et al., 1994; Janssens et al., 2001; Goossens et al., 2007).

Another group of immunoglobulin adhesion molecules occurring in AJs is the nectin-afadin-ponsin complex (Asakura et al., 1999). Through the binding of the transmembrane glycoprotein nectin to the cytoplasmic protein afadin this complex can anchor actin filaments (Takai et al., 2008) and thereby can also be linked to the cadherin-catenin complex (e.g., Tachibana et al., 2000; Pokutta et al., 2002; for a recent review see also Meng and Takeichi, 2009). In addition, afadin can also bind the cytoplasmic protein ponsin, which is either connected to actin filaments or may indirectly bind to the cadherin-catenin complex through vinculin (Mandai et al., 1999).

1.1.3 Mixed-type cell-cell adhering junctions

In recent years, it has become clear that several other junction types exist that cannot readily be subsumed under the general textbook classification of adhering junctions (for reviews see Franke, 2009; Franke et al., 2009).

a) Complex junctions (*complexus adhaerentes*)

This mixed-type junction can be found in cells of the lymph node sinus and other portions of the lymphatic vascular system which contain VE-cadherin – with or without N-cadherin – together with the plaque-forming proteins α- and β-catenin, plakoglobin, proteins p120, p0071 as well as afadin. In addition, this junction type also includes the desmosomal plaque protein desmoplakin and typical TJ proteins such as claudin-5 and the immunoglobulin-type transmembrane protein JAM-A ("junctional adhesion molecule-A"; Schmelz et al., 1990, 1994; Schmelz and Franke, 1993, Hämmerling et al., 2006; Baluk et al., 2007; Hofmann et al., 2008; Pfeiffer et al., 2008; Dejana et al., 2009; for reviews see, e.g., Dejana, 2004; Moll et al., 2009).

b) Adherens cortex (*cortex adhaerens*)

This junction type can be observed in the anucleate prismoid fiber cells of the vertebrate eye lens. These cells are very densely packed, nearly without any extracellular spaces and reveal a huge cytoplasmic plaque with two different kinds of cortical

complexes: In the region at the short polar sides, these junctions contain N-cadherin and cadherin-11 as transmembrane glycoproteins in combination with the plaque-building proteins α- and β-catenin, plakoglobin, proteins p120 and p0071 as well as protein ARVCF and afadin. These molecules are further accompanied by the actin-binding protein ezrin. In the region along the longer lateral side, this junction type further contains protein ZO-1, members of the membrane-associated guanylate kinase (MAGUK) protein family as well as spectrin and plectin, in addition to the aforementioned protein ensemble (Straub et al., 2003).

c) Composite junctions (*areae compositae*)

According to the current textbook description of the cell-cell junctions of the cardiomyocytes of the heart, both AJs and desmosomes occur as separate junctions side by side in varying numbers. Moreover, in some species, notably avian, desmosomes have often been described to represent only 10 % or even less of the total cell-cell junction area (e.g., McNutt and Fawcett, 1969; McNutt, 1970; Forbes and Sperelakis, 1985). Detailed immunoelectron microscopic research on the special adhering junctions of the adult mammalian heart, however, has revealed a generally more complex junction type: A fusion of the desmosomal and AJ molecules postnatally accumulating in the IDs (for the development of embryonic desmosomes from epithelioid structures, including keratin filaments and aggregates, see Kuruc and Franke, 1988; van der Loop et al., 1995). The desmosomal and AJ molecules here have amalgamated into the *area composita*, a composite junction (Borrmann, 2002; Borrmann et al., 2006; Franke et al., 2006; Goossens et al., 2007; Pieperhoff and Franke, 2007, 2008). This amalgamation is indeed a rather late, postnatal process occurring in mammals as has been demonstrated in special detail for mouse developmental stages (Pieperhoff and Franke, 2007; see also Hirschy et al., 2006). The composition of the *area composita* and its importance has recently gained increasing attention as it has been shown that the desmosomal-type molecules of this newly defined type of junction are, as demonstrated by mutations, responsible for various forms of hereditary, life-threatening arrhythmogenic right ventricular cardiomyopathies (ARVC; for further literature see Perriard et al., 2003; for reviews see Bazzi and Christiano, 2007; Marcus et al., 2007; Awad et al., 2008; Corrado et al., 2009; Herren et al., 2009; Saffitz, 2009; Li and Radice, 2010; Sen-Chowdhry et al., 2010).

d) Minimal dot junctions (*puncta adhaerentia minima*)

In cultures of mesenchymal stem cells (MSCs) derived from human bone marrow, placenta or adipose tissue, remarkably long filopodial processes can often be observed which are frequently decorated by very small punctate AJs (Wuchter et al., 2007) differing in size from AJs described for other mesenchymal cells in culture (cf. Hinz et al., 2004). Biochemical and electron microscopical immunolocalization has shown the involvement of N-cadherin and cadherin-11 and α- and β-catenin as well as plakoglobin, together with afadin, proteins p120, p0071 and ARVCF, in these small AJ structures.

e) Taproot AJs (*manubria adhaerentia*)

In the aforementioned cultures of cells of mesenchymal origin, another class of mixed-type junctions can often be observed: Here the cells also form cell-cell contacts via filopodial processes, some can be very long, which protrude tight-fittingly into deep invaginations of neighbouring cells, and are connected by AJ structures, an association called a taproot-like junction (Wuchter et al., 2007). The molecular components of these taproot junctions are AJ-typical with N-cadherin and cadherin-11 as transmembrane glycoproteins and the plaque proteins α- and β-catenin with – less frequently – also plakoglobin, together again with the proteins afadin, p120, p0071 and ARVCF.

1.2 Junctions connecting the valvular interstitial cells

1.2.1 Anatomy and function of the heart valves

Due to the ability of mammals to develop a blood system which separates the pulmonary from the systemic circulation, the four-chambered mammalian heart also needs four heart valves, each of which ensures unidirectional blood flow and prevents regurgitation and obstruction. As a result of the torsion of the heart tube during development, leading to adjoining positions of the in- and outflow tracts, the four heart valves are arranged in one plane, called the “fibrous skeleton” of the heart (Misfeld and Sievers, 2007).

The heart valves are usually divided into two groups: 1) the semilunar valves, i.e. the pulmonary valve (*valva trunci pulmonalis*; PV) and the aortic valve (*valva aortae*; AV) and 2) the atrioventricular valves, i.e. the mitral valve (*valva mitralis*; MV) and the tricuspid valve (*valva tricuspidalis*; TV). The AV connects the left ventricle with the aortic root and consists of three leaflets. The PV connects the *conus arteriosus* of the right ventricular

outflow tract with the *truncus pulmonalis* of the pulmonary artery. The MV connects the left atrium and the left ventricle, and the TV in turn connects the right atrium and the right ventricle (Figure 3; Misfeld and Sievers, 2007).

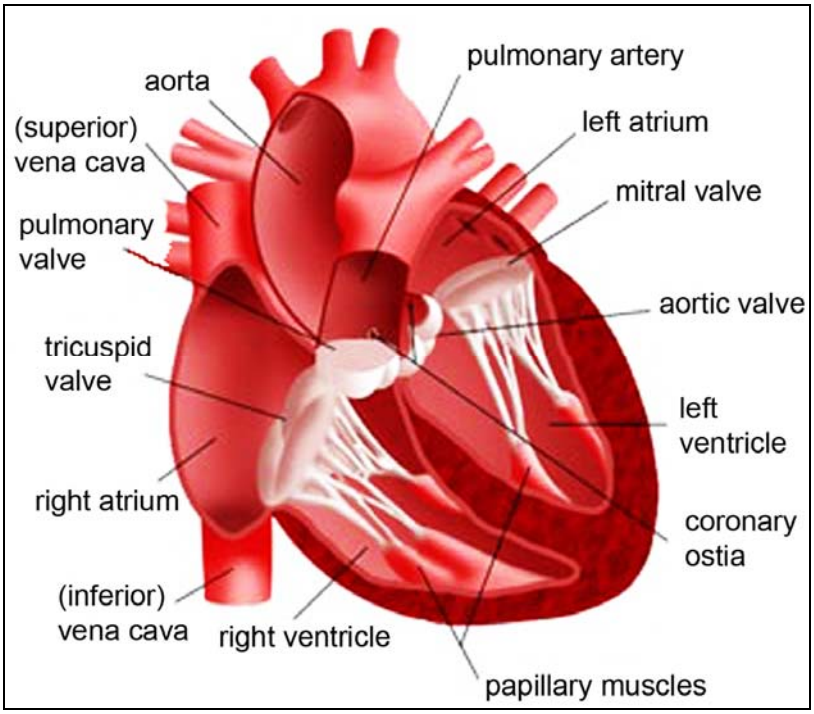

Figure 3: Schematic presentation of a human heart with exposed atria and ventricles. Taken from www.ars-medicina.designblog.de

In the closed state of a normal heart, the PV and the TV have to withstand a pressure of about 30 mm Hg, the AV a pressure of about 100 mm Hg, and the MV has to withstand even pressures up to 150 mm Hg (cf. Yoganathan et al., 2004). The heart valves open and close about three billion times over an average lifetime (Joyce et al., 2009) and have the ability to guide up to 20 L blood per minute through the system, while coping with substantial changes in blood pressure and flow rates. A highly organized and imperishable structure of the heart valve is therefore essential to fulfil these demands.

1.2.2 Structure of the heart valves

All heart valves are covered with a single layer of endothelial and endothelium-associated cells: The endocardium, which continues with the endocardium of the ventricle and the atria, the endothelium of the sinus and the greater vessels. Recent studies have indicated that the endothelial layer of the valvular endocardium has some special features, compared with the endothelium occurring elsewhere in the vascular system (Butcher et al., 2004, 2006): While vascular endothelium is most important as a regulator of blood vessel tonus, the valvular endothelial cell layers are primarily involved in mechanotransduction pathways, thereby regulating valve relaxation and cusp stiffness (e.g., Yacoub et al., 1999; Grande-Allen et al., 2001; El-Hamamsy et al., 2009).

It is widely agreed that the valve interior consists of a trilaminar structure (Figure 4): The *fibrosa*, the *spongiosa* and the *ventricularis* (Mönckeberg, 1904; Gross and Kugel, 1931; Mitomo et al., 1969). The *fibrosa* is mainly built up by collagen fibers oriented parallel with the free edge of the valve cusp. The *spongiosa* is located in between of the *fibrosa* and the *ventricularis* and mainly consists of loose connective tissue rich in glycosaminoglycans (GAGs). Due to ability of GAGs to bind water, the *spongiosa* maintains hydration and thereby ensures a high viscoelasticity of the valve leaflet (Torii et al., 1965; Vesely et al., 1995; Carew et al., 1999, 2000). The *ventricularis* is composed of elastin sheets aligned perpendicular to the vessel wall. It has been suggested that elastin mainly serves to maintain the collagen orientation and reorganization after external forces occurring during the loading cycles (Scott and Vesely, 1996; Vesely, 1998). Being the major protein of the heart valve, collagen represents 55 % of the dry weight, whereas the weight of elastin makes up about 10 % only (Bashey et al., 1967). In healthy mammalian valves the amount of collagen is divided into collagen type I (74 %), type III (24 %) and type V (2 %) as for example reported by Cole et al. (1984). Besides these collagen types, in developing heart valves as well as in adult valves collagen types II, VI and XI have also been found (Klewer et al., 1998; Lincoln et al., 2004, 2006). In addition, the heart valve ECM contains fibronectin and vitronectin (Akhtar et al., 1999).

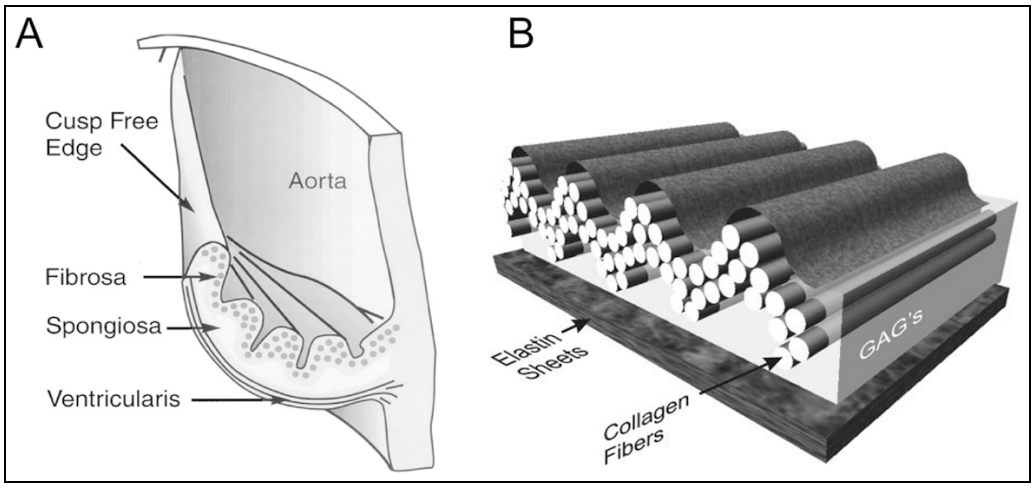

Figure 4: Simplified schematic presentation of the three different layers of the aortic heart valve. (**A**) Aortic heart valve leaflet showing the localization of the layers in the heart valve leaflet (adapted from Vesely, 1998). (**B**) Components of the layers with elastin sheets in the *ventricularis*, GAGs in the *spongiosa* and collagen fibers in the *fibrosa* (cf. Vesely, 2005).

1.2.3 Valvular interstitial cells

The ECM of the valve interior is loosely dispersed and this meshwork is produced by and based on the mesenchymally derived, so-called valvular interstitial cells (VICs). Besides the endothelial cells, the VICs represent about 30 % of the volumetric density of the valve (see, e.g., Filip, 1984). In addition to endothelial cells and VICs, another cell population has been described in the valvular leaflets: Smooth muscle α-actin-positive cells (Bairati and DeBiasi, 1981; Mulholland and Gotlieb, 1996; Bertipaglia et al., 2003; Taylor et al., 2003; Schenke-Layland et al., 2004) which are assumed to have contractile or even partly motile properties and to be involved in the maintenance of the valve tonus. The amount of this cell population seems to increase under diseased conditions (Rabkin-Aikawa et al., 2004) and in times of tissue stress where it contributes to the heart valve stiffness (Merryman et al., 2006).

VICs in culture, their phenotype and their behavior were objects of specific investigation since the middle of the 1980s (e.g., Filip et al., 1986; Zacks et al., 1991; Lester et al., 1992, 1993). As these cells are able to develop actin “stress fibers” and to contract when taken in culture, they are often called “myofibroblastoidal” cells (Filip et al., 1986; Messier et al., 1994; Mulholland and Gotlieb, 1996; Della Rocca et al., 2000; Taylor et al., 2000; for general reviews see Gabbiani, 1996; Hinz and Gabbiani, 2003). Similar to (myo-) fibroblastoidal cells of other origins, VICs have also secretory properties and produce not only collagen and elastin but also matrix metalloproteinases, fibronectin, chondroitin sulfate and GAGs (Messier et al., 1994; Dreger et al., 2002; Butcher and

Nerem, 2004; see there for earlier references). Moreover, VICs can respond to exogenous stimuli by contraction, e.g., after treatment with adrenalin, angiotensin-II, bradykinin, potassium chloride, carbachol or endothelin, and typically show relaxation after treatment with isoprotenerol (see, e.g., Filip et al., 1986; Messier et al., 1994).

However, the VIC population is heterogeneous and different phenotypes are known to be specifically associated with physiological heart valve integrity. Recently, studies dealing with phenotype-function relationships of the VIC population have led to the identification of six distinguishable phenotypes of VICs: 1) quiescent VICs, which maintain the valvular structure and inhibit angiogenesis, are located in the heart valve leaflet; 2) embryonic progenitor endothelial or mesenchymal cells which according to some authors can give rise to the future resident quiescent VICs through a process called “endothelial-to-mesenchymal transition” (EMT; Armstrong and Bischoff, 2004; Trinh and Stainier, 2004; Snarr et al., 2008; Hinton and Yutzey, 2011), located in the embryonic cardiac cushions; 3) activated VICs, also located in the leaflet, with a “myofibroblast” appearance and the ability to proliferate, migrate, remodel the ECM and to respond to valve injury; 4) osteoblastic-type VICs, located in the leaflet, responsible for calcification processes, but also for chondrogenesis, a process based on secretions of osteocalcin, osteopontin and alkaline phosphatase; 5) progenitor VICs, located in the bone marrow or in the circulating blood, which, when located in the heart valve leaflet, induce activated VICs to repair the heart valve (see, e.g., Liu et al., 2007), and 6) adipogenic cells characterized by adipogenesis-typical lipid droplets and certain amphiphilic proteins (Dunmore-Buyze et al., 1995; Chen et al., 2009).

1.2.4 Cell-cell junctions of valvular interstitial cells

Contacts between VICs and the surrounding ECM structures, including the collagen fibers, have been demonstrated by electron microscopists in the past (Filip et al., 1986). Moreover, VICs have been shown to be connected via typical albeit sparse GJs (Filip et al., 1986; Lester and Gotlieb, 1988; Lester et al., 1993). Moreover, the functionality of these GJs has been demonstrated using cultured VICs (Filip et al., 1986; Latif et al., 2006). In addition, VICs have also been claimed to be connected by some sort of AJs (Lester and Gotlieb, 1988; Messier et al., 1994). Other reports describing the presence of desmosomes in VICs were – and are – doubtful (e.g., Messier et al., 1994). Using immunohistochemistry and cell sorting (FACS) as well as immunoblot analysis, the

synthesis of N-cadherin, α- and β-catenin, connexins-26 and -43 and desmogleins has recently been reported (Latif et al., 2006).

1.3 Aim of the work

The textbook categories of cell-cell junctions postulate that there are four major junction types: 1) the desmosomes, 2) the AJs, 3) the TJs and 4) the GJs. However, as mentioned before, research on cell- and tissue-specific cell-cell junctions has revealed a broader and more diversified spectrum of cardiac adhering junctions. In the heart specifically, the myocardial composite junctions, representing an amalgamation of desmosomal and AJ molecules, have been characterized (for recent reviews see Marcus et al., 2007; Franke et al., 2009). By contrast, the proteins involved in the cell-cell contacts between the mesenchymally derived cells of the heart valves – the VICs – still have not yet been elucidated to a reasonable level.

Research on heart valves and their cells started already at the end of the 19th century with histological and later – after 1950 – with electron microscopic studies (Joseph, 1858; Mönckeberg, 1904; Gross and Kugel, 1931; Kühnel, 1965) and was more recently extended by biochemical and immunocytochemical analyses (for a general review, including anatomical and physiological features of VICs, see Flanagan and Pandit, 2003). However, even to date there are only few publications presenting only with sparse and rather non-systematic analyses of the cell-cell contact proteins connecting the VICs of heart valves (Latif et al., 2005, 2006).

Therefore, it has been the aim of this thesis to characterize the cell and molecular biology of the cell-cell contacts of the VICs of different mammalian species *in situ* and in cell culture. This also might provide a better basis for the molecular design and the preparation of cells grown *in vitro* and in three-dimensional meshwork structures which would be useful for preparations of artificial heart valves that may raise cell biologically optimized objects for a therapeutic heart valve replacement (“heart valve engineering”).

2 Materials

2.1 Primary and established cell culture lines

All cell lines used were treated and passaged either as recommended by the distributor or the manufacturer or - in case of primary cell culture lines - as based on experience in the laboratory. Generally, the cells were passaged every 3 to 4 days by treatment with trypsin (0.25 %)/EDTA (0.7 %) in PBS and plated on coated or uncoated cell culture dishes supplied with fresh DMEM medium (Dulbecco's modified Eagle's medium with glutamine; GIBCO BRL, Eggenstein, Germany) containing 10 % FCS (PAA Laboratories, Cölbe, Germany), 1 % glutamine (GIBCO BRL) and 1 % penicillin/streptomycin (PAA Laboratories).

2.1.1 Human cell culture lines

Table 1 Human cell culture lines

Cell line	Reference
U333/glioma	astrocytoma cell line (Osborn et al., 1981; for earlier reports see references cited therein)
MCF-7	cell line of human breast carcinoma; ATCC HTB-22 (Soule et al., 1973)
PLC	cell line of primary human liver carcinoma; ATCC CRL-8024 (Alexander et al., 1976)
SV80	SV40-transformed human WI38 fibroblasts; ATCC CCL-75.1 (Girardi et al., 1966)
HG261	human skin fibroblasts; ATCC CCL-122 (Todaro et al., 1966; Todaro, 1968)
HaCaT	human keratinocytes cell line (Boukamp et al., 1988)

2.1.2 Non-human cell culture lines

Table 2 Non-human cell culture lines

Cell line	Reference
B1	bovine dermal fibroblasts (Cowin et al., 1986)
HL-1	murine cardiac muscle cell line (Claycomb et al., 1998)
Rat2	rat fibroblasts; ATCC CRL-1764 (Topp, 1981)

2.1.3 Human tissues and primary cell culture lines

Human hearts or heart valve tissues and primary cell culture lines were obtained from freshly dissected hearts or heart valves of patients of both sexes and different ages, undergoing heart or heart valve transplantation (cooperation with Prof. Dr. Artur Lichtenberg, Department of Cardiac Surgery, University Hospital Heidelberg, 2006-2009, and Department of Cardiothoracic Surgery, University Hospital Düsseldorf, since 2009). For cell culture details see chapter 3.1.1.

Papillary fibroelastoma samples were kindly provided by Prof. Dr. Waldemar Hort (Institute of Pathology, University Hospital Düsseldorf), and myxomatous degenerated human mitral heart valves as well as several other human tissues for comparison were kindly provided by Prof. Dr. Roland Moll (Institute of Pathology, University Hospitals Giessen and Marburg). Fetal heart samples were provided by Prof. Dr. Ingrid Moll (Dermatology and Venereology Department and Clinic, University Clinic of Hamburg-Eppendorf).

2.1.4 Non-human tissues and primary cell culture lines

Bovine tissues from freshly slaughtered animals were obtained from a local abattoir (Schlachthof Mannheim). Ovine tissues were obtained through the “Heidelberg Initiative for Cardiovascular Tissue Engineering” (Coordinator: Dr. Payam Akhyari, Department of Cardiac Surgery, University Hospital Heidelberg, 2006-2009). Fetal and adult porcine tissues were provided by Prof. Dr. Heiner Niemann (Institute of Farm Animal Genetics, Friedrich-Loeffler-Institute Mariensee, Neustadt am Rübenberge).

2.2 Antibodies

2.2.1 Primary antibodies

Table 3 Primary antibodies

Antigen	Antibody, category, species	Source	References
Cadherins			
N-cadherin	mcl[1], m[2]	Transduction Labs (Lexington, KY, USA)	Bhowmick et al., 2001; Nürnberger et al., 2002
N-cadherin	pcl[3], rb[4]	QED Biosciences Inc. (San Diego, CA, USA)	
P-cadherin	mcl, m	Transduction Labs	Nose and Takeichi, 1986; Tao et al., 1996
E-cadherin	mcl, m	Transduction Labs	Vestweber and Kemler, 1984, 1985
Cadherin-11	mcl, m	Zymed Laboratories (South San Francisco, CA, USA)	Okazaki et al., 1994
VE-cadherin	mcl, m	Transduction Labs	Lampugnani et al., 1995; Dejana, 1996; Dejana et al., 2000
VE-cadherin	pcl, rb	Cayman Chemical Company (Ann Arbor, MI, USA)	
Desmoglein 1+2	mcl, m (DG3.10)	Progen Biotechnik (Heidelberg, Germany)	Schmelz et al., 1986a, b
Desmoglein 3	mcl, m	Progen Biotechnik	Schäfer et al., 1996; Kurzen et al., 1998
Desmocollin 1	mcl, m (clone U100)	Progen Biotechnik	Nuber et al., 1995, 1996
Desmocollin 3	mcl, m (clone U114)	Progen Biotechnik	Nuber et al., 1996
Transmembrane Tight Junction Proteins			
Occludin	mcl, m	Invitrogen (Paisley, UK)	Furuse et al., 1993
Claudin 1	pcl, rb	NeoMarkers (Fremont, CA, USA)	Furuse et al., 1998a, b
Claudin 2	pcl, rb	Zymed Laboratories	
Claudin 3	pcl, rb	Zymed Laboratories	Tsukita and Furuse, 1998; Morita et al., 1999a, b; Rahner et al., 2001
Claudin 4	mcl, m	Zymed Laboratories	
Claudin 5	pcl, rb	Zymed Laboratories	
Claudin 7	pcl, rb	Zymed Laboratories	
Tricellulin-α	pcl, rb	Kindly provided by Sachiko Tsukita, Osaka	Ikenouchi et al., 2005

Continuation of Table 3

Antigen	Antibody, category, species	Source	References
Other Transmembrane Proteins/Glycoproteins			
Nectin 2	pcl, rb	Santa Cruz Biotech. (Santa Cruz, CA, USA)	Lopez et al., 2000; Fabre et al., 2002
Nectin 3	pcl, rb	Santa Cruz	
Myozap	mcl, m (517.67)	Kindly provided by Sebastian Pieperhoff, Edinburgh	Seeger et al., 2010
Hemidesmosomal glycoproteins	mcl, m (HD233)	Kindly provided by Katsushi Owaribe, Nagoya	Owaribe et al., 1990, 1991
JAM-A	pcl, rb	Zymed Labs	Kostrewa et al., 2001; Konopka et al., 2007
JAM-C	pcl, rb	Zymed Labs	
Armadillo Proteins			
Plakoglobin	mcl, m (PG5.1)	Progen Biotechnik	Cowin et al., 1986
Plakoglobin	mcl, m (11E4)	Kindly provided by Margaret J. Wheelock, Omaha	
β-Catenin	mcl, m	Transduction Labs	Ozawa et al., 1990b; Eger et al., 2000
β-Catenin	pcl, rb	Zymed Labs	Ozawa et al., 1990b; McCrea et al., 1991
Protein p120	mcl, m	Transduction Labs	Reynolds et al., 1994, 1996a, b
Protein p120	pcl, rb	Sigma (St. Louis, MO, USA)	
Protein p0071	pcl, gp^5 (GP71)	Progen Biotechnik	Hofmann et al., 2008, 2009
Protein ARVCF	pcl, gp (GP155)	Progen Biotechnik	Walter et al., 2008
Plakophilin-1 (Pkp1)	mcl, m (PP1-2D6)	Progen Biotechnik	Heid et al., 1994
Plakophilin-2 (Pkp2)	mcl, m (PP2-62, -86, -150)	Progen Biotechnik	Mertens et al., 1996
Plakophilin-2 (Pkp2)	mcl, m (Pkp2-518)	Progen Biotechnik	Rickelt et al., 2010
Plakophilin-2 (Pkp2)	pcl, gp (GP-PP2)	Progen Biotechnik	Rickelt, 2010
Plakophilin-3 (Pkp3)	mcl, m (PP3-270.6.2)	Progen Biotechnik	Schmidt et al., 1999

Continuation of Table 3

Antigen	Antibody, category, species	Source	References
Other Plaque Proteins			
α-Catenin	mcl, m	Zymed Labs	Herrenknecht et al., 1991; Nagafuchi et al., 1991
α-T-Catenin	pcl, rb	USBiological (Swampscott, MA, USA)	Janssens et al., 2001, 2003
α-E-Catenin	pcl, rb	Cell signaling (Danvers, MA, USA)	Herrenknecht et al., 1991; Nagafuchi et al., 1991
α-N-Catenin	pcl, rb	Sigma	Hirano et al., 1992; Uchida et al., 1994
Desmoplakin I+II	mcl, m (DP-2.15, -2.17 and -2.20)	Progen Biotechnik	Franke et al., 1982b, 1983a; Cowin et al., 1985
Desmoplakin I	pcl, gp (DP-1)	Progen Biotechnik	Köser, 1999; Köser et al., 2003
Vinculin	mcl, m (11-5)	Sigma	Geiger, 1979; Geiger et al., 1980
Vinculin	pcl, rb	Sigma	
α-Actinin	mcl, m (BM-75.2)	Sigma	Abd-el-Basset et al., 1991
l/s-Afadin	pcl, rb	Sigma	Mandai et al., 1997
ZO-1	mcl, m	Invitrogen	Stevenson et al., 1986; Anderson et al., 1989
ZO-1	pcl, rb	Zymed Labs	
ZO-3	pcl, rb	Zymed Labs	Haskins et al., 1998; Itoh et al., 1999; Inoko et al., 2003
ZO-3	mcl, m	Millipore (Schwalbach, Germany)	
Intermediate-sized Filament Proteins			
Vimentin	mcl, m (Vim3B4)	Progen Biotechnik	Heid et al., 1988; Herrmann et al., 1989
Vimentin	pcl, gp (GP53)	Progen Biotechnik	Magin et al., 1990
Desmin	mcl, m (D9)	Progen Biotechnik	Van Muijen et al., 1987
Nestin	mcl, m	Millipore	Lehndahl et al., 1990; Tohyama et al., 1993
Keratins (cytokeratins) 8 and 18	mcl, m (NCL-5D3)	Progen Biotechnik	Angus et al., 1987
Keratin 20	pcl, gp (K20.2)	Progen Biotechnik	Moll et al., 1982a, b
Pan-Keratin	mcl, m (Lu5)	Acris (Herford, Germany)	von Overbeck et al., 1985
Neurofilament (NF)	mcl, m	Boehringer Ingelheim (Ingelheim am Rhein, Germany)	Wood and Anderton, 1981
Gliafilament (GFAP)	pcl, rb	Millipore	Uyeda et al., 1972

Continuation of Table 3

Antigen	Antibody, category, species	Source	References
Cytoskeletal Proteins			
β-, γ-, -non-muscle actin	mcl, m	Sigma	Gimona et al., 1994; Hanft et al., 2006
α-smooth muscle actin	mcl, m (ASM-1)	Progen Biotechnik	Skalli et al., 1986
Cardiac α-actin	mcl, m (AC1-20.4.2)	Progen Biotechnik	Franke et al., 1996
Extracellular Matrix Proteins			
Elastin	mcl, m (BA-4)	Sigma	Wrenn et al., 1986
Collagen type I	pcl, rb	Abcam (Cambridge, MA, USA)	French et al., 2008; Yue et al., 2008
Collagen type II	pcl, rb	Abcam	Sohaskey et al., 2008
Collagen type IV	pcl, rb	Abcam	McColl et al., 2008
Collagen type VI	pcl, rb	Abcam	Snipstad et al., 2010
Collagen type VII	pcl, rb	Linaris (Wertheim-Bettingen, Germany)	Sakai et al., 1986
Other Proteins or Glycoproteins			
Perilipin	mcl, m (Peri112.17.1)	Kindly provided by Hans Heid, DKFZ, Heidelberg	
Adipophilin	mcl, m (125)	Progen Biotechnik	Heid et al., 1998
Tubulin	mcl, m	Sigma	Gao et al., 2008
Moesin	mcl, m	Transduction Labs	Furthmayr et al., 1992
Ezrin	mcl, m	Sigma	Bretscher, 1986
S-100	pcl, rb	Dako (Hamburg, Germany)	Zuckerman et al., 1970; Herschman et al., 1971
Lamin A/C	mcl, m (X67)	Progen Biotechnik	Krohne and Benavente, 1986
Ki-67	mcl, m	Zymed	Gerdes et al., 1983
Ki-67	pcl, rb	Zymed	
Periostin	pcl, rb	Acris	Horiuchi et al., 1999
PERP	pcl, rb	Sigma	Attardi et al., 2000; Ihrie and Attardi, 2005
Osteopontin	pcl, rb	Sigma	Oldberg et al., 1986
Paxillin	mcl, rb	Epitomics (Burlingame, CA, USA)	Turner et al., 1990

[1]monoclonal antibody, [2]mouse, [3]polyclonal antibody, [4]rabbit, [5]guinea pig

2.2.2 Secondary antibodies

Secondary antibodies conjugated with fluorochromes used for immunofluorescence microscopy were directed against species-specific immunoglobulins and had been generated in goats. Cy3- and Alexa488-conjugated secondary antibodies against mouse, rabbit or guinea pig immunoglobulins were used (Cy3: Dianova, Hamburg, Germany; Alexa488: Invitrogen, Karlsruhe, Germany). Antibodies were diluted according to the manufacturer's recommendations.

Immunoblot analysis was performed using HRP- (horseradish peroxidase) conjugated secondary antibodies against rabbit, guinea pig or mouse immunoglobulins (Dianova).

2.2.3 Other fluorescent markers

Alexa Fluor®488- or Alexa Fluor®594-coupled phalloidin was used for the specific staining of F-actin. In addition, staining of the nuclear chromatins was performed with 4', 6-diamidino-2-phenylindole (DAPI; Serva, Heidelberg, Germany).

2.3 Buffers, media and solutions

All chemicals used for buffers, media and other solutions were obtained from Merck (Darmstadt, Germany), Sigma-Aldrich (München, Germany), Roche Diagnostics (Mannheim, Germany), Serva (Heidelberg, Germany) or Roth (Karlsruhe, Germany).

Table 4 Buffers, media and solutions

Buffer	Composition and concentration
10X PBS	1.4 M NaCl 27 mM KCl 17 mM KH_2PO_4 81 mM Na_2HPO_4 pH 7.4
Tris-urea buffer	Stock solution: 20.18 g Tris-HCl ad 1L H_2O_{dest}, pH 11 Working solution: 150 mL stock solution + 100 mL H_2O_{dest} + 12.5 g urea
Citrate buffer	Solution A: 21.01 g Citric acid ad 1L H_2O Solution B: 29.41 g Sodium citrate ad 1L H_2O_{dest} 9 mL A + 41 mL B ad 500 mL, H_2O_{dest}, pH 6
0.5 M Sodium cacodylate buffer	107 g Sodium cacodylate ad 1L H_2O_{dest}, pH 7.2
2.5 % Glutardialdehyde*	2.4 mL Glutardialdehyde (25 %) 1.25 mL 1M KCl 62.5 µL 1 M $MgCl_2$ 2.5 mL 0.5 M Sodium cacodylate buffer ad 25 mL H_2O_{dest}
4 % Osmium tetroxide	1 g Osmium tetroxide ad 25 mL H_2O_{dest}
0.5 % Uranylacetate	125 g ad 25 mL H_2O_{dest}
2 % Uranylacetate	500 mg ad 25 mL Methanol
Lead citrate solution	0.67 g Lead nitrate 0.88 g Sodium citrate 0.2 g NaOH ad 50 mL H_2O_{dest} pH 12
RIPA buffer	1 % Triton-X-100 0.2 % SDS 0.5 % Sodium desoxycholat 20 mM HEPES 150 mM NaCl ad 300 mL H_2O_{dest} pH 7.4
ADS buffer	116 mM NaCl 20 mM HEPES 9 mM NaH_2PO_4 5mM Glucose 5 mM KCl 0.4 mM $MgSO_4$ pH 7.4

Continuation of Table 4

Buffer	Composition and concentration
Dissociation buffer	150 mg Collagenase type II (0.05 %) 180 mg Pancreatin (0.06 %) ad 300 mL 1X ADS buffer
2X SDS buffer	40 mM DTT 125 mM Tris-HCl 20 % Glycerol 4 % SDS 0.1 % Bromphenol blue pH 6.8
10X electrophoresis running buffer	350 mM Tris-HCl, pH 8.8 1 % SDS 1.92 M Glycine
Coomassie staining solution	0.2 % Coomassie briliant blue 40 % Isopropanol 7 % Acetic acid
PVDF membrane destaining solution	40 % Isopropanol 7 % Acetic acid
DMEM High Glucose 1X (GIBCO BRL)	25 mM Glucose 3.97 mM L-Glutamine 0.0399 mM Phenol red
10X Reverse transcriptase (RT) buffer	0.4 M Tris-HCl pH 8 0.4 M KCl 60 mM $MgCl_2$ 10 mM DTT 15 nM dNTP (4X)
1X TAE buffer	40 mM Tris-HCl 1 mM EDTA
2% Formaldehyde solution	2 g Paraformaldehyde in 100 mL 1X PBS, pH 7.4
Sodium thiosulfate pentahydrate solution	200 mL 50 mM HEPES 12.4 g sodium thiosulfate pentahydrate pH 5.8

*glutardialdehyde is named glutaraldehyde in the following

2.4 Technical equipment

Table 5 Technical equipment

Instruments and glassware	Name	Manufacturer
Incubators	Function Line	Heraeus (Hanau, Germany)
Electron microscope	EM 900	Zeiss(Oberkochen, Germany)
Confocal laser scanning microscope	LSM 510	Zeiss
Fluorescence microscope	Axiophot	Zeiss
Diamond knifes, 45°	DiATOME ultra	Diatome AG (Biel, Switzerland)
Digital camera	Axio Cam HRc/MRc	Zeiss
Ultramicrotome	Ultracut	Leica (Wetzlar, Germany)
Microtome	HM 355 S	Microm (Walldorf, Germany)
Cryotome	Jung CM 3050 S	Leica
Microtome blades	Leica 819	Leica
Microwave instrument	RHS Rapid Microwave Histoprocessor	Milestone (Sorisole, Italy)
Water bath		GFL (Burgwedel, Germany)
Sterile laminar flow bench	SterilGardHood	The Baker Company. Inc. (Sanford, ME, USA)
Heating block	Thermomixer 5436	Eppendorf (Hamburg, Germany)
pH meter	765 Calimatic	Knick (Egelsbach, Germany)
Magnetic stirrer	Ikemag®Reo	Ika Labortechnik (Staufen, Germany)
Gelelectrophoresis chamber	X Cell Sure Lock	Novex (San Diego, CA, USA)
Electrophoresis power supply	Phero-stab.500	Biotec-Fischer (Reiskirchen, Germany)
Blotting chamber		cti (Idstein/Taunus, Germany)
Shaker	Silent Rocker	cti
Scanner	Epson Perfection 4870	Epson (Long Beach, CA, USA)
Scales	PB 3002-S/PB 135-S	Mettler-Toledo (Giessen, Germany)
Heating cabinet		Memmert (Schwabach, Germany)
Centrifuge	5415R	Eppendorf
Centrifuge	Minifuge RF	Heraeus
Vortex	Reax2000	Heidolph (Schwabach, Germany)
Developer	Optimum Typ TR	MS Laborgeräte (Heidelberg, Germany)
Rotator	tiny turner	cti
Thermocycler	MJR Research	Biozyme, Oldendorf, Germany

3 Methods

3.1 Cell cultures

3.1.1 Primary and secondary cultures of human, bovine, ovine and porcine valvular interstitial cells

One to two heart valve leaflets of human, bovine, ovine or porcine origin were minced with small scissors into pieces (ca. 1 mm side lengths) in 4°C cold 1X ADS buffer (see Table 4). The pieces were then collected in 12 mL 37°C warm dissociation buffer containing 0.05 % collagenase type II (Invitrogen, Karlsruhe, Germany) and 0.06 % pancreatin (Sigma, München, Germany) in 1X ADS buffer (see Table 4). Afterwards, the pieces were slowly agitated on a magnetic stirrer for 30 min at room temperature (RT). After sedimentation of the tissue pieces, the supernatant was discarded and the tissue pieces were incubated with another 10 mL of the dissociation buffer and again slowly agitated on a magnetic stirrer at RT. After sedimentation of the tissue pieces, the supernatant suspension was collected, centrifuged at 1000 rpm to remove collagenase and pancreatin, and the resulting pellet was stored in 4 mL newborn calf serum at 37°C.

The remaining tissue pieces were again incubated with the digestion solution and the supernatant was collected. This procedure was repeated three times. Afterwards, all pellets in newborn calf serum were pooled and centrifuged at 1000 rpm for 5 min. The resulting pellet was washed twice with 37°C warm 1X ADS buffer and was re-centrifuged. The resulting pellet was resuspended in 2 mL 37°C warm DMEM with 10 % FCS and 1 % penicillin/streptomycin (v/v). Finally, the cells were plated on collagen-coated dishes and cultivated until they had reached confluency at 37°C in a humidified incubator. By treating the cells with trypsin/EDTA they were detached from the dish and either plated on collagen-coated dishes for further passages or on collagen-coated glass coverslips.

3.1.2 Primary valvular interstitial cells in three-dimensional cultures

3.1.2.1 Matrigel™*/collagen type I three-dimensional cultures*

Matrigel™/collagen type I three-dimensional (3D) cultures were prepared with ovine VICs. Cells (passage two to five) grown in 10 mL culture dishes were rinsed twice with 37°C warm PBS, then detached from the dish by treatment with trypsin/EDTA and finally diluted to a concentration of ca. 4.2 x 10^6 cells/mL with 1X DMEM with 10 % FCS and 1 % penicillin/streptomycin. For preparations of the final Matrigel™/collagen type I matrix a volume of 1.17 mL, 100 µL 2X DMEM and 100 µL rat tail collagen type I (5 mg/mL; BD Biosciences, Franklin Lakes,NJ, USA) were mixed in an Eppendorf reaction tube on ice.

In a second tube, 340 µL Matrigel™ (with basement matrix; BD Biosciences) was mixed with 277 µL of the diluted cell suspension. To neutralize the low pH of the collagen type I/DMEM solution, 340 µL 0.1 M NaOH were added, mixed by pipetting up and down and added to the cell/Matrigel™ solution. This solution was mixed by pipetting up and down, kept on ice, and the wells of a 24-well plate with membrane inserts of a mean pore size of 0.4 µm (BD Biosciences) were each filled with 150 µL and incubated for 1 h to polymerize the Matrigel™/collagen type I solution. After the solution had polymerized to gel, the Matrigel™/collagen type I matrix 3D constructs were covered with 0.5 mL DMEM (10 % FCS and 1 % penicillin/streptomycin) containing 50 µg/mL ascorbic acid. Matrigel™/collagen type I matrix 3D constructs were cultivated for 2 weeks and were fixed in 4 % formaldehyde in PBS (w/v) for 24 h and embedded in paraffin after dehydration, in 2.5 % glutaraldehyde (v/v) at 4°C for electron microscopy, or were frozen for cryostat sections (for detailed protocols of fixation of tissue pieces and 3D constructs see chapters 3.2.2, 3.2.3 and 3.4.1).

3.1.2.2 Collagen type I three-dimensional cultures

To obtain ca. 3.12 mL of a 3D collagen type I culture suspension, five 10 mL culture dishes with confluent grown ovine VICs were detached and diluted in 0.75 mL DMEM (containing 10 % FCS and 1 % penicillin/streptomycin). 2 mL rat tail collagen type I with a concentration of 5 mg/mL (BD Biosciences) were mixed with 0.25 mL 10X DMEM and neutralized with 120 µL 10 M NaOH (all steps were performed on ice) and mixed with the VIC cell suspension to a final collagen concentration of 2 mg/mL. The 3D construct was polymerized at 37°C in an incubator for 1 h, then covered with DMEM medium

containing 10 % FCS, 1 % penicillin/streptomycin and 50 µg/mL ascorbic acid and incubated for one week with changes of the medium every two days. The 3D constructs were fixed as described for the Matrigel™/collagen constructs (for detailed protocols of fixation of tissue pieces and 3D constructs see chapters 3.2.2, 3.2.3 and 3.4.1).

3.1.2.3 Re-seeding of decellularized heart valve structures with valvular interstitial cells

Freshly obtained pulmonary valve conduits including valve annulus, valve leaflets and pulmonary artery wall of young lambs (about 4 months old) were decellularized with a concomitant removal of the basal membrane material (Grauss et al., 2003; Kasimir et al., 2003). To this end, valve conduits were washed twice in sterile PBS and incubated under shaking in 0.5 % trypsin in PBS containing 0.2 % EDTA at 37°C for 48 h (Bader et al., 1998; Cebotari et al., 2002, 2006). The detergent solution was changed every 12 hours. To remove residual detergent, the valve conduits were finally washed twice in sterile PBS and stored in serum- and antibiotic-free DMEM medium at 4°C. Before the final utilization, decellularized valve conduits were incubated overnight at RT in serum- and antibiotic-free DMEM medium, to exclude potentially unsterile heart valves.

The pulmonary heart valve leaflets were dissected (Figure 5) and five decellularized heart valve leaflets were fixed in a custom-designed culture chamber (Figure 6; Akhyari et al., 2009b). The leaflets were covered with ca. 300 µL serum-free DMEM medium containing 1 % penicillin/streptomycin. The valves were incubated overnight at 37°C in an incubator. The next day, ca. 250,000 ovine VICs in DMEM medium containing 10 % FCS and 1 % penicillin/streptomycin were seeded on each decellularized valve and incubated for 10 days with changing of the medium every three days. Afterwards the re-seeded heart valves were fixed and prepared for paraffin-embedding, cryosectioning, electron microscopical and biochemical analysis (for detailed protocols of fixation of 3D constructs see chapters 3.2.2, 3.2.3 and 3.4.1).

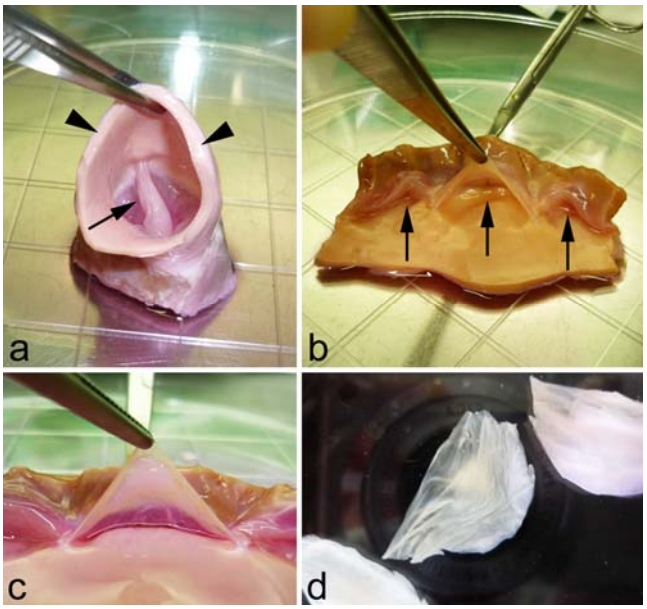

Figure 5: Preparations of decellularized ovine pulmonary valves. (**a**) Decellularized ovine pulmonary valve conduit with closed pulmonary heart valve (see arrow) and adjacent pulmonary artery walls (arrowheads). (**b**) Dissected, opened valve conduit showing the three pulmonary heart valve leaflets (see arrows). (**c**) Higher magnification of decellularized heart valve leaflets.
(**d**) Dissected decellularized pulmonary heart valve leaflets.

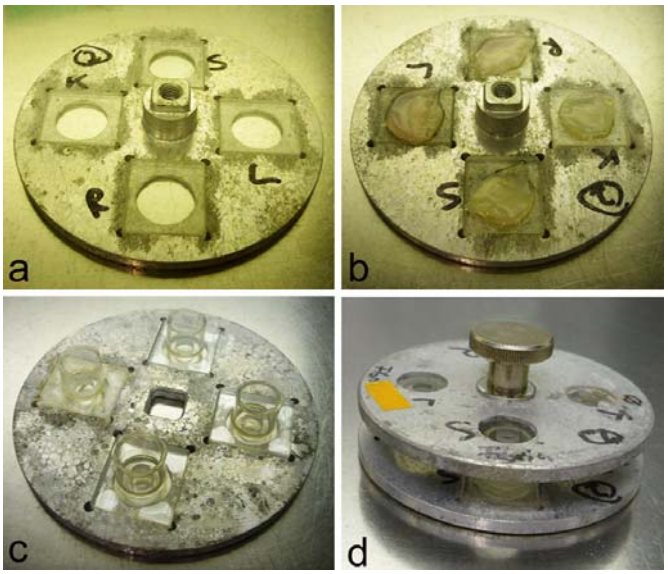

Figure 6: Custom-designed culture chamber. (**a**) Bottom part with four circular holes, each of them covered with a square glass disk. A screw thread is located in the middle. (**b**) Bottom part with four heart valve leaflets placed on the glass disks. (**c**) Upper part of the culture chamber with four circular holes, each covered with a glass disk. In the middle of each disk, a cylindrical plastic tube is attached leaving a fourfold circular hole in the glass. In the center of the incubation chamber, a hole corresponding to the screw thread of the bottom part of the chamber, is left. (**d**) Upper part tightened to the bottom part. The heart valve leaflets are placed and fixed between the glass disks of the bottom part and the plastic tubes of the upper part of the chamber. Medium changes can be performed through the holes in the glass disks of the upper part without opening the culture chamber.

3.1.3 Small interference RNA transfection

For small interference RNA (siRNA) transfection (Elbashir et al., 2001; Tuschl and Borkhardt, 2002), siRNA specific for mRNA encoding human plakophilin-2 and N-cadherin as well as control siRNAs (ON-TARGETplus SMARTpool, non-targeting control siRNA) and lamin A/C siRNA were obtained from Dharmacon (Chicago, USA). Primary cultures of VICs derived from human mitral heart valves (passage 5-8) were plated on 6-well plates covered with poly-L-lysine (each well was supplied with three glass cover slips) with DMEM containing 10 % FCS and 1 % penicillin/streptomycin. In total, one 6-well plate for each time point (48 h, 72 h and 96 h) was used. The cells were used 2-3 days after seeding at a mean confluency of ca. 70 %.

The siRNA transfection experiments were basically performed according to the manufacturer's protocol using minor modifications as described elsewhere (Pieperhoff et al., 2008) and serum- as well as antibiotic-free DMEM medium. The cells of the six wells of each 6-well plate were treated as follows: 1) plakophilin-2 siRNA with transfection reagent, 2) N-cadherin siRNA with transfection reagent, 3) lamin A/C siRNA with transfection reagent, 4) control siRNA with transfection reagent, 5) medium with transfection reagent without siRNA, 6) DMEM medium without transfection reagent or siRNA. The cells were then incubated at 37°C in an incubator. After 48 h, the samples for the first time point were taken, whereas the medium of the other 6-well plates was replaced by normal culture medium (10 % FCS, 1 % penicillin/streptomycin) to avoid cytotoxicity caused by the siRNA or the transfection reagent, respectively.

The coverslips with the cells were briefly washed twice in 37°C warm PBS and fixed for 5 min in -20°C cold methanol, following by a fixation step for 30 sec in -20°C cold acetone. The subsequent preparations for immunofluorescence microscopy are described in chapter 3.3. For the analysis of the siRNA knock-down results monoclonal antibodies (mAbs) against plakophilin-2, N-cadherin and lamin A/C were used. Nuclei were stained with DAPI. Cells which have grown in the wells beside the glass coverslips were taken for lysates used for immunoblot analysis (for details of the biochemical analysis see chapter 3.5).

3.2 Light microscopy

3.2.1 Fixation of cultured cells

Cells grown on glass coverslips coated with collagen type I or poly-L-lysine were fixed either by incubation in -20°C cold methanol and acetone or by 37°C warm 2 % formaldehyde, freshly prepared from paraformaldehyde powder, in PBS, pH 7.4 (see Table 4).

3.2.1.1 Methanol/acetone fixation

Cells grown on glass coverslips were washed twice with 37°C warm 1X PBS and fixed in -20°C cold methanol for 5 min, followed by an incubation step in -20°C cold acetone for 30 sec. After the coverslips had dried, they were either used directly for immunofluorescence microscopy or were stored frozen at -20°C.

3.2.1.2 Formaldehyde fixation

Cells grown on glass coverslips were washed twice with 37°C warm PBS and incubated for 3-5 min in 37°C warm 2 % formaldehyde in PBS (w/v). After fixation, the cells were washed twice with PBS for 5 min and used immediately for immunofluorescence microscopy. To this end, the fixed cells were incubated twice each for 5 min in PBS containing 50 mM NH_4Cl to saturate free reactive aldehyde groups. Afterwards the cells were incubated with Triton-X-100 (0.1 %; w/v) or saponin (0.1 %; w/v) in PBS for 5 min. After two washing steps with PBS for 5 min, the cells were incubated with the primary antibodies (for the following immunofluorescence microscopy see chapter 3.3).

3.2.2. Preparation of snap-frozen tissue and fixation of cryotome sections

Tissues or 3D cultures with entrapped VICs were washed gently in 37°C warm PBS to remove residual blood or culture medium. Then the tissues or 3D cultures were frozen in isopentane cooled to the temperature of liquid nitrogen. The specimens were incubated in isopentane for a few minutes (duration depended on the specific size of the frozen samples) and were then stored in plastic vials with ca. 5 mL isopentane at -80°C. For immunofluorescence microscopy, frozen specimens were cut with a cryotome into ca.

4 µm thin sections at -20°C. The sections were immediately placed on Menzel Super Frost glass object slides (Thermo Fisher Scientific, Rockford, IL, USA) and dried at RT for 30 min. For initial histological investigations, some sections were incubated in 0.5 % methylene blue (w/v), washed with H_2O_{dest} and examined under the microscope to define the "area of interest". The sections to be used for immunofluorescence microscopy were fixed with incubation with -20°C cold acetone for 10 min, then dried at RT for 5 min, and then either used or stored frozen at -20°C. Before incubation with antibodies, the frozen sections were treated with Triton-X-100 (0.1 %; w/v) for 5 min (for immunofluorescence microscopy see chapter 3.3).

3.2.3 Preparation of paraffin-embedded tissue and microwave-assisted antigen-retrieval

Tissues or 3D cultures with entrapped VICs were cut into small pieces of ca. 0.5 cm side length and fixed in freshly prepared 4 % formaldehyde in PBS, pH 7.4 (w/v) for 24 h at 4°C. After passage through an increasing ethanol dehydration series, the dehydrated samples were embedded in low-melting paraffin. The paraffin-embedded specimens were pre-cooled at -20°C for 1-2 h and then cut into 3-4 µm thin sections. The sections were placed on Menzel Super Frost glass object slides and dried overnight at 40°C in a heating chamber. Then the sections were stored in a dark and dry place at RT until they were used for immunofluorescence microscopy.

After the fixation with formaldehyde and the embedding in paraffin, tissue structures are usually relatively well preserved but the accessibility of the antigenic molecules may be reduced. To overcome this problem, sections through paraffin-embedded tissues were treated by antigen-retrieval; a microwave-assisted method to reveal protein epitopes to the antibodies (Shi et al., 1991). Before microwave treatment, the sections were rehydrated in a decreasing ethanol series (2X xylene, 2X 100 %, 1X 90 %, 1X 80 %, 1X 70 % and 1X 50 % ethanol, each step for 5 min, following a washing step with H_2O_{dest}). Sections were then treated in a special microwave pressure cooking pot either at 115°C in a Tris-urea buffer at pH 11 for 10 min or at 98°C in a citrate buffer at pH 6 for 10 min in a microwave processor (for compositions of the buffers see Table 4). After treatment, the microwave pressure cooking pot was cooled for 12 min with cold water. Afterwards the sections were taken out of the pot and were washed in H_2O. Then the sections were incubated in 2 % milk powder (w/v) in PBS containing 0.2 % Triton-X-100 (w/v) for 20 min at RT (for the further immunofluorescence microscopy see

chapter 3.3). Sections through paraffin-embedded tissues were also used to perform hematoxylin-eosin (HE) and Masson-Goldner trichrome stainings (Masson, 1929; Goldner, 1938).

3.2.4 Preparations of ventricular endothelium

Sheets of endothelial cells were prepared from bovine ventricular endocardium of a heart freshly obtained from a local abattoir. Ventricles of the heart were opened and rinsed with PBS to remove erythrocytes from residual blood. The cell sheets were then scraped with a glass object slide and transferred to a fresh slide (Franke et al., 1979a, 1987b, 1988; Cowin et al., 1986). The sheets were shortly dried at RT, the puritiy was observed under the microscope and the sheets were fixed with methanol/acetone fixation (chapter 3.2.1.1). Immunofluorescence microscopy was performed as described in chapter 3.3.

3.3 Immunofluorescence microscopy

For immunofluorescence microscopy, the cells grown on coverslips or the tissue sections were fixed as described in chapter 3.2. After treatment with either Triton-X-100 or saponin, the sections or the cells grown on glass coverslips were washed three times in PBS at RT for 5 min and then incubated with the primary antibodies (Abs) in varying dilutions (supernatants were used undiluted, purified antibodies were diluted according to the manufacturer's recommendations) in a wet chamber for 1 h. After three washing steps with PBS at RT for 5 min, the samples were incubated with the secondary Ab (dilution 1:500) for 30 min, following an incubation step with DAPI (1:10,000) for another 5 min. For double-immunolabeling microscopy, the primary as well as the secondary Ab was used in double concentration.

Afterwards, the specimens were washed twice with PBS for 5 min and once with H_2O_{dest} for 1 min and fixed in 100 % ethanol for 5 min at RT. The coverslips or tissue sections were dried at RT for 5 min and then mounted with Fluoromount-G (Southern Biotechnology Associates, Birmingham, AL, USA) and cover glasses. The cells on the coverslips or the tissue sections were observed either with an Axiophot 2 (Zeiss) or with a confocal laser scanning microscope (LSM) 510 (Zeiss). Micrographs were obtained by an AxioCam MRc camera. Image processing was performed with the commercial programs LSM Image Browser Rel. 4.2, Axiovision LE. Rel. 4.4 and Adobe® Photoshop® CS3.

3.4 Electron microscopy

Buffers and chemicals used for electron microscopy are listed in Table 4.

3.4.1 Conventional transmission electron microscopy

For conventional transmission electron microscopy, cells grown on glass coverslips were washed twice with 37°C warm PBS and incubated in 2.5 % glutaraldehyde in sodium cacodylate buffer (v/v; Serva, Heidelberg, Germany) at 4°C for 10 min. Pieces of freshly obtained tissues or 3D cell cultures were dissected immediately into smaller pieces (ca. 1 x 1 mm side length) and incubated in 2.5 % glutaraldehyde in sodium cacodylate buffer (Table 4) at 4°C for 20 min (Sabatini et al., 1963; Fahimi and Drochmans, 1965; for review see Hayat, 1970). Both cells grown on glass coverslips or tissue pieces were then washed three times for 5 min with 4°C cold sodium cacodylate buffer (50 mM) and incubated in 2 % osmium tetroxide in sodium cacodylate buffer (v/v) for 2 h at 4°C in order to fix lipids, in particular membranes (for reviews see Hayat, 1970; Glauert, 1975). The specimens were then washed three times in H_2O_{dest} for 5 min and incubated overnight in 0.5 % uranylacetate in distilled water (w/v) at 4°C, followed by three washes each for 10 min (cells on glass coverslips) or 20-30 min (tissue pieces) in H_2O_{dest}, dehydration in an ethanol series (1X 50 %, 1X 60 %, 1X 70 %, 1X 80 %, 1X 90 %, 1X 95 %) on ice, finally twice each in 100 % ethanol, and by incubation in propylene oxide at RT.

After dehydration, cells on glass coverslips or tissue pieces were incubated overnight in a 1:1 (v/v) mixture of Epon 812 (Serva) and propylene oxide at RT. Tissue pieces were rotated to ensure penetration of the resin into the tissue. The propylene oxide was then allowed slowly to evaporate, ensuring complete penetration of both the cells on coverslips and the tissue pieces by the epoxy resin. The next day, the specimens were incubated with fresh Epon 812 for another 4-5 h and finally embedded in fresh Epon 812. Cells on glass coverslips were mounted with a gelatin capsule filled with Epon 812 and tissue pieces were embedded in silicone rubber molds (Plano, Wetzlar, Germany) filled with Epon 812.

The embedded tissue pieces and the cells grown on coverslips were incubated for 2 days in a heating chamber at 60°C which led to maximal hardening of the resin. The glass coverslips were removed (with a “crack”) from the gelatin capsules after freezing in liquid nitrogen for a few minutes. Then the tissues or cells embedded were cut with an ultramicrotome into ultrathin sections of ca. 60 nm, and the sections were placed on 100 mesh copper grids covered with a very thin film of 1 % pioloform in chloroform (w/v) to enhance the adhesion and the stability of the section.

Staining of ultrathin sections was performed by incubating the sections in 4°C cold 2 % uranylacetate in methanol (w/v) for 15 min, followed by three washing steps (1X in methanol, 2X in H_2O_{dest}, for 3 min each), incubation in lead citrate for 5 min (Table 4; Reynolds, 1963) and three washes in H_2O_{dest} for 3 min each. The sections were finally dried and observed with an EM 900 (Zeiss) at 80 kV. Pictures were taken on Kodak electron microscopy negative films (No. 4489; 3.25X4 inch; Sigma-Aldrich) and the negatives were developed (developer D19 Kodak and fixer Agefix Agfafoto 51) in a darkroom. The negatives were then scanned with an Epson scanner and processed further by Adobe® Photoshop® CS3.

3.4.2 Immunoelectron microscopy

For immunoelectron microscopy, the “pre-embedding” method was chosen, which means that the antibody reactions were performed before the specimens were embedded in the resin. To this end, cells grown on glass coverslips or sections of snap-frozen tissues or through 3D cultures were placed on glass coverslips and fixed in 2 % formaldehyde, freshly prepared from paraformaldehyde powder, in PBS pH 7.4 (w/v) at RT for 3-7 min, then shortly washed in PBS and immediately transferred into 50 mM NH_4Cl in PBS (w/v) twice for 5 min. After a short wash in PBS, followed by detergent treatment with 1 % saponin in PBS (w/v) for 3-5 min, cells grown on coverslips or tissue sections mounted on coverslips were washed twice in PBS for 5 min, and incubated with the primary Ab solution in a wet chamber for usually 1 h, using dilutions as in immunofluorescence microscopy.

After three 5 min washing steps in PBS, the coverslips were incubated with Nanogold-coupled secondary Abs specific for the species of the primary antibodies used (anti-mouse, or anti-rabbit or anti-guinea pig IgG, usually in a dilution of 1:50 [v/v]; Nanoprobes, Yaphank, NY, USA) for 3-4 h. The samples on coverslips were then washed in PBS twice for 5 min each and incubated in 2.5 % glutaraldehyde in sodium cacodylate buffer for 15 min at 4°C. The glutaraldehyde-containing solution was then gently washed away with sodium cacodylate buffer (50 mM), and the coverslips bearing the samples were incubated in a sucrose solution (13.6 g sucrose in 200 mL 50 mM HEPES buffer, pH 5.8) twice for 3 min each. This was followed by a silver-enhancement step (Nanoprobes, HG Silver™ Enhancement Kit) for which usually three different time points were chosen: 6 min, 7 min or 8 min.

Finally, the coverslips with the fixed material were directly incubated in a sodium thiosulfate pentahydrate solution (see Table 4) twice for 3 min each. After two washing

steps in H_2O_{dest} for 3 min each the coverslips bearing the samples were incubated in 0.2 % osmium tetroxide at 4°C for 30 min. The osmium tetroxide was then carefully washed away with H_2O_{dest} and the coverslips were dehydrated and embedded as already described for conventional ultrathin section electron microscopy (see chapter 3.4.1).

3.5 Protein gel electrophoresis

For the identification of proteins present in cultured cells or tissues, sodium dodecyl sulfate-polyacrylamide gel electrophoresis (SDS-PAGE) and immunoblot analysis using specific antibodies were performed.

3.5.1 Preparation of cell culture and tissue lysates for gel electrophoresis

Cultured cells in 6-well plates or in culture dishes (5 or 10 cm in diameter) were washed twice gently with 37°C warm PBS to remove dead cells, debris and residual medium. The cells were covered with 200-300 µL 2X Laemmli buffer (Laemmli, 1970) containing dithiothreitol (DTT) and SDS for cell lysis, to dissociate proteins and protein-complexes into polypeptides and to negatively charge the polypeptides present. 1 µL benzonase (Merck, Darmstadt, Germany) was added and incubated for 30 sec at RT under agitation to remove DNA and RNA. The cells were then collected with a cell scraper (Sarstedt, Nümbrecht, Germany), transferred into an Eppendorf reaction tube and heated at 95°C for 5 min under agitation to denature and SDS-couple the polypeptides. The samples were centrifuged at 13,000 rpm for 3 min at RT and the resulting supernatants were either used directly or stored frozen at -20°C.

Tissue lysates were obtained from ca. 10 µm thin sections of frozen tissues or areas dissected therefrom (Moll et al., 1982b; for freezing procedures and preparations of cryotome sections see chapter 3.2.2), collected in pre-cooled (-20°C) Eppendorf reaction tubes and supplemented with 200 µL 2X Laemmli buffer containing 1 µL benzonase. The suspensions were homogenized with a glass homogenizer, heated and centrifuged at 13,000 rpm for 3 min. The resulting supernatant was used directly or was stored frozen at -20°C.

3.5.2 SDS-PAGE

SDS-PAGE is based on the principle that glycopolypeptides or polypeptides modified otherwise can be separated according to their electrophoretic mobility in the SDS-coupled states in a reduced form. Therefore DTT is added as a reducting agent to destroy disulfide bridges. SDS solutions at elevated temperatures are used to break up the secondary and tertiary structures of the proteins by destroying hydrogen bonds and dissociate the resulting SDS-modified polypeptide-based chains. SDS-modification also charges the polypeptide-based chains negatively, so that the polypeptide chains migrate in the electric field in relation to their specific charge and mass.

15 µL of the supernatant of the sample were filled per slot of the gel (Tris-glycine 4-20 % gels; Anamed, Groß-Bieberau, Germany), and the gel was placed in a gel chamber filled with 1X electrophoresis running buffer (Table 4). As reference system for the molecular weight of the polypeptide-based chains, a marker set (broad range 2-212 kDa; New England Biolabs, Ipswich, MA, USA) with 13 polypeptides of known molecular weight and SDS-gelelectrophoretic mobility was used (Table 6).

Table 6 Components, sources and molecular weights of the polypeptide markers

Polypeptides	Source	Calculated MW[1] in kDa
Myosin, heavy chain	rabbit muscle	212
MBP2[2]-β-galactosidase	*E.coli*	158
β-galactosidase	*E.coli*	116
Phosphorylase b	rabbit muscle	97.2
Serum albumin[3]	**bovine**	**66.4**
Glutamic dehydrogenase	bovine liver	55.6
MBP2	*E.coli*	42.7
Thioredoxin reductase	*E.coli*	34.6
Triosephosphate isomerase[3]	***E.coli***	**27**
Trypsin inhibitor	soybean	20
Lysozyme	chicken egg white	14.3
Aprotinin	bovine lung	6.5
Insulin A	bovine pancreas	3.4

[1]MW=molecular weight, [2]MBP=maltose-binding-protein, [3]serum albumin and triosephosphate isomerase are at double intensity to serve as reference points

3.5.3 Transfer of polypeptides onto a membrane

The polypeptides separated on SDS-PAGE (see chapter 3.5.2) were transferred from the gel onto a polyvinyliden fluoride membrane (PVDF; Immobilon-P, Millipore) using a special semi-dry transfer technique (Kyhse-Andersen, 1984). To this end, a PVDF-membrane sheet was rinsed in isopropanol and equilibrated in transfer buffer 2 (25 mM Tris, 20 % isopropanol, pH 10.4). The gel was equilibrated in buffer 3 (40 mM norleucine, 24 mM Tris, pH 9.4). Whatman® 3MM-Paper sheets (Sigma-Aldrich) were equilibrated in transfer buffer 1 (300 mM Tris, 20 % isopropanol, pH 10.4), in transfer buffers 2 and 3, respectively, and arranged with the gel and the PVDF-membrane in the following order in the blotting chamber (see scheme below). The semi-dry blot was run for 1.5 h at 130 mA.

cathode
3 Whatman-Paper in transfer buffer 3
SDS-gel in transfer buffer 3
PVDF-membrane in transfer buffer 2
2 Whatman-Paper in transfer buffer 2
3 Whatman-Paper in transfer buffer 1
anode

Then the membrane with the separated polypeptide-containing bands was stained for 1 min in Coomassie brilliant blue staining solution (Table 4) to visualize the polypeptide bands. Background staining was reduced by washes in destaining buffer (Table 4). The membranes were then dried, marker bands marked with a “permanent pen”, and the membranes were scanned and documented.

3.5.4 Antigen detection by immunoblotting reaction

The detection of the polypeptides bound to the PVDF-membrane was usually performed using an indirect enzyme-immuno-assay. To block non-specific binding reactions, the PVDF-membranes were rinsed in isopropanol and incubated for 30 min at RT in a “blocking solution” with 5 % milk powder in PBS containing 0.05 % Tween®20 (Sigma). For the immunodetection (“Western blot”) of the bound proteins, primary antibodies were diluted in this blocking solution according to the manufacturer’s recommendations. In general, purified antibodies were diluted 1:1000 and hybridoma cell

culture supernatants 1:5 or 1:10. The membranes were incubated with the Ab solutions on a shaker at RT for 1 ½ h. Afterwards, the membranes were washed in PBS containing 0.05 % Tween®20 for 10 min and then twice with the blocking solution for 10 min each to remove residual primary antibodies.

The membranes were then incubated with the secondary Abs on a shaker at RT for 1 h. The secondary Abs (mostly in a dilution of 1:5,000 in blocking solution) used for immunoblots were species-specific Abs coupled to HRP. Thereafter, the membranes were washed three times in PBS at RT for 5 min to remove residual secondary Abs and to diminish background reactions. The antibody-HRP complexes were then visualized by a chemiluminescent immunoblotting substrate containing luminol (ECL; Thermo Fisher Scientific). The ECL-reaction leads to the emission of low intensity light at 428 nm which was detected on a medical film (18X24 cm; Konika-Minolta, Langenhagen). The films were scanned and images processed further by Adobe® Photoshop® CS3.

3.6 Immunoprecipitations

To identify potential binding partners and protein complexes of specific polypeptides, immunoprecipitations (IPs) were performed with lysates of cultured pulmonary VICs of ovine and bovine origin. For this purpose, twelve cell culture dishes (10 cm in diameter) with VICs grown to confluency were washed gently twice with 4°C cold PBS and the cells were immediately lysed with 6 mL RIPA buffer (Table 4) containing a protease inhibitor cocktail (Complete Mini Inhibitor Tabs; Roche Diagnostics, Mannheim, Germany) and 2 µL benzonase (Merck). The cell lysate was homogenized using a Dounce glass homogenizer and incubated at 4°C for 1 h.

In the meanwhile, 50 µL of magnetic “Dynabeads” (“pan-mouse Dynabeads” coated with human anti-mouse IgG mAb; Dynal, Hamburg, Germany) were washed three times with 4°C cold RIPA buffer in an Eppendorf reaction tube. The buffer was replaced by 1 mL of the cell lysate and incubated on a rotator at 4°C for 3 h.

In parallel, in a second reaction tube 50 µL magnetic beads were washed three times with 1 mL 4°C cold 50 mM Tris-HCl buffer at pH 7.5. The buffer was replaced by 1 mL of the specific Ab (mouse mAbs were diluted 1:100 and hybridoma cell culture supernatants 1:5 or 1:10 in 50 mM Tris-HCl buffer) and incubated on a rotator at 4°C for 3 h. The remaining Ab-containing solution was aspirated and the beads were washed five times with RIPA buffer for 1 min. Then, the “bead-treated” cell lysate was incubated with the antibody-coupled beads and incubated on a rotator at 4°C over night. The resulting

supernatant was then aspirated and the beads were again washed five times with RIPA buffer for 1 min each. After a very short centrifugation step, the residual buffer was removed and the beads were treated with 100 µL 2X Laemmli buffer and incubated at 95°C for 3 min. Subsequently SDS-PAGE and immunoblotting of the polypeptides bound to the antibody-beads was performed.

To show the presence of the essential proteins studied, an aliquot of the original cell lysate obtained before the IP was used. Moreover, lysates of tissue material obtained from dissected ventricle tissues as well as corresponding control lysates of cultured pulmonary VICs were used in parallel. To control for unspecific binding of proteins present in the initial cell lysate to the beads, aliquots of bead suspension before IP ("pre-clear", negative control) and of "control" mAbs (desmocollin 1 and 3 and VE-cadherin) against unrelated proteins were used.

3.7 Polymerase chain reaction

3.7.1 Preparation of total RNA from heart valve tissue and cultured valvular interstitial cells

For the preparation of total RNA from heart valve tissue or cultured VICs of bovine origin, the commercial Rneasy Mini Kit from Qiagen (Hilden, Germany) was used. Cells grown in culture or sections of frozen tissue were used. Scraped cells or tissue sections were dispensed in 600 µL "RLT" buffer with guanidine thiocyanate (containing 10 µL/mL β-mercaptoethanol). The resulting lysates were transferred in 2 mL "QIAshredder" columns and centrifuged at RT at 13,000 rpm for 2 min to separate the DNA from the RNA. The eluate was mixed with 600 µL 70 % ethanol and homogenized. This solution was then transferred to an "Rneasy mini" column and centrifuged again at RT at 13,000 rpm for 2 min. The flow-through was discarded and the column was washed with 700 µL "RW1" buffer with ethanol. To remove residual buffer, the column was shortly centrifuged and again washed twice with 500 µL "RPE". Afterwards, the column was centrifuged for 2 min at RT at 13,000 rpm to remove the buffer from the column. The RNA was then eluted into a fresh Eppendorf reaction tube with 30-50 µL Rnase-free water. The column was centrifuged another minute at RT at 13,000 rpm to elute the bound RNA. The RNA was then used directly for cDNA synthesis or stored at -80°C.

3.7.2 cDNA synthesis

Using the reverse transcriptase reaction (according to Frohman et al., 1988) and random hexamer oligonucleotide primers, mRNA was transcribed into cDNA for the further analysis by polymerase chain reaction (PCR). 10 µg of the isolated mRNA were denatured in 12 µL Rnase-free water at 65°C for 3 min, and 2 µL 10X reverse transcription buffer (RT buffer, Table 4), 0.74 µg "random primer" (Roche Diagnostics), 10 units AMV transcriptase and 20 units Rnase inhibitor (Roche Diagnostics) were added for incubation at 42°C for 1 h, followed by an incubation step at 52°C for 30 min.

3.7.3 Polymerase chain reaction

The PCR was used to amplify specific DNA fragments. To this end, specific oligodesoxyribonucleotides (primers) were synthesized so that one primer was complementary to the coding sequence (*forward*) and the other primer was complementary to the non-coding sequence (*reverse*) of the DNA sequence of the gene of interest. To allow the binding of the primers to the double-stranded DNA sequence, the DNA was denatured by heat. The Taq (*Thermus aquaticus*)-polymerase (1 units/µL; Fermentas, St. Leon-Rot, Germany) was used to synthesize the specific complementary strand in a thermocycler.

For an experimental volume of 50 µL, the composition of the reaction solution was as follows:

2 µL cDNA,
35 µL $H_2O_{dest,}$
5 µL dNTPs (10 mM),
5 µL 10X PCR buffer,
1 µL *forward* primer (10 pmol/µL),
1 µL *reverse* primer (10 pmol/µL),
1 µL Taq-polymerase

The thermocycler was programmed according to the following protocol:

95°C	2 min	
95°C	30 sec	30 cycles
58°C	30 sec	
72°C	45 sec	
72°C	10 min	

Depending on the specific sizes of the amplified fragments and on the compatibility of the primer pairs, respectively, the protocol was optimized with variations both in temperature and duration.

Primers used (5'-3')

α-E-catenin *forward*: TTT CTC AAG GAG GAG CTT GTG
reverse: TGC CTG GGA TGC AGT ATA GA

α-N-catenin *forward:* ATG ACT TCG GCA ACT TCA CC
reverse: CTC ATG ACA TCT GCC ATG TC

α-T-catenin *forward:* GAA AAG ATT GCT GAG CAA GT
reverse: GAC ATT TTC ACT GTT TGC ACT A

GAPDH *forward:* CCA TCA CCA TCT TCC AGG AG
reverse: ATC CAC AGT CTT CTG GGT GG

3.7.4 Agarose gel electrophoresis

To analyze the PCR fragments obtained, the DNA was separated by electrophoresis on an agarose gel. Here the mobility of double-stranded DNA is reciprocally proportional to the logarithm of the numbers of base pairs, so that the DNA fragments can be separated in an electrical field according to their sizes. Ethidium bromide is able to intercalate in guanine-cytosine-base pairs and is therefore used for the visualization of the DNA fragments in the agarose gel under ultraviolet light.

Depending on the sizes of the DNA fragments, the proportion of agarose in the gels differed between 0.8 % (w/v) and 1.5 % (w/v). The agarose was dissolved in 1X TAE buffer (Table 4) and boiled. After cooling down to 50-60°C, the agarose/TAE solution was mixed with 0.75 µg/µL ethidium bromide and filled into a gel chamber with a separating ridge. The DNA samples were then mixed with loading buffer (1/6 of the total volume; 0.25 % bromphenol blue, 0.25 % xylene cyanol, 15 % ficoll) and filled into the gel pockets. One of the pockets was filled with a DNA-size reference (Bluescribe vector digested by Hinf I; Roche Diagnostics). Depending on the length of the gel, the voltage used differed between 80-120 V. The DNA bands obtained were documented under ultraviolet light (E-Box, 1000/20M; Peqlab, Erlangen, Germany) using a wavelength of 312 nm.

4 Results

4.1 *Coniunctiones adhaerentes* – Plakophilin-2-containing adherens junctions, a novel type of cell-cell connections in the heart valve

According to current textbooks, there are three – and only three – types of plaque-asscociated cell-cell junctions (Farquhar and Palade, 1963; Campbell and Campbell, 1971; Staehelin, 1974): (1) The desmosomes (*maculae adhaerentes*; for recent reviews see Green and Simpson, 2007; Holthöfer et al., 2007; Desai et al., 2009), (2) adherens junctions (AJs; *zonulae adhaerentes, fasciae adhaerentes and puncta adhaerentia*; for recent reviews see Perez-Moreno et al., 2003; Ebnet, 2008; Harris and Tepass, 2010), and (3) tight junctions (TJs; *zonulae occludentes*; for recent reviews see Matter and Balda, 2003; Niessen, 2007; Ebnet, 2008). Since the mid-1990s, however, it has become clear that there are further types of related junctions which morphologically and with respect to their molecular composition cannot easily be subsumed under the hitherto known junction categories. Such novel types of junctions include extreme forms connecting mesenchymal cells such as the minimal dot junctions (*puncta adhaerentia minima*; see Wuchter et al., 2007) as well as the variously-sized, often gigantic forms of “taproot” AJs (*manubria adhaerentia*; Wuchter et al., 2007), the *cortex adhaerens* structures connecting vertebrate eye lens fiber cells (Straub et al., 2003), the so-called “sandwich junctions” described in various stratified squamous epithelia and carcinomas derived therefrom, as well as in the Hassall bodies of the thymus *(iuncturae structae*; Langbein et al., 2002, 2003), the *puncta occludentia* (Schlüter et al., 2007) and the complex junctions connecting the special endothelial cells of the lymphatic vessel system (*complexus adhaerentes*; Schmelz et al., 1990, 1994; Schmelz and Franke, 1993; Hämmerling et al., 2006; Moll et al., 2009; see there for further references).

The composite junctions (*areae compositae*) have gained special importance for the evolution and the ontogenic development of the mammalian heart. These mostly extended adhering junction structures occupy most of the intercalated disk (ID) regions connecting cardiomyocytes, and their formation is only postnatally completed (Borrmann, 2002; Borrmann et al., 2006; Franke et al., 2006; Pieperhoff and Franke, 2007). Here, the findings that mutations in some of the desmosomal proteins amalgamated in these composite junctions can lead to hereditary arrhythmogenic right ventricular cardiomyopathy/dysplasie (ARVC/D), often resulting in the so-called “sudden death” of

otherwise healthy human beings, has greatly stimulated a special field of clinical, epidemiological and cardiological research (for references see, e.g., Bazzi and Christiano, 2007; Marcus et al., 2007; Awad et al., 2008; Corrado et al., 2009; Herren et al., 2009; Saffitz, 2009; Pieperhoff et al., 2010; Sen-Chowdhry et al., 2010).

4.1.1 The adhering junctions of valvular interstitial cells in the adult heart valve *in situ*

The cell-cell junction proteins of valvular interstitial cells (VICs) *in situ* and in cell culture have been studied by immunocytochemical and biochemical methods.

4.1.1.1 Histological appearance of the adult mammalian heart valve

The heart valve interior consists of large amounts of extracellular matrix (ECM), including collagen and elastin fibers in various degrees of thickness and in spatial patterns often related to VIC processes. In initial immunofluorescence microscopical studies I have noted that the adhering junctions connecting the interstitial cells of the heart, notably those of the valves, *grosso modo* appear to be of a basic AJ-type but also show certain specialties. On the other hand, at that time the group of Latif and coworkers had just reported that the junctions connecting these VICs would contain desmosomal “marker” molecules such as desmoglein (Latif et al., 2005, 2006). Therefore, and because of the importance of VICs and their connections and interactions in the ECM in *in vitro* constructs as well as *in situ*, I have decided to study the VIC structures and their molecular junction complement in detail.

The hematoxylin-eosin staining (Figure 7a; nuclei are stained dark blue and the cytoplasm is stained purple) showed that the VICs were dispersed loosely throughout the heart valve matrix. The amounts and the distribution pattern of the collagen fibrils, stained in red, differ in relation to the compartmentalization of the heart valve into three different layers: The *ventricularis*, the *spongiosa* and the *fibrosa*. The *ventricularis* (Figure 7a, right hand side of the heart valve section) shows a semi-dense packing of collagen fibril bundles, whereas the *spongiosa* – seen in the central portion – is characterized by a rather loose (“spongy”) distribution of collagen. By contrast again the *fibrosa* consists of rather densely packed collagen fibrils (Figure 7a, left hand side of the heart valve). The trichrome staining of the cross-section through an ovine heart valve shows that the heart valve matrix extends over the adjacent myocardium with relatively thin protrusions into the

myocardial region (Figure 7b; muscle tissue is stained red, nuclei deep-blue, cytoplasm light red and the collagen fibril bundles green).

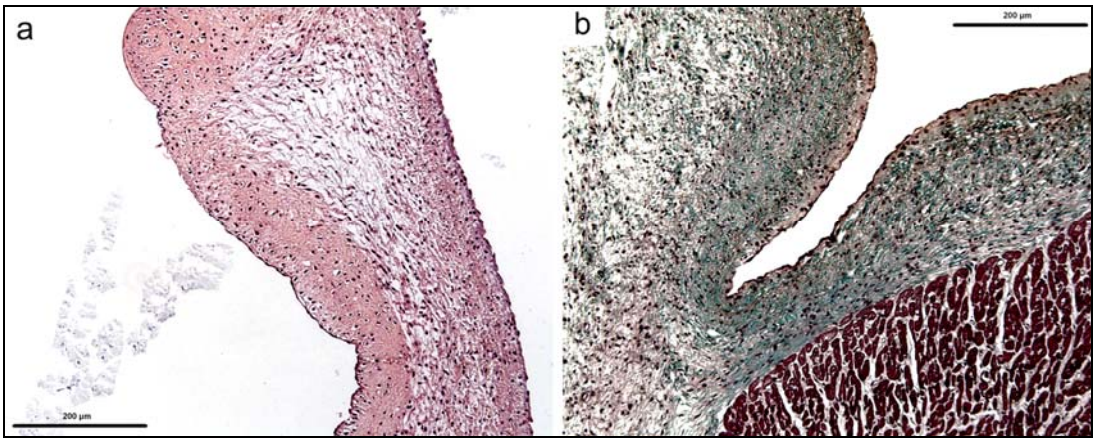

Figure 7 Cross-sections through formaldehyde-fixed, paraffin-embedded ovine heart valves. (**a**) Hematoxylin-eosin staining of an ovine aortic heart valve. (**b**) Trichrome staining according to Masson-Goldner of an ovine aortic heart valve with adjacent myocardium (lower right). Bars: 200 µm

4.1.1.2 The extracellular matrix components of the heart valve

In all species studied, elastin fibers are prominent components of the valvular ECM of the heart valve. Most of them are located at the *ventricularis* but decent amounts can be also found in central regions of the *spongiosa* and close to the collagen-rich area as of the *fibrosa* (Figure 8a). Obviously, collagen fibril bundles make up the major part of the ECM and occur in various molecular types. The most abundant collagen type I, often appears to be restricted to the *fibrosa* (Figure 8b), but in some places can also extend and protrude into the *spongiosa* (Figure 8c) or extend throughout the whole leaflet up to the tip of the heart valve (Figure 8d). Fibrils containing collagen type VI, in contrast, are abundant in the *ventricularis* (Figure 9a), sometimes with a few protrusions towards the middle part of the valve and into the *spongiosa* (Figure 9b). Similar to the distribution of collagen type I, collagen type VI is also located all over the valvular cusp up to the most distal regions of the valve (Figure 9c). Finally, collagen type VII is not restricted to a special layer and occurs rather ubiquitously in the valve (Figure 9d).

The non-collagenous ECM protein osteopontin, mainly described to occur in calcified valves (e.g., Mohler et al., 1999; Canver et al., 2000), as well as periostin, reported to be involved in the development of heart valves (Norris et al., 2008; Snider et al., 2008; for

review see Markwald et al., 2010), essentially have been absent in all the heart valves studied, independent from the species or the age of the donor.

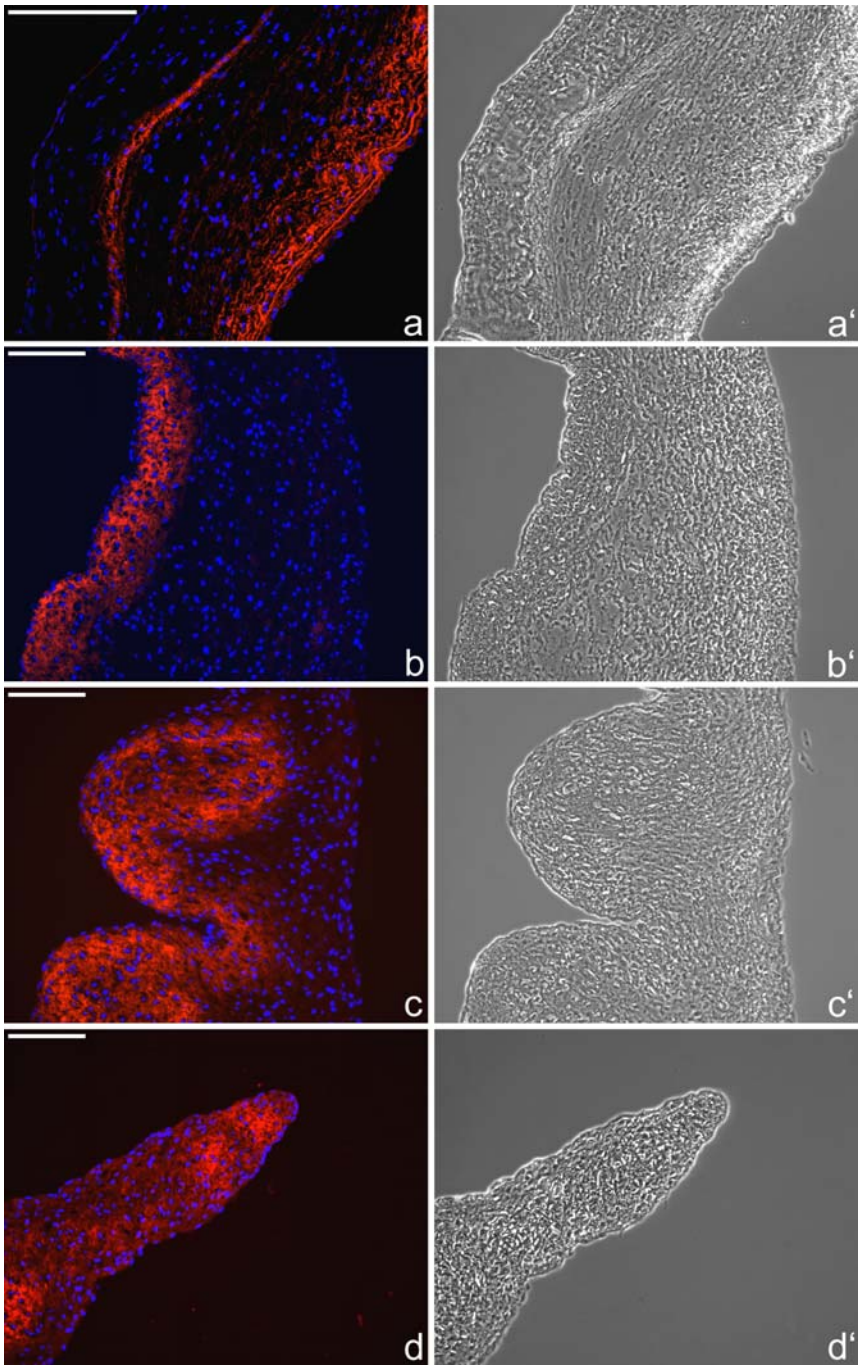

Figure 8: Immunofluorescence micrographs showing the distribution of elastin and collagen type I in sections through frozen human (**a**) and ovine (**b-d**) pulmonary heart valves. (**a**) Elastin is located mainly in the *ventricularis* (right hand side) and to a lesser degree also in the *spongiosa* (middle part of the valve). (**b-d**) Distribution of collagen type I in an ovine heart valve where it mainly occurs in the *fibrosa* (**b**, left hand side of the valve) but can also protrude into the *spongiosa* (**c**) or even is located throughout the cusp (**d**). Nuclei are stained blue (DAPI). Bars: 100 µm

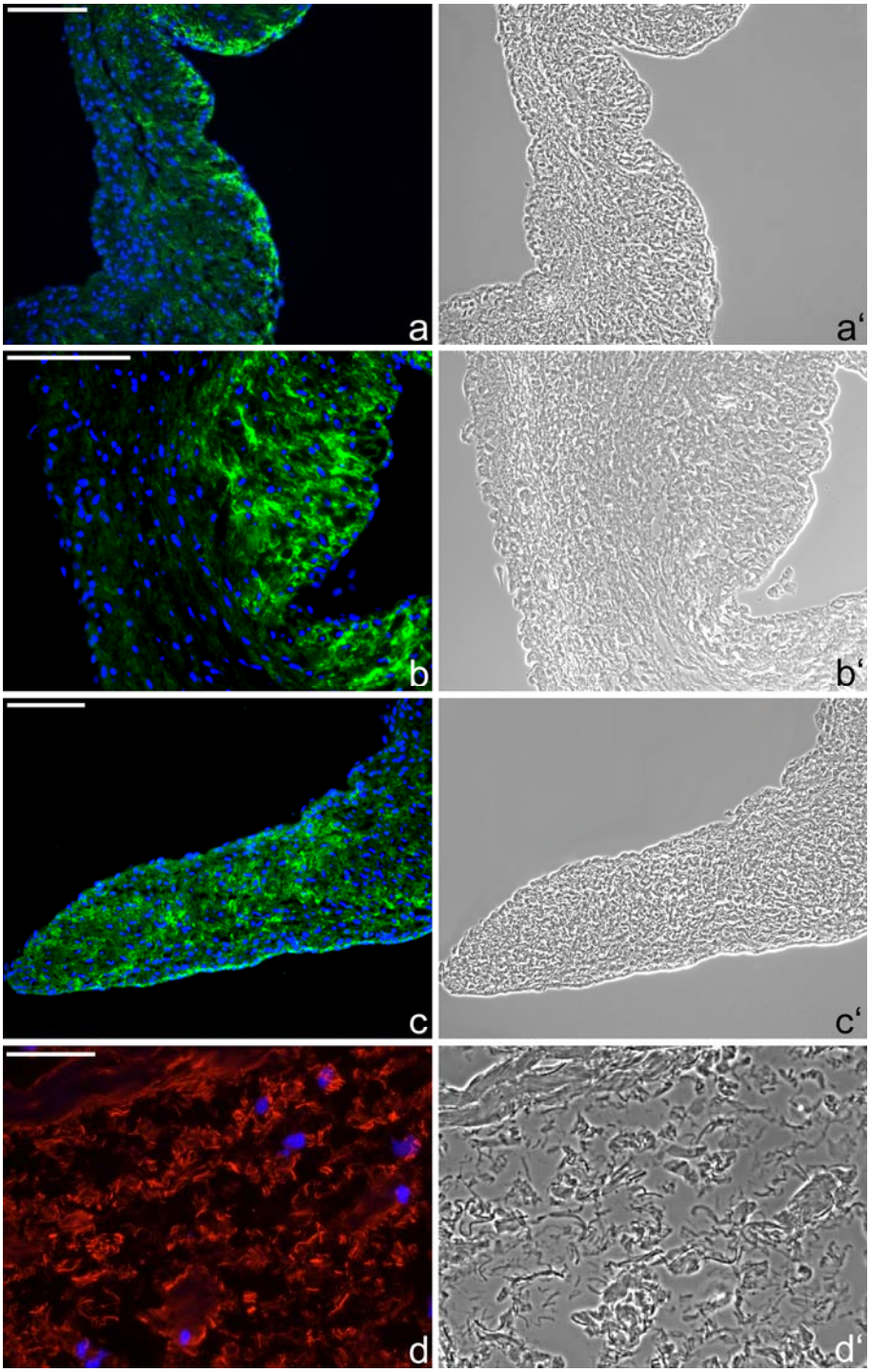

Figure 9: Immunofluorescence micrographs showing the distribution of collagens of type VI and type VII in ovine and bovine pulmonary heart valves. (**a-b**) Collagen type VI is mainly located in the *ventricularis* (**a** and **b**, right hand side) but is also abundant in the distal parts of the valve, as shown here for an ovine heart valve (**c**). (**d**) Collagen type VII is not restricted to a special layer as can be seen here in a bovine heart valve. Nuclei are stained blue. Bars: 100 µm (a-c), 50 µm (d)

4.1.1.3 The endothelial cells of the heart valves

As the inner surface of the heart is exposed to the blood flow, it is – like any other blood vessel in the body – covered with a continuous endothelial cell layer as the adluminal component of the endocardium (for a definition of the term “endocardium” in this thesis see page 115). Consequently, the heart valve leaflets are also lined with endothelial cells of the endocardium, together with some subjacent mesenchymal tissue cells, i.e. in essence a situation as in all other cardiac vascular elements.

4.1.1.3.1 The endothelial cell layer of the endocardium covering the heart valves

Immunofluorescence microscopy of the endothelial cell sheets covering the endocardium (for detailed preparation protocols see chapter 3.2.4) shows positive reactions for the endothelial cell-specific junctional marker protein VE-cadherin (Figure 10). Often the transmembrane AJ protein cadherin-11 is also recognized at these cell-cell junctions (Figure 11a) whereas reactions for N-cadherin are always indistinct and may in some places be interpreted as rather negative (Figure 12a). P-cadherin is always negative in endocardial cells (not shown). Specific antibodies against α-catenin (Figure 11c) and the *armadillo* proteins plakoglobin (Figure 11b and 12b), β-catenin (Figure 11d) as well as protein p120 (Figue 12c) all have shown positive reactions. Desmosomal proteins like the glycoproteins desmoglein and desmocollin as well as the plaque proteins desmoplakin and plakophilin-2 are totally negative (not shown). The occurrence of the novel, *area composita*-associated plaque junction protein myozap (Seeger et al., 2010) is inconsistent and often interrupted at cell-cell contacts of the endothelial cell layer. For an overview of proteins involved in the AJs of adult endothelial cells of the endocardium see Table 8.

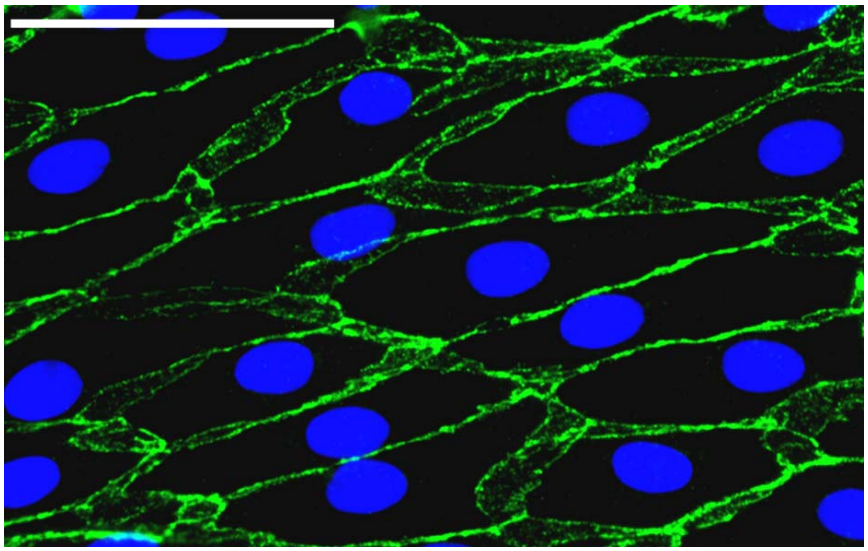

Figure 10: Immunofluorescence micrograph of endothelial cell sheets scraped off from bovine ventricular endocardium (see chapter 3.2.4). The cell-cell junctions connecting the endothelial cells show positive staining for the endothelial cell-specific protein marker VE-cadherin (green). Nuclei are stained blue. Bar: 50 µm

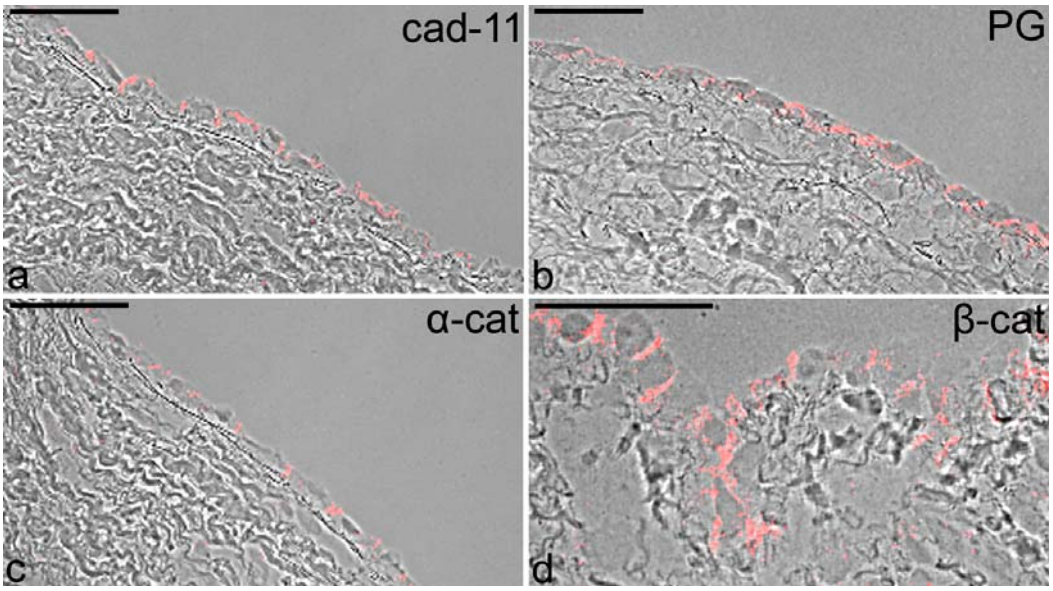

Figure 11: Immunofluorescence micrographs showing the endothelial cell layer covering the heart valve endocardium. Cross-sections through formaldehyde-fixed, paraffin-embedded bovine pulmonary heart valves treated with monoclonal antibodies show positive reactions (red) for the typical AJ proteins plakoglobin (**a**), α-catenin (**b**), cadherin-11 (**c**) and β-catenin (**d**). The background is in phase contrast optics. Bars: 50 µm

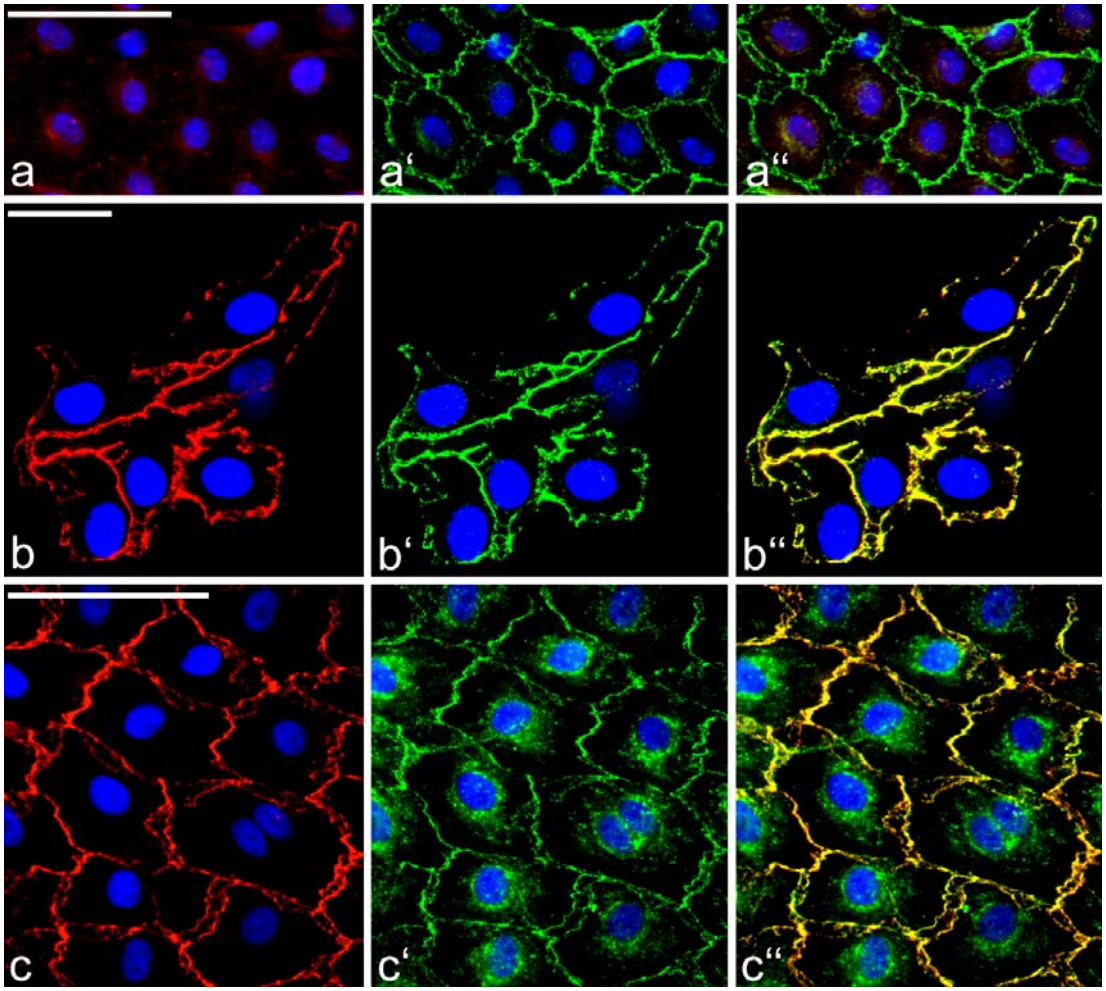

Figure 12: Double-label immunofluorescence micrographs of endothelial cell sheets scraped off from bovine ventricular endocardium (see chapter 3.2.4). (**a**) Double-staining of N-cadherin (red) and VE-cadherin (green) here shows the absence of N-cadherin in endocardial cells of the heart. (**b**) Colocalization (yellow) of plakoglobin (red) and VE-cadherin (green). (**c**) Colocalization (yellow) of protein p120 (red) and VE-cadherin (green). Nuclei are stained blue. Bars: 50 µm (a, c), 20 µm (b)

4.1.1.3.2 The endothelial cells of the vascular structures of the heart valve

Depending on the specific thickness of a valvular leaflet, relatively prominent vascular structures are found at the basis of the valvular cusp. Cross-sections through cryopreserved heart valve tissues of bovine origin reveal the occurrence of an organized vascular system, in particular in immunofluorescence microscopy, using smooth muscle-specific markers such as antibodies against smooth muscle α-actin (Figure 13a) or desmin (Figure 13b).

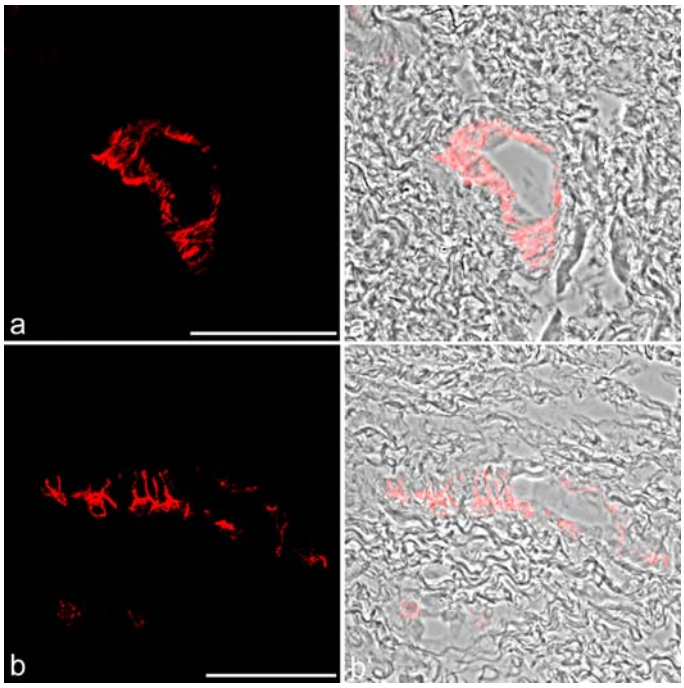

Figure 13: Immunofluorescence micrographs of cross-sections through frozen bovine mitral valves, showing the presence of vascular structures. Vascular lumen-lining cells are labeled (red) with a specific antibody against smooth muscle α-actin (**a**) and desmin (**b**). For combinations with corresponding phase contrast images see **a'** and **b'**. Bars: 50 µm

The cell-cell contacts of the endothelia of vascular structures in heart valves are primarily formed by VE-cadherin. The transmembrane AJ glycoprotein, cadherin-11, also shows a positive reaction whereas the reactions for N-cadherin are rather inconsistent (not shown). Moreover, these AJ cell-cell contacts are positive for the plaque protein α-catenin (Figure 14a) as well as for the *armadillo* proteins β-catenin (Figure 14b), protein p120 (Figure 14c), plakoglobin (Figure 14d) and protein p0071 (not shown; see however, the reactions in other vascular structures as published by Hofmann et al., 2008).

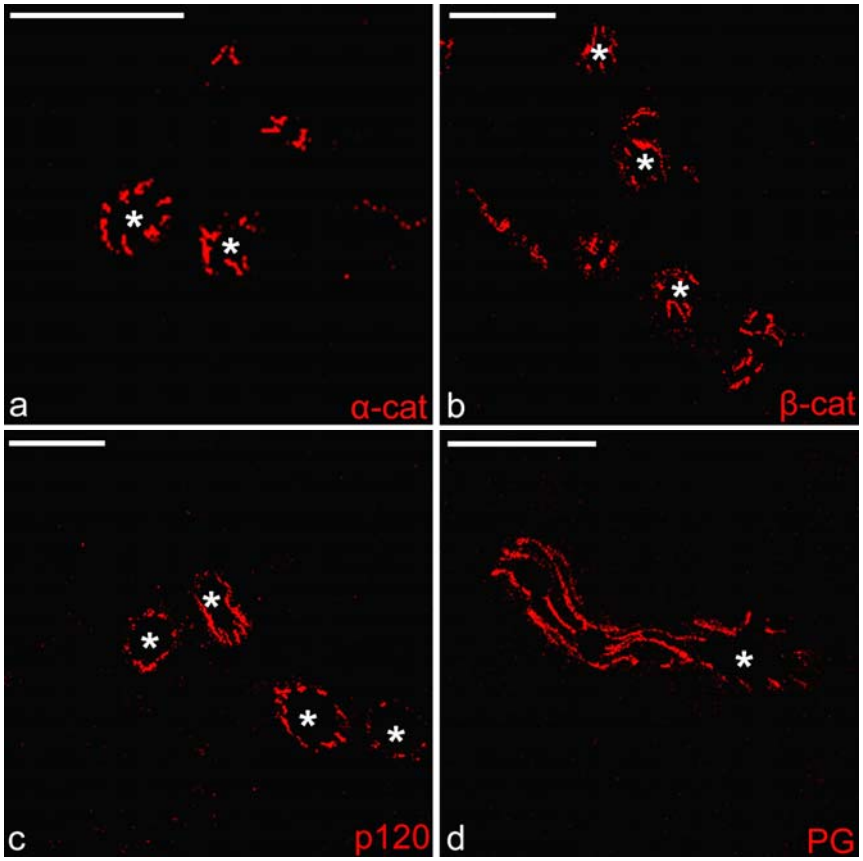

Figure 14: Immunofluorescence micrographs of cryostat sections through a frozen bovine mitral heart valve, showing the localization of AJ proteins at the cell-cell contacts of endothelial cells of vascular structures in the valve interior. Positive reactions with specific antibodies against α- and β-catenin (**a**, **b**), protein p120 (**c**) and plakoglobin (**d**) show the typical endothelial appearance (vascular lumina are denoted by asterisks). Bars: 50 µm

4.1.1.4 The appearance of valvular interstitial cells of heart valves and their extracellular environment in the electron microscope

VICs represent the most abundant cell type of the heart valve. They are loosely distributed throughout the heart valve interior as already shown by hematoxylin-eosin staining (Figure 7). This dispersed arrangement seems to be due to the large amounts of accompanying ECM material such as collagen fiber bundles which thus separate the VICs from each other. Remarkably, although the VICs appear tight-packed by collagen fibrils they tend to form long and thin cellular processes (Figure 15). Many of these often ramified, variously long, filopodia-like cell processes are closely associated with the aforementioned collagen fiber bundles, thus forming a three-dimensional (3D) meshwork that is quite characteristic for the organization of heart valve tissue in general, independent from the specific type of heart valve. Processes of VICs are not only separating the collagen fiber bundles, resulting in a phenomenon best described as a segmental

compartmentalization (for a survey see Figure 16a and, for higher magnification, Figure 16b), but also show a partial or even total engulfment of collagen bundles (see Figures 15 and 16).

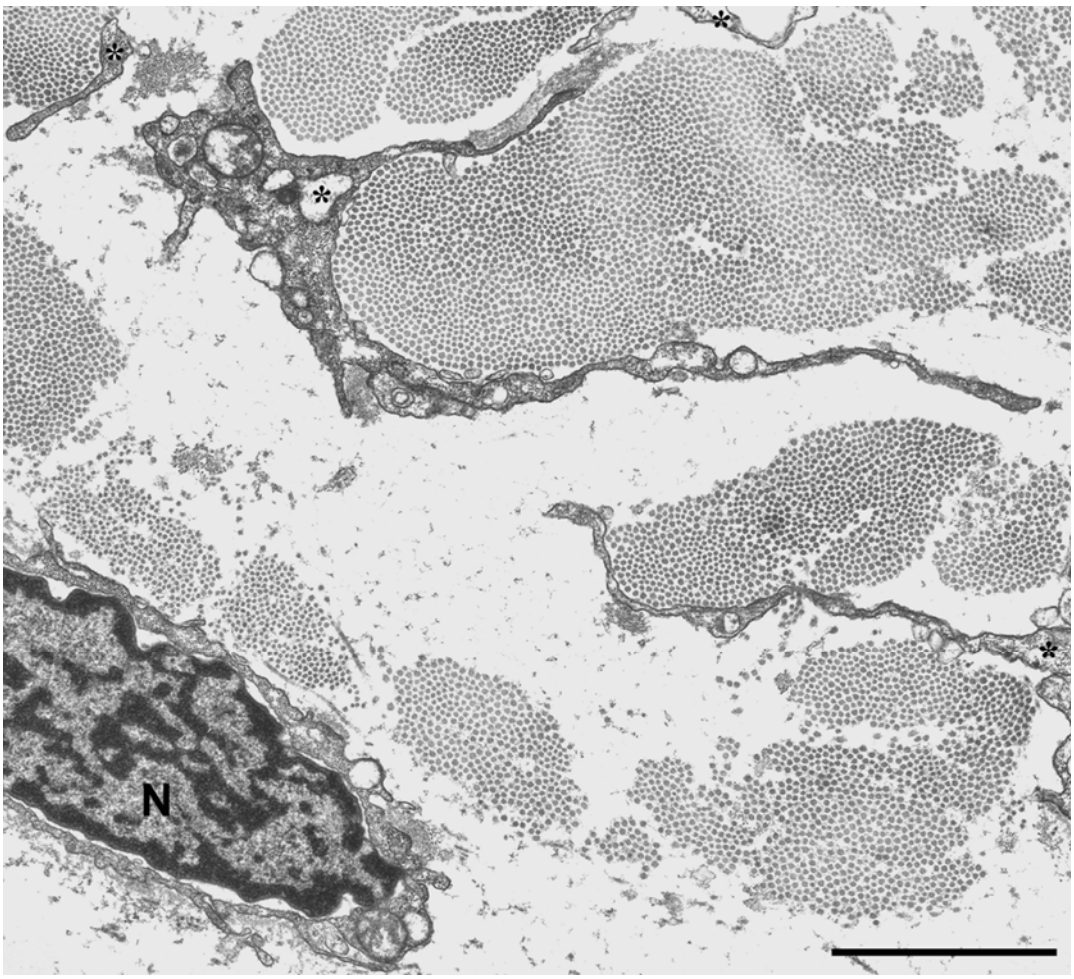

Figure 15: Electron micrograph of an ultrathin section through a human aortic heart valve. Note the cell processes of several VICs (indicated by asterisks; N, nucleus) and the close and somewhat regular association of such processes with collagen fiber bundles. Bar: 2 µm

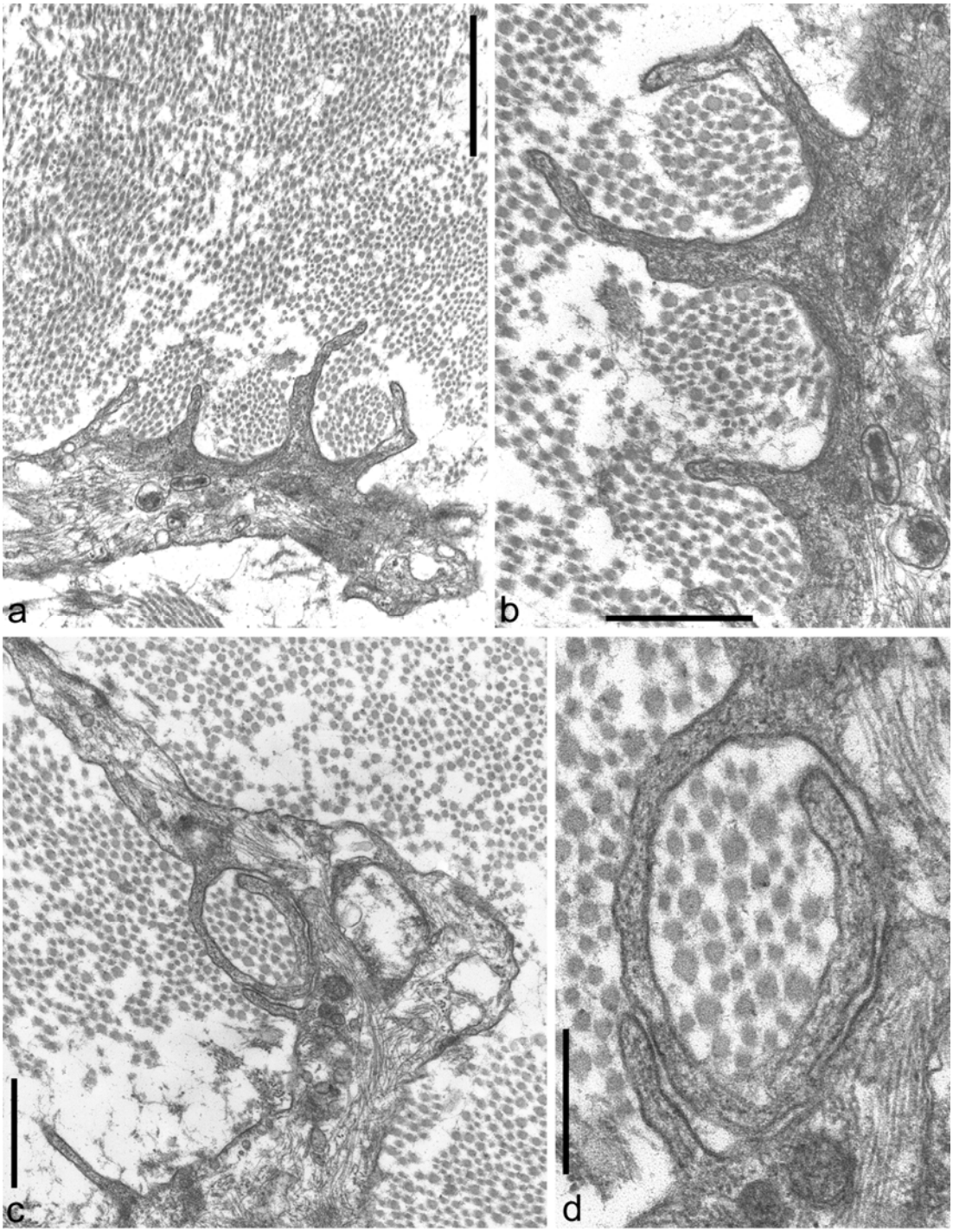

Figure 16: Electron micrographs of ultrathin sections through a bovine tricuspid heart valve, showing several processes of VICs. Such cell processes are often closely associated with collagen fiber bundles which they often separate from each other in almost periodic arrangements (**a**, **b**). Note also the total engulfment of collagen fiber bundles by such cell processes (**c;** for higher magnification see **d**). Bars: 1 µm (a), 0.5 µm (b, c), 0.25 µm (d)

4.1.1.5 The intermediate-sized filaments of valvular interstitial cells

Given that VICs and the endothelial cells surrounding the valve interior are mesenchymally derived cells, they can be visualized and identified by specific antibodies against the intermediate-sized filament (IF) protein vimentin (Franke et al., 1978, 1979a, b; Herrmann et al., 2007), as shown for bovine heart valve tissue in Figure 17. Besides this main cell type, another cell type can be found in the valve interior, which is characterized by additional smooth muscle α-actin-positive microfilament bundles (e.g., Bairati and DeBiasi, 1981) which often occur close to the valve surface, just beneath the endothelial cell layer (Figure 17a and b). The frequency and distribution patterns of these smooth muscle α-actin-positive cells show marked regional variations.

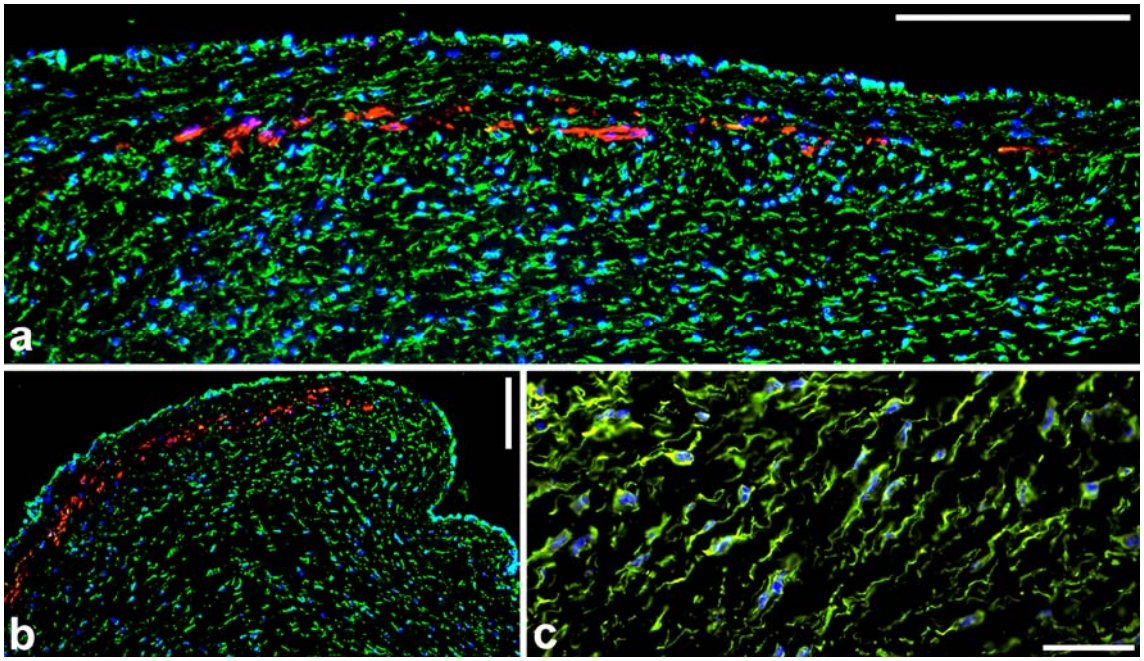

Figure 17: Immunofluorescence micrographs of cross-sections through formaldehyde-fixed, paraffin-embedded bovine aortic heart valves. Note the loose and widespread distribution of vimentin-positive VICs in the endocardial lining and in the heart valve interior (green; **a**-**c**) as well as the scattered clusters of smooth muscle α-actin-positive cells near the valve margin (red; **a** and **b**). Nuclei are stained blue. Bars: 100 µm (a), 50 µm (b and c)

4.1.1.6 The cell-cell contacts of valvular interstitial cells in situ

Independent from the species and from the specific valve type, all heart valves examined have shown the complete set of typical mesenchymal AJ proteins, although in arying proportions. VICs are negative for the endothelial cell marker VE-cadherin as well as for the epithelial cell markers E-cadherin and P-cadherin. As to the transmembrane AJ glycoproteins, the occurrence of N-cadherin in heart valve cell-cell contacts (Latif et al., 2006) has been confirmed (Figure 18a). In contrast to previously published work reporting the absence of cadherin-11, this cadherin has now been confirmed as a general VIC-AJ component (see Figure 18b for immunofluorescence microscopy and Figure 19b for colocalization with N-cadherin). Also in contrast to observations of others (Latif et al., 2005, 2006), the desmosomal transmembrane glycoproteins, desmoglein-1-3 are totally absent. Similarly, other typical desmosomal proteins like the plaque proteins plakophilin-1-3 and desmoplakin as well as the transmembrane glycoproteins desmocollin-1-3 have also been absent in the VICs of all species examined. In a direct comparison, the occurrence of plakophilin-2 in the IDs of the myocardium and its absence in the adjacent valvular tissue can be seen in Figure 20. The novel plaque junction protein myozap (Seeger et al., 2010), a member of the *area composita* junction protein ensemble has also not been seen in VICs (not shown).

With respect to the plaque proteins of AJs, VICs often show a rather complex composition. In contrast to reports that plakoglobin would be absent in VIC-AJs of heart valves (Latif et al., 2006), this *armadillo* protein has been demonstrated in all VIC junctions (not shown). Moreover, the co-existence of α- and β-catenin has been confirmed (for single immunofluorescence label of β-catenin see Figure 18c; for double-label immunofluorescence with N-cadherin see Figure 19a; for immunoelectron microscopy see Figure 21). Protein p120 as another *armadillo* protein is also generally present (for single immunofluorescence micrographs see Figure 18d; for double-label immunolocalization with N-cadherin see Figure 19c). In addition, VICs sometimes have shown a positive – albeit weak – reaction for the plaque protein p0071, whereas proteins ARVCF and neurojungin appear to be absent in VICs (not shown). Moreover, actin-binding junction-associated proteins like protein ZO-1-3, afadin, vinculin and α-actinin have also been detected in the majority of the contacts between VICs (not shown).

Biochemical analysis using SDS-PAGE, followed by immunoblot analysis, has essentially confirmed the results of the immunofluorescence experiments (Figure 22). Here, tissue samples from all four heart valves of ovine origin have shown positive reactions for vimentin but predominantly negative reactions for cardiac α-actin (not

shown), thus also indicating that the microdissected heart valves were free from adjacent myocardium. The VICs of all four heart valves (AV, PV, MV, and TV) have also shown positive reactions for N-cadherin and cadherin-11, for the α-catenin as well as for β-catenin and plakoglobin (not shown). Desmosomal glycoproteins like desmogleins and desmocollins are definitely also absent from heart valve tissue (not shown).

Reports of electron microscopic observations of extensive “desmosomal” structures in VICs of heart valves as published in the early 1990s (Messier et al., 1994), have been repeteadly cited by others (Latif et al., 2006) but the results of the present study show that desmosomal structures and molecules are totally absent in heart valve tissue of the species examined. On the other hand, besides some sporadic gap junction (GJ) structures, AJ structures are generally observed in VICs *in situ*, where they often occur between the cell processes of different cells, mostly as rather small *puncta adhaerentia* (see, e.g., Figure 23a and b). Occasionally, p*uncta adhaerentia* structures are also observed at sites of contact between two cell processes, developing a somewhat interdigitating AJ contact (Figure 23c) or – rather rarely – between cell processes of the same or a neighboring cell process (Figure 23d). For an overview of proteins involved in the AJs of adult VICs *in situ* see Table 8.

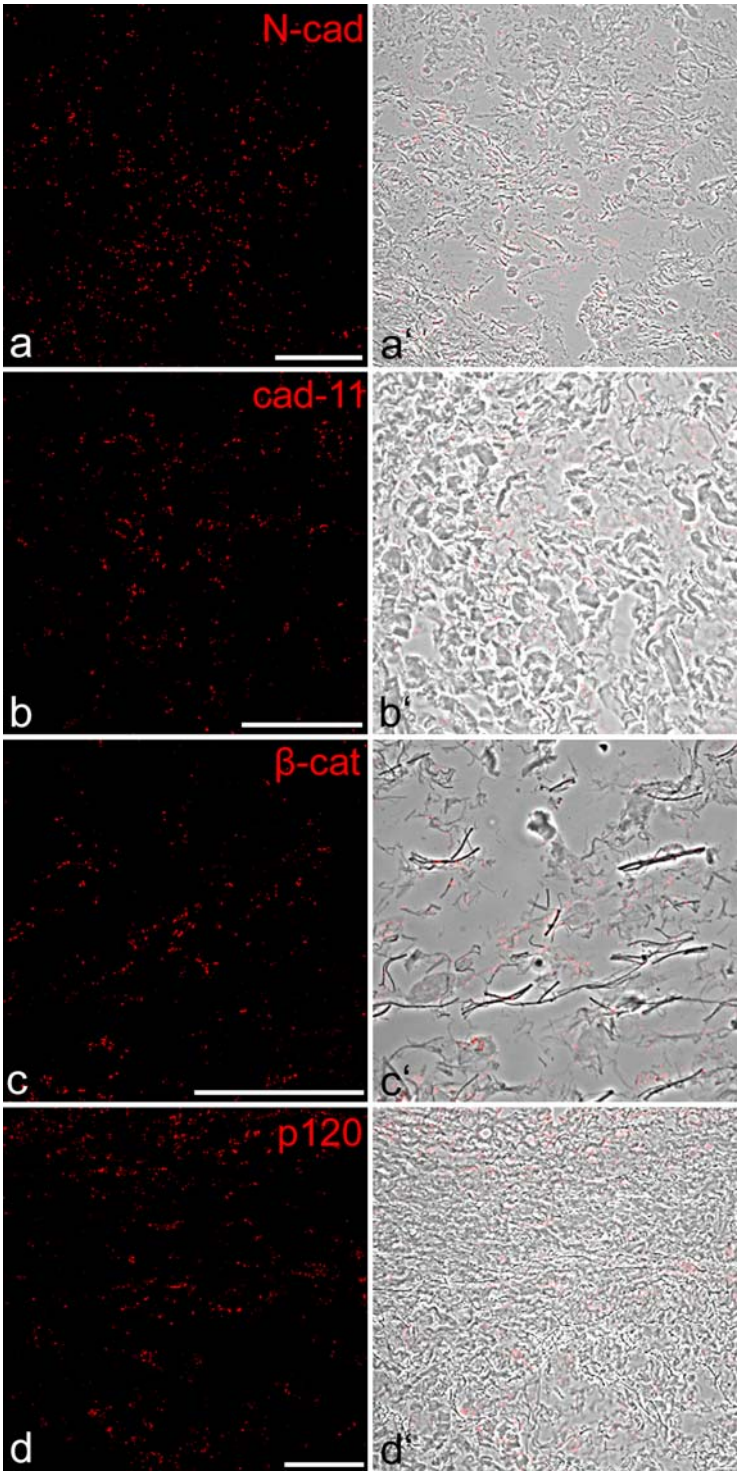

Figure 18: Immunofluorescence micrographs of cross-sections through frozen bovine heart valves labeled with antibodies against AJ proteins (red), showing the typical scattered, dot-like junctions connecting the VICs. Shown are reactions of antibodies against N-cadherin (**a**) and cadherin-11 (**b**) as well as against β-catenin (**c**) and protein p120 (**d**) by immunofluorescence alone or in combination with phase contrast images (**a'-d'**). Bars: 50 µm

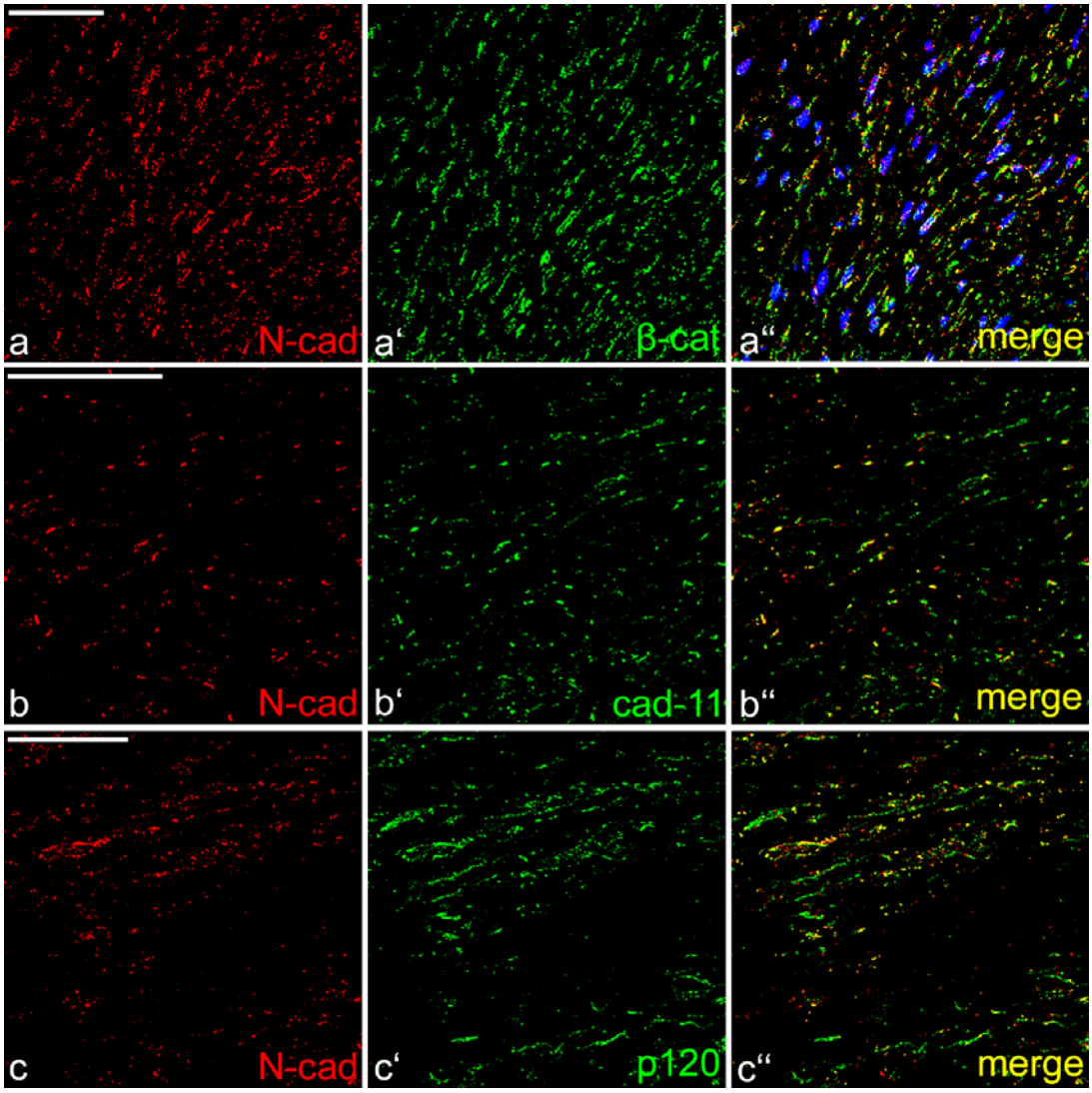

Figure 19: Double-label immunofluorescence micrographs of cross-sections through formaldehyde-fixed and paraffin-embedded samples of human and bovine heart valves, treated for antigen retrieval and showing colocalization of AJ proteins. VIC contacts are positive for N-cadherin (**a-c**, red) colocalizing with β-catenin (**a'**), cadherin-11 (**b'**) and protein p120 (**c'**) appearing in green color (colocalization is shown by merged color in yellow). Nuclei are stained blue. Bars: 50 µm

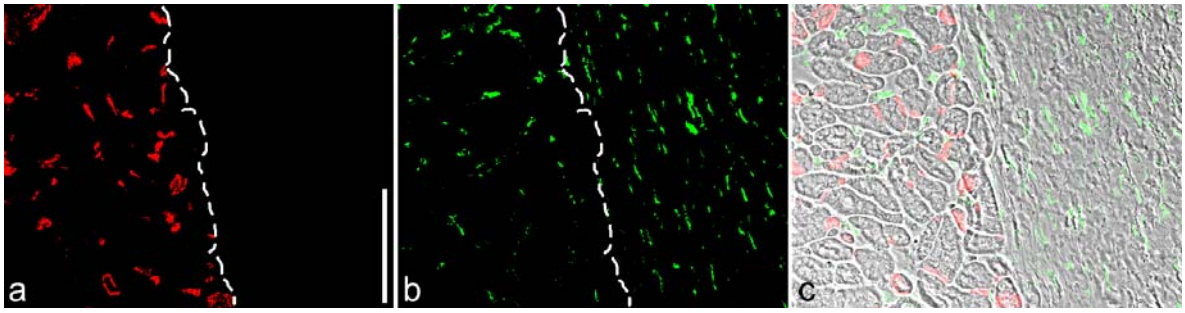

Figure 20: Double-label immunofluorescence micrograph of a section through a formaldehyde-fixed pulmonary valve of an ovine heart. Note the positive staining of plakophilin-2 in the composite junctions (*areae compositae*) of the myocardial IDs (**a**, red, on the left hand side of the dashed line) and its absence in the cell-cell contacts between the VICs in the heart valve (**b**, right hand side of the dashed line). Note the widespread occurrence of vimentin-positive VICs, including cardiac fibroblasts and various kinds of interstitial cells (**b**, green). Comparison of the double-label merged image with phase contrast (**c**) allows a clear distinction of myocardial tissue (left) and interstitial cells of the valve matrix (right). Bar: 50 µm

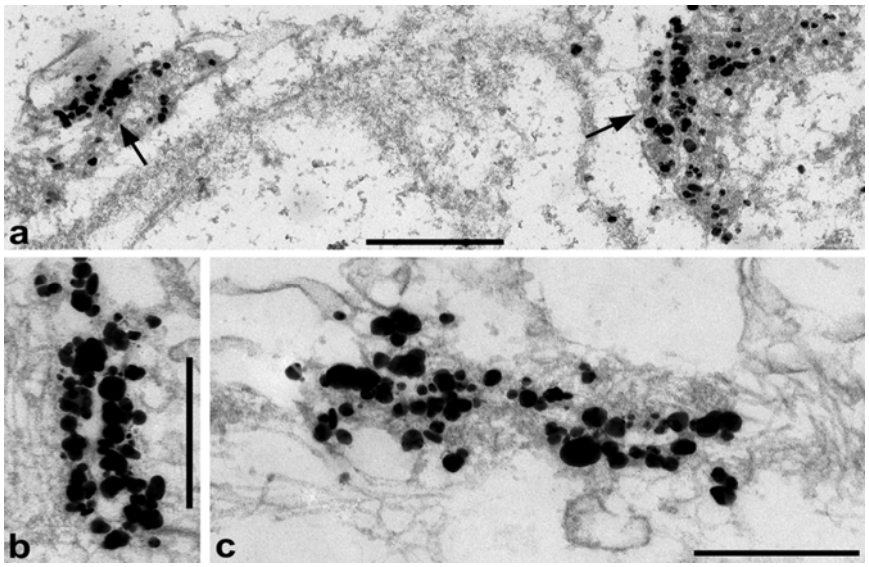

Figure 21: Immunogold-label electron micrographs of cross-sections through cryo-fixed bovine aortic heart valves. Antibodies against β-catenin localize to AJs of VICs. Note a *punctum adhaerens* in **a** (arrow in the left) as well as an association of a junctional plaque of a thin VIC cell process with an IF bundle (arrow in the right). High resolution showing the specific accumulations of immunogold-labeled β-catenin with both AJ plaques (**b, c**) demonstrate its specific occurrence in the VIC AJ plaques. Bars: 0.25 µm

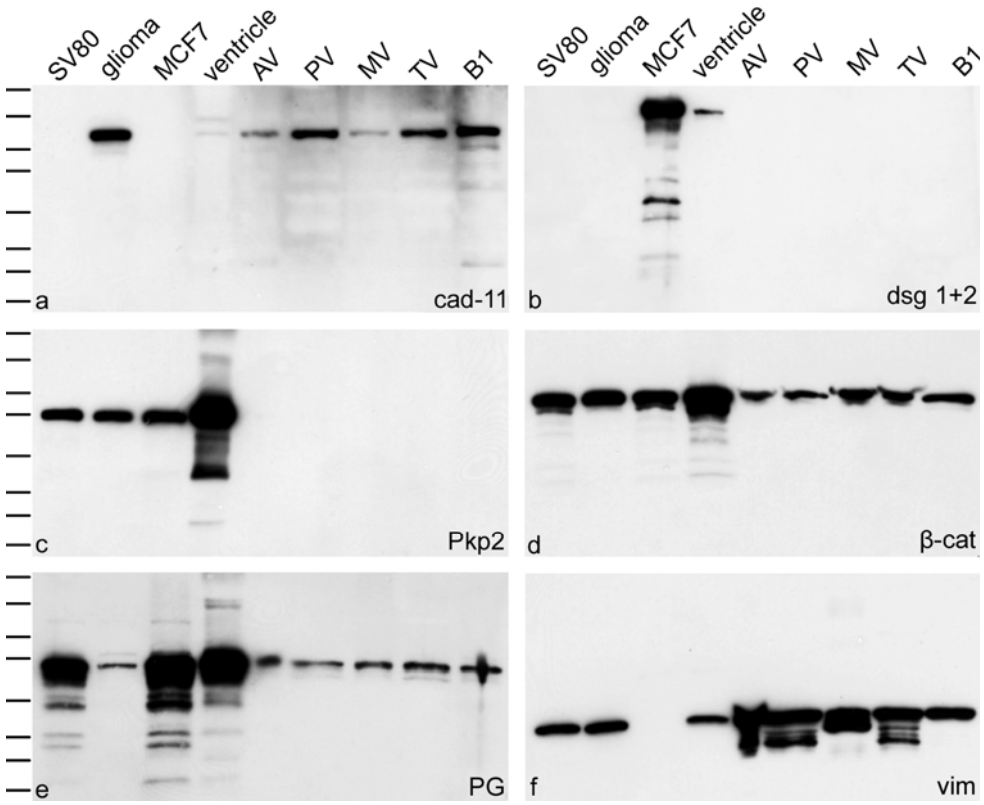

Figure 22: SDS-PAGE followed by immunoblot analysis of proteins and glycoproteins of microdissected frozen ovine heart valves. Reactions were similar for VICs occurring in aortic valves (AVs), pulmonary valves (PVs), mitral valves (MVs) and tricuspid valves (TVs). Note positive reactions for antibodies against cadherin-11 (cad-11, **a**), β-catenin (β-cat, **d**), plakoglobin (PG, **e**) and vimentin (vim, **f**). Reactions for desmogleins 1 and 2 (dsg 1+2, **b**) and plakophilin-2 (Pkp2, **c**) are negative. Cultured human SV80 cells (SV40-transformed fibroblasts), U333 astrocytoma glioma cells, breast carcinoma cells of line MCF-7 (MCF7) and bovine fibroblast cells of line B1 and ovine ventricle tissue were analyzed in parallel as controls in the same electrophoresis and immunoblot reaction. Polypeptide marker bands (bars, left margin) correspond to 212, 158, 116, 97.2, 66.4, 55.6, 42.7 and 34.6 kDa (top to bottom).

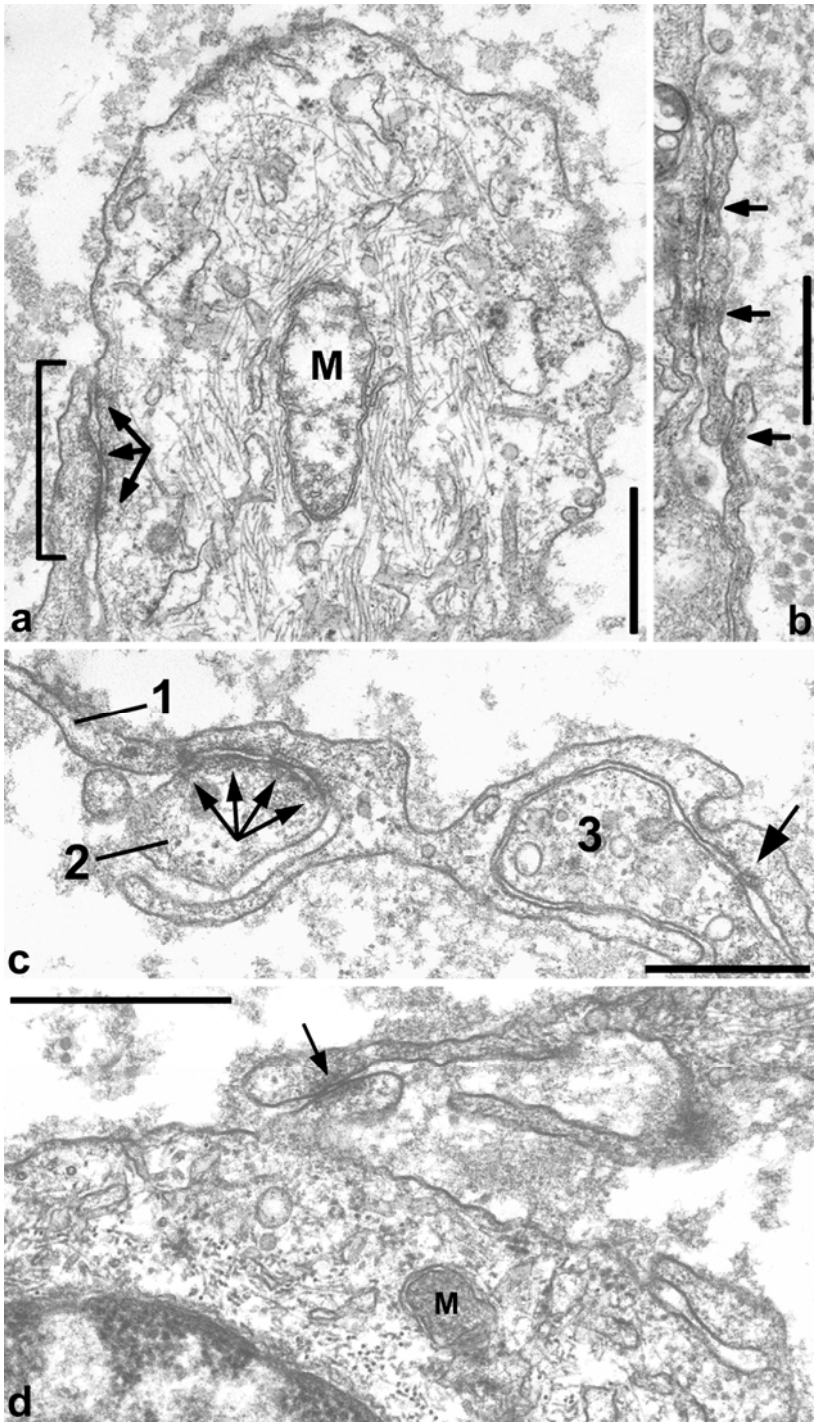

Figure 23: Electron micrographs of ultrathin sections through human aortic and bovine tricuspid heart valves. (**a, b**) Cell-cell contacts (*puncta adhaerentia*) between VIC processes or cell bodies are shown in a human aortic (**a**) and a bovine tricuspid (**b**) heart valve. The *puncta adhaerentia* are indicated by arrowheads. (**c, d**) Cross-sections through the matrix of a human aortic heart valve, showing long VIC processes connected by cell-cell AJ contacts of the *puncta adhaerentia* type (**c**, note connections between three processes, designated 1-3) which are often clustered (e.g., at the group of arrows at the left hand side); the single arrow at the right hand side points to an individual *punctum adhaerens*. (**d**) Cell-cell contacts infrequently also occur between a short cell process of one cell and a longer process of the other cell. M: mitochondrium. Bars: 0.5 µm

4.1.2 The adhering junctions of valvular interstitial cells grown in cell culture

Human aortic heart valves of patients of different ages (18-58 years), bovine aortic, pulmonary, mitral and tricuspid heart valves as well as ovine pulmonary heart valves were used to prepare primary cultures of adult VICs. These cultures were usually grown up to passage 6 and then used for immunofluorescence microscopy, biochemical analysis or electron microscopy.

4.1.2.1 The intermediate-sized filaments of valvular interstitial cells in culture

VICs in culture grow as flattened substratum-adherent cells and often form very long filopodial processes. As in heart valves *in situ*, VICs growing in culture are rich in bundles of IFs identified by immunofluorescence staining with antibodies against vimentin (Figure 24a). In contrast to VICs *in situ*, a remarkable number of the cultured VICs are also positive for smooth muscle α-actin (Figure 24b and c). Moreover, occasionally IFs containing glial filament acidic protein (GFAP) can be observed in cultured VICs (Figure 24d and e), representing up to 10 % of the cells. Reactions for other IF types like desmin or cytokeratins as well as for cardiac α-actin have been negative. Moreover, based on immunoreactions osteopontin as well as periostin appear to be absent in VICs in culture. Some cells show positive reactions for the lipid droplet-associated protein perilipin which has been found to be absent in VICs *in situ* (not shown).

Cultured VICs also show intensive phalloidin reactions of actin filament bundles (Figure 25a and b). Moreover, the typical actin-binding proteins vinculin (Figure 25a and c), paxillin (Figure 25b and c') and α-actinin (not shown) are generally present in cultured VICs (Figure 25c'' shows a typical colocalization of vinculin and paxillin at sites of attachment of the actin microfilament bundles at "focal adhesions" contacting the substratum).

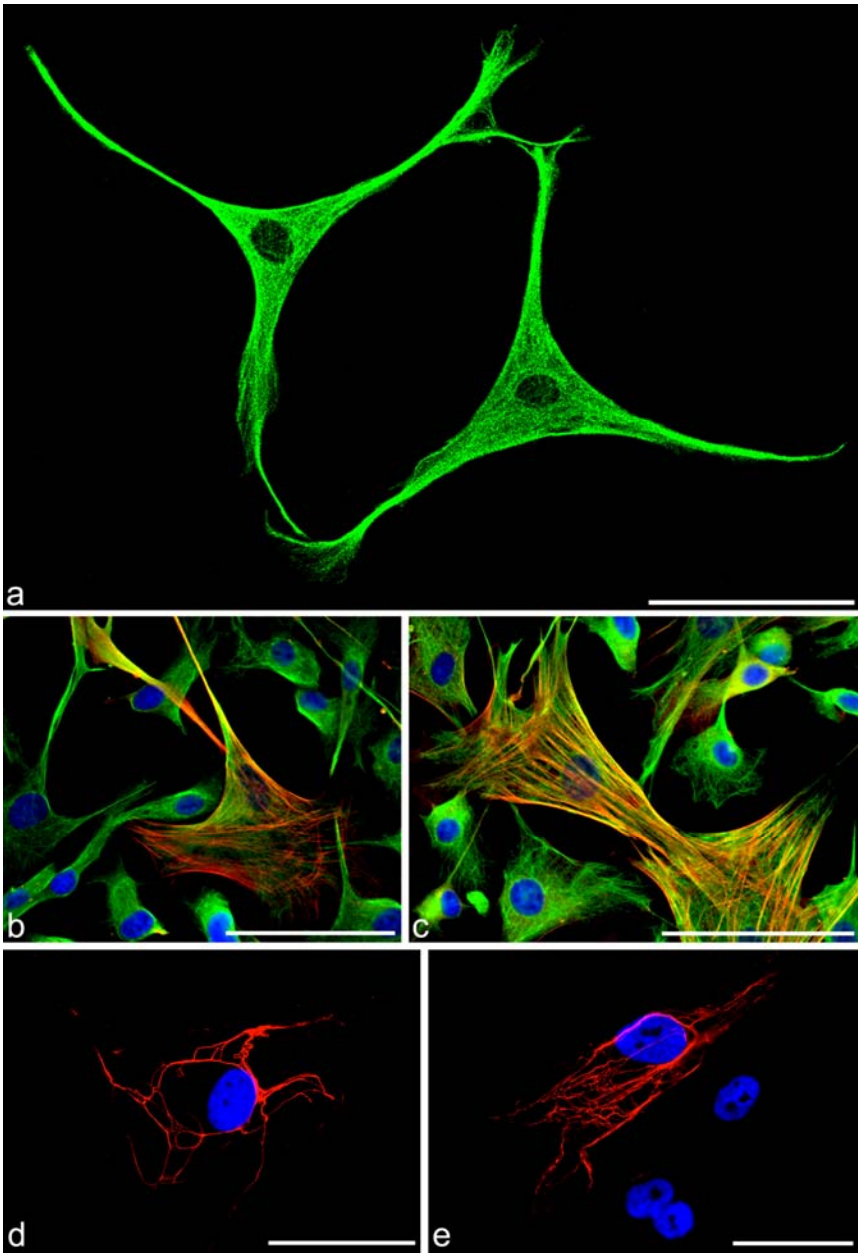

Figure 24: Immunofluorescence micrographs showing the organization of IFs in cultured VICs isolated from ovine pulmonary heart valves. (**a**) Typical appearance of cultured VICs grown to subconfluency which form cell-cell contacts with their filopodial processes (IFs stained with antibodies against vimentin, green). (**b, c**) Partial colocalization of smooth muscle α-actin (red) and vimentin (green). Note that actin filaments do not only appear in the protruding tips of the cells (**b**) but can also occur in the juxtanuclear cytoplasm (**c**). (**d, e**) Immunofluorescence micrographs of the localization of the IF protein GFAP in cultured VICs, showing typical IF bundle arrays. GFAP occurs only in some of the cultured VICs; some cells are positive while neighboring cells often are not (**e**). Nuclei are stained blue. Bars: 100 µm (a), 50 µm (b-e)

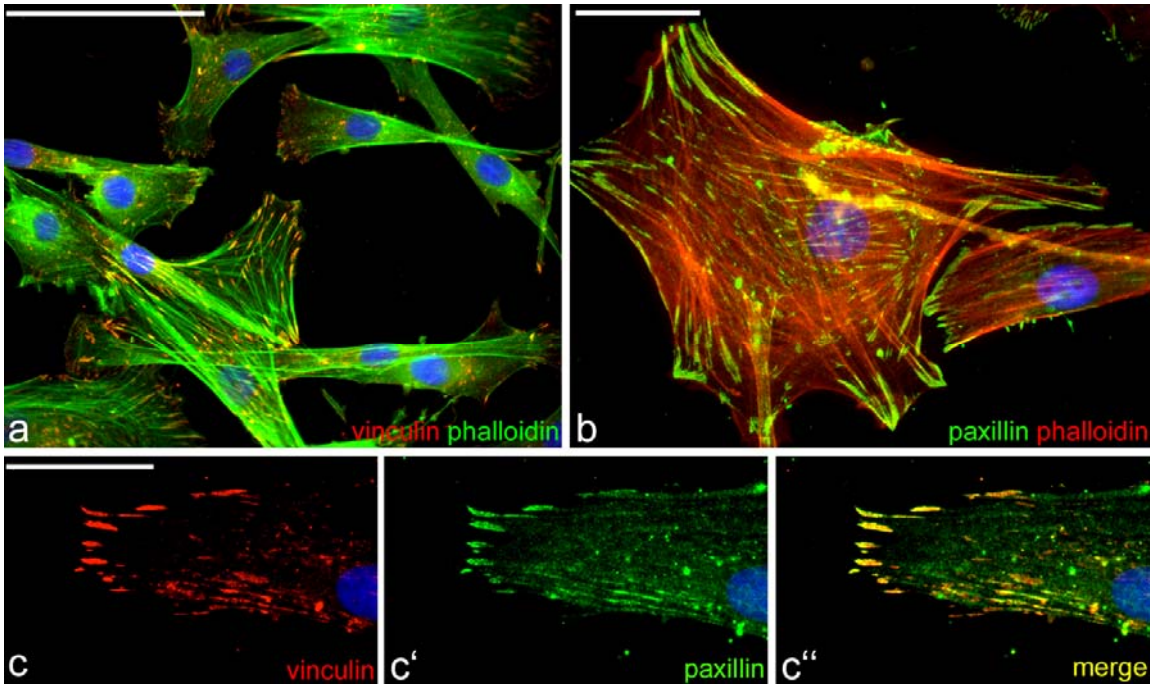

Figure 25: Double-label immunofluorescence micrographs of cultured VICs, presenting filament bundles by phalloidin, coupled to fluorescent secondary antibodies (**a**, green; **b**, red). The actin-binding proteins vinculin (**a, c**, red) and paxillin (**b**, **c'**, green) show positive reactions at the asymmetrical "focal adhesions". Vinculin and paxillin also colocalize in these focal adhesions of VICs (see yellow color in the merged picture in **c''**). Nuclei are stained blue. Bars: 50 µm (a), 20 µm (b, c)

4.1.2.2 The cell-cell contacts of valvular interstitial cells in culture

AJs of the *puncta adhaerentia* type frequently occur in cultured VICs and are already seen in early phases of culture, i.e. in non-confluent states (Figure 26). Cell-cell contacts often occur in groups of junctions, either between the ends of two cell processes (Figure 26a and b) or between the end of one process and a central cell element of another VIC (Figure 27b). Coincidentally, cell-cell contacts can also be formed between the plasma membranes of two adjacent cells, either in a distinct punctate fashion (Figure 27a, d and e; Figure 28b and Figure 29a) or in a seemingly bridge-forming manner (Figure 26c; Figure 27c and Figure 28a). As it has already been shown for mesenchymal stem cells derived from human bone marrow, umbilical cord blood or adipose tissue (Wuchter et al., 2007), VICs can also form cell-cell contacts of the so-called *manubrium adhaerens*-type between cell bodies of two adjacent cells, i.e. tight-fittingly and often deeply invaginated connections between the cells (Figure 28c and Figure 29b). Sometimes, AJs of VICs are recognized over remarkably long distances of cell processes (Figure 29).

However, VICs grown in culture generally show a very characteristic morphology, commonly seen as typical of “myofibroblastoidal” cells: VICs of all the species examined here mostly appear as spindle-shaped, elongated and – for the most part – bipolar cells (Figure 24, 25 and 26). Quite often such cells can display a broad lamellipodial front and a thin and sometimes astonishingly long uropod-like “tail process” (up to 150 µm long; Figure 26 and 27).

The cell-cell contacts often occur as punctate clusters or appear as cell-cell bridges positive for N-cadherin (Figure 27a-c) as well as for protein p120 (Figure 27d, e). N-cadherin also colocalizes with cadherin-11, plakoglobin, protein p120 (Figure 28) and α- and β-catenin (not shown). Generally, the AJs of such culture cells show colocalization of α- and β-catenin as well as of both these proteins with plakoglobin (Figure 29). Immunoreactions with antibodies against protein p0071 are mostly negative (Figure 30) which may reflect the presence of very minor amounts of this protein in these AJs. As in VICs *in situ*, proteins ARVCF and neurojungin appear to be absent in cultured VICs (not shown). Negative reactions are also found for PERP protein (not shown; Attardi et al., 2000) and for the novel *area composita*-associated plaque protein myozap. On the other hand, actin-binding proteins such as proteins ZO-1-3 (Figure 30), afadin and α-actinin all have shown positive reactions in cultured VICs (not shown).

Subforms or tissue-specific types of α-catenin such as α-E-catenin (Rimm et al., 1994, 1995), α-N-catenin (Hirano et al., 1992; Uchida et al., 1994) and α-T-catenin (Janssens et al., 2001; Goossens et al., 2007), show very variable immunofluorescence reactions. In general, α-E-catenin appears to be positive in cultured cells as well as *in situ*, whereas α-T-catenin and α-N-catenin under the conditions have only shown negative reactions both in cultured VICs as well as in heart valves *in situ* (not shown). Moreover, VICs of different mammalian species are negative for VE-cadherin, indicating that the VIC primary cultures are not derived from – or contaminated with – residual endothelial cells. Negative immunoblot reactions have also been seen for E- and P-cadherin (Figure 30). In the electron microscope, VICs in culture – as in VICs *in situ* (Figure 23) – show solely cell-cell contacts of the AJ type (Figure 31), together with some – quite rare – GJs (Figure 31e).

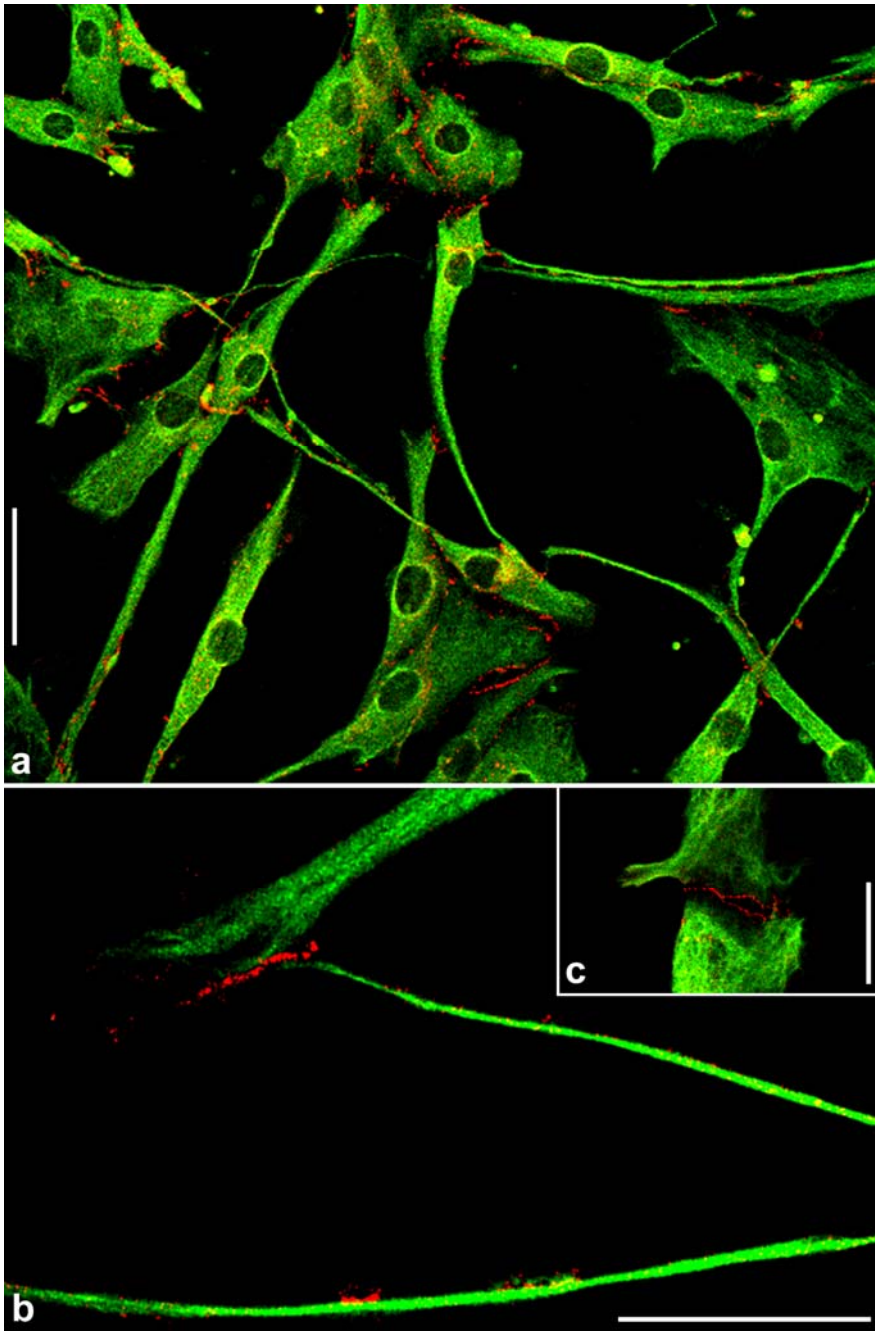

Figure 26: Double-label immunofluorescence micrographs of cultured ovine VICs derived from a pulmonary valve, grown to subconfluency. (**a**) The survey image shows VICs with their typical long processes (vimentin, green) connected to other cells over – partly – very long distances. Note the high frequency of AJs (cell-cell contacts are stained with antibodies against N-cadherin, red). (**b**) Extremely long filopodial processes (here the process shown in the bottom region exceeds 100 µm in length), connecting cultured ovine VICs via AJs containing N-cadherin (red). Note the group of AJs in the upper left which connects the ends of two filopodial VIC processes. (**c**) Plasma membrane regions of two adjacent cells forming an extended AJ-rich cell-cell contact region. Bars: 50 µm (a), 30 µm (b), 25 µm (c)

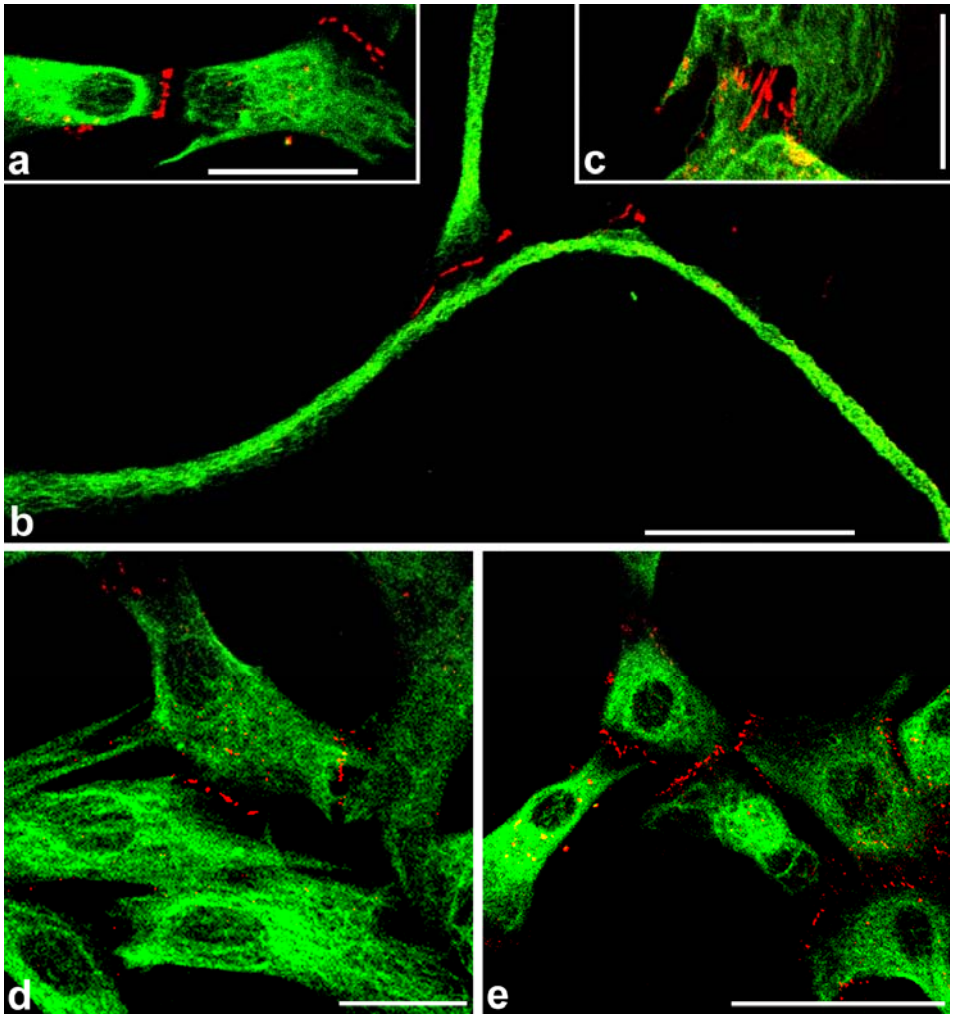

Figure 27: Double-label immunofluorescence micrographs of ovine VICs from a pulmonary heart valve, grown in culture and showing different forms of *puncta adhaerentia* type AJs. N-cadherin-mediated cell-cell contacts (red) can occur as punctate arrays between two cell bodies (**a**; vimentin, green). Higher magnification shows the structure of a subtype of AJ occurring at the end of a cell process and forming an extended contact region with the middle segment of a long cell process exceeding 150 µm in length (**b**). These AJs can also occur as groups of cell-cell bridges (**c**). Cell-cell contacts of the *puncta adhaerentia* type are not only positive for N-cadherin (**a-c**) but also for rotein p120 (**d, e**). Bars: 25 µm (a-c), 20 µm (d), 50 µm (e)

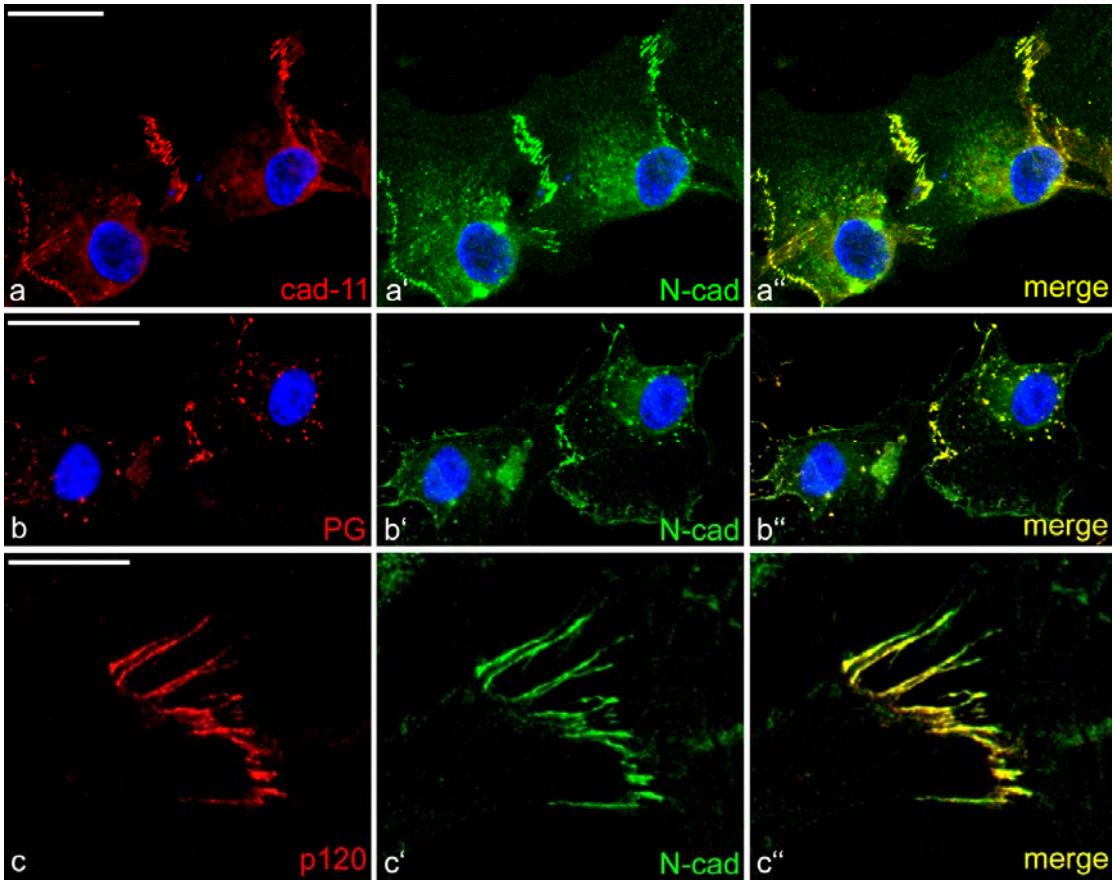

Figure 28: Double-label immunofluorescence micrographs of cultured VICs of human and ovine origin, showing colocalization of AJ transmembrane glycoproteins with typical plaque proteins. (**a**) Colocalization of cadherin-11 (red) with N-cadherin (green) in ovine VICs (note the yellow merged color in **a''**). (**b**) Plakoglobin as a typical plaque protein (PG, red) colocalizes with N-cadherin (green) in a typical punctate pattern in AJs connecting ovine VICs (**b''**, merged yellow color). (**c**) Protein p120 (red) colocalizes with N-cadherin (green) in tight-fitting invaginations of cell-cell contacts of human VICs (yellow merged color). Nuclei are stained blue. Bars: 20 µm (a, b), 10 µm (c)

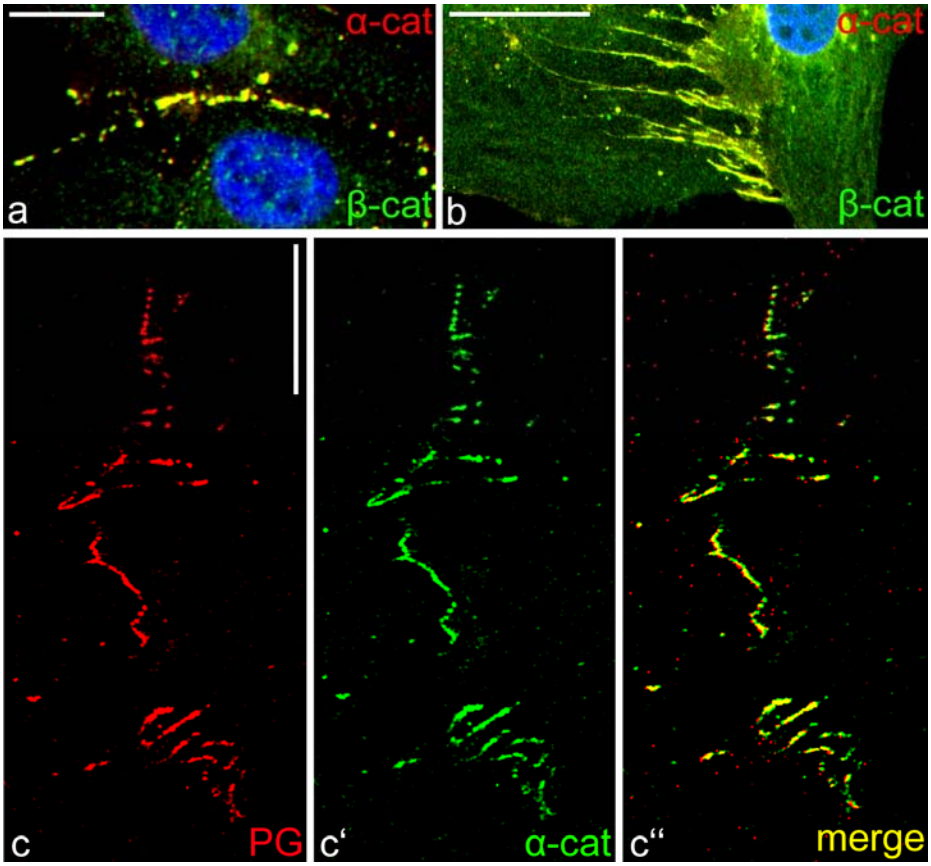

Figure 29: Double-label immunolabeling of cultured VICs showing colocalization of typical AJ plaque proteins. (**a**) Colocalization (yellow, merged images) of α-catenin and β-catenin in *puncta adhaerentia* type cell-cell junctions over a relatively long distance connecting the cell membranes of two adjacent VICs of bovine origin. (**b**) Human VICs showing colocalization of α-catenin (red) and β-catenin (green) in AJ plaques (yellow, merged image). Note that here the processes of one cell deeply and tight-fittingly insert into invaginations of the other cell, forming junctions of the *manubrium adhaerens* type. (**c**) Extended AJ-rich contact region of ovine VICs with numerous junctions positive for plakoglobin (**c**, red) and α-catenin (**c'**, green). Colocalization can be seen in the merged picture (**c''**, yellow). Nuclei are stained blue. Bars: 5 µm (a), 20 µm (b, c)

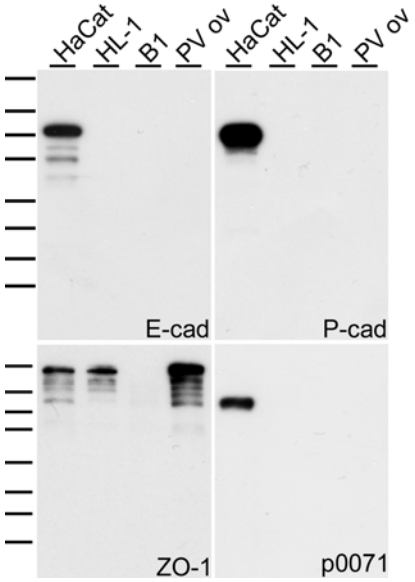

Figure 30: SDS-PAGE, followed by immunoblot analysis of proteins of the human epidermal keratinocytes cell line HaCat, a murine cardiomyocyte-like cell line (HL-1), a bovine fibroblastoidal cell line (B1) and cultured ovine VICs derived from a pulmonary heart valve (PV ov). E-cadherin (E-cad) and P-cadherin (P-cad) show negative reactions in PV ov. Protein ZO-1 shows a positive reaction in PV ov, whereas the reaction of protein p0071 is negative here, probably due to the presence of very low amounts of this protein. Polypeptide marker bands (bars, left) correspond to 212, 158, 116, 97.2, 66.4, 55.6, 42.7 and 34.6 kDa (top to bottom).

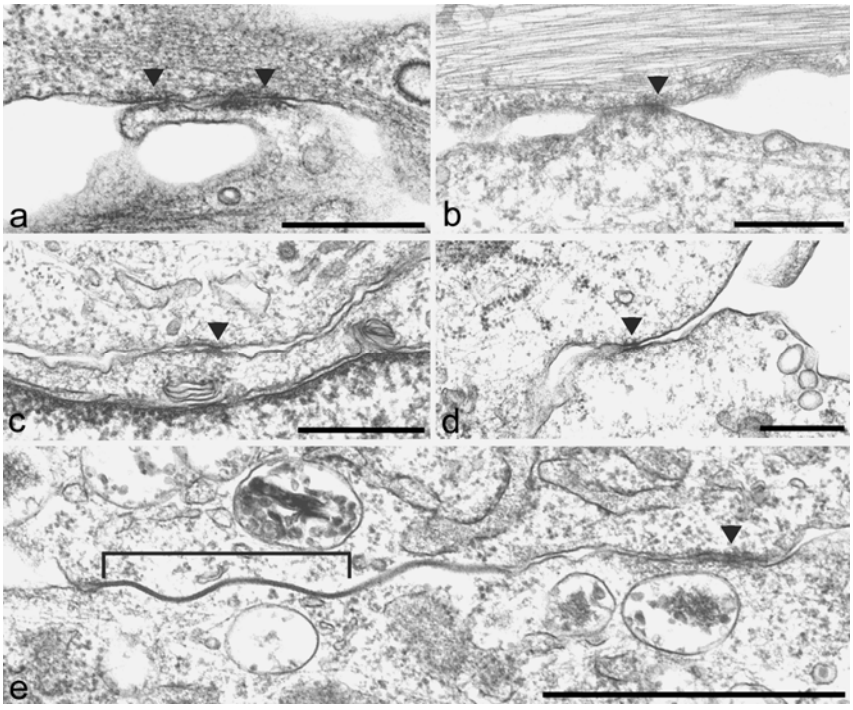

Figure 31: Electron micrographs of cultured ovine VICs of a pulmonary heart valve, showing contacts and interactions of VICs in culture. Arrowheads indicate small individual cell-cell contacts of the *puncta adhaerentia* type (**a**-**e**). Sometimes, GJs are also present in the contact areas of two neighboring cells (see bracket in **e**). Bars: 0.5 µm (a-d), 1 µm (e)

4.1.2.3 The acquisition of plakophilin-2 to the adherens junctions of cultured valvular interstitial cells

As desmosomal proteins are absent in VICs of different mammalian species *in situ*, it is quite surprising to detect the selectively rapid acquisition of an additional desmosomal plaque protein – plakophilin-2 – in AJs of cultured VICs (Figure 32). This *de novo* appearance of plakophilin-2 can be observed from early culture passages on and is conserved – or even enhanced – when these cells are passaged further. In contrast, plakophilins-1 and -3 have never been detected in the AJs of cultured VICs (Figure 33). Other desmosomal proteins such as cadherins of the desmoglein and desmocollin subfamilies as well as plaque proteins, including desmoplakin are – and remain – absent in cultured VICs (not shown).

In VIC cultures of bovine, ovine or human origin, plakophilin-2 always colocalizes with N-cadherin and cadherin-11 (Figure 34) as well as with α- and β-catenin (Figure 35), plakoglobin, proteins p120 and p0071 (not shown).

Although plakophilin-2 is abundant in the cell-cell contacts of cultured VICs and always colocalizes with other AJ proteins, this relationship is not reciprocal and complete: Not every junction which is positive for N-cadherin, for example, is also positive for plakophilin-2 (e.g., Figure 36a-a'').

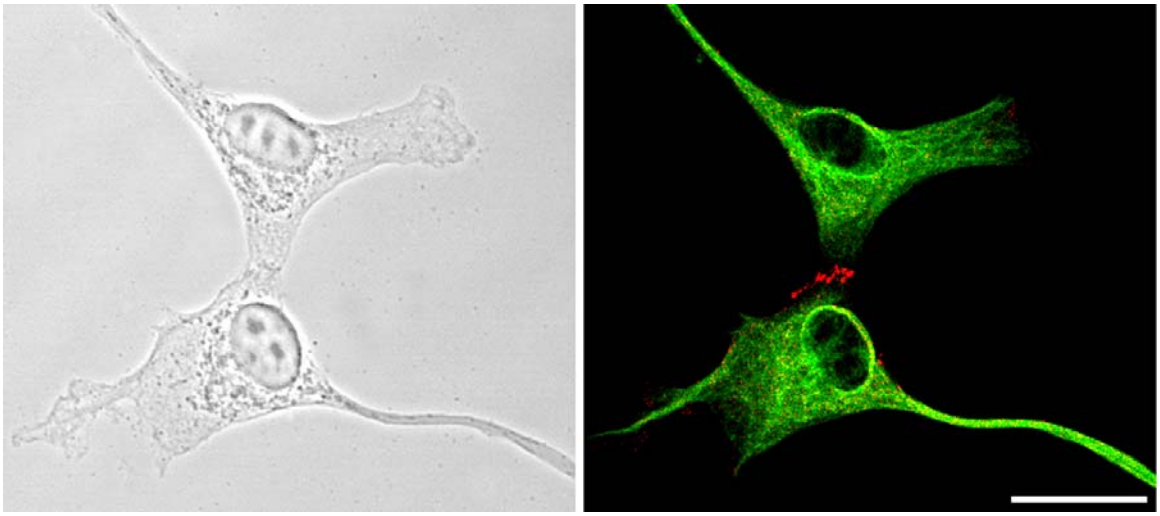

Figure 32: Double-label immunofluorescence micrograph of cultured ovine VICs, immunostained for vimentin (green), showing a positive reaction for the desmosomal plaque protein, plakophilin-2 (red). Bar: 25 μm

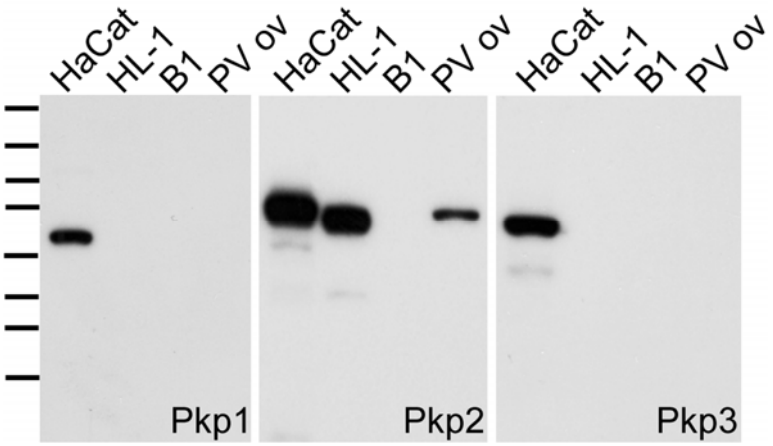

Figure 33: SDS-PAGE, followed by immunoblot analysis of proteins of a human epidermal keratinocyte cell line (HaCat), a murine cardiomyocyte-like cell line (HL-1), a bovine fibroblastoidal cell line (B1) and cultured ovine VICs derived from a pulmonary heart valve (PV ov). Reactions for plakophilins 1 and 3 (Pkp1 and 3) are negative in PV ov. By contrast, note that plakophilin-2 (Pkp2) shows positive reactions in PV ov. Polypeptide marker bands (bars, left) correspond to 212, 158, 116, 97.2, 66.4, 55.6, 42.7 and 34.6 kDa (top to bottom).

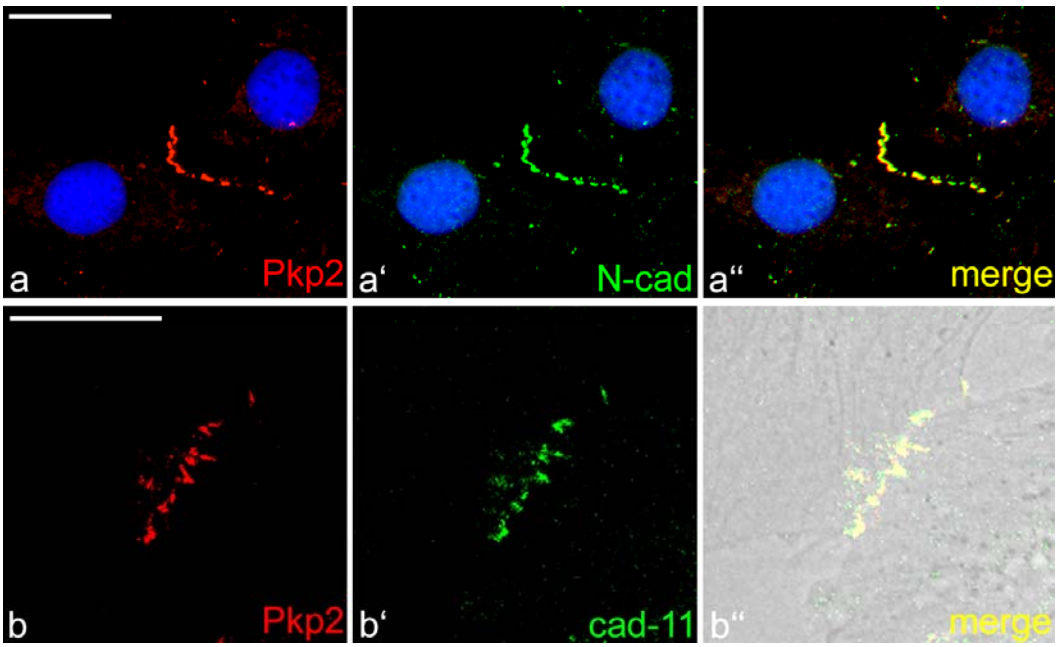

Figure 34: Double-label immunofluorescence micrographs of cultured ovine VICs, showing the colocalization (yellow merged color) of plakophilin-2 (**a, b**, red) with N-cadherin (**a-a’’**, green) or cadherin-11 (**b-b’’**, green). See the phase contrast in the merged picture (**b’’**) for IF anchorage in the plaque region. Nuclei are stained blue. Bars: 100 µm (a), 20 µm (b)

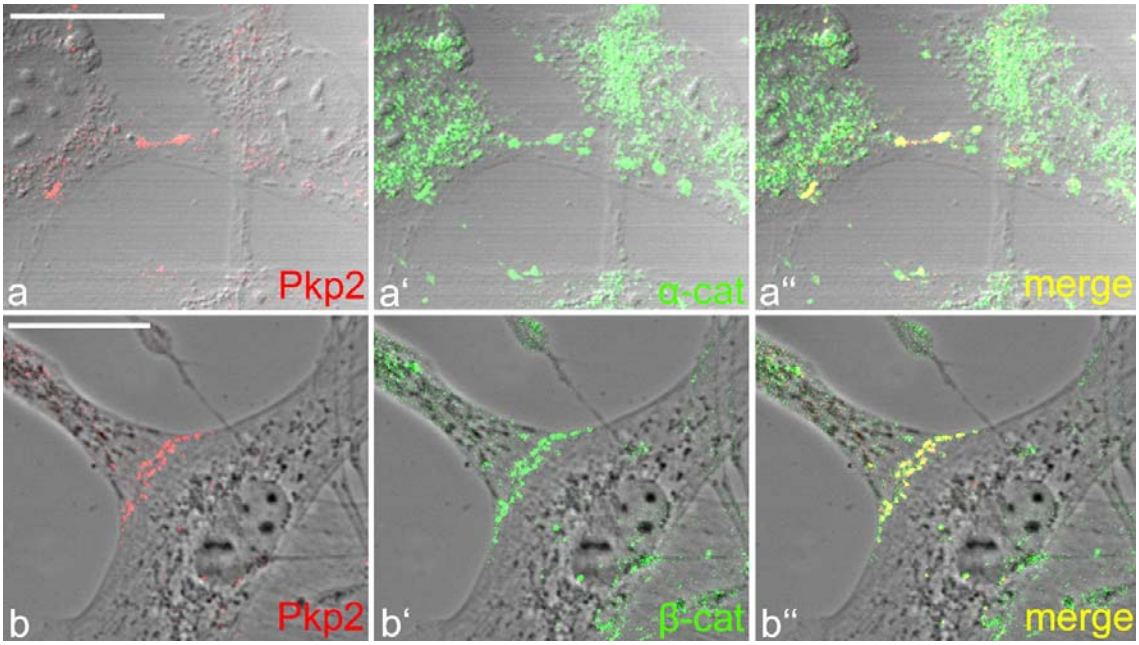

Figure 35: Double-label immunofluorescence micrographs of cultured human and ovine VICs, showing colocalization (yellow merged color) of plakophilin-2 (red) with the typical AJ plaque proteins α- and β-catenin (green). Note the characteristic dot-like structures of the junctions of the *puncta adhaerentia* type which occur either as single dots (**a-a’’**) or as clusters of *puncta adhaerentia* (**b-b’’**). Bars: 20 µm

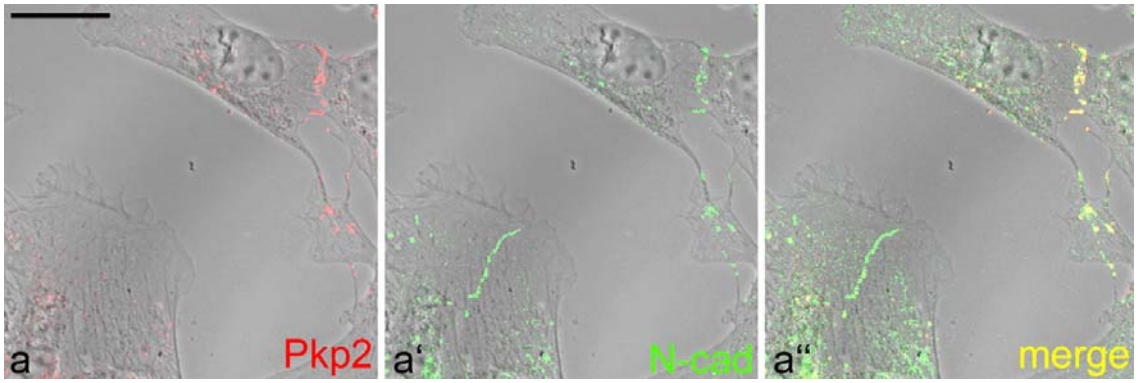

Figure 36: Double-label immunofluorescence micrographs of cultured ovine VICs labeled with specific antibodies against plakophilin-2 (red) and N-cadherin (green). Note that plakophilin-2 (red) may be absent in some cell-cell contacts (between the cells in the lower left), whereas in other cell-cell contacts it may be present and show colocalization with N-cadherin (yellow merged color; neighboring cell-cell contact between two other VICs in the upper right). Bar: 20 µm

4.1.2.4 Biochemical analyses of adherens junctions of cultured adult valvular interstitial cells from different mammals, types of heart valve and culture passage numbers

To compare directly the molecular composition of the AJs connecting adult VICs in culture, biochemical analyses of cultured VICs from three different mammalian species (human, bovine and ovine) were performed by SDS-PAGE, followed by immunoblot analysis. In all experiments, cultured human astrocytoma cells (glioma line U333), human breast carcinoma cells (line MCF-7) and bovine fibroblasts (line B1) were analyzed for comparison. Additionally, lysates of ventricular myocardial tissue of the analyzed species were used for comparison.

None of the three analyzed species (cow, sheep and man) present any significant difference between the four different heart valves (AV, PV, MV, TV), neither in the type of the proteins found nor in their relative amounts, as demonstrated for bovine VIC cultures in Figure 37a-f. There are obviously no significant differences in the reaction with antibodies specific for N-cadherin or cadherin-11 as well as for α-catenin (not shown), β-catenin, protein p120 or plakoglobin. The immunoblot reaction with specific antibodies against plakophilin-2 also shows the presence of this protein in VICs derived from all four different heart valves (Figure 37f). Moreover, among the three species compared, there are no significant differences in the AJ proteins in the course of cell culture passages, as can be seen, e.g., for ovine VICs of passages one to six (P1-P6; Figure 37g-j). Immunoblot reactions with specific antibodies against N-cadherin, cadherin-11, plakoglobin, and plakophilin-2 show a consistent and stable presence of these junction proteins. VICs derived from aortic heart valves of patients who had to undergo heart valve replacement and differed in age (18-58 years) and sex (Figure 37k-p), also reveal near equal amounts of N-cadherin, cadherin-11, plakoglobin, β-catenin and plakophilin-2.

Desmosomal proteins such as Dsg 1 and 2 (Figure 37o), Dsc 1-3 and desmoplakin are absent in all VIC cultures (not shown). Typical cardiac proteins like desmin and cardiac muscle α-actin as well as myozap are always found to be negative in cultured VICs whereas HL-1 cells generally show positive reactions for these proteins (for cultured ovine VICs see Figure 38). For a summary of the proteins involved in the AJs of adult VICs in culture see Table 8.

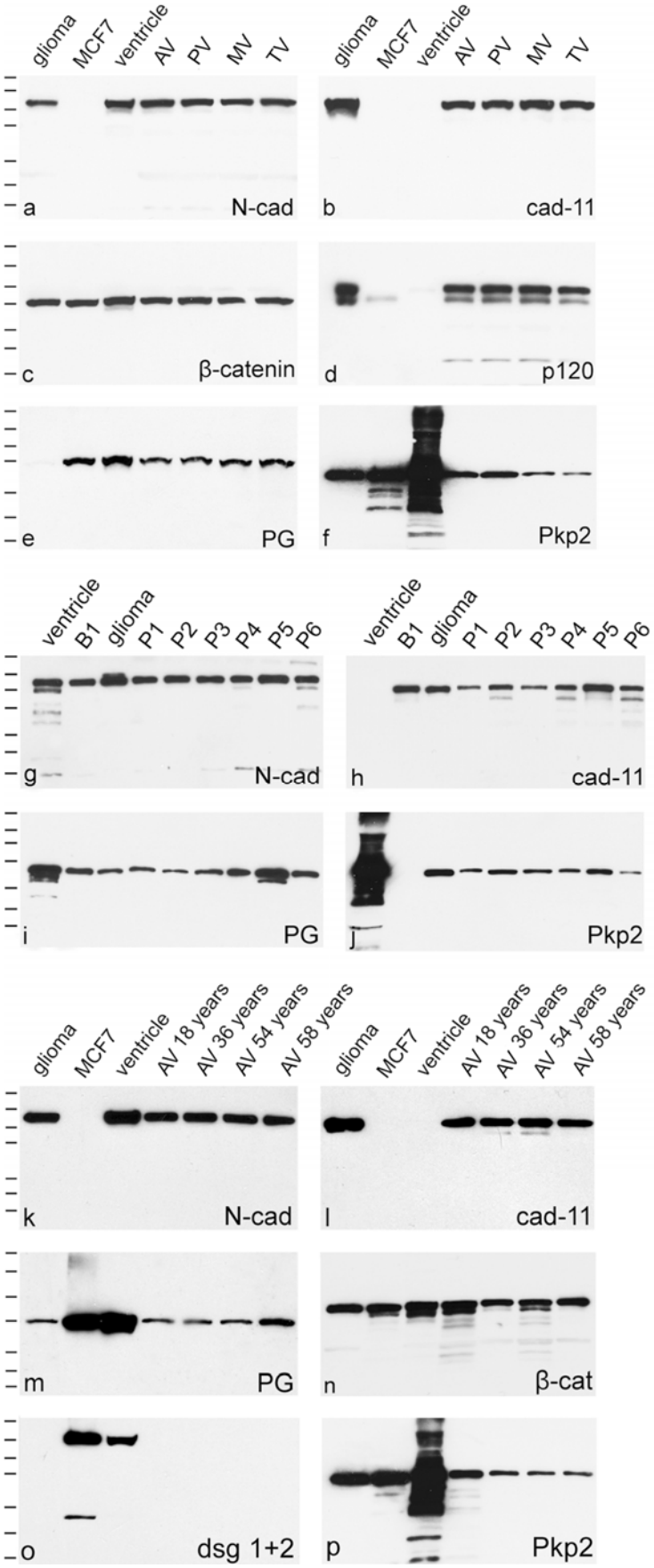
glioma
MCF7
ventricle
AV
PV
MV
TV
a
N-cad
b
cad-11
c
β-catenin
d
p120
e
PG
f
Pkp2
ventricle
B1
glioma
P1
P2
P3
P4
P5
P6
g
N-cad
h
cad-11
i
PG
j
Pkp2
AV 18 years
AV 36 years
AV 54 years
AV 58 years
k
N-cad
l
cad-11
m
PG
n
β-cat
o
dsg 1+2
p
Pkp2

Figure 37

Figure 37: SDS-PAGE, followed by immunoblot analyses of proteins in primary cultures of VICs from heart valves of three different species (cow, sheep and man). **a-f** Immunoblot reactions of proteins of bovine VICs derived from the aortic valve (AV), pulmonary valve (PV), mitral valve (MV) and tricuspid valve (TV). Reactions of various specific antibodies against N-cadherin (N-cad, **a**), cadherin-11 (cad-11, **b**), β-catenin (β-cat, **c**), protein p120 (p120, **d**), plakoglobin (PG, **e**) and plakophilin-2 (Pkp2, **f**) are shown here. **g-j** Immunoblot reactions of proteins of ovine VICs with increasing passages (P1-P6) were performed with antibodies against N-cadherin (**g**), cadherin-11 (**h**), plakoglobin (**i**) and plakophilin-2 (**j**). **k-p** Immunoblot reactions of human aortic VICs of patients differing in age (18-58 years old) and sex were performed with antibodies against N-cadherin (**k**), cadherin-11 (**l**), plakoglobin (**m**), β-catenin (**n**), desmogleins 1 and 2 (dsg 1+2, **o**) and plakophilin-2 (**p**). Ventricular myocardial tissue of bovine, ovine and human origin (ventricle), human breast carcinoma cells of the MCF-7 cell culture line (MCF7), and human astrocytoma cells (glioma U333) have been analyzed in parallel as controls. Polypeptide marker bands (bars, left) correspond to 212, 158, 116, 97.2, 66.4, 55.6 and 42.7 kDa (top to bottom).

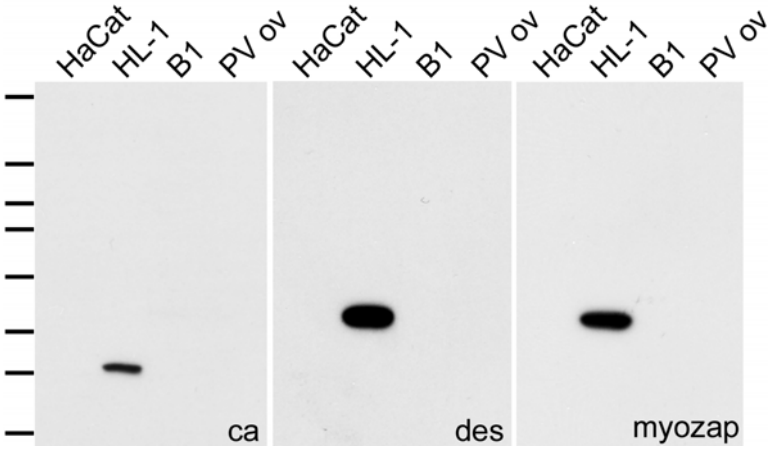

Figure 38: SDS-PAGE, followed by immunoblot analysis of proteins of a human epidermal keratinocyte line (HaCat), a murine cardiomyocyte-derived line (HL-1), a bovine fibroblastoidal cell line (B1) and cultured ovine VICs derived from a pulmonary heart valve (PV ov). Antibody reactions against cardiac α-actin (ca), desmin (des) and protein myozap are negative in PV ov. All three proteins show positive reactions in the cardiomyocyte-derived cell line HL-1 and negative reactions in HaCat and B1 cells. Polypeptide marker bands (bars, left) correspond to 212, 158, 116, 97.2, 66.4, 55.6, 42.7 and 34.6 kDa (top to bottom).

4.1.2.5 Small interference RNA knock-down experiments of plakophilin-2 and N-cadherin in primary cultures of human valvular interstitial cells

Pieperhoff et al. (2008) have shown that in cultures of neonatal rat cardiomyocytes the loss of the desmosomal plaque protein plakophilin-2 can cause the complete disintegration of the *area composita* structures of the residual ID structures seen in such cell cultures (for similar experiments and results with cardiomyocytes see Oxford et al., 2007, and Fidler et al., 2009; for knock-down experiments of plakophilin-3 in epithelial cells see Kundu et al., 2008). Moreover, Rickelt (2010) has shown that the treatment with

siRNA against plakophilin-2 of general kinds of cultures of mesenchymally derived cells or malignantly transformed SV80 fibroblasts can result in a loss of immunolabeling of plakophilin-2 and that treatment with siRNA against N-cadherin can result in a loss of N-cadherin. In cells treated with plakophilin-2 siRNA, N-cadherin remains stable at cell-cell contacts and so does plakophilin-2 in cells treated with N-cadherin siRNA.

Therefore, knock-down of plakophilin-2 and N-cadherin mRNA was performed with primary cultures of human VICs derived from mitral heart valves (for protocols see chapter 3.1.3 and Pieperhoff et al., 2008). Although control experiments using cells without treatment yielded reliable results, inconsistent results were obtained with control groups in which siRNA against lamin A/C was applied. This was also the case with the “true” knock-down experiments using plakophilin-2 or N-cadherin siRNAs. In such experiments, however, cells treated with siRNA often showed a strongly increased rate of cell death rates, presumably caused by the cytotoxicity of the siRNA reagents, although rather low amounts of siRNA were used. Consequently, safe conclusions could not be drawn from these experiments.

4.1.2.6 The occurrence of α-N-catenin in the adherens junctions of cultured valvular interstitial cells

The junctional plaque protein α-catenin occurs in three different isoforms: α-E-catenin, which apparently is near-ubiquitously expressed (Herrenknecht et al., 1991; Nagafuchi et al., 1991), α-T-catenin, which is predominantly expressed in cardiomyocytes and in peritubular myoid cells of the testis (Janssens et al., 2001, 2003), and α-N-catenin, known for its occurrence in neural tissues (Hirano et al., 1992; Uchida et al., 1994). Recently, α-T-catenin has also been reported to be localized in the composite junctions of the IDs in the myocardium together with α-E-catenin (Janssens et al., 2001; Goossens et al., 2007). And, even more interestingly, α-T-catenin also colocalizes in these composite junctions with the desmosomal plaque protein plakophilin-2 whereas α-E-catenin does not (Goossens et al., 2007).

Therefore, mRNA of cultured bovine VICs and heart valve tissue of bovine origin was used for reverse transcription and the cDNA obtained was then used for PCR-reactions with specific primers against the sequences of bovine α-E-, α-N- and α-T-catenin (for detailed protocols and primer sequences see chapter 3.7). Figure 39 shows that cultured VICs as well as heart valve tissue *in toto* synthesize α-E-catenin, which has also been confirmed by immunofluorescence microscopy (not shown). By contrast, α-T-

catenin is synthesized neither in cultured VICs nor in heart valve tissue, which corresponds to the findings in immunofluorescence microscopy (not shown). Surprisingly, α-N-catenin has shown a weak positive signal in cultured VICs whereas heart valve tissue does not reveal this subform of α-catenin, a finding which has been confirmed by immunoblot analysis (see Figure 40).

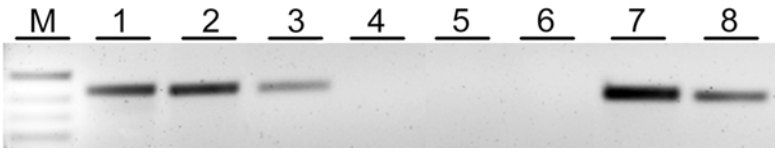

Figure 39: RT-PCR detection of α-E-catenin- (lanes 1 and 2), α-N-catenin- (lanes 3 and 4) and α-T-catenin-mRNA (lanes 5 and 6) in cultured VICs of bovine origin (lanes 1, 3, 5 and 7) as well as in bovine heart valve tissue (lanes 2, 4, 6 and 8). GAPDH primers have been used as typical housekeeping gene (lanes 7 and 8). Marker bands (M) correspond to 517, 396, 356, 247 and 75 bp (top to bottom).

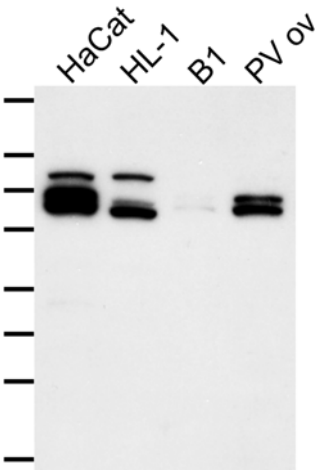

Figure 40: SDS-PAGE followed by immunoblot analysis of proteins from the human keratinocyte cell line HaCat, a murine cardiomyocyte-derived cell line (HL-1), a bovine fibroblastoidal cell line (B1) and cultured ovine VICs derived from a pulmonary heart valve (PV ov). Antibodies against α-N-catenin show positive reactions in HaCat as well as in HL-1, PV ov and only a very weak reaction in B1 cells. Polypeptide marker bands (bars, left) correspond to 212, 158, 116, 97.2, 66.4, 55.6, 42.7 and 34.6 kDa (top to bottom).

4.1.2.7 Immunoprecipitation analyses of cultured valvular interstitial cells of ovine origin

To further characterize the adhering junctions of the VICs growing in culture, primary cultures of pulmonary heart valves were used for immunoprecipitation analyses (IPs). The cultured cells were lysed in RIPA buffer (Table 4) and the relevant polypeptides were enriched by specific antibodies coupled to magnetic "Dynabeads", separated by SDS-PAGE and reacted by immunoblot analyses. In addition to the precipitated protein samples, proteins from ovine ventricular myocardial tissue or from primary cultures of ovine pulmonary valves were examined in parallel and samples of the specific supernatants obtained before the immunoprecipitation as well as "pre-clear" samples were also run in parallel (for protocol see chapter 3.6).

The results (Table 7, Figure 41) show that N-cadherin co-immunoprecipitates with plakoglobin and β-catenin but not with plakophilin-2 or cadherin-11 (Figure 41a and b). Cadherin-11 in turn co-immunoprecipitates with plakoglobin and β-catenin, but not with N-cadherin or plakophilin-2 (Figure 41c and d). Finally, β-catenin co-immunoprecipitates with N-cadherin, whereas the reaction of β-catenin with the cadherin-11-IP has been inconsistent (for a positive reaction see Figure 41e and for negative reaction see Figure 41f). Plakoglobin shows a positive reaction in N-cadherin-IPs, but somewhat surprisingly, has not been found to co-immunoprecipitate with plakophilin-2 (Figure 41g). Protein p0071 co-immunoprecipitates with N-cadherin- and β-catenin-IPs but not with plakophilin-2- and cadherin-11-IPs (Figure 41h). Moreover, plakophilin-2 has not been found to co-immunoprecipitate with N-cadherin, cadherin-11 or with β-catenin or plakoglobin (Figure 41i and j). For a summary of the results obtained by immunoprecipitation analyses see Table 7.

Table 7 Summary of the results of the immunoprecipitation analyses of cell-cell junction proteins of ovine valvular interstitial cells grown in culture

		Antibodies bound to "Dynabeads"				
		N-cad IP	cad-11 IP	β-cat IP	PG IP	Pkp2 IP
Immunoblots	N-cad	+	-	+	+	-
	cad-11	-	+	+	+	-
	β-cat	+	+	+	+	-
	PG	+	+	-	+	-
	p0071	+	-	+	ns	-
	Pkp2	-	-	-	-	+

+: positive reaction of the specific antibody in the immunoblot; -: negative reaction of the specific antibody in the immunoblot; ns: not shown

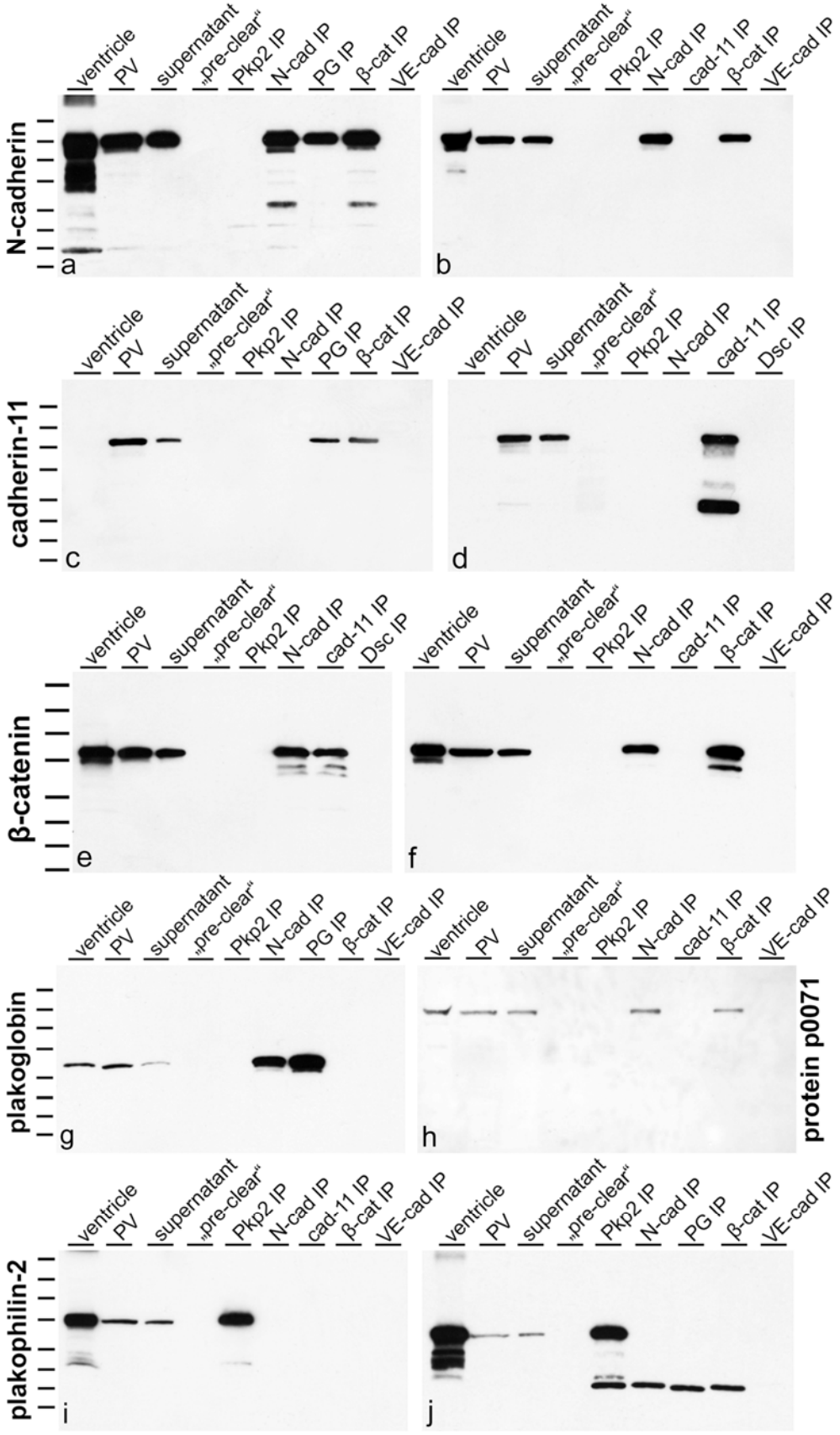
N-cadherin
ventricle
PV
supernatant
„pre-clear"
Pkp2 IP
N-cad IP
PG IP
β-cat IP
VE-cad IP
cad-11 IP
a
b
cadherin-11
Dsc IP
c
d
β-catenin
e
f
plakoglobin
g
h
protein p0071
plakophilin-2
i
j

Figure 41

Figure 41: Immunoprecipitation analyses (IPs) performed with primary cultures of ovine pulmonary heart valve. N-cadherin (N-cad) and cadherin-11 (cad-11), β-catenin (β-cat) and plakoglobin (PG) and plakophilin-2 (Pkp2) proteins were coupled to magnetic beads by using specific antibodies and incubated with cell lysate ("precipitation"). The protein-complexes coupled to the magnetic beads were separated by SDS-PAGE, followed by immunoblot reactions with antibodies against N-cadherin (**a, b**), cadherin-11 (**c, d**), β-catenin (**e, f**), plakoglobin (**g**), protein p0071 (**h**) and plakophilin-2 (**i, j**; vertical names on the left and right hand side). Ovine ventricular myocardial tissue (ventricle), primary cell cultures of ovine pulmonary heart valves (PV), IPs with VE-cadherin (VE-cad) or other antibodies to desmocollins-1 and -3 (Dsc) were used as internal controls. Lysates taken before incubation with antibody-coupled beads (supernatants) were used as positive controls and samples obtained with magnetic beads without antibodies ("pre-clear") were also used as negative controls in parallel. Polypeptide marker bands (bars, left) correspond to 212, 158, 116, 97.2, 66.4, 55.6 42.7 and 34.6 kDa (top to bottom).

4.1.2.8 Cell-cell junctions of valvular interstitial cells grown on different substrates

Recently it has been shown that protein coating of biological material scaffolds can enhance endothelial cell attachment (Akhyari et al., 2009a, b). In view of this finding the influence of different coating strategies on VICs grown in culture has been noted (Gwanmesia et al., 2010) and, therefore, the influence of different cell culture substrates on the types and patterns of cell-cell junctions connecting cultured ovine VICs has been studied to some detail.

To test whether the specific cell growth substrate influences the advent of plakophilin-2 and the ensemble of the other aforementioned AJ proteins of ovine VICs, several different substrates were examined by immunofluorescence microscopy and biochemical analysis. In addition to coating of the plates with collagen I, ovine VICs were also seeded on plates coated with fibronectin, gelatine or poly-L-lysine. In parallel, VICs seeded on plates without coating, were used as controls. The cells were then fixed with methanol/acetone, followed by immunofluorescence microscopy, or prepared for SDS-PAGE followed by immunoblot analysis.

VICs cultured on different substrates showed no essential differences in the molecular composition of AJs. N-cadherin and cadherin-11 were always present (Figure 42a and b) as well as α-catenin (not shown), β-catenin (Figure 42d), plakoglobin and protein p120 (not shown). Likewise, the ability of VICs to form IFs was not influenced by the specific coating substrate (for smooth muscle α-actin containing VICs see, e.g., Figure 42e; for vimentin see Figure 42f). Plakophilin-2 was positive in immunoblot analyses without significant increases or decreases of the amount of protein (Figure 42c). In addition, plakophilin-2 generally colocalized with the other AJ proteins (i.e., see

colocalization with N-cadherin in Figure 43a-e) as shown before for VICs grown on collagen type I-coated plates.

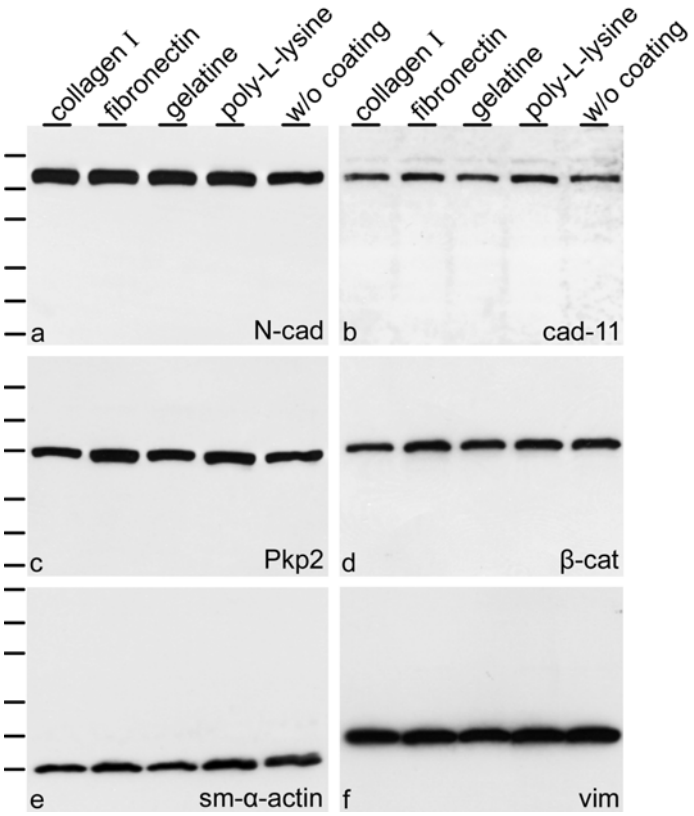

Figure 42: SDS-PAGE, followed by immunoblot analysis of proteins of ovine VICs from pulmonary heart valves cultured on different substrate-coating materials. Collagen type I, fibronectin, gelatine, poly-L-lysine or absence of coating (w/o coating) was. Immunoblot reactions of proteins with antibodies against N-cadherin (N-cad, **a**), cadherin-11 (cad-11, **b**), plakophilin-2 (Pkp2, **c**), β-catenin (β-cat, **d**), smooth muscle α-actin (sm-α-actin, **e**) and vimentin (vim, **f**) do not show markerd differences between the different substrates and coatings. Polypeptide marker bands (bars, left) correspond to 158, 116, 97.2, 66.4, 55.6 and 42.7 kDa (top to bottom).

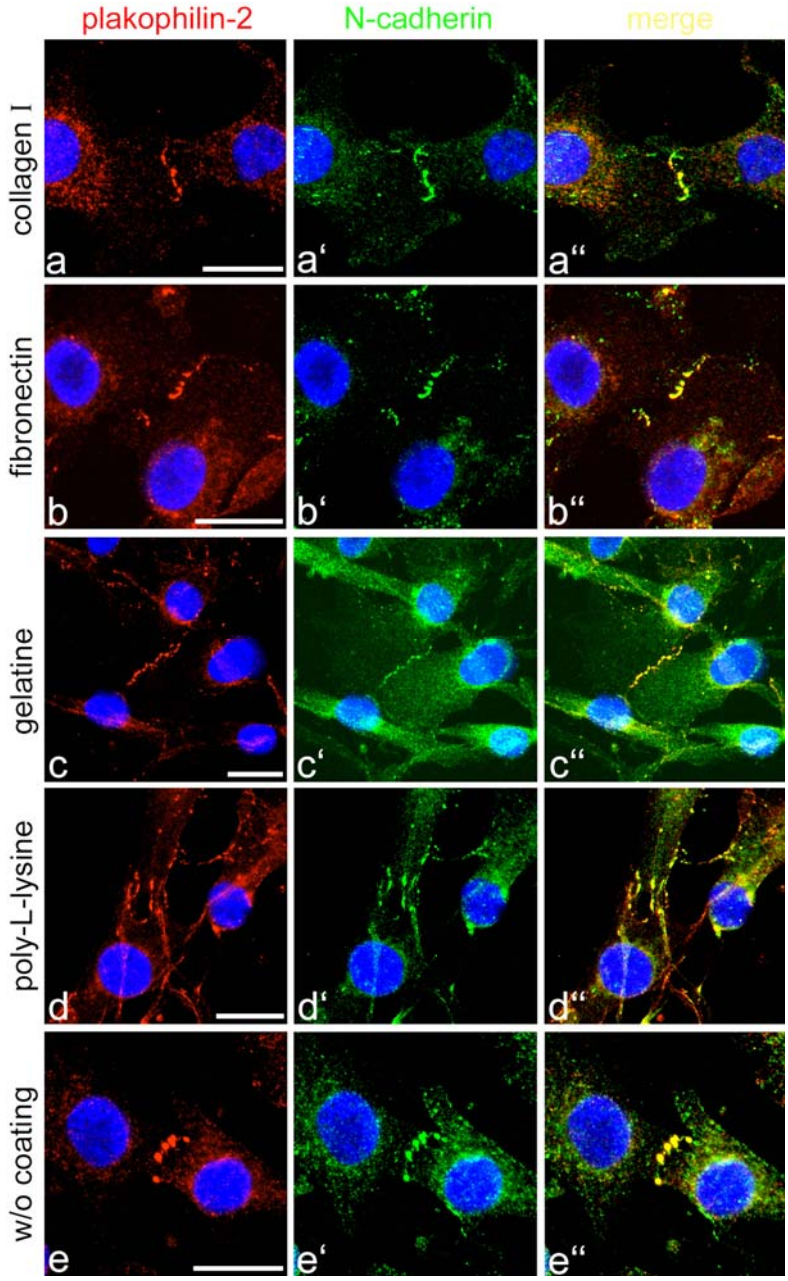

Figure 43: Double-label immunofluorescence micrographs of ovine VICs from pulmonary heart valves cultured on different substrates. Collagen type I (**a-a’’**), fibronectin (**b-b’’**), gelatine (**c-c’’**), poly-L-lysine (**d-d’’**) or absence of coating substance (w/o coating; **e-e’’**) was tested. Antibodies against plakophilin-2 (**a-e**, red) and N-cadherin (**a’-e’**, green) show colocalization at the cell-cell contacts (**a’’-e’’**, yellow). Bars: 20 µm

4.1.2.9 Cell-cell junctions of valvular interstitial cells treated with growth factors

The influence of different growth factors on VIC growth, especially on the advent of plakophilin-2 in the AJs in cultured VICs, was examined by immunofluorescence microscopy and biochemical analyses. VICs were incubated for one week with several

growth factors as additives under serum-free conditions. The following growth factors at various concentrations were tested: TNF-α 0.5 mM, PDGF-BB 5 ng/mL, heparin 50 µg/mL, TGF-β1 1 ng/mL, VEGF 25 ng/mL, INF-γ 10 ng/mL, EGF 10 ng/mL, bFGF 5 ng/mL, bFGF 25 ng/mL and bFGF 10 µg/mL (for general reviews see Brown et al., 2005; Posner and Laporte, 2010; Witsch et al., 2010; for the role of certain growth factors in myocardial tissue regeneration see Santini, 2005). In parallel, VICs were incubated without any growth factor. The AJs of the VICs treated with growth factors showed no significant differences in their ensemble or localization pattern in contrast to untreated VICs. In addition, the appearance of plakophilin-2 and its colocalization with other AJ proteins was also not significantly altered in the presence of the various growth factors added to the culture medium.

4.2 Growth of valvular interstitial cells in three-dimensional systems

To study the spatial arrangements and patterns of behavior of cultured VICs – in particular of those containing plakophilin-2 – a 3D growth model resembling the properties of the native heart valve matrix has been established. Here, three different 3D systems were chosen: 1) VICs growing in a collagen type I gel matrix; 2) VICs growing in a collagen type I gel matrix in combination with an extract of basal lamina matrix material (Matrigel™; for review see Kleinman and Martin, 2005); and 3) VICs allowed to grow on a decellularized heart valve scaffold, using a custom-designed incubation chamber disk (Chapter 3.1.2.3; Figure 6; Akhyari et al., 2009b). The constructs prepared were used for biochemical and immunohistochemical analyses and (immuno-) electron microscopy.

VICs of ovine origin grown in artificial 3D systems composed of collagen type I (with or without Matrigel™) or on a decellularized ovine heart valve matrix, formed cell bodies with numerous processes, as can be seen in hematoxylin-eosin or Masson-Goldner stainings of cross-sections through such preparations (Figure 44a-d). In such preliminary histological studies, the cells appeared well-adapted to their artificial environment, independent from the specific type of 3D construct. Therefore, such 3D matrix constructs repopulated with proliferiferating VICs were embedded for – and examined by – electron microscopy.

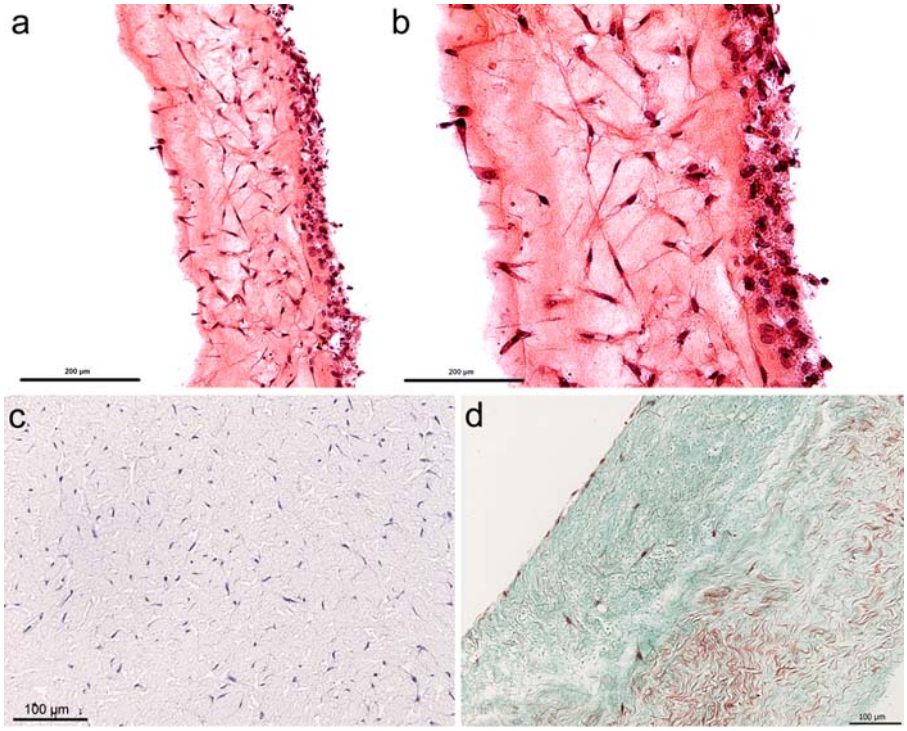

Figure 44: Cross-sections of different formaldehyde-fixed, paraffin-embedded artificial 3D constructs stained with hematoxylin-eosin (**a-c**) or according to Masson-Goldner (**d**). In collagen type I 3D constructs (**a**), some cells have accumulated at one side of the construct, whereas the cells grown in the interior show spreading and the formation of tentacle-like cell processes (higher magnification in **b**). In collagen type I plus Matrigel^{TM} 3D constructs, the cells show less spreading (**c**). In decellularized ovine heart valves re-populated with VICs (**d**), cells have hardly migrated into the scaffold interior and instead are mostly located at the surfaces of the constructs (green: collagen; red: muscle cells). Bars: 200 µm (a and b), 100 µm (c and d)

Collagen type I 3D constructs

Cells growing in collagen type I-based matrix only (Figure 44a and b) form tentacle-like filopodial processes quite similar to those seen in the native valve. Remarkably, some VICs seem to accumulate in higher packing density at one side of the construct, apparently in response to the contacts with the cell-covered culture dish. In general, cells located in the interior of the 3D construct appear to be in contact with each other. Electron microscopy indicates that VICs grown in this artificial 3D scaffold composed only of collagen type I fibers, look healthy for a cultivation period of 1-2 weeks without any additional supply in spite of frequent changes of the DMEM medium containing serum and antibiotics. Under these conditions, the cells effectively colonize in the collagen scaffold provided with frequent cell-cell contacts of the *puncta adhaerentia* type (Figure 45).

Collagen type I / Matrigel™ 3D constructs

VICs grown in 3D constructs composed of collagen I together with Matrigel™ (Figure 44c) apparently do not form as many tentacle-like processes as in the system containing collagen type I only. Moreover, VICs grown in collagen type I enriched by Matrigel™ appear to be more densely packed. However, in the electron microscope these cells often appear somewhat degenerated and stress-damaged, showing a relatively high proportion of cytoplasmic vacuoles (Figure 46a).

Decellularized heart valve scaffolds re-populated with VICs

VICs grown on decellularized heart valve matrix have shown the least promising results: The cells are hardly able to penetrate – and to migrate or extend into – the matrix and show only very few cell-cell contacts (Figures 44d and 46b). Moreover, in individual cells which managed to migrate into the construct system rarely showed cell-cell contact regions with an AJ-type ultrastructure (Figure 46c and d).

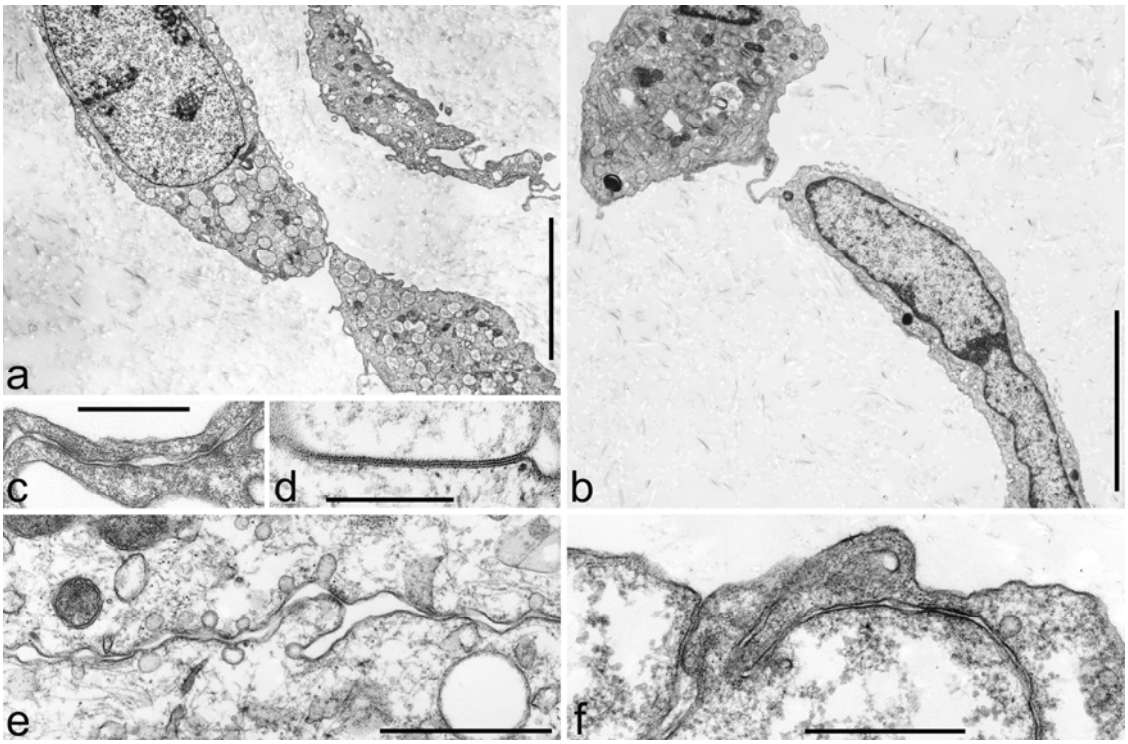

Figure 45: Electron micrographs of ultrathin sections through 3D matrix constructs containing collagen type I with entrapped VICs. Cells are loosely dispersed and form cell-cell contacts either at cell processes (**a-c**) or between juxtanuclear cell bodies of adjacent cells (**d-f**). The cell contacts are of the AJ *puncta adhaerentia* type (**c**, **e**). GJs are also present but occur quite infrequently (**d**). VICs show the typical invagination appearance of the so-called *manubrium adhaerens*-type junction (**f**; Wuchter et al., 2007). Note that some of the cells are very rich in cytoplasmic vesicles indicating shortness in oxygen or nutritives. The empty-looking regions in **f**) may represent glycogen-storage aggregates. Bars: 5 µm (a, b), 0.6 µm (c, f), 0.3 µm (d), 0.8 µm (e)

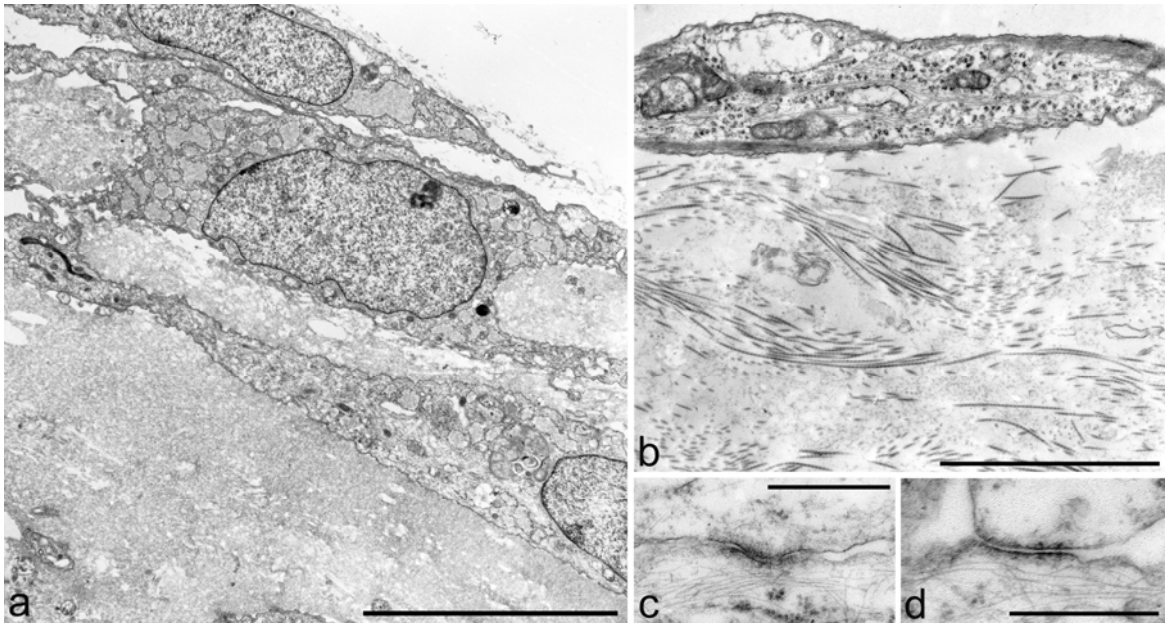

Figure 46: Electron micrographs of ultrathin sections through 3D matrix constructs composed of collagen type I and Matrigel™ or decellularized heart valves seeded with VICs. The cells of collagen type I 3D constructs are densely packed, which may partly reflect the enormous shrinkage, and some also show signs of stress and cell death (**a**). Electron micrographs of ultrathin sections through decellularized heart valves of ovine origin show that only few cells migrate into the depth of the heart valve scaffolds, most of them remain at the outside (**b**).VICs present cell-cell contact structures resembling VIC-AJs (**c**-**d**). The ECM of the decellularized heart valve consists of seemingly intact collagen bundles, in some places interspersed with residual cell debris (**b**). Cells which have managed to migrate into the scaffold at some places form cell-cell contacts of the AJ type (**c**, **d**). Bars: 8 µm (a), 3 µm (b), 0.5 µm (c, d)

4.2.1 The proteins involved in the cell-cell contacts between valvular interstitial cells in three-dimensional constructs

3D constructs composed of collagen type I, collagen type I/Matrigel™ or preparations of decellularized heart valve scaffolds were seeded with cultured VICs and these were allowed to grow after various periods of time, followed by examination using immunofluorescence microscopy to identify and characterize the specific growth forms and the AJs formed.

Collagen type I 3D constructs

Here the cells grow in sparse, widely distributed arrays throughout the artificial matrix region, mostly appearing with long filopodial processes which in certain patterns form cell-cell contacts (Figure 47a and b). In these cells smooth muscle α-actin filament bundles seem highly decreased, notably in comparison with the vimentin IFs (Figure 47a-c''). In comparison with VICs grown in 2D monolayer cultures, the amount of nuclei

positive for the proliferation marker Ki-67 is strongly decreased (for double immunolabeling with vimentin see Figure 47d and for a survey comparison with Ki-67-positive cells see Figure 47e; for references see also Taylor et al., 2002; Butcher and Nerem, 2004; Benton et al., 2009).

Collagen type I / Matrigel™ 3D constructs

The VICs located in the cortical parts of the 3D constructs are generally positive for both vimentin and smooth muscle α-actin, whereas the cells that have penetrated deeper into the construct often show a decrease in smooth muscle α-actin immunostaining intensity (Figure 48a). As already suggested in the interpretations of hematoxylin-eosin stainings (Figure 44c) and electron micrographs (Figure 46a), VICs here form relatively few AJs. Nevertheless, the AJs present are positive for N-cadherin (Figure 48b) and cadherin-11 (not shown) as well as for α-catenin (not shown), β-catenin (Figure 48c), plakoglobin and protein p120 (not shown).

Decellularized heart valve scaffolds re-populated with VICs

Double-label immunofluorescence microscopy using sections through frozen or fixed and paraffin-embedded 3D constructs has shown that cells that have remained in the periphery of the construct bodies are positive both for vimentin and smooth muscle α-actin (Figure 49a-a'') whereas cells deeper in the interior of the scaffold seem to contain reduced smooth muscle α-actin (Figure 49a). Cross-sections of fixed and paraffin-embedded 3D constructs show the typical dot-like *puncta adhaerentia* AJs positive for N-cadherin (Figure 49b) and cadherin-11 (not shown), α-catenin (not shown), β-catenin (Figure 49c), together with protein p120 and plakoglobin (not shown). These AJs often occur in clusters (double-label immunofluorescence staining of vimentin and β-catenin in Figures 49d and e).

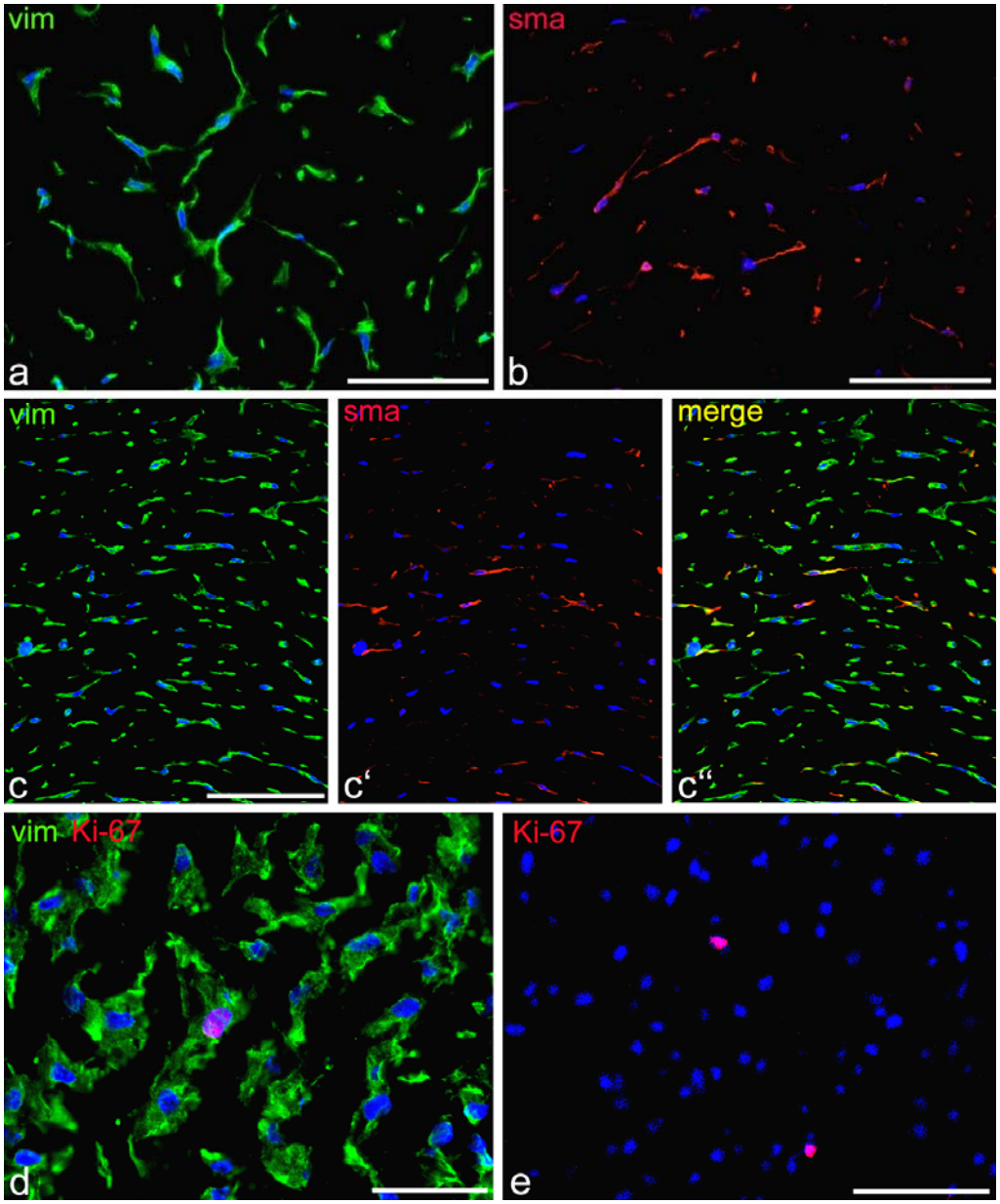

Figure 47: Immunofluorescence micrographs of cross-sections through frozen or paraffin-embedded 3D constructs containing ovine pulmonary VICs grown in a collagen type I gel matrix. The VICs often form cell processes positive for vimentin (vim, green, **a**) and smooth muscle α-actin (sma, red, **b**) but some of them may give the impression of reduced smooth muscle α-actin labeling (**c-c''**) and reduced cell proliferation as indicated by the reaction of protein Ki-67 antibodies (red, **d**; green, vimentin; single staining in a lower magnification in **e**). Bars: 100 µm (a, b, c, e), 50 µm (d)

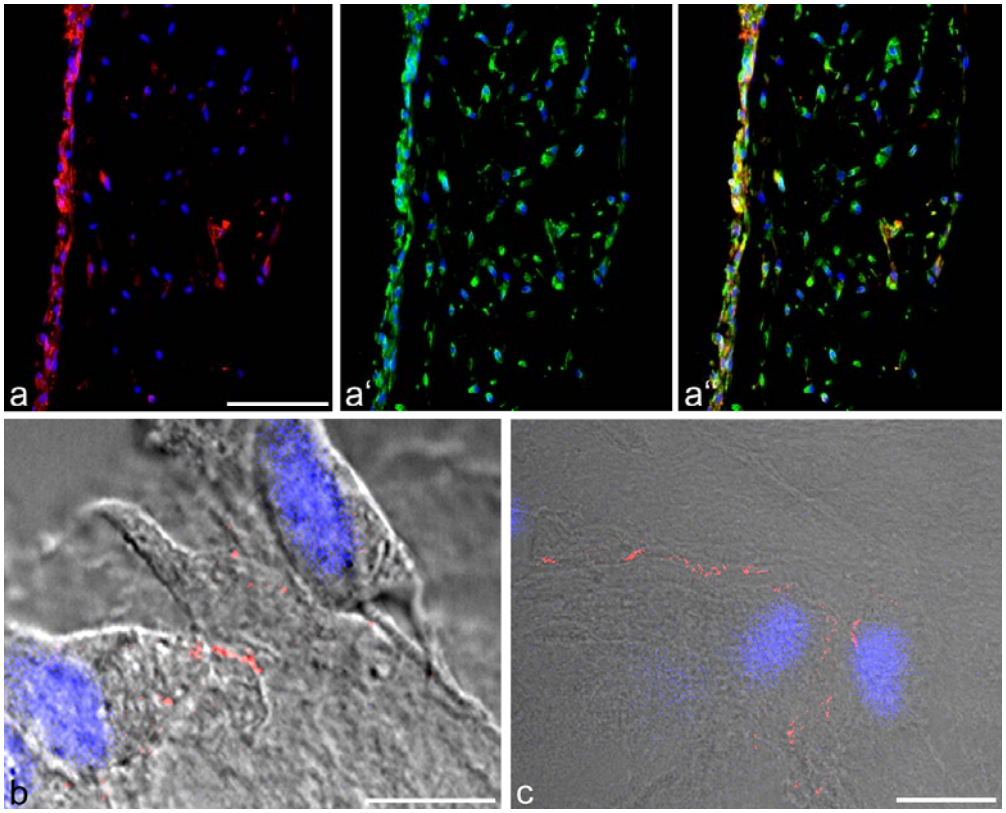

Figure 48: Immunofluorescence micrographs of cross-sections through paraffin-embedded 3D constructs containing collagen type I and Matrigel™ with entrapped VICs of ovine origin. VICs located in the outer parts of the constructs show strong reactions for smooth muscle α-actin, whereas cells grown in the interior are mostly negative for this actin (**a**). Cells growing both near the surface and in the interior are all positive for vimentin (**a'**; for a merged image see **a''**). Cell-cell AJs between adjacent cells are positive for N-cadherin (**b**) and β-catenin (**c**). Bars: 100 µm (a), 10 µm (b), 20 µm (c)

Due to the insufficient ultrastructural quality of the decellularized re-seeded scaffolds and the collagen type I / Matrigel™ constructs (see, e.g., Figure 46), these two approaches were not followed up in the subsequent experiments. Instead, the following examinations were focused exclusively on constructs composed of VICs grown in collagen type I gels.

Here, N-cadherin and cadherin-11 are generally noted at AJs (Figure 50). The appearance of these AJs strongly resembles those described for native valves, and most of them are of the *puncta adhaerentia* type. In contrast to the AJ plaque proteins involved, i.e. α-catenin (not shown), β-catenin, protein p120 and plakoglobin (Figure 51), plakophilin-2 and other desmosomal proteins always appear negative in immunofluorescence microscopy (not shown). Double-label immunofluorescence stainings of N-cadherin with either β-catenin or plakoglobin show on the one hand perfect colocalization of the transmembrane glycoproteins and the plaque proteins. On the other

hand, however, certain AJ regions are also detected in which the colocalization of AJ glycoproteins and plaque proteins is not evident (Figure 52). Electron micrographs of cross-sections through frozen 3D constructs reacted with antibodies against certain AJ proteins and immunogold-labeled secondary antibodies (Figure 53; for a detailed description of this method see chapter 3.4.2) demonstrate that N-cadherin shows the by far the most extensive and contiguous labeling of the junctional ultrastructure (Figure 53a), whereas cadherin-11 has been localized to a much smaller extent (Figure 53b). Among the plaque proteins, protein p120 (Figure 53c) and β-catenin (Figure 53d) immunogold-labeling have been the most intense, whereas plakoglobin has shown marked differences from AJ to AJ (Figure 53d).

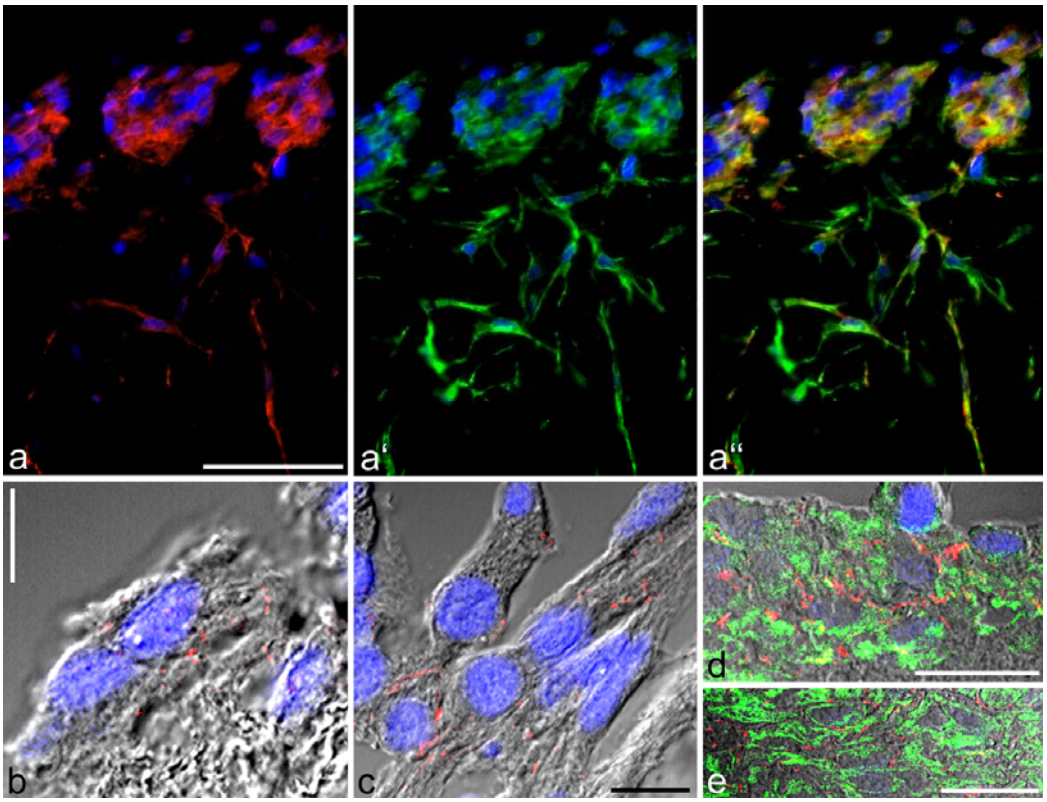

Figure 49: Immunofluorescence micrographs of cross-sections through formaldehyde-fixed, paraffin-embedded 3D constructs of decellularized ovine heart valves re-populated with ovine VICs and allowed to grow for 1-2 weeks in a custom-designed incubation chamber. (**a-a''**) Double-labeling of the outer part of such a construct with antibodies against smooth muscle α-actin (red, **a**) and vimentin (green, **a'**), showing the distribution of VICs. Only the cells which remain near the surface of the construct show strong overall double-labeling (**a''**, yellow merged image), whereas the cells that are located in the depth of the construct are characterized by decreased smooth muscle α-actin labeling (merged picture, **a''**). Cell-cell AJ contacts of the *puncta adhaerentia* type contain N-cadherin (red, **b**) and the plaque-building protein β-catenin (red, **c**; for double-label results see **d** and **e**). Bars: 100 µm (a), 10 µm (b, c), 20 µm (d, e)

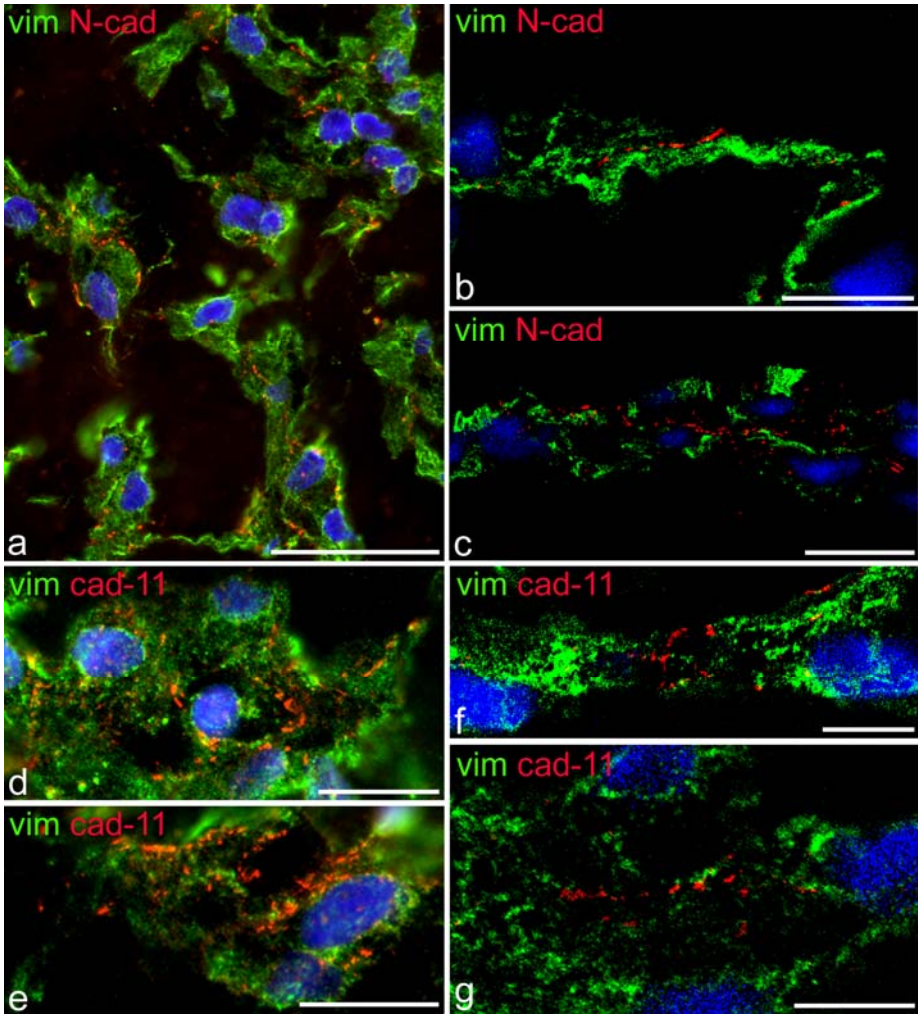

Figure 50: Immunofluorescence micrographs of cross-sections through formaldehyde-fixed, paraffin-embedded 3D collagen type I constructs re-populated with ovine VICs and immunostained with antibodies against N-cadherin (red, **a-c**) and cadherin-11 (red, **d-g**), both in double-label staining with vimentin (green). Bars: 50 µm (a), 20 µm (b, c, d, e), 10 µm (f, g)

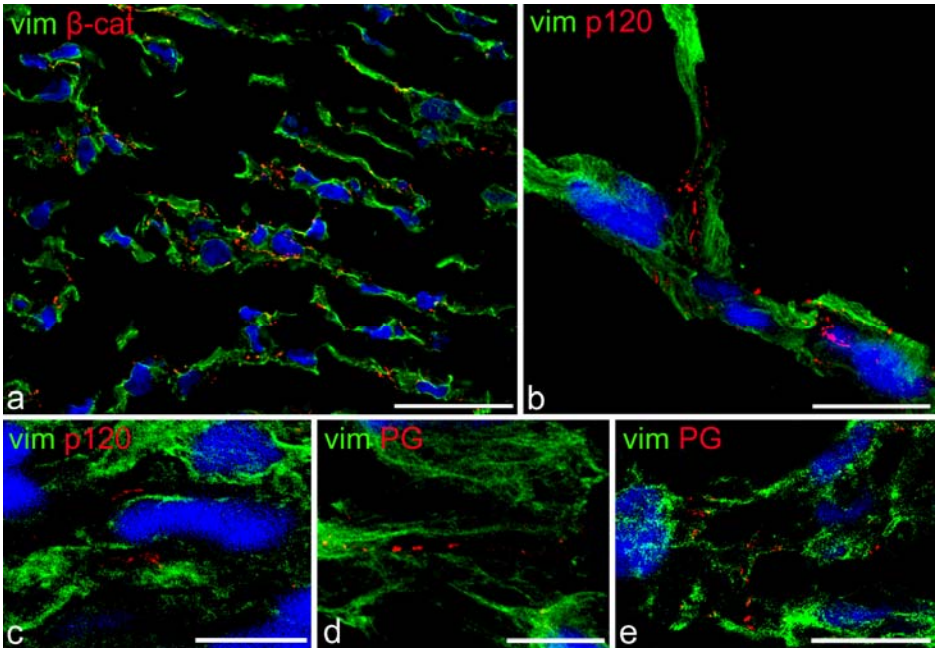

Figure 51: Double-label immunofluorescence micrographs of cross-sections through frozen samples of collagen type I 3D constructs with entrapped ovine VICs, using antibodies against vimentin (green) and β-catenin (**a**, red), protein p120 (**b, c**, red) and plakoglobin (**d, e**, red). Note the characteristic *puncta adhaerentia*-like appearance of most AJs. Bars: 50 µm (a), 20 µm (b, e), 10 µm (c, d)

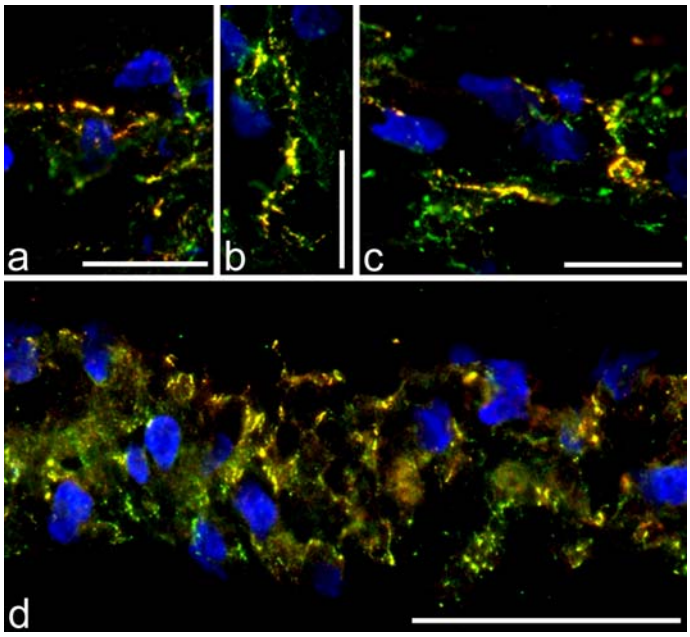

Figure 52: Double-label immunofluorescence micrographs of cross-sections through formaldehyde-fixed, paraffin-embedded collagen type I 3D constructs with entrapped ovine VICs. Neighboring VICs show several punctate cell-cell contacts indicating colocalization (yellow) of N-cadherin (green) and β-catenin (red, **a-c**) or plakoglobin (red, **d**). Shown are the merged label pictures. Bars: 20 µm (a, b, c), 50 µm (d)

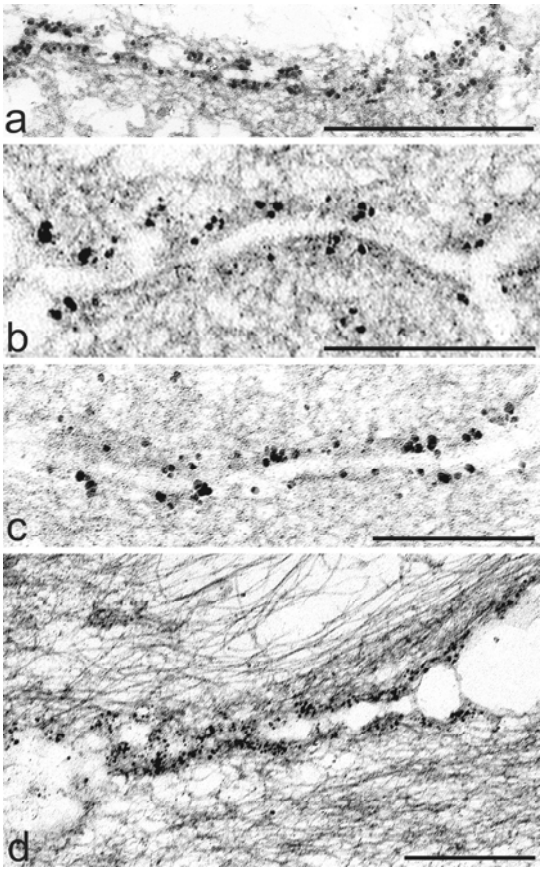

Figure 53: Immunogold-label electron micrographs of cross-sections through frozen collagen type I 3D constructs of ovine VICs, showing AJs decorated with antibodies against N-cadherin (**a**), cadherin-11 (**b**), protein p120 (**c**), and β-catenin (**d**). Bars: 0.5 µm (a, d), 0.3 µm (b, c)

4.2.2 Valvular interstitial cells grown in three-dimensional collagen type I constructs re-isolated and grown as primary culture

To test whether the process leading to the absence of plakophilin-2 in AJs of 3D collagen type I constructs is reversible, primary cultures of VICs obtained from the 3D constructs aforementioned were examined by immunofluorescence microscopy and biochemical analysis.

VICs isolated from 3D collagen type I constructs and grown again as primary 2D monolayer cell cultures show again an increase of the proportion of smooth muscle α-actin-positive cells (Figure 54a). Moreover, such VICs also start to proliferate to a relatively higher proportion as indicated by immunofluorescence staining with Ki-67 (Figure 54; for a comparison with VICs grown in 3D model systems see Figure 47d and e). As already reported for primary cultures of VICs freshly derived from ovine, bovine and human heart valves, VICs re-isolated from 3D collagen type I constructs and grown again as primary cultures also form AJs with N-cadherin and cadherin-11, complexed with α- and β-catenin,

protein p120 and plakoglobin (for double-label immunofluorescence micrographs see Figure 55). And again, plakophilin-2 is rapidly acquired in AJs of such VICs re-isolated from 3D collagen type I constructs and grown again as primary cultures. In such cultures AJs showed colocalization of all the AJ proteins aforementioned (for an example see Figure 56).

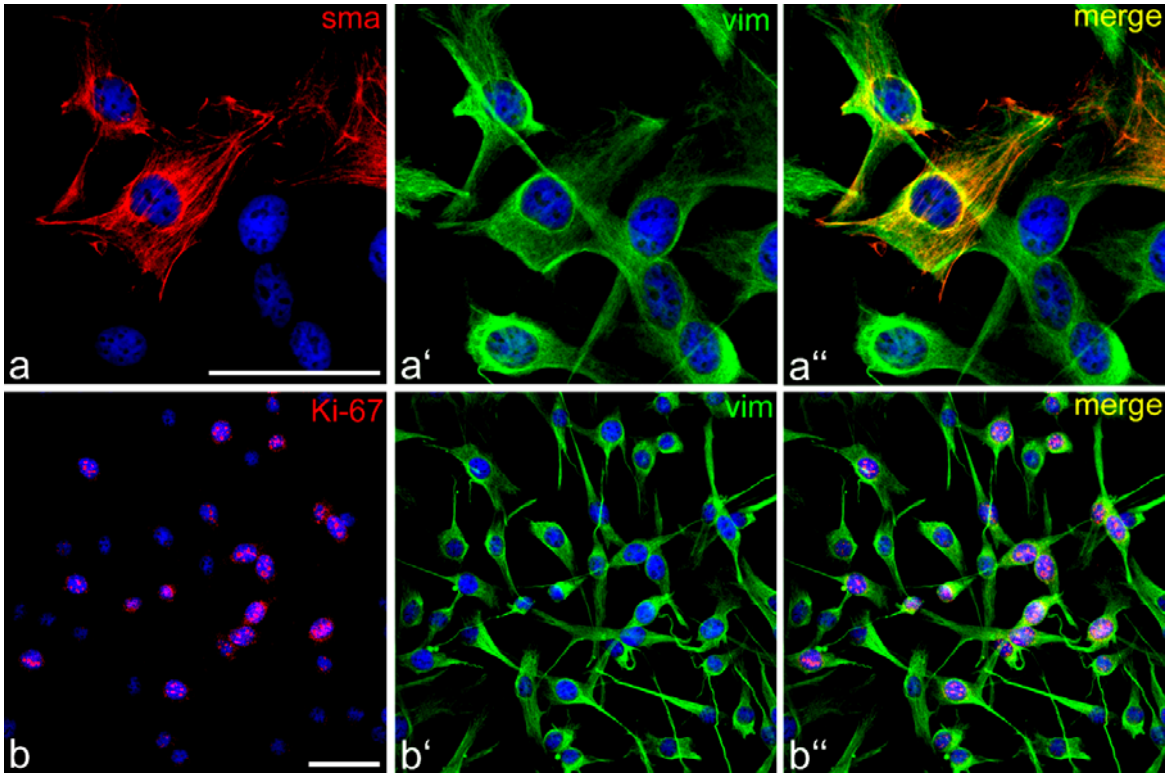

Figure 54: Double-label immunofluorescence micrographs of ovine pulmonary VICs grown first in 3D collagen type I constructs, then re-isolated and grown as primary cultures. (**a-a’’**) VICs labeled with antibodies against smooth muscle α-actin (red, **a**) and vimentin (green, **a’**), show an increase of the amount of smooth muscle α-actin-positive cells in comparison to the ubiquitous marker vimentin (merged picture, **a’’**). (**b-b’’**) The proliferation activity is also markedly increased as indicated by double-label immunostainings for vimentin (green, **b’**) and the nuclear protein Ki-67 (red, **b**): Here nearly every cell is positive for Ki-67 (merged picture, **b’’**). Bars: 50 µm

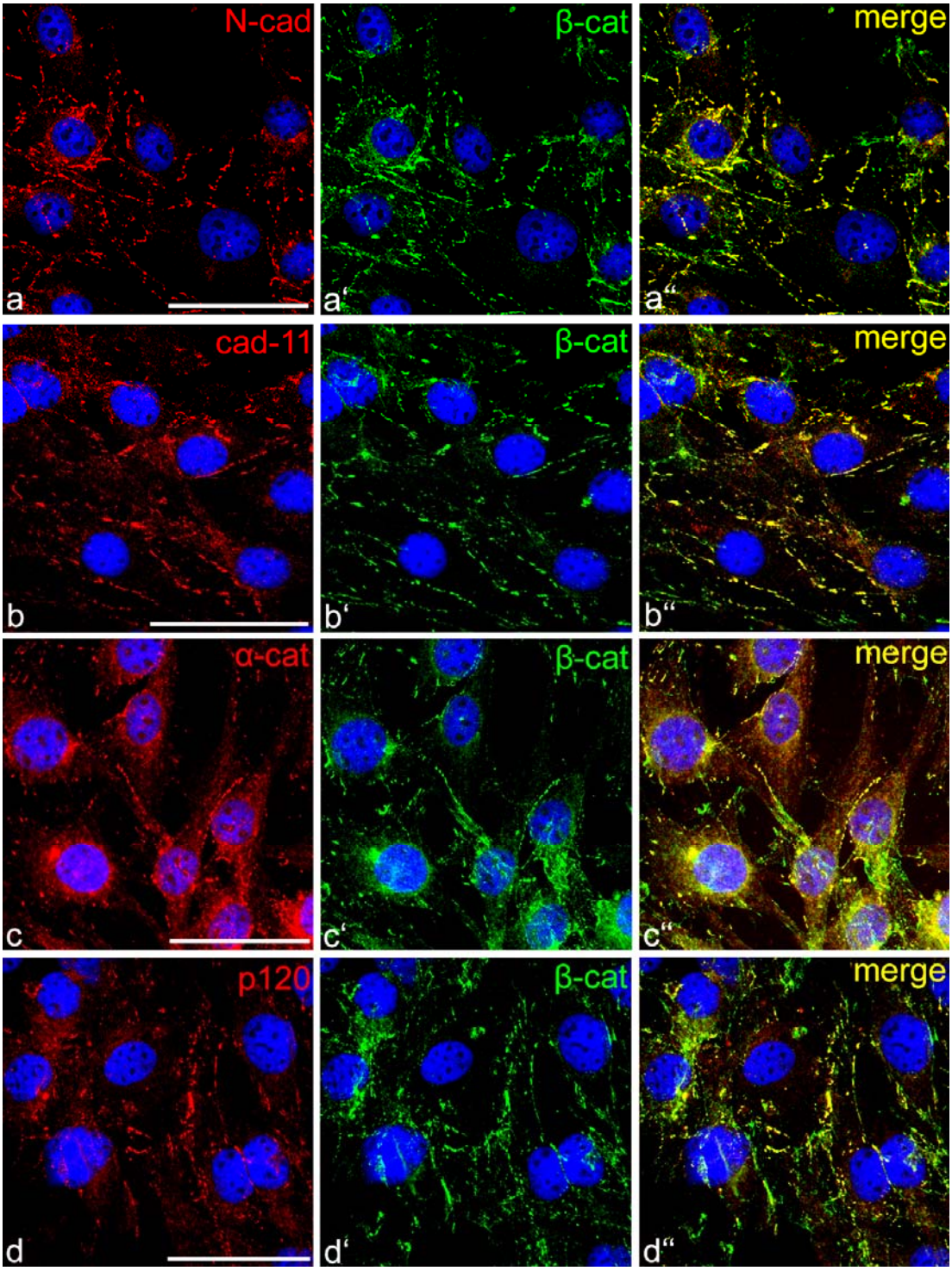

Figure 55: Double-label immunofluorescence micrographs of ovine pulmonary VICs grown first in 3D collagen type I constructs, re-isolated and grown as primary cultures. Antibodies against N-cadherin (red, **a**), cadherin-11 (red, **b**), α-catenin (red, **c**) and protein p120 (red, **d**) or antibodies against β-catenin (green, **a'-d'**) show far-reaching colocalization in characteristic *puncta adhaerentia* AJ structures (merged pictures: a''-d''). Bars: 50 µm

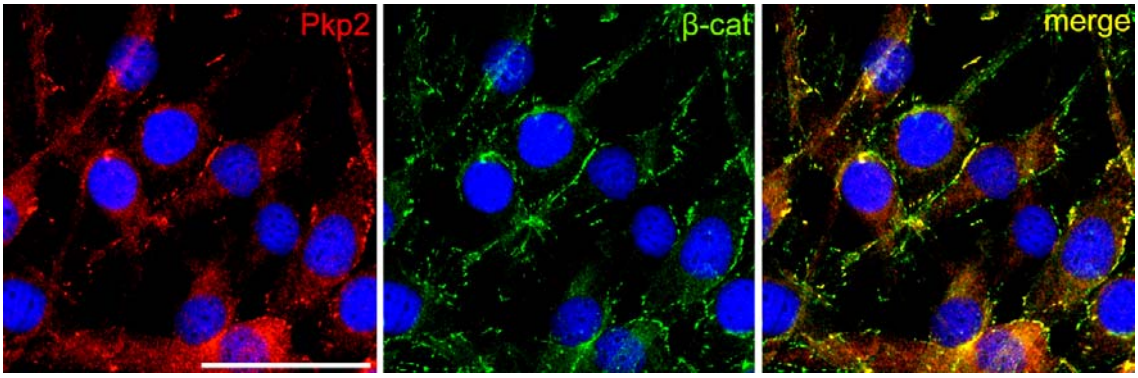

Figure 56: Double-label immunofluorescence micrographs of ovine pulmonary VICs grown first in 3D collagen type I constructs, re-isolated and grown as primary cultures. Antibodies against plakophilin-2 (red) show frequent sites of colocalization (yellow, merged picture) with β-catenin (green). Bar: 50 µm

4.2.3 Immunoblot analyses of the adherens junction molecule ensembles of valvular interstitial cells in three-dimensional collagen type I constructs – a summary

As demonstrable in immunoblot analyses, I have shown that VICs growing in collagen type I 3D constructs – in contrast to reports of others (for a review see Flanagan and Pandit, 2003) – are able to modify their ECM environment by *de novo* secretion of elastin and fibronectin (Figure 57). This holds for both ovine and bovine VICs grown in 3D constructs, using two differently distributed collagen type I preparations (Figure 57, lanes 1-4). Ovine and bovine VICs in primary cultures derived from freshly prepared heart valves (Figure 57, lanes 5 and 6) show elastin and fibronectin in similar amounts and deposition patterns as VICs grown in 3D collagen type I constructs, re-isolated and grown again in primary cultures (Figure 57, lane 9).

N-cadherin (Figure 58a) and cadherin-11 (Figure 58b) as well as α-catenin (not shown), β-catenin (Figure 58c), plakoglobin (Figure 58d) and protein p120 (Figure 58e) show positive reactions in immunoblot analyses of both ovine and bovine VICs grown in 3D constructs composed of collagen type I (Figure 58, lanes 1-4) as it is also seen with VICs grown in primary cultures derived from freshly prepared ovine or bovine heart valves (Figure 58, lanes 5 and 6). VICs grown in 3D collagen type I constructs, re-isolated and grown again as primary cultures (Figure 58, lane 9) also show positive reactions for N-cadherin (Figure 58a) and cadherin-11 (Figure 58b) as well as for α-catenin (not shown), β-catenin (Figure 58c), plakoglobin (Figure 58d) and protein p120 (Figure 58e).

VICs grown in 3D constructs composed of collagen type I contain strongly decreased amounts or even an absence of plakophilin-2 (Figure 58f, lanes 1-4). VICs grown in 3D collagen type I constructs, re-isolated and grown again as primary culture also acquire plakophilin-2 (Figure 58f, lane 9).

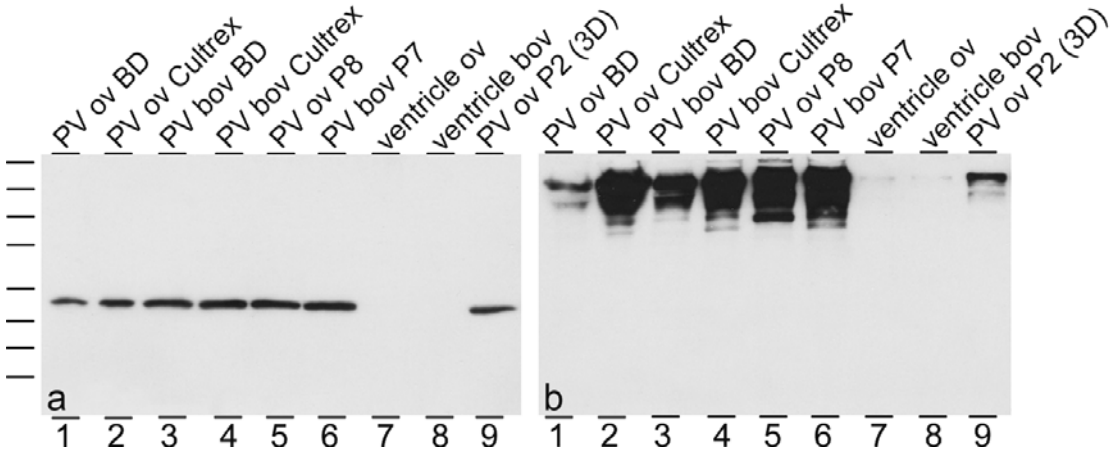

Figure 57: SDS-PAGE followed by immunoblot analyses using antibodies against elastin and fibronectin. PK ov/bov BD, PK ov/bov Cultrex as well as PK ov P8/PK bov P7 and PV ov P2 (3D) show positive reactions for both elastin (**a**) and fibronectin (**b**). Ventricle ov/bov is used as control and shows negative reactions for both antibodies.
Abbreviations: lanes 1 and 3: PK ov/bov BD, ovine/bovine VICs grown in 3D constructs using collagen type I from BD Biosciences; lanes 2 and 4: PK ov/bov Cultrex, ovine/bovine VICs grown in 3D constructs using collagen type I from Cultrex; lanes 5 and 6: PK ov P8/PK bov P7, VICs grown in primary culture of passage 8/7, originally derived from freshly prepared ovine/bovine pulmonary heart valve; lanes 7 and 8: ventricle ov/bov, ovine/bovine ventricular myocardial tissue; lane 9: PV ov P2 (3D), ovine VICs grown first in 3D collagen type I constructs, then re-isolated and again grown as primary cultures of passage 2. Polypeptide marker bands (bars, left) correspond to 212, 158, 116, 97.2, 66.4, 55.6 and 42.7 kDa (top to bottom).

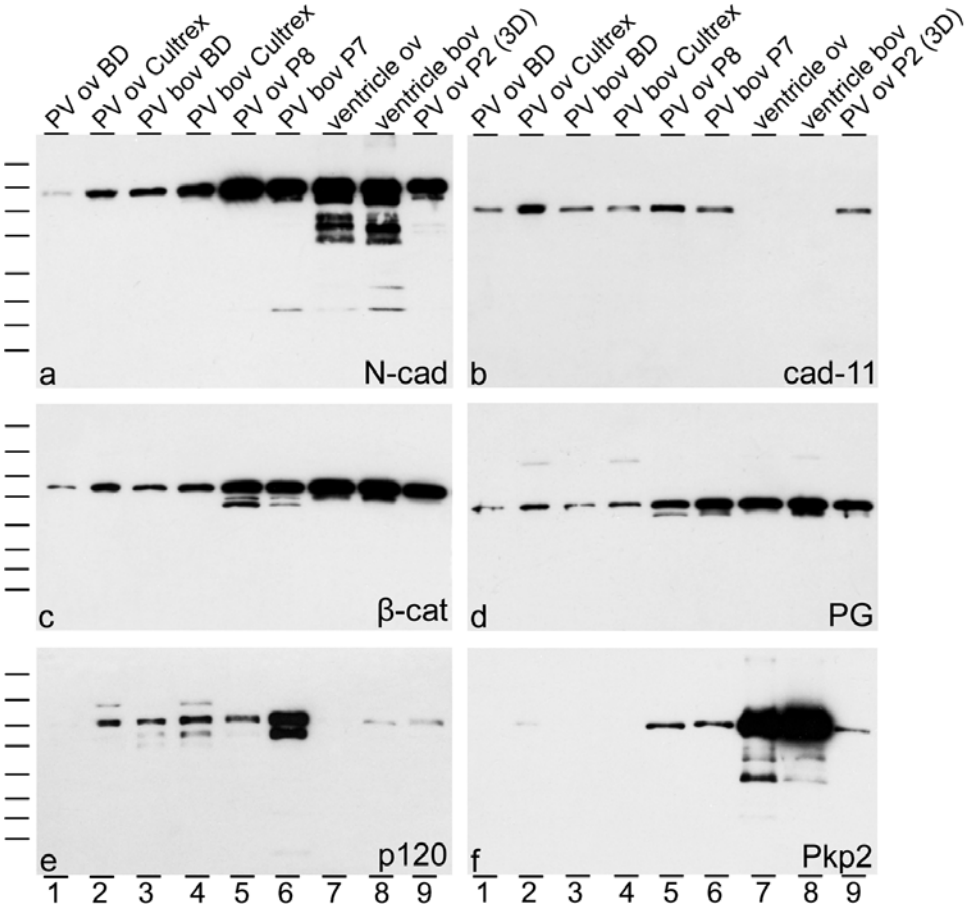

Figure 58: SDS-PAGE followed by immunoblot analyses using antibodies against N-cadherin (N-cad, cadherin-11, β-catenin, plakoglobin, protein p120 and plakophilin-2. PK ov/bov BD, PK ov/bov Cultrex, PK ov P8/PK bov P7 and PV ov P2 (3D) show positive reactions for N-cadherin (N-cad; **a**), cadherin-11 (cad-11; **b**), β-catenin (β-cat; **c**), plakoglobin (PG; **d**) and for protein p120 (p120; **e**), with minor reactions seen for PV ov BD using antibodies against N-cadherin and protein p120. Plakophilin-2 (Pkp2; **f**) shows positive reactions only in 2D VIC cultures (PK ov P8/PK bov P7 and PV ov P2 [3D]) as well as in ventricle ov/bov but no or only very weak reactions in 3D culture constructs (lanes 1-4). Reactions for cadherin-11 (**b**) and protein p120 (**e**) are weak in ventricle ov/bov, maybe due to minor proportions of these proteins in the samples used whereas reactions for N-cadherin, β-catenin, plakoglobin and plakophilin-2 are clearly positive in ventricle ov/bov (lanes 7 and 8).
Abbreviations: lanes 1 and 3: PK ov/bov BD, ovine/bovine VICs grown in 3D constructs using collagen type I from BD Biosciences; lanes 2 and 4: PK ov/bov Cultrex, ovine/bovine VICs grown in 3D constructs using collagen type I from Cultrex; lanes 5 and 6: PK ov P8/PK bov P7, VICs grown in primary culture of passage 8/7, originally derived from freshly prepared ovine/bovine pulmonary heart valve; lanes 7 and 8: ventricle ov/bov, ovine/bovine ventricular myocardial tissue; lane 9: PV ov P2 (3D), ovine VICs grown first in 3D collagen type I constructs, then re-isolated and again grown as primary cultures of passage 2. Polypeptide marker bands (bars, left) correspond to 212, 158, 116, 97.2, 66.4, 55.6 and 42.7 kDa (top to bottom).

4.3 Valvular interstitial cells in fetal hearts

As the AJ-type cell-cell contacts between the VICs of adult hearts *in situ* and in culture had shown distinct differences, in particular by the advent of plakophilin-2 in cell culture, I have also examined fetal mammalian heart valves, comparing VICs *in situ* and in culture in prenatal hearts. For these studies I have used heart valves from fetal pigs at day 85 post-fertilization and human heart valves derived from a fetus of week 20 of pregnancy.

4.3.1 Valvular interstitial cells in fetal hearts *in situ*

In the electron microscope, porcine fetal VICs present a compact morphology, mostly without long filopodial processes, but where they are present, their cell-cell contacts mostly occur at these structures (Figure 59a). These AJ contacts are also of the *puncta adhaerentia* type, not infrequently with prominent plaques providing attachment for IFs or microfilament-bundles (Figure 59). The ECM structures, especially the collagen fiber bundles, seem to be relatively sparse and not as homogenously extending throughout the valve interior as typical for adult heart valves (for comparisons see Figures 15 and 16). Similar to adult VICs *in situ*, however, fetal VICs also tend to "embrace" and align collagen fiber bundles with filopodial processes in tentacle-like patterns (Figure 59b; for comparison with adult VICs see Figure 16). Like adult VICs, fetal VICs *in situ* also are positive for vimentin IFs (Figure 60). In addition – and in stark contrast to the situation observed for adult heart valves – the fetal valves studied have shown a marked subpopulation of cells positive for smooth muscle α-actin (Figure 60b'; for comparison with adult heart valves see Figure 17), which occur either in clusters or as individual cells in the matrix cell meshwork (Figure 60b'). Numerous vimentin-positive interstitial cells can also be seen to form cell processes which protrude into – and extend throughout – the adjacent myocardial tissue (Figure 60a; compare with adult myocardium, e.g., Figure 20). Finally, fetal VICs *in situ* lack the cardiac muscle-specific IF protein desmin as can best be seen in double-label immunostainings of heart valve tissue with adjacent myocardium, using antibodies specific for cardiac α-actin (cf. Moll et al., 2006) in comparison with antibodies against vimentin or against desmin (Figure 61).

In immunofluorescence microscopy the cell-cell AJs connecting fetal VICs *in situ* show an ensemble of proteins similar to that found in VICs of adult hearts, i.e. N-cadherin (Figure 62a) and cadherin-11 (not shown), together with α- and β-catenin (Figure 62a and b), plakoglobin as well as proteins p120 and p0071 (not shown).

Surprisingly, plakophilin-2 has been found in fetal VICs *in situ*, a finding which has only been seen so far in adult VICs growing in culture (see preceeding chapters). This occurrence of plakophilin-2 in fetal VICs has been noted in AJs between vimentin-positive VICs in typical dot-like patterns (Figure 63a) or at AJ contacts of VICs in close vicinity to the endocardial cells lining the valve (Figure 63b). Moreover, plakophilin-2 here again shows colocalization with α- and β-catenin (Figure 63c-c''), proteins p120 and p0071, plakoglobin and proteins ZO-1-3 (not shown). Remarkably, plakophilin-2 is not restricted to certain clusters of cells within the valvular matrix (Figure 64a) but also occurs in AJs connecting VICs deep in the interior of the heart valve (Figure 64b). Other desmosomal molecules, including desmoglein and desmocollin as well as desmoplakin, have consistently been found to be absent in AJs of fetal heart valve tissue (not shown). As a final remark, the occurrence of plakophilin-2 does not correlate with the spatial distribution of smooth muscle α-actin-positive cells in the valves (not shown). For an overview of proteins involved in the AJs of fetal VICs *in situ* see Table 8.

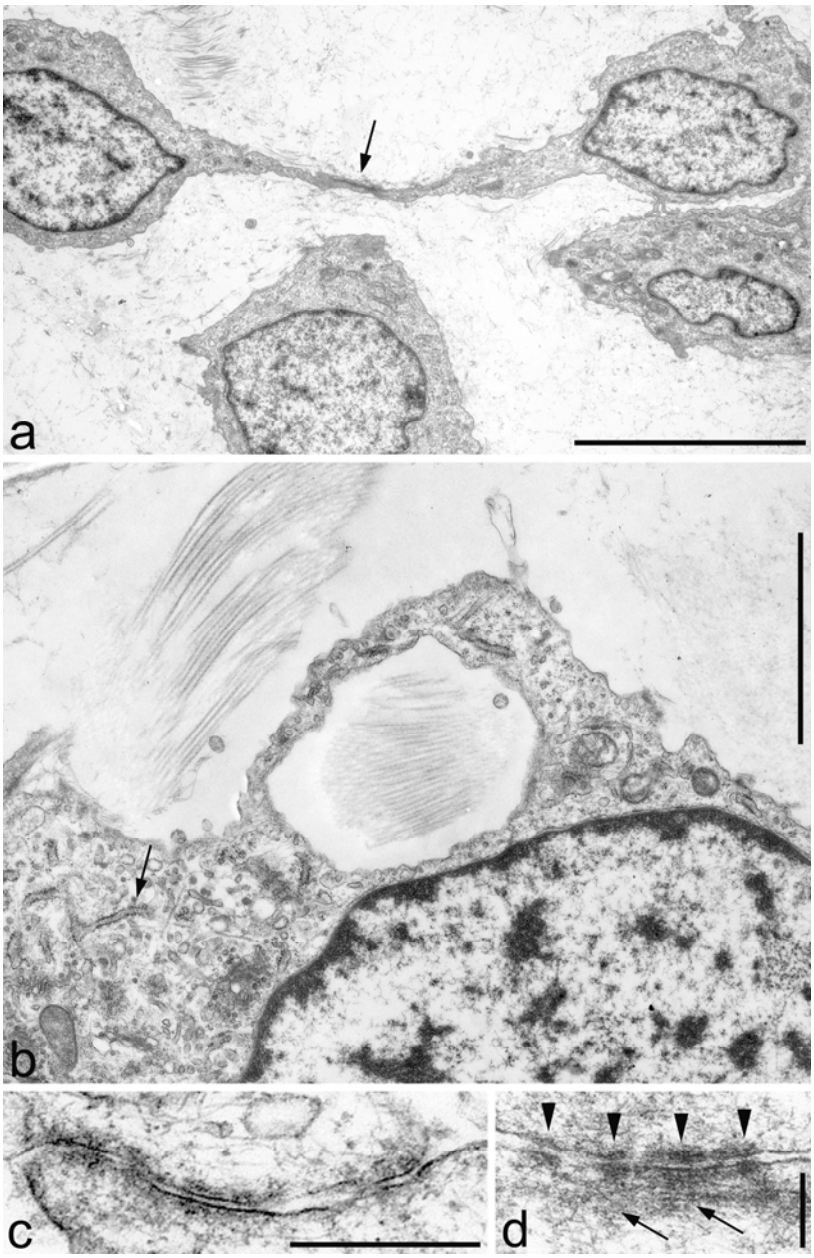

Figure 59: Electron micrographs of cross-sections through fetal porcine aortic heart valves. (**a**) The cells are embedded in ECM and tend to form thin filopodial processes with cell-cell contacts of the AJ type connecting such processes (e.g., arrow in **a**). (**b**) Some of the filopodial processes also wrap around collagen fiber bundles. Note the abundant amount of endoplasmatic reticulum and Golgi cisternae in the cytoplasm of the fetal VICs (arrow in **b**). Cell-cell contacts of the AJ type occur as clusters, can be observed in some places which may suggest usion (**c**), while in other regions distinct individual *puncta adhaerentia* can be resolved (**d**; see arrowheads). Note occasional lateral associations of AJ plaque structures with IF bundles (**d**; arrows). Bars: 5 µm (a), 2 µm (b), 0.5 µm (c), 0.2 µm (d)

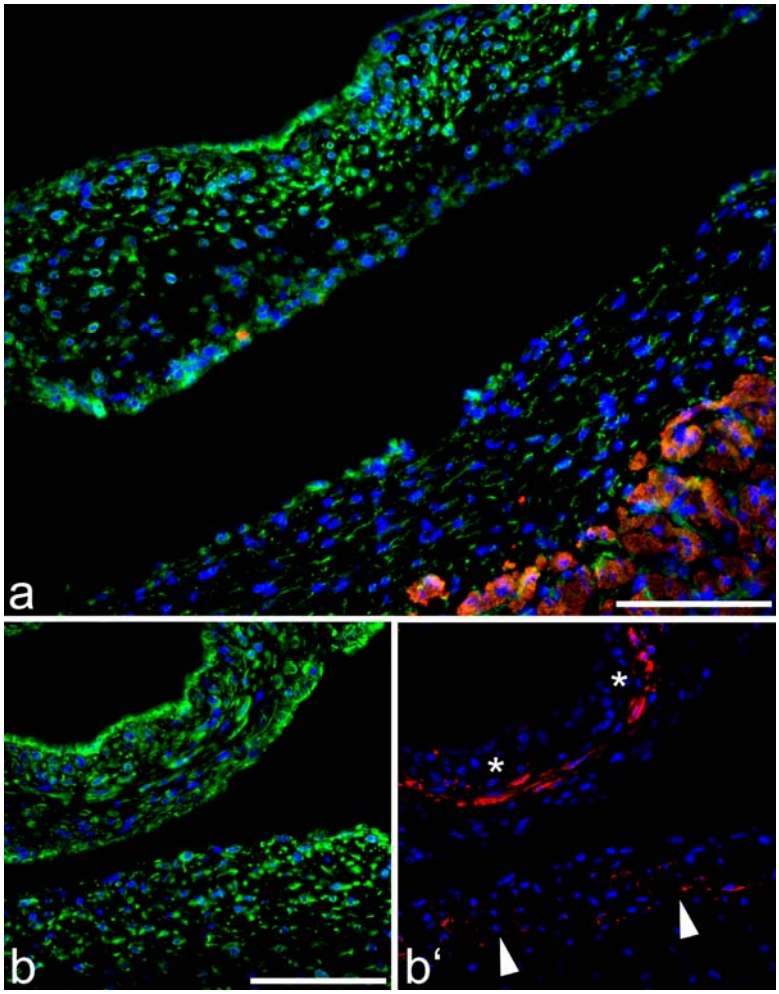

Figure 60: Double-label immunofluorescence micrographs of cross-sections through formaldehyde-fiexd, paraffin-embedded fetal porcine mitral heart valves with adjacent myocardium. (**a**) Mesenchymal connective tissue cells (VICs) are stained with antibodies against vimentin (green) and cardiomyocytes with antibodies against cardiac α-actin (red). Vimentin-positive VICs and endothelial cells are present in the heart valve (upper part in **a**) as well as in the layer of connective tissue bordering the myocardium. Vimentin-positive cells are also found between the myocardial cells. (**b-b'**) Besides the vimentin-positive VICs (**b**, green), the heart valves also harbor a population of cells positive for smooth muscle α-actin (**b'**; red; see also arrowheads and asterisks in **b'**). Nuclei are stained blue. Bars: 100 µm

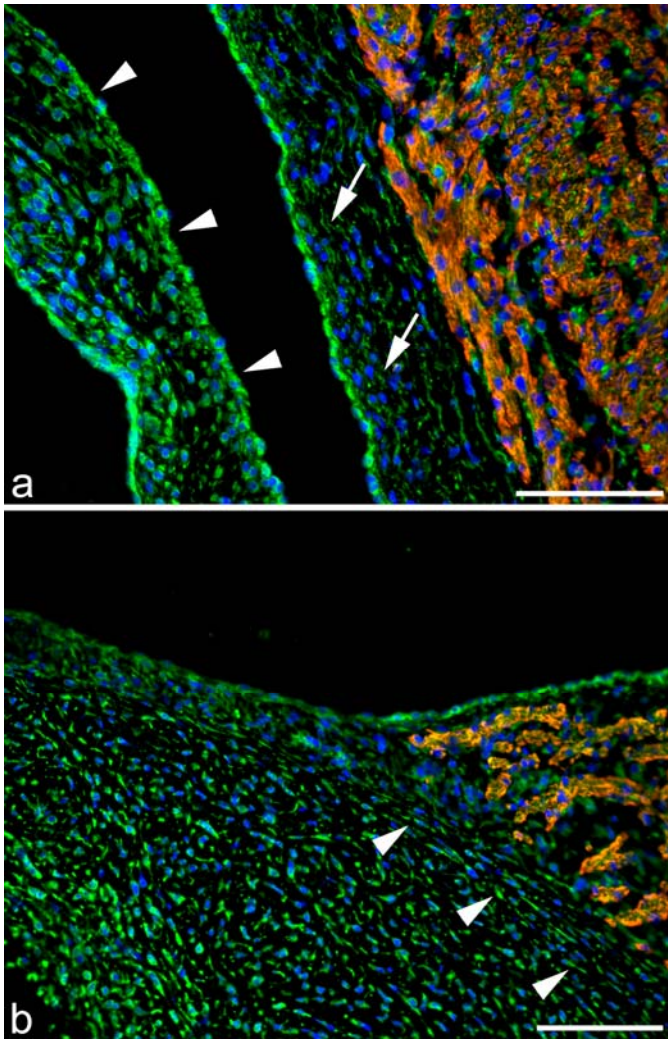

Figure 61: Double-label immunofluorescence micrographs of cross-sections through formaldehyde-fixed, paraffin-embedded fetal porcine tricuspid heart valves with adjacent myocardium. Mesenchymal cells are labeled with antibodies for vimentin (green) and cardiomyocytes with antibodies against desmin (red). Heart valve leaflets are positive for vimentin only and do not contain any desmin-positive cells (arrowheads in **a**). Moreover, the connective tissue adjacent to the myocardium shows only vimentin-positve cells (arrows in **a**). The intersection of the myocardium and the valve is clearly recognizable by the lack of desmin-positive cells in the valvular base (arrowheads in **b**). Note the vimentin-positive endothelial cells and cardiac fibroblasts interspersed between the cardiomyocytes. Nuclei are stained blue. Bars: 100 µm

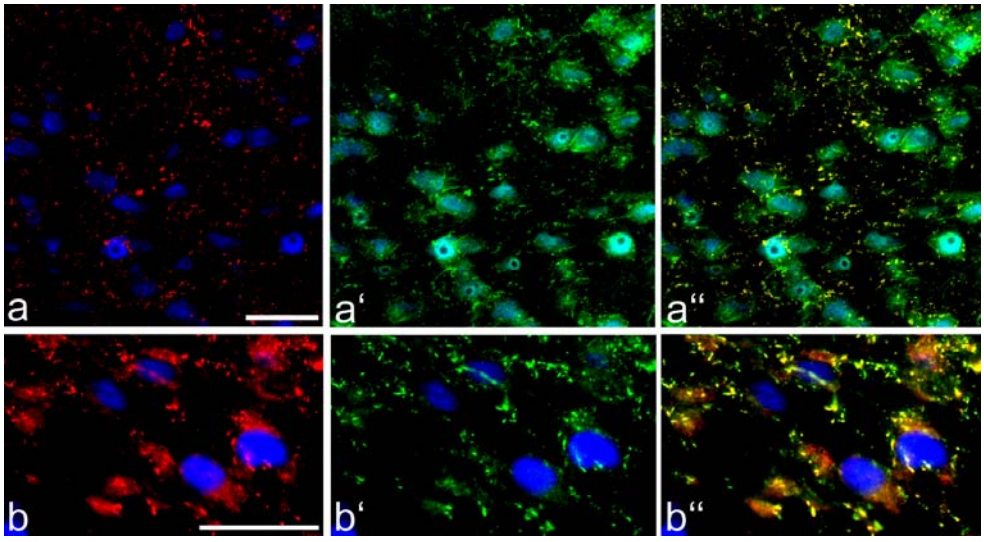

Figure 62: Double-label immunofluorescence micrographs of cross-sections through frozen fetal human and porcine heart valve tissue immunostained with antibodies against cell-cell junction proteins. (**a-a’’**) Several cell-cell contacts of the AJ type connect VICs in fetal porcine heart valve tissue containing N-cadherin (**a**, red) and the plaque protein β-catenin (**a’**, green), colocalizing in some AJ structures (merged picture **a’’**, yellow). (**b-b’’**) Here α-catenin (**b**, red) and β-catenin (**b’**, green) colocalize in cell-cell contacts between the VICs of the valve interior (**b’’**, yellow). Nuclei are stained blue. Bars: 20 µm

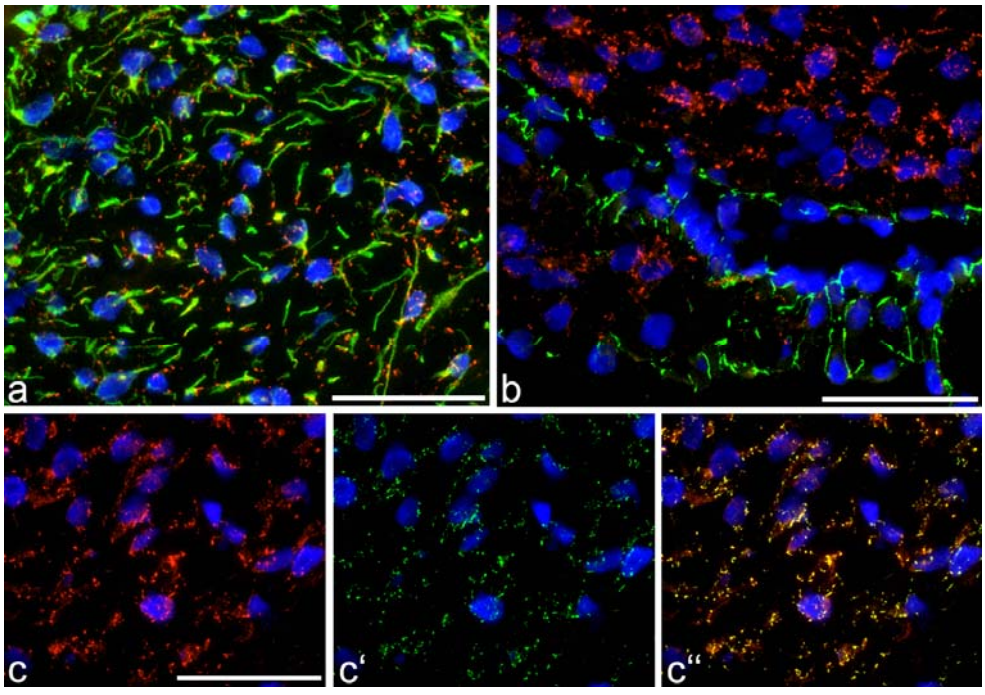

Figure 63: Double-label immunofluorescence micrographs of cross-sections through human fetal heart valves, showing the additional desmosomal plaque protein plakophilin-2 occurring in the cell-cell junctions connecting VICs of the heart valve interior. (**a**) Vimentin-positive VICs, showing cell-cell AJ contacts labeled with a specific antibody against plakophilin-2 in the central position of the valve (vimentin, green; plakophilin-2, red). (**b**) Plakpophilin-2 (red) also occurs in regions just beneath the endocardium (labeled by VE-cadherin, green). (**c-c’’**) Colocalization of β-catenin (**c**, red) and plakophilin-2 (**c’**, green; for merged picture see **c’’**). Nuclei are stained blue. Bars: 50 µm

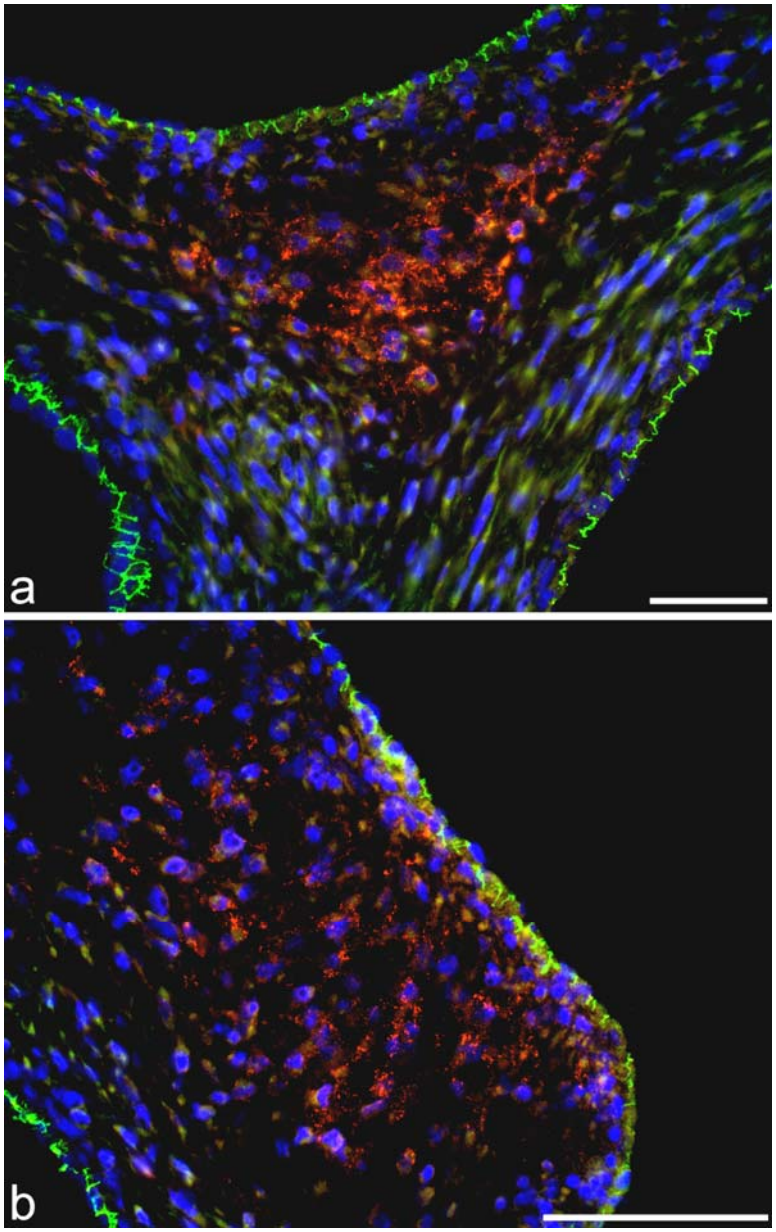

Figure 64: Double-label immunofluorescence survey micrographs of cross-sections through formaldehyde-fixed, paraffin-embedded porcine fetal heart valve tissue, showing the spatial distribution of plakophilin-2-positive (red) VICs in the heart valve interior. (**a**) Clusters of VICs positive for plakophilin-2 are located in the center of a heart valve, whereas cells more adjacent to the endothelial lining (VE-cadherin; green) appear to be negative for this protein. (**b**) Dispersed localization of plakophilin-2-positive VICs (red) in the heart valve in direct comparison with some cells occurring in close vicinity to the endothelial lining (VE-cadherin, green). Nuclei are stained blue. Bars: 50 µm (a), 100 µm (b)

4.3.2 The fetal endocardium[1]

In the electron microscope, one category of the cells of the embryonal and the fetal endocardium shows a typical endothelial ultrastructural appearance with some cell processes, a basal lamina (Figure 65a) and zonula-type as well as distinct individual cell-cell contacts, including an extended, AJ-type *zonula adhaerens* (for reviews see Palade, 1988; Wagner, 1988; Heimark and Schwartz, 1988; Franke et al., 1988; Madri et al., 1988). The specific organization of the fetal endocardium, with special details of its endothelial AJs is presented in Figure 65. Concerning the proteins involved in the cell-cell AJs of the endocardial endothelium, VE-cadherin is present as a typical endothelial cell marker in all contacts, whereas the immunolocalization results for N-cadherin have been rather inconsistent and sometimes appear to be interrupted (Figure 66a and b). By contrast, cadherin-11 consistently appears in colocalization with VE-cadherin (Figure 66c). The plaque proteins α- and β-catenin, afadin, ZO-1 and -3 as well as proteins p120 and p0071 also colocalize with VE-cadherin in endothelial cells (not shown). JAM-A, specific claudins and occludin all show positive reactions as expected for an endothelial cell-cell junction (not shown; Lampugnani et al., 1995; for related reviews see, e.g., Dejana et al., 1995, 2000; Bradfield and Imhof, 2004; Dejana, 2004; Bazzoni, 2006; Ferreri and Vincent, 2008; Moll et al., 2009).

While desmosomal proteins like desmoglein-2 and desmocollin-2 as well as desmoplakin are always absent in fetal endocardial cell-cell junctions (Figure 67), the desmosomal plaque protein plakophilin-2 surprisingly can show positive reactions in the endothelial cells of the endocardium (for colocalization of plakophilin-2 and β-catenin in VICs as well as in adjacent endothelial cells of the endocardium see Figure 68). This occurrence is not ubiquitous but seems to be spatially restricted to some parts of the valves (for a survey of a valve leaflet with colocalization of plakophilin-2 and β-catenin see Figure 69 as well as Figure 70c and d). Plakophilin-2 is also often seen to colocalize with N-cadherin and cadherin-11 as well as with α-catenin, afadin and proteins ZO-1 and -3 (not shown). Remarkably, the cells of the endocardial endothelium which are positive for VE-cadherin and cover the connective tissue above the myocardium are mostly negative for plakophilin-2, whereas in these plakophilin-2 is of course psitive in the IDs of the adjacent cardiomyocytes (Figure 70a). Endothelial AJs of other blood vessels like fetal

[1] In this thesis the term “endocardium” is used in a strictly histological meaning and shall include (i) the primary and definitive cardiac endothelium as a continuous layer of cells characterized by endothelial cell type marker structures and molecules as well as (ii) all the dispersed connective tissue cells located in the subjacent matrix (“cardiac cushion matrix”). The term does not include any implication related to the specific origin and process of differentiation of the cells mentioned (for review articles see Mikawa, 1999; Mjaatvedt et al., 1999).

aorta and arterioles of various calibres, which have been examined as controls, do not contain plakophilin-2-positive junctions (Table 8; not shown). For an overview of proteins involved in the AJs of fetal endocardial endothelium *in situ* see Table 8.

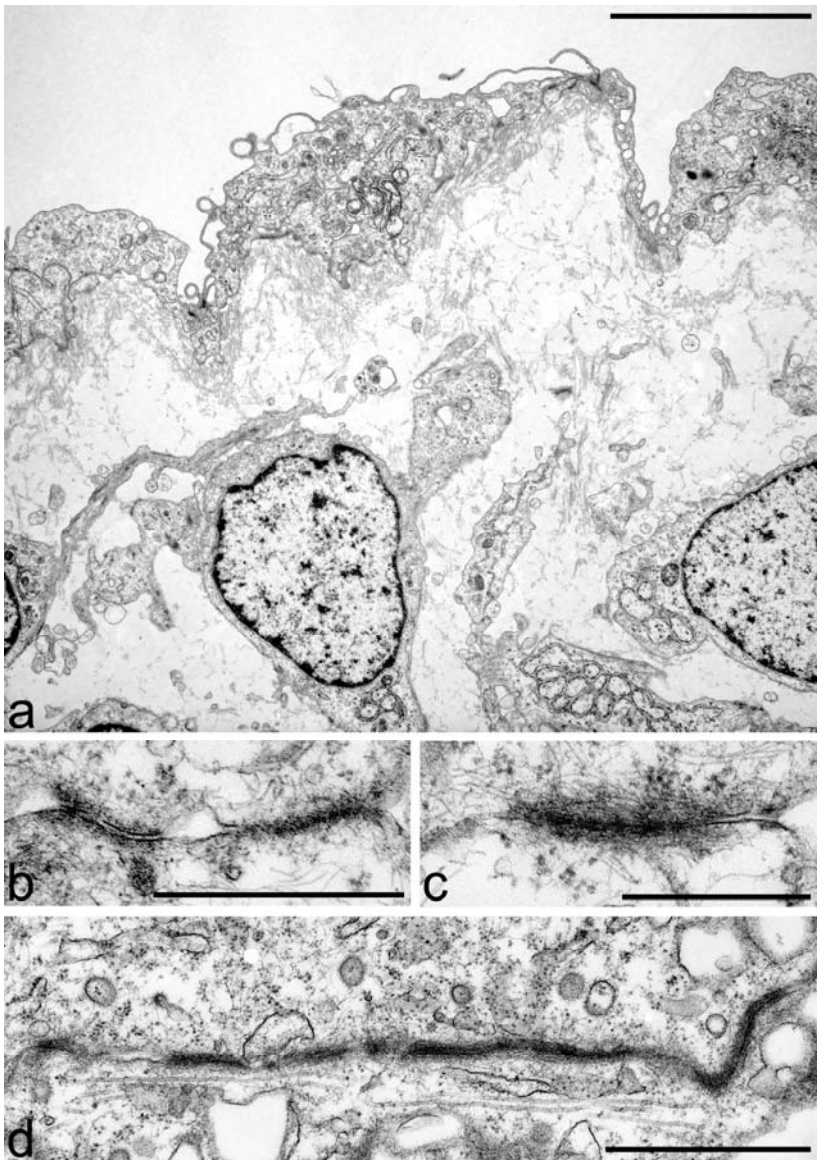

Figure 65: Electron micrographs of cross-sections trough fetal porcine mitral and tricuspid heart valve tissue, showing the endothelial cell layer of the endocardium and their cell-cell contacts. (**a**) Endothelial cell layer (top), coat of a tricuspid heart valve (bottom part) in which some VICs are embedded in collagenous ECM. (**b-d**) Cell-cell structures of the AJ type connecting endothelial cells of a mitral heart valve. Note the prominent IF bundles associated with the AJ shown in (**c**) and the microtubule bundle associated with the extended junction in (**d**). Bars: 5 µm (a), 1 µm (b), 0.5 µm (c), 1.5 µm (d)

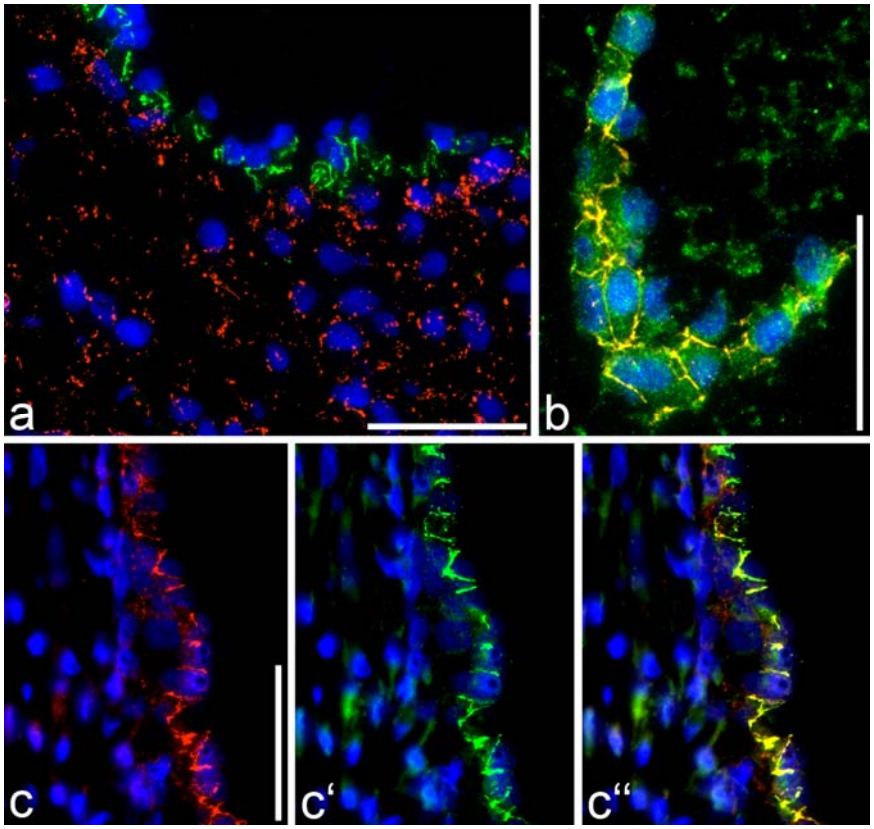

Figure 66: Double-label immunofluorescence micrographs of cross-sections through frozen fetal human heart valve tissue. (**a-b**) The reaction of N-cadherin is not fully coincident with the endothelial cells lining the heart valve. In some areas of the valve, N-cadherin-positive structures (red) clearly do not colocalize with VE-cadherin structures (**a**; green), whereas in other regions such a colocalization is seen (**b**; yellow). Note the abundance of N-cadherin in the cell-cell contacts of the VICs underneath the endothelial layer (**a**, red). (**c-c’’**) Cadherin-11 (**c**; red), in contrast, always colocalizes with VE-cadherin (**c’**; green) as demonstrated in the merged picture (**c’’**; yellow). Nuclei are stained blue. Bars: 50 µm

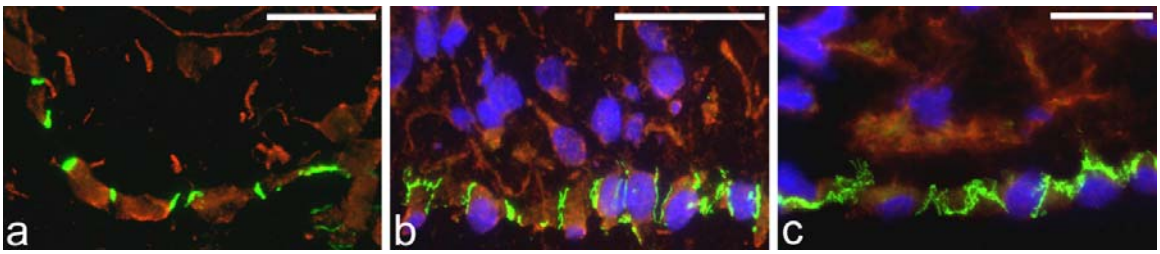

Figure 67: Double-label immunofluorescence micrographs of cross-sections through formaldehyde-fixed, paraffin-embedded fetal human (**a**, **b**) and porcine (**c**) heart valves. Dsg-2 (**a**; red) and Dsc-2 (**b**; red) as well as desmoplakin (**c**; red) are absent in the cell-cell contacts of fetal human endocardial endothelium, which in turn shows positive reactions for VE-cadherin only (**a-c**; green). Note also that the adjacent VICs show no positive reactions for antibodies against any of these desmosomal proteins. Nuclei are stained blue. Bars: 20 µm (a, c), 40 µm (b)

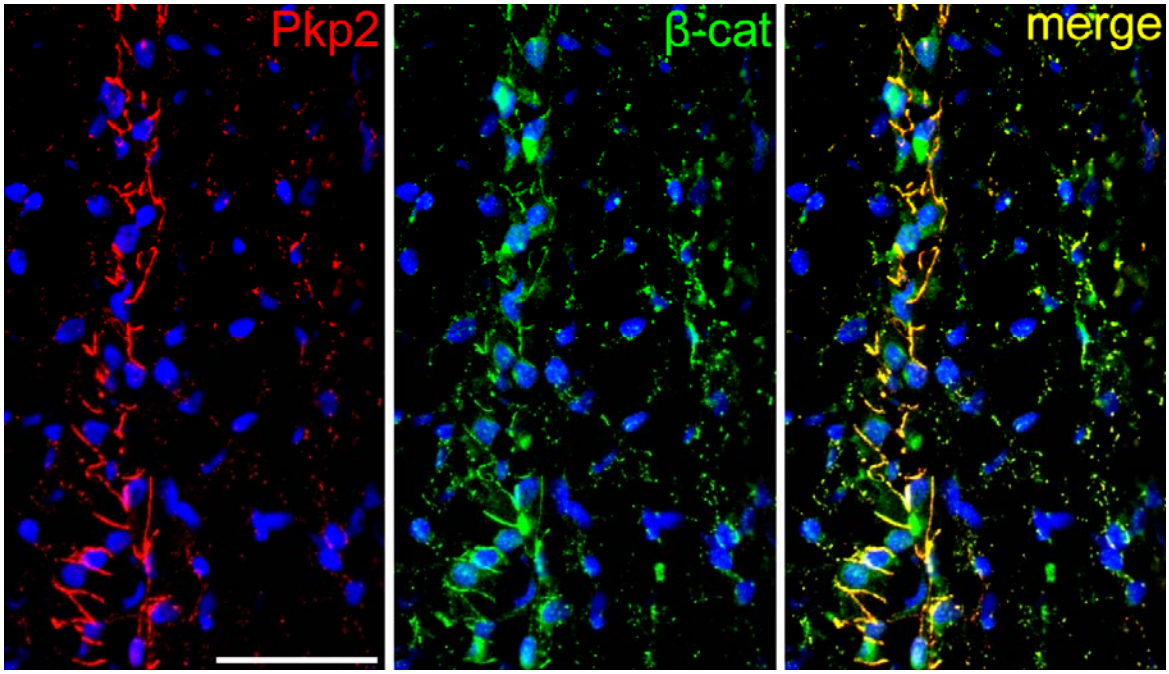

Figure 68: Double-label immunofluorescence micrograph of cross-sections through a frozen fetal human heart valve, showing plakophilin-2 in endothelial cells of the endocardium lining the heart valve and in adjacent VICs. Plakophilin-2 (Pkp2; red) colocalizes with β-catenin (β-cat; green) in the endothelial cells of the endocardium as well as in several of the AJs of the VICs (see the merged picture; yellow). Nuclei are stained blue. Bar: 50 µm

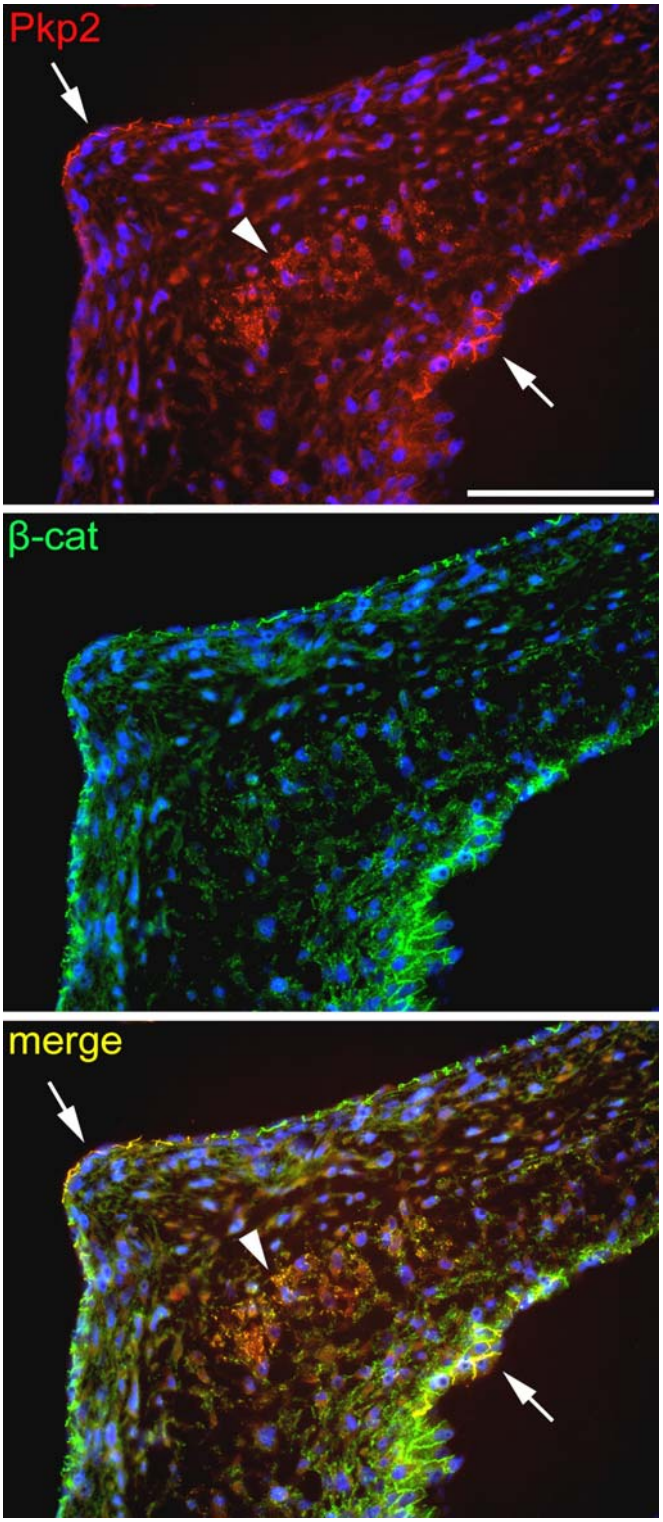

Figure 69: Double-label immunofluorescence survey micrograph of cross-sections through frozen fetal porcine heart valve tissue, showing the distribution and partial colocalization of plakophilin-2 and β-catenin. Plakophilin-2 (Pkp2; red) is present in several cell-cell contacts of VICs located deep in the center of the heart valve (white arrowheads) as well as at some AJ sites of the endothelial cells lining the heart valve interior (white arrows) and β-catenin (β-cat; green) is also present in AJs both of VICs and endothelial cells. Colocalizations are demonstrated by the yellow merged color. Nuclei are stained blue. Bar: 100 µm

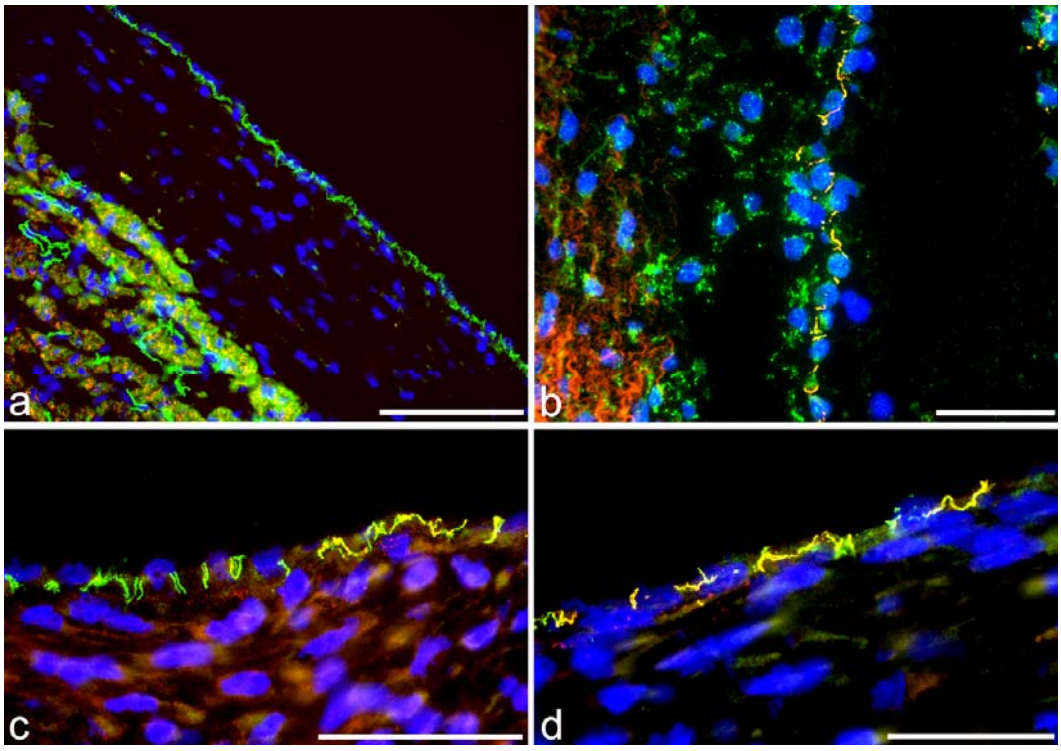

Figure 70: Double-label immunofluorescence micrographs of cross-sections through fetal porcine and human heart valve tissues with adjacent myocardium, showing the distribution of VE-cadherin and plakophilin-2 in detail. (**a**) Porcine endocardium, which is directly located above the myocardium, shows endothelial cells (labeled with VE-cadherin; green) which are here mostly negative for plakophilin-2 (red), which in turn is predominant in the IDs connecting the cardiomyocytes. (**b**) Human endocardium located at the edges of the heart valves shows colocalization of VE-cadherin (red) and plakophilin-2 (green) in many endothelial cells. Note also the occurrence of plakophilin-2 in junctions connecting VICs adjacent to the endocardium. (**c**-**d**) Colocalization of plakophilin-2 (red) and VE-cadherin (green) in the endothelial cells of the endocardium is not complete but interrupted or of different intensities in some regions (see **c** and **d**; yellow color shows colocalization). Nuclei are stained blue. Bars: 100 µm (a), 50 µm (b, c, d)

4.3.3 Primary cultures of fetal valvular interstitial cells

Primary cultures of VICs derived from fetal porcine heart valve tissue display a slightly different phenotype compared to adult VICs in cell culture, as they are generally not only positive for vimentin but also for smooth muscle α-actin (Figure 71 a and b; for comparison with adult VIC cultures see Figures 24b and c). Moreover, a certain proportion of the cultured fetal VICs shows positive reactions for the IF protein desmin which has always found to be absent in adult cultured VICs. Surprisingly, the fetal VICs in culture reveal a rather low amount of proliferatively active cells (Figure 71d) which is in stark contrast to the results obtained with cultures of adult VICs (not shown). The amount of glial filament acidic protein (GFAP)-positive cells, however, resembles that of adult VICs in culture (not shown). AJ contacts of cultured fetal VICs present a similar ensemble of

molecular constituents as shown for cultures of adult VICs, i.e. N-cadherin and cadherin-11 (Figure 72), in combination with α- and β-catenin (Figure 73), plakoglobin and protein p120 (not shown), often together with proteins ZO-1-3 (Figure 73). Again, plakophilin-2 is present in cultured fetal VICs as shown before for cultured adult VICs. VE-cadherin, P-cadherin and E-cadherin as well as desmogleins and desmocollins are always absent in cultures of fetal VICs (not shown). For a summary of the proteins of the AJs of fetal VICs in culture see Table 8.

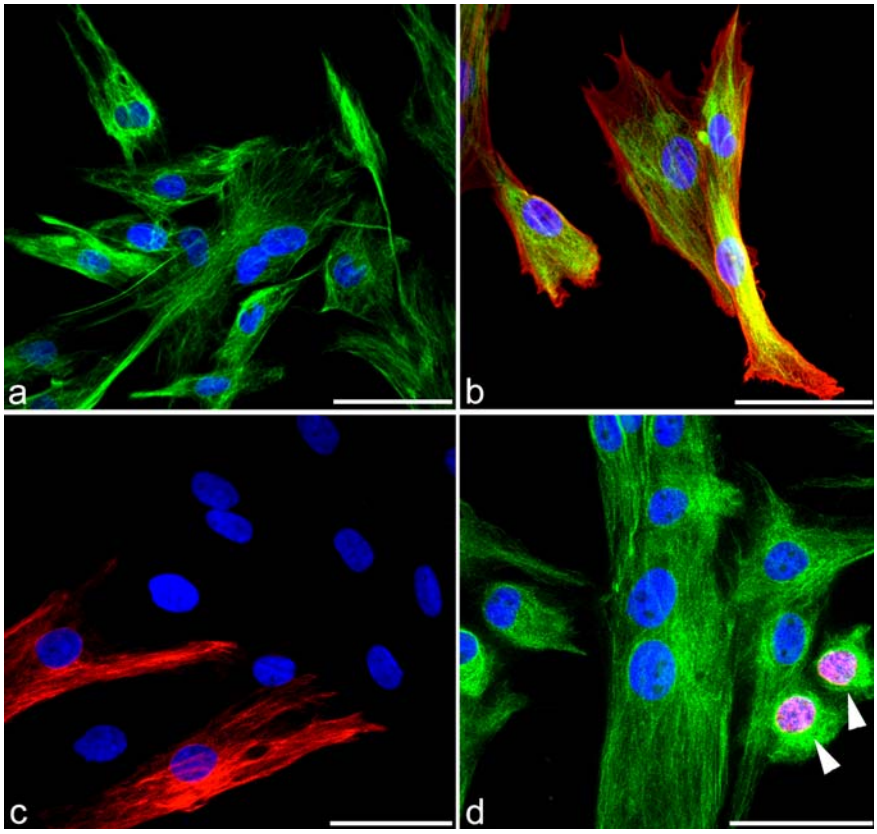

Figure 71: Double-label immunofluorescence micrographs of primary cultures of fetal VICs derived from porcine mitral heart valves. (**a**) All cells show positive reactions for vimentin (green), indicative of their mesenchymal origin. Note the long and thin filopodial-like processes. (**b**) Vimentin-positive cells (green) often also show a positive reaction for smooth muscle α-actin (red). (**c**) Some cells in addition show positive staining for the cardiomyocyte-typical IF protein desmin (red). (**d**) Only few VICs (vimentin, green) show proliferative activity as demonstrated by nuclear staining with Ki-67 (red; see arrowheads). Nuclei are stained blue. Bars: 50 µm

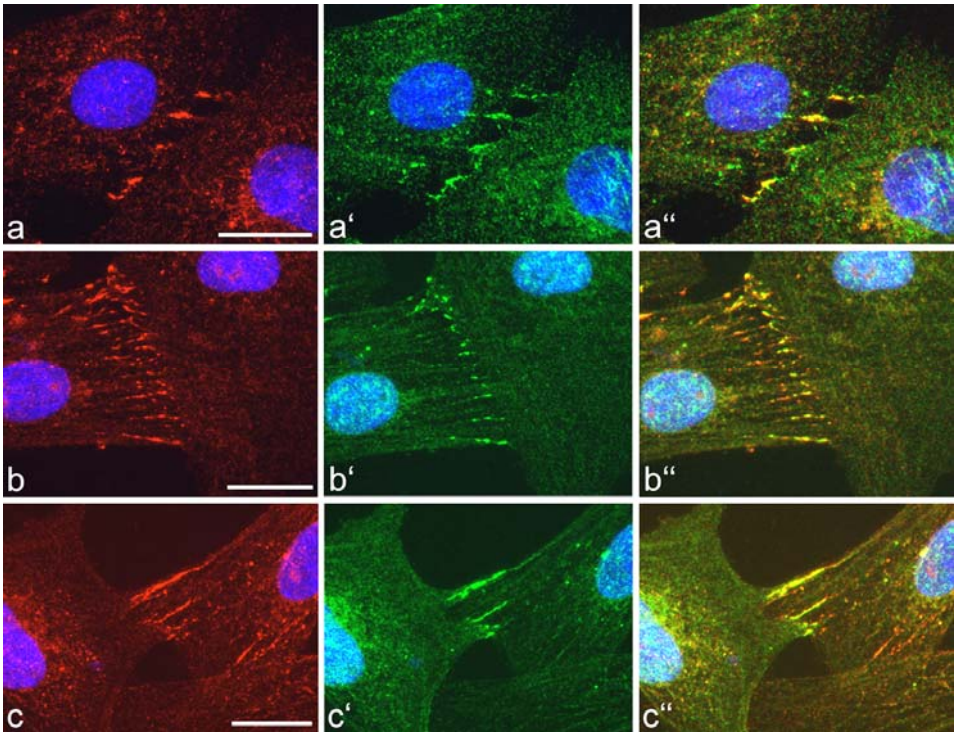

Figure 72: Double-label immunofluorescence micrographs of primary cultures of fetal porcine VICs derived from mitral heart valves, showing colocalization of transmembrane AJ glycoproteins and the "desmosomal" plaque protein plakophilin-2. (**a-a''**) Colocalization of N-cadherin (**a**; red) and plakophilin-2 (**a'**; green) in the AJs. (**b-c''**) Colocalization of cadherin-11 (**b** and **c**; red) and plakophilin-2 (**b'** and **c'**; green), here mostly in both the typical *puncta adhaerentia* type (**b-b''**) and the more tight-fittingly and deeply invaginated AJ type (*manubrium adhaerentes*), shown by the yellow merged color. Nuclei are stained blue. Bars: 20 µm

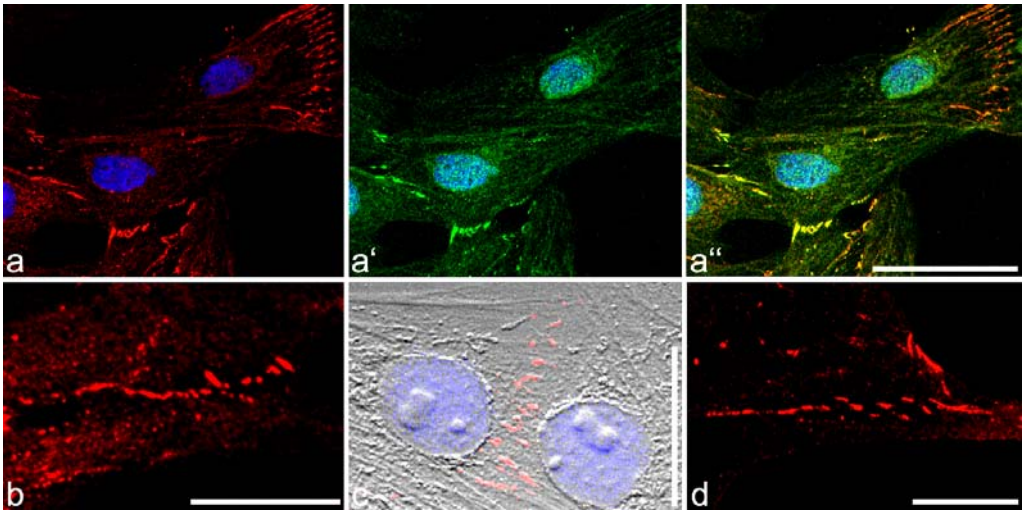

Figure 73: Double-label immunofluorescence micrographs of primary cultures of fetal porcine VICs derived from mitral heart valves, showing the occurrence of AJ plaque proteins in cell-cell contacts. (**a-a''**) Colocalization of plakoglobin (**a**, red) and plakophilin-2 (**a'**; green). Note that plakoglobin does also occur in places negative for plakophilin-2 (see merge picture, **a''**). (**b-d**) Localization of α-catenin (**b**), β-catenin (**c**) and protein ZO-1 in AJs (**d**). Nuclei are stained blue. Bars: 50 µm (a-a''), 20 µm (b-d)

4.4 Valvular interstitial cells in pathologically altered heart valve tissue

4.4.1 Myxomatous degenerated heart valves

To determine the nature of the AJs in pathologically altered valvular tissues, ten cases of myxomatous degenerated human heart valves have been examined by immunofluorescence microscopy using microwave-assisted antigen-retrieval techniques. These AJs show a normal composition, i.e. N-cadherin (Figure 74a) and cadherin-11 (not shown), together with α- and β-catenin (Figure 74c), protein p120 (Figure 74b) and plakoglobin (not shown) and are consistently negative for all desmosomal marker molecules examined, including plakophilin-2 (Figure 75).

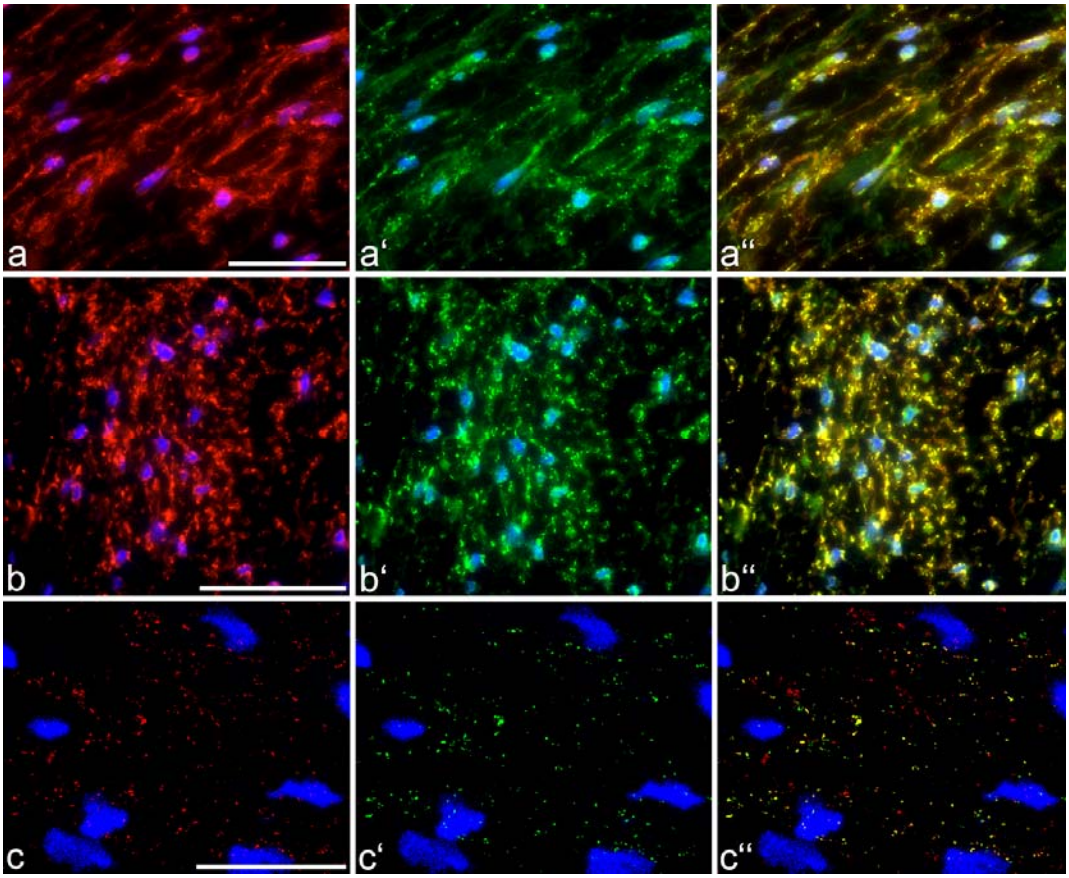

Figure 74: Double-label immunofluorescence micrographs of cross-sections through formaldehyde-fixed, paraffin-embedded samples of myxomatous degenerated heart valve tissue, showing the occurrence of AJ proteins in cell-cell junctions of VICs. (**a**) N-cadherin (red) and β-catenin (green) colocalize in AJs of VICs. (**b**) Protein p120 (red) and β-catenin (green) colocalize in VIC-rich regions of a myxomatous degenerated heart valve. (**c**) Reactions for α-catenin (red) are weak and somewhat inconsistent but generally show colocalization with β-catenin (green). Nuclei are stained blue. Bars: 50 µm

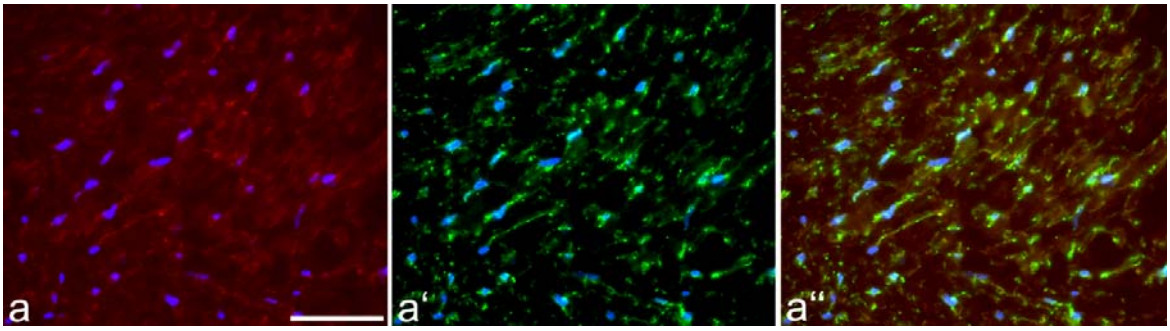

Figure 75: Double-label immunofluorescence micrograph of cross-sections through a formaldehyde-fixed, paraffin-embedded myxomatous degenerated heart valve tissue, showing the absence of plakophilin-2 (**a**, red) in contrast to the ubiquitous presence of β-catenin (**b**, green). Nuclei are stained blue. Bar: 50 µm

4.4.2 The cell-cell junctions in papillary fibroelastomas

The papillary fibroelastoma is a rare tumor occurring in heart valves and sometimes (13 % of the cases) within the confinements of the myocardium, usually affecting both, the atrial and the ventricular myocardium (cf. McAllister and Fenoglio, 1978). Only a few and partly controversial reports about the histogenesis of these tumors are available (Valente et al., 1992; Rubin et al., 1995; Hort and Horstkotte, 2006). Degenerative changes occurring in the morphology of the endothelial cells of the endocardium, mostly characterized by abnormal depositions of extracellular fibrous material, are often regarded as results of lesions or viral infections (Hurle et al., 1986; Grandmougin et al., 2000).

However, there is so far no decisive report on the AJs of such endothelial cells or of VICs of the affected heart valves. As has been shown afore in this thesis, the AJs of endothelial cells of the fetal endocardium usually differ from the endothelial cells of the adult endocardium by their content of the additional desmosomal plaque protein plakophilin-2, as it has also been seen in VICs grown in culture and in diverse types of malignantly transformed mesenchymal cells originating from other parts of the body (Rickelt et al., 2009).

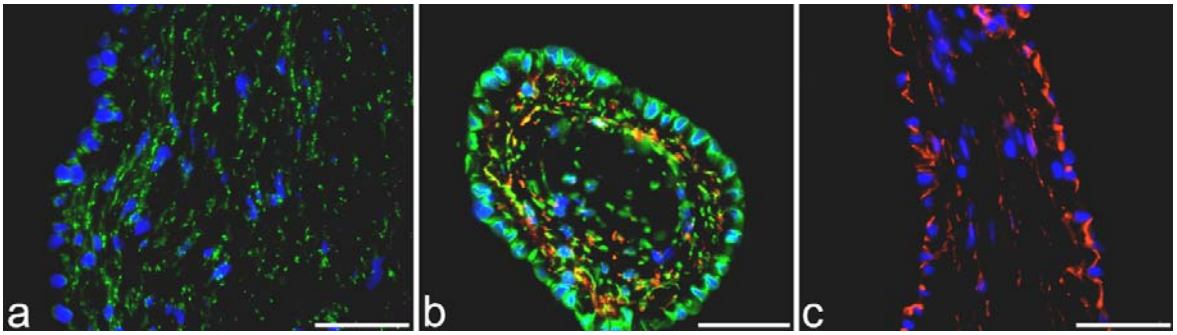

Figure 76: Double-label immunofluorescence micrographs of cross-sections through a formaldehyde-fixed, paraffin-embedded papillary fibroelastoma. (**a**) AJs of VICs in such a fibrotic region near the tumor show positive reactions for N-cadherin (green). Note the apparent absence of N-cadherin[2] in the endothelial cells lining the valve surface in this region. (**b**) Interstitial cells stained with antibodies against vimentin (green) in protrusions of the tumor show positive reactions for N-cadherin (red) whereas the endothelial cells are negative. (**c**) β-catenin (red) shows positive reactions both in AJs connecting the endothelial cells and the VICs. Nuclei are stained blue. Bars: 50 µm

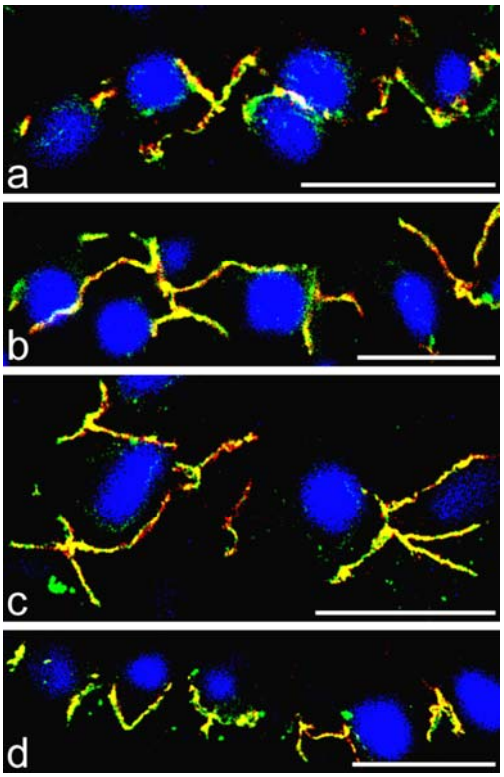

Figure 77: Double-label immunofluorescence micrographs of an oblique grazing section through a formaldehyde-fixed, paraffin-embedded papillary fibroelastoma, showing colocalization of cadherin-11 (red; **a**) and β-catenin (red; **b**), plakoglobin (red; **c**) and protein p120 (red; **d**) with VE-cadherin (green; **a-d**) in the AJs of endothelial cells of the endocardium of the tumor. Nuclei are stained blue. Bars: 20 µm

[2] It cannot be excluded that negative reactions of N-cadherin antibodies in some endothelial parts may reflect local differences of epitope accessibility or the specific antibody used rather than absence of the antigen.

AJs of the sparse VICs occurring in some regions of the tumor show a typical composition, i.e. N-cadherin (Figure 76a and b) and cadherin-11 (not shown) together with α-catenin (not shown), β-catenin (Figure 76c), protein p120 and plakoglobin (not shown). Reactions for desmosomal marker molecules, including plakophilin-2, have consistently been negative (not shown). The endothelial cells of endocardial regions bordering the tumor show an AJ composition similar to that found for endothelial cells lining healthy valves (for comparison see Figure 11 in chapter 4.1.1.3.1). Here, VE-cadherin colocalizes with cadherin-11 (Figure 77a), whereas the reaction for N-cadherin is always inconsistent[2] (Figure 76a and b). Moreover, VE-cadherin colocalizes with α-catenin (not shown), β-catenin (Figure 77b), plakoglobin (Figure 77c) and protein p120 (Figure 77d). Desmosomal proteins, including plakophilin-2, have generally found to be absent in AJs of these endothelial cells (not shown).

4.5 *Coniunctiones adhaerentes* – Molecular ensembles of the adhering junctions of heart valve cells

Table 8 The molecular ensembles of the adhering junctions of mammalian heart valves

Molecules / Occurrence	Valvular Interstitial Cells (VICs)				Endothelial Cells		
	adult VICs *in situ*[1]	fetal VICs *in situ*[2]	adult VICs in culture[3]	fetal VICs in culture[4]	fetal endocardium *in situ*[2]	adult endocardium *in situ*[1]	fetal aorta *in situ*[2]
Transmembrane glycoproteins							
N-cadherin*	+	+	+	+	–/+	–/+	–/+
VE-cadherin**	–	–	–	–	+	+	+
E-cadherin***	–	–	–	–	–	–	–
P-cadherin****	–	–	–	–	–	–	–
Cadherin-11*****	+	+	+	+	+	+	+
JAM-A	–	–	–	–	+	+	+
JAM-C	–	–	–	–	+	+	+
Desmoglein 1 (Dsg1)	–	–	–	–	–	–	–
Desmoglein 2 (Dsg2)	–	–	–	–	–	–	–
Desmoglein 3 (Dsg3)	–	–	–	–	–	–	–
Desmocollin 1 (Dsc1)	–	–	–	–	–	–	–
Desmocollin 2 (Dsc2)	–	–	–	–	–	–	–
Desmocollin 3 (Dsc3)	–	–	–	–	–	–	–
Plaque proteins							
α-Catenin	+	+	+	+	+	+	+
β-Catenin	+	+	+	+	+	+	+
Plakoglobin	+	+	+	+	+	+	+
Protein p120	+	+	+	+	+	+	+
Protein p0071	(+)	(+)	(+)	(+)	(+)	+	+
Neurojungin	–	–	–	–	–	–	–
Protein ARVCF	–	–	–	–	–	–	–
Protein myozap	–	–	–	–	–	–/+	+
Plakophilin-1	–	–	–	–	–	–	–
Plakophilin-2	–	+	+	+	+	–	–
Plakophilin-3	–	–	–	–	–	–	–
Desmoplakin	–	–	–	–	–	–	–
Actin-binding proteins							
Protein ZO-1-3	+	+	+	+	+	+	+
Afadin	+	+	+	+	+	+	+
Vinculin	+	+	+	+	+	+	+
Paxillin	+	+	+	+	+	+	+
α-Actinin	+	+	+	+	+	+	+
Associated filaments							
Vimentin	+	+	+	+	+	+	+
Smooth muscle α-actin	(+)	(+)	(+)	+	–	–	–
Desmin	–	–	–	(+)	–	–	–
Cytokeratins	–	–	–	–	–	–	–
Glial filament protein	(+)	(+)	(+)	(+)	nd	nd	nd

[1]human, bovine, ovine, porcine origin; [2]human, porcine origin; [3]human, bovine, ovine origin; [4]porcine origin; +, generally present; -, consistently negative; (+), weak reactions or differences between cells; -/+, inconsistent reactions; nd, not determined; synonymic names (for nomenclature see Angst et al., 2001; Hulpiau and van Roy, 2009): *, cadherin-2; **, cadherin-5; ***, cadherin-1; ****, cadherin-3; *****, OB-cadherin

5 Discussion

Over the past two decades remarkable efforts have been made in the field of heart valve "tissue engineering" (TE) to improve the results of heart valve transplantations or replacements (e.g., Vesely, 2005; Mendelson and Schoen, 2006). However, as a fundamental problem it soon became obvious that the knowledge of the cell and molecular biology of the heart valves and in particular of the cells populating the valve interior, the valvular interstitial cells (VICs), was and is still rather limited. In particular, a sufficient characterization of the cell-cell junctions of VICs and the molecules involved has been missing. The results of this thesis should – and hopefully can – essentially contribute to our knowledge of the cell and molecular biological characteristics of adherens junctions (AJs) of VICs in adult and fetal heart valves – *in situ*, in culture and in artificial heart valve constructs, thus providing a basis for heart valve TE and for analyses of pathological alterations in heart valves and also an alternative model for the development of VICs. A second, basically biological aim of this study has been to provide such a basis not only for human heart valves but also for various other mammalian species such as bovine, ovine and porcine valves.

5.1 Valvular interstitial cells in the adult mammal – *in situ* and in culture

In the electron microscope adult VICs *in situ* appear as a loose meshwork dominated by intimate relationships to elements of their extracellular matrix (ECM) environment, especially to the collagen fiber bundles and elastin structures. As it has already been shown for the endothelial/virgultar cells (SEVCs) of lymph node sinus (Moll et al., 2009) and for fibroblasts in tendon development (Birk and Trelstad, 1984, 1986; Canty et al., 2004, 2006; Richardson et al., 2007), VICs – or more precisely, their filopodial processes – enwrap and surround collagen fiber bundles in a peculiar way and thereby seem to contribute to the stability and flexibility of the heart valve leaflet. This architectonic interaction of VICs and ECM elements in the heart valve has apparently been ignored so far, except for a few marginal mentions in the literature (e.g., Icardo and Colvee, 1995).

In the present study, the characteristic features of heart valve structure have been further elucidated, including diseased valves with pathologically high proportions of ECM protein depositions and calcifications. Here, the elucidation of the focal adhesion molecules and structures that connect the actin cytoskeleton with the ECM such as α-

actinin, vinculin, paxillin, talin, integrins and syndecans might help in the understanding of valvular cell functions (Zamir and Geiger, 2001; Hinz et al., 2003; Fayet et al., 2007; Liu and Gotlieb, 2007; for reviews see, e.g., Hynes, 2002; Hinz and Gabbiani, 2003; Koster et al., 2004; Banno and Ginsberg, 2008; Cortesio et al., 2008; La Flamme et al., 2008; Tumbarello et al., 2008; Yoo and Guan, 2008).

VICs *in situ* display a marked cell type heterogeneity as some of them possess – besides the ubiquitous vimentin intermediate-sized filaments (IFs) and non-muscle type actins – also some smooth muscle α-actin-positive microfilaments (e.g., Bairati and DeBiasi, 1981; Mulholland and Gotlieb, 1996; Bertipaglia et al., 2003). This subpopulation has been hypothesized by some authors to originate from a heart valve cell population with special “stem cell” characteristics (Pho et al., 2008) which, however, has yet not been satisfactorily characterized and this problem is still discussed somewhat controversially.

Adult VICs in culture often comprise a remarkably high proportion of smooth muscle α-actin-positive cells, indicative of a switch from a rather fundamental mesenchymal phenotype towards a more myofibroblastoidal character, probably representing an activated state (in terms of contractility and stability see, e.g., Filip et al., 1986; Messier et al., 1994; Della Rocca et al., 2000; for general literature on myofibroblasts and myofibroblastoidal differentiation see Gabbiani et al., 1971; Gabbiani, 1996; Eyden, 2001; Grotendorst et al., 2004; for general reviews see Majno, 1979; Schürch et al., 1998; Powell et al., 1999; Walker et al., 2001). In cell cultures, the occurrence of gliafilament protein or the fat droplet-associated protein perilipin in certain VIC subtypes also emphasizes their heterogeneous nature. As lipid droplet-associated proteins often appear in conspicuously close vicinity of IF bundles in certain cell types (Franke et al., 1987b; Almahbobi et al., 1992; Evans, 1994; Almahbobi, 1995; Lieber and Evans, 1996; Heid et al., 1998; Schweitzer and Evans, 1998; see also Bloom and Fawcett, 1975) their occurrence in specific VICs may reflect local changes toward adipogenic differentiation.

5.1.1 The adhering junctions of adult valvular interstitial cells *in situ*

Besides descriptions of gap junctions between VICs (e.g., Filip et al., 1986; Lester and Gotlieb, 1988; Lester et al., 1993) there are also some reports mentioning AJs connecting VICs (e.g., Lester and Gotlieb, 1988; Messier et al., 1994). A dubious report on the presence of desmosomal structures connecting VICs (Messier et al., 1994) has surprisingly survived in the literature over more than a decade without molecular

characterization (Latif et al., 2006). However, the discussions on the presence of desmosomes or desmosomal cadherins in VICs can now be ended as it has been shown in the present thesis by both electron microscopy and biochemistry that VICs *in situ* are not connected by desmosomal cadherins and structures but exclusively by small AJs of the so-called *puncta adhaerentia* type, mostly located on their long and slender filopodial processes.

In molecular terms, two transmembrane glycoproteins have been recognized in VICs in nearly isostoichiometric amounts: N-cadherin which has already been noted in AJs by Latif et al. (2006) and cadherin-11, another typical mesenchymal cadherin. The existence of these two glycoproteins has been reported before in various mesenchymal cells (e.g., Kimura et al., 1995; Simonneau et al., 1995; Kiener and Brenner, 2005; Richardson et al., 2007; Wuchter et al., 2007; Agarwal et al., 2008), and especially cadherin-11 has been specifically shown to play an important role in the development of bone and cartilage structures (Kiener and Brenner, 2005; Richardson et al., 2007). Both N-cadherin and cadherin-11 are anchored in cytoplasmic plaques containing α-and β-catenin, confirming Latif et al. (2006), together with proteins p120 and p0071 as well as plakoglobin, in contrast to the reports by Latif and colleagues. Desmosomal molecules such as desmogleins and desmocollins as well as desmoplakin and plakophilins are clearly absent, in contrast to previous reports (e.g., Latif et al., 2006; Chester and Taylor, 2007). In conclusion, the junctions connecting VICs are quite normal and complete mesenchymal type AJs (for a recent review see Franke, 2009).

5.1.2 The advent of plakophilin-2 in adult valvular interstitial cells growing in culture

The AJ protein and glycoprotein composition of adult VICs grown in culture is similar to that of adult VICs *in situ* and other mesenchymal cells such as bone marrow- or cord blood-derived mesenchymal stem cells (Wuchter et al., 2007). In contrast to other authors reporting increases in the proportion of cadherin-11 to N-cadherin in the change from a fibroblastoidal to a myofibroblastoidal cell type in cell culture (Hinz et al., 2004), these two glycoproteins occur in nearly equal amounts in the AJs of adult VICs growing in culture.

Plakophilin-2 has hitherto been known only as a characteristic plaque constituent of desmosome-containing epithelial tissues or tumors derived therefrom as well as of meningothelial cells (Kartenbeck et al., 1984; Akat et al., 2003, 2008) and cardiomyocytes

(Mertens et al., 1996, 1999; Borrmann, 2000; Franke et al., 2006; Goossens et al., 2007; Pieperhoff et al., 2008). However, the advent of plakophilin-2 in AJs of non-epithelial cells, as described here for VICs growing in culture or in fetal development, is not an isolated phenomenon as it has recently also been found in the AJs of some soft tissue tumors *in situ*, some malignantly transformed mesenchymal cell lines and in highly proliferative non-malignant mesenchymal stem cells derived from bone marrow (Rickelt et al., 2009). Plakophilin-1 (Kapprell et al., 1988; Schäfer et al., 1993; Hatzfeld et al., 1994; Heid et al., 1994; Schmidt et al., 1994) and plakophilin-3 (Schmidt et al., 1999; Borrmann et al., 2000; Borrmann, 2002) have not been identified in adult VICs growing *in situ* or in culture. Although plakophilin-3 could not be identified in the biochemical analyses of this study, it has to be emphasized that the presence of minor amounts of this plaque protein cannot rigorously ruled out (for a similar problem with cardiac myxomata see Rickelt et al., 2010). In this context it should be mentioned that in certain malignantly transformed mesenchymal cell culture lines the presence of decent amounts of plakophilin-3 has been demonstrated (Rickelt et al., 2009).

As has been found in this thesis, plakophilin-2 is also absent in AJs connecting VICs of myxomatous degenerated heart valves and heart valve-derived, benign papillary fibroelastomas, the cellular origin of which, however, is still controversially discussed (see, e.g., Hort and Horstkotte, 2006). The absence of this desmosomal protein might be due to a basic difference between the special VICs and mesenchymal cells originating from “cardiac fibroblasts” involved in the development of cardiac myxomata (for a recent review on myofibroblastoidal cells in tumors see also Eyden et al., 2009). A comprehensive general comparison of the AJs occurring in the various subtypes of cardiac fibroblastoidal cells is still missing (e.g., Goldsmith et al., 2004; Banerjee et al., 2007; Snider et al., 2009; for reviews see also Brown et al., 2005; Camelliti et al., 2005; Baudino et al., 2006; Souders et al., 2009; for reports on interactions between special cardiac fibroblasts and cardiomyocytes see Brown et al., 2005; Banerjee et al., 2006; Camelliti et al., 2006; Chilton et al., 2007; Baudino et al., 2008; Pedrotty et al., 2008).

On the other hand, in certain plakophilin-2-cDNA-transfected cells and in cardiomyocytes, plakophilin-2 has been shown to occur in complexes with α- and β-catenin and plakoglobin (Chen et al., 2002; Köser et al., 2003; Borrmann et al., 2006). Similarly, in malignantly transformed fibroblasts, plakophilin-2 could be recovered in immunoprecipitation analyses in complexes with N-cadherin and β-catenin (Rickelt et al., 2009). In the present study, however, such attempts to identify possible binding partners of plakophilin-2 in the AJs of adult VICs grown in culture have not been successful. Further

studies to identify not yet characterized binding partners using transgenic animals might be valuable in the elucidation of the molecular interactions in this subtype of AJs.

Certainly, plakophilin-2 is a protein of prime interest in cardiology. In myocardial cells, mutations in genes encoding desmosomal molecules can result in severe arrhythmogenic cardiomyopathies (ARVC/D), demonstrating the fragility and functional sensitivity of the composite junction complexes involved (for the biochemistry of the *areae compositae* and recent reviews on ARVC/D see Bazzi and Christiano, 2007; Marcus et al., 2007; Awad et al., 2008; Corrado et al., 2009; Herren et al., 2009; Saffitz, 2009; Pieperhoff et al., 2010; Sen-Chowdhry et al., 2010). Here, in particular the gene encoding plakophilin-2 seems to be most often affected (Mertens et al., 1996; Gerull et al., 2004; Grossmann et al., 2004; Franke et al., 2009; for related results of siRNA-mediated knock-down experiments of plakophilin-2 in cultured neonatal rat cardiomyocytes see, e.g., Oxford et al., 2007; Pieperhoff et al., 2008; Fidler et al., 2009; for related experimental results see also Sato et al., 2009). At present it cannot yet be concluded whether the acquisition of plakophilin-2 to the AJ plaques of VICs simply reflects a molecular equipment related to the higher proliferation rates of these cells or whether it is involved in other VIC functions.

5.1.3 The adult endocardium

The endothelial cells of the endocardium have been described already in the 1970s by electron microscopy and compared to endothelial cells in vascular structures (e.g., Anversa et al., 1975; Lupu and Simionescu, 1985; Andries and Brutsaert, 1994; for a review see Brutsaert and Andries, 1992), whereas the existence of – or the need for – a vascular system within the heart valves has been discussed rather controversially (e.g., Ritter et al., 1928; Gross and Kugel, 1931; for recent publications see, e.g., Weind et al., 2000, 2001, 2002; Filion and Ellis, 2003). Although both kinds of endothelium share some similar characteristics such as the basic ultrastructural morphology of their cell-cell junctions (Lupu and Simionescu, 1985; Andries and Brutsaert, 1994), they do not seem to be identical, as also indicated by reports on differences in their permeability properties as well as in cell shape (e.g., Brutsaert and Andries, 1992; Andries and Brutsaert, 1994). Nevertheless, little is yet known about the cell-cell junctions of endothelial cells of the endocardium, especially in comparison to vascular endothelia.

In this thesis, the junctional ensemble of endothelial cells of the endocardium has been compared to that of vascular endothelial cells (for comparison of AJ proteins in VICs,

endothelial cells of the endocardium and vascular endothelial cells see Table 9). In accordance with other endothelia, VE-cadherin as the major AJ cadherin colocalizes with typical AJ plaque proteins (Lampugnani et al., 1995; Dejana, 1996; Lampugnani and Dejana, 1997; Navarro et al., 1998; Hämmerling et al., 2006; Boda-Heggemann et al., 2009; see also Franke et al., 1987c, 1988; for the special relation between VE-cadherin and β-catenin and its functional importance in endothelial cell assembly and vascular development see also Carmeliet et al., 1999). The colocalization of cadherin-11 with VE-cadherin in contrast to a different distribution of N-cadherin has also been reported for specific other endothelial tissues (for references see above) but is still controversially discussed as some other authors have reported a colocalization of VE-cadherin with N-cadherin in endothelial *zonulae adhaerentes* (e.g., Schulze and Firth, 1993; Luo and Radice, 2005; for further references see Hayes et al., 2003; Moll et al., 2009). Other authors disagree and claim that N-cadherin is dispersed on the endothelial cell surface and not restricted to AJs (Salomon et al., 1992; Lampugnani et al., 1995; Dejana, 1996, 2004; Lampugnani and Dejana, 1997; Navarro et al., 1998; for a recent review see also Ferreri and Vincent, 2008). Clearly, desmosomal proteins have not been detected in the AJs of endothelial cells of the endocardium, in contrast to certain other endothelial cell types such as those typical of the lymph node sinus (*complexus adhaerentes*) and specific other regions of the lymphatic system where VE-cadherin has been shown to co-exist with desmoplakin (Schmelz et al., 1990; 1994; Schmelz and Franke, 1993; Valiron et al., 1996; Ebata et al., 2001a, b; Cattelino et al., 2003; Hämmerling et al., 2006; Baluk et al., 2007; Pfeiffer et al., 2008; for reviews see Stacker et al., 2002; Moll et al., 2009).

Surprisingly, the most recently identified cardiovascular AJ plaque protein myozap (Seeger et al., 2010) has been detected in various kinds of endothelia (Pieperhoff et al., 2011) but it occurred in somewhat inconsistent and interrupted patterns in endothelial cells of the endocardium. A summary of the present knowledge on the molecular composition of the AJs examined is presented in Table 9.

Table 9 The adhering junctions of valvular interstitial cells and (endocardial) endothelial cells of the adult mammalian heart

Molecules / Occurrence	adult VICs *in situ*	adult endocardial endothelium *in situ*	adult aorta *in situ*
Transmembrane glycoproteins			
N-cadherin	+	–/+	–/+
VE-cadherin	–	+	+
E-cadherin	–	–	–
P-cadherin	–	–	–
Cadherin-11	+	+	+
JAM-A	–	+	+
JAM-C	–	+	+
Desmoglein 1 (Dsg1)	–	–	–
Desmoglein 2 (Dsg2)	–	–	–
Desmoglein 3 (Dsg3)	–	–	–
Desmocollin 1 (Dsc1)	–	–	–
Desmocollin 2 (Dsc2)	–	–	–
Desmocollin 3 (Dsc3)	–	–	–
Plaque proteins			
α-Catenin	+	+	+
β-Catenin	+	+	+
Plakoglobin	+	+	+
Protein p120	+	+	+
Protein p0071	(+)	+	+
Neurojungin	–	–	–
Protein ARVCF	–	–	–
Protein myozap	–	–/+	+
Plakophilin-1	–	–	–
Plakophilin-2	–	–	–
Plakophilin-3	–	–	–
Desmoplakin	–	–	–

+, generally present; -, consistently negative; (+), weak reactions or differences between cells;
-/+, inconsistent reactions (regionally and in different experiments)

5.2 Valvular interstitial cells in fetal heart valves

5.2.1 Heart valve development

In human embryos, major contributions of mesodermal cells to the formation of the heart are noted already in the early pregnancy. They form the heart tube consisting of the endothelial cells and thus represent the inner tube of the endocardium as well as myocardial cells forming the outer tube (Figure 78). Although it is clear that both the endothelial and the myocardial cells develop from a mesodermal precursor sharing both vascular and cardiogenic differentiation potential, the lineage relationships between the endothelial cells of the endocardium and the myocardial cells are still disputed (Figure 78D; see also Linask and Lash, 1993; Lough and Sugi, 2000; Kattmann et al., 2006; Misfeldt et al., 2009; for reviews see Mikawa, 1999; Mjaatvedt et al., 1999; Trinh and Stainier, 2004; Snarr et al., 2008; Harris and Black, 2010). An important step in heart formation is the separation of the endocardial and myocardial tubes by the so-called cardiac jelly, an acellular, ECM-enriched mass (e.g., Manasek et al., 1970, 1973; Markwald et al., 1977; Krug, 1985; Hurle et al., 1994; for a recent review see Butcher and Markwald, 2007). After the so-called “looping” of the heart “anlage” the cardiac jelly contributes to the “endocardial cushions” and mesenchymal cells start to populate the cushion matrix (Figure 79; see, e.g., Moorman et al., 2003; Trinh and Stainier, 2004). The origin of these mesenchymal cushion cells has been somewhat controversially discussed (e.g., Person et al., 2005b) as the invading cells are seen as descendants either of the endocardial endothelium (Patten et al., 1948) or of the myocardium (Chang, 1932). More recently, it has been hypothesized that these mesenchymal cells may be derived from the endothelial layer of the endocardium and result from a process referred to as “epithelial-mesenchymal transition” (EMT; or, with a here more appropriate meaning, “endothelial-mesenchymal-transition”; see also Kinsella and Fitzharris, 1980; Bernanke and Markwald, 1982; Runyan and Markwald, 1983; Mjaatvedt et al., 1987; for reviews see Armstrong and Bischoff, 2004; Trinh and Stainier, 2004; Snarr et al., 2008; Hinton and Yutzey, 2011). Subsequently, formation of valvular structures, septation and compartmentalization of the heart into four chambers begins (Anderson, 2003a, b; Moorman et al., 2003). Embryonal blood already flows through the heart before the completion of chamber development (Gui et al., 1996).

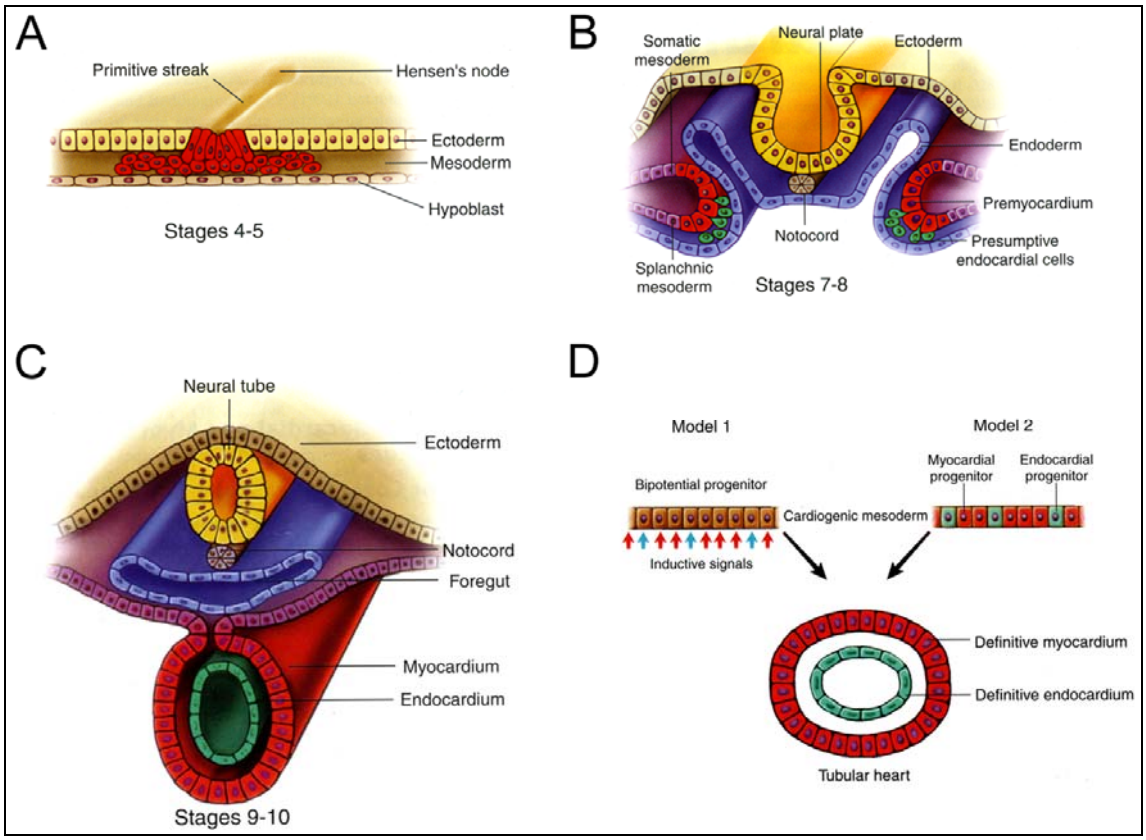

Figure 78: Morphogenetic events in early heart development of chicken developmental stage HH 4-10 and models for the development of myocardial and endothelial heart lineages (taken from Mikawa, 1999). (**A-C**) Mesodermal cells (red) in the gastrula stage (**A**) segregate into premyocardial (red) and presumptive endocardial cells (green) in the neurula stage (**B**). Myocardial (red) and endocardial (green) cells form the tubular heart (**C**). Different models for the genesis of myocardial (red) and endocardial (green) cells originating from the cardiogenic mesoderm (**D**).

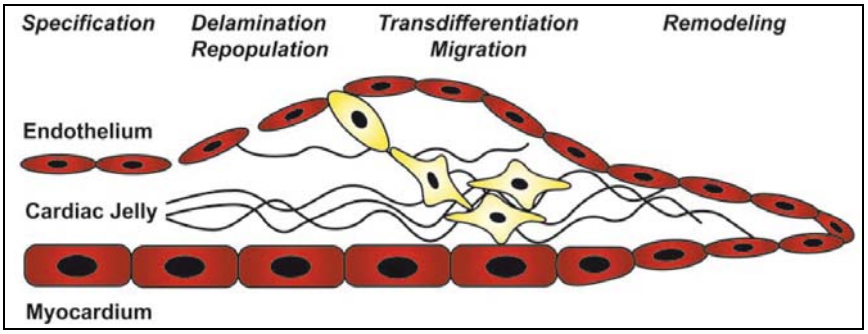

Figure 79: Schematic survey showing mesenchymal cells originating from delaminating endothelial cells of the endocardium which transdifferentiate and migrate into the cardiac jelly, populating and remodeling the heart valve matrix (cf. Armstrong and Bischoff, 2004).

5.2.2 The appearance of plakophilin-2 in adhering junctions of fetal valvular interstitial cells and endothelial cells of the endocardium

Although in the electron microscope the general appearance of fetal VICs *in situ* is quite similar to that of adult VICs, e.g. even showing the aforedescribed engulfment of collagen bundles by filopodial processes, there are remarkable molecular differences: Fetal VICs *in situ* are connected by AJs containing plakophilin-2 which appears to be absent in AJs of adult VICs. Moreover, in cultured fetal VICs, high proportions of smooth muscle α-actin-containing VICs reflect the "activated" phenotype of VICs in this specific developmental stage (Rabkin-Aikawa et al., 2004; Aikawa et al., 2006).

The endothelial cells of the fetal endocardium also show a very similar junctional ensemble as the endothelial cells of the adult endocardium, with the remarkable exception that the endothelial cells covering the heart valves of the fetal endocardium, but not those covering the adjacent myocardium are often connected by AJs containing plakophilin-2 (Table 10).

The spatial specification of endothelial cells in different endocardial regions of the future valves has been extensively described in the context of cushion development, emphasizing that cushion mesenchyme does only form in the future valve regions but never in atrial or ventricular regions, apparently due to the absence of inductive signals from the underlying myocardium (e.g., Bernanke and Markwald, 1982; Runyan and Markwald, 1983; Mjaatvedt et al., 1987, 1999; Mikawa, 1999). This supports the hypothesis that the integration of plakophilin-2 in AJs of a certain portion of the endocardial endothelium and in underlying VICs might result from some kind of induction in specific developmental stages. Moreover, a participation of plakophilin-2 located in the nucleus cannot yet be excluded (Mertens et al., 1996, 2001; for reviews see also Klymkowsky, 1999; Schmidt and Koch, 2007; McCrea et al., 2009; for discussions of canonical Wnt-signaling in heart valve formation see Hurlstone et al., 2003; Person, 2005a, b; Tzahor, 2007; Cohen et al., 2008; Alfieri et al., 2010; for general effects of Wnt-signaling in cadherin-based cell adhesion see Chen et al., 2002; Nelson and Nusse, 2004; Heuberger and Birchmeier, 2009).

Table 10: The adhering junctions of fetal valvular interstitial cells and endothelial cells of the endocardium

Molecules / Occurrence	fetal VICs *in situ*	fetal endocardial endothelium *in situ*	adult endocardial endothelium *in situ*
Transmembrane glycoproteins			
N-cadherin	+	–/+	–/+
VE-cadherin	–	+	+
E-cadherin	–	–	–
P-cadherin	–	–	–
Cadherin-11	+	+	+
JAM-A	–	+	+
JAM-C	–	+	+
Desmoglein 1 (Dsg1)	–	–	–
Desmoglein 2 (Dsg2)	–	–	–
Desmoglein 3 (Dsg3)	–	–	–
Desmocollin 1 (Dsc1)	–	–	–
Desmocollin 2 (Dsc2)	–	–	–
Desmocollin 3 (Dsc3)	–	–	–
Plaque proteins			
α-Catenin	+	+	+
β-Catenin	+	+	+
Plakoglobin	+	+	+
Protein p120	+	+	+
Protein p0071	(+)	(+)	+
Neurojungin	–	–	–
Protein ARVCF	–	–	–
Protein myozap	–	–	–/+
Plakophilin-1	–	–	–
Plakophilin-2	+	+	–
Plakophilin-3	–	–	–
Desmoplakin	–	–	–

+, generally present; -, consistently negative; (+), weak reactions or differences between cells;
-/+, inconsistent reactions (regionally and in different experiments)

5.3 Valvular interstitial cells in three-dimensional matrix constructs and the potential role of plakophilin-2 for tissue engineering

An important field in the interdisciplinary research of medicine and biology is heart valve TE due to the increasing shortage of donor heart valves and the fact that cardiovascular diseases are the most frequent cause of death in the industrialized

Western countries and that the surgical treatments of valves represent the second most frequent kind of operation (Gummert et al., 2009).

Regarding the aforediscussed additional occurrence of plakophilin-2 in cultured VICs and other mesenchymal cells, one has to consider the effective benefit of the use of those cells for *in vitro* re-seeding of artificial heart valve constructs and that the knowledge about the cell-cell junctions of VICs in artificial heart valve models is still very limited (Taylor et al., 2002; Flameng, 2004; Schenke-Layland et al., 2004; Benton et al., 2009; Iop et al., 2009; for reviews see Rabkin and Schoen, 2002; Flanagan and Pandit, 2003; Schmidt and Hoestrup, 2005; Vesely, 2005; Mendelson and Schoen, 2006; Dohmen and Konertz, 2009 and references cited therein). In AJs of VICs grown in 3D constructs plakophilin-2 seems to decrease strongly or to be totally lost but otherwise the AJ protein ensemble is still indistinguishable from that of VICs *in situ*, which might be due to the high viscosity, even rigidity of the surrounding matrix (Taylor et al., 2002; Butcher and Nerem, 2004; Benton et al., 2009). This process is obviously reversible as VICs grown in 3D culture constructs, re-isolated and grown again in monolayer 2D cultures again can show the acquisition of plakophilin-2 in their AJs.

At any rate, the use of cultured VICs as a reliable cell source for the construction of artificial heart valves should still be carefully examined, as the functional effects of the advent and the loss of this protein in the AJs of mesenchymally derived cells is not clear yet in the context of pathological changes resulting in tumorous growth (for fibroblasts in general see also Kalluri and Zeisberg, 2006; Rickelt et al., 2009, 2010; for possible pathological changes in VICs see also Gwanmesia et al., 2010). Alternatively, approaches using decellularized heart valve matrices may be favored (Akhyari et al., 2010; for review see Knight et al., 2008).

5.4 An alternative view of the development of valvular interstitial cells

Based on the results of this thesis, an alternative concept of the development of VICs and heart valves different from EMT may be proposed: In stages of invasion of mesodermal cells into the future heart region not only myocardial and endothelial cells are originating from common mesodermal precursors, but also some – initially perhaps sparse – mesenchymal cells; the future VICs (Figure 80A). These VICs *in statu nascendi*, interspersed between the endocardial and the cardiomyocyte tube (Figure 80B) as well as the endothelial cells of the endocardium are still plakophilin-2-negative at this stage.

Due to inductive stimuli, the existence and nature of which has already been discussed by other authors (Bernanke and Markwald, 1982; Runyan and Markwald, 1983; Mjaatvedt et al., 1987), or due to a not yet identified mechanism, endothelial cells and VICs then are selectively activated only in regions of the future endocardial cushions (Figure 80B; lower part of the heart tube), a process accompanied by the acquisition of plakophilin-2 in the AJs of these mesenchymally derived cells. After heart valve development, plakophilin-2 in these AJs may decrease rapidly and may disappear completely in the AJs of VICs of mature heart valves.

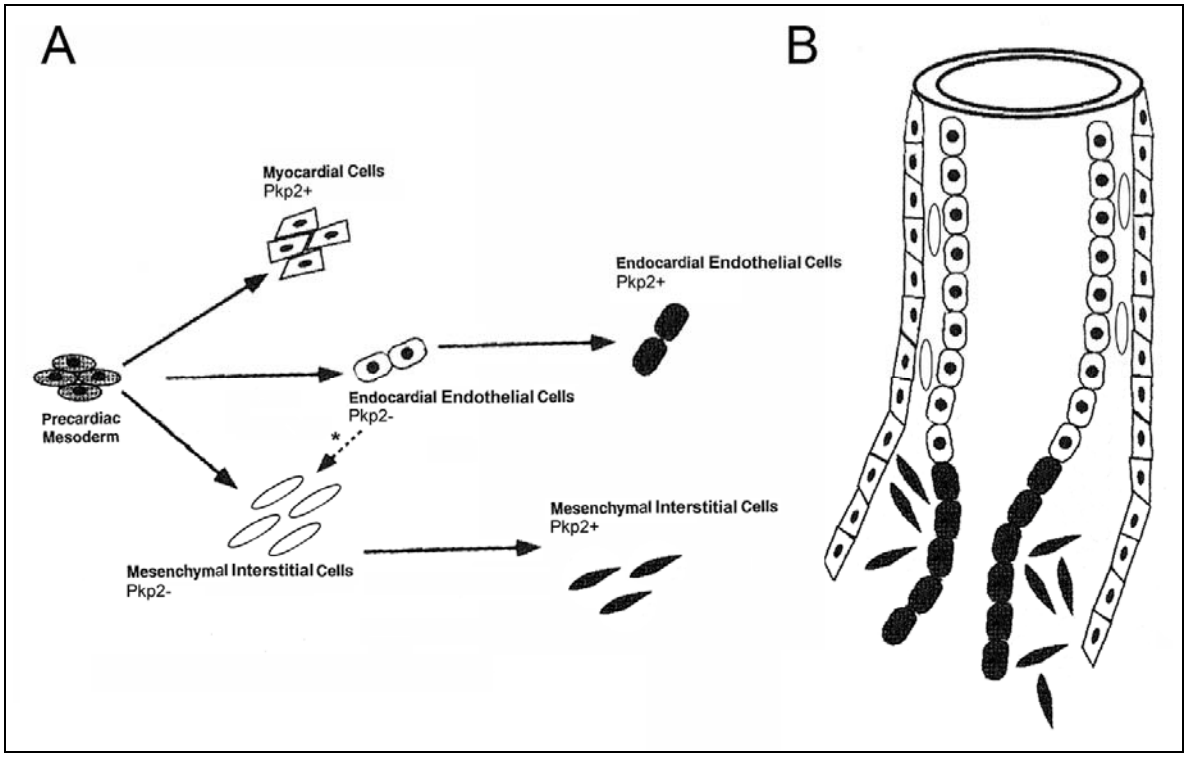

Figure 80: Schematic survey of an alternative model of the early valvulogenesis (modified from Eisenberg and Markwald, 1995). (**A**) Myocardial and endothelial cells of the endocardium as well as mesenchymal interstitial cells originate from the precardiac mesoderm. (**B**; upper part of the image) Myocardial cells (white-colored angled cells) build the outer heart tube, endothelial cells of the endocardium (white-colored roundish cells) build the inner endocardial tube and mesenchymal interstitial cells (white colored spindle-shaped cells) are located dispersed in between. Only at regions of prospective endocardial cushions, endothelial cells of the endocardium and mesenchymal interstitial cells become activated, thus plakophilin-2(Pkp2)-positive (black-colored cells; lower part of the image). It should also be noted that this concept does not exclude conversions of endothelial of the endocardium to dispersed mesenchymal interstitial cells (asterisk in **A**).

References

Abd-el-Basset, E.M., Ahmed, I., and Fedoroff, S. (1991). Actin and actin-binding proteins in differentiating astroglia in tissue culture. J Neurosci Res 30, 1-17.

Achtstätter, T., Fouquet, B., Rungger-Brändle, E., and Franke, W.W. (1989). Cytokeratin filaments and desmosomes in the epithelioid cells of the perineurial and arachnoidal sheaths of some vertebrate species. Differentiation 40, 129-149.

Agarwal, S.K., Lee, D.M., Kiener, H.P., and Brenner, M.B. (2008). Coexpression of two mesenchymal cadherins, cadherin 11 and N-cadherin, on murine fibroblast-like synoviocytes. Arthritis Rheum 58, 1044-1054.

Aghib, D.F., and McCrea, P.D. (1995). The E-cadherin complex contains the src substrate p120. Exp Cell Res 218, 359-369.

Aikawa, E., Whittaker, P., Farber, M., Mendelson, K., Padera, R.F., Aikawa, M., and Schoen, F.J. (2006). Human semilunar cardiac valve remodeling by activated cells from fetus to adult: implications for postnatal adaptation, pathology, and tissue engineering. Circulation 113, 1344-1352.

Akat, K., Mennel, H.D., Kremer, P., Gassler, N., Bleck, C.K., and Kartenbeck, J. (2003). Molecular characterization of desmosomes in meningiomas and arachnoidal tissue. Acta Neuropathol 106, 337-347.

Akat, K., Bleck, C.K., Lee, Y.M., Haselmann-Weiss, U., and Kartenbeck, J. (2008). Characterization of a novel type of adherens junction in meningiomas and the derived cell line HBL-52. Cell Tissue Res 331, 401-412.

Akhtar, S., Meek, K.M., and James, V. (1999). Immunolocalization of elastin, collagen type I and type III, fibronectin, and vitronectin in extracellular matrix components of normal and myxomatous mitral heart valve chordae tendineae. Cardiovasc Pathol 8, 203-211.

Akhyari, P., Kamiya, H., Gwanmesia, P., Ziegler, H., Barth, M., Tschierschke, R., Lichtenberg, A., and Karck, M. (2009a). In vivo endothelialisation of allogenic detergent decellularized heart valves can be enhanced by surface coating using autologous fibrin. Poster presented at: 56th Annual Meeting of Southern Thoracic Surgical Association (Marco Island, FL, USA), pp.30.

Akhyari, P., Ziegler, H., Mambou, P., Barth, M., Hoffman, S., Kamiya, H., Berger, I., Franke, W.W., Karck, M., and Lichtenberg, A. (2009b). Impact of protein coating strategies on the re-endothelialization of biological heart valve scaffolds. Poster presented at: German Society for Thoracic and Cardiovascular Surgery, 38th Annual Meeting (Stuttgart), pp.118.

Akhyari, P., Kamiya, H., Gwanmesia, P., Aubin, H., Tschierschke, R., Hoffmann, S., Karck, M., and Lichtenberg, A. (2010). In vivo functional performance and structural maturation of decellularised allogenic aortic valves in the subcoronary position. Eur J Cardiothorac Surg 38, 539-546.

Alexander, J.J., Bey, E.M., Geddes, E.W., and Lecatsas, G. (1976). Establishment of a continuously growing cell line from primary carcinoma of the liver. S Afr Med J 50, 2124-2128.

Alfieri, C.M., Cheek, J., Chakraborty, S., and Yutzey, K.E. (2010). Wnt signaling in heart valve development and osteogenic gene induction. Dev Biol 338, 127-135.

Almahbobi, G., Williams, L.J., and Hall, P.F. (1992). Attachment of steroidogenic lipid droplets to intermediate filaments in adrenal cells. J Cell Sci 101 (Pt 2), 383-393.

Almahbobi, G. (1995). Adhesion of intermediate filaments and lipid droplets in adrenal cells studied by field emission scanning electron microscopy. Cell Tissue Res 281, 387-390.

Anastasiadis, P.Z., and Reynolds, A.B. (2000). The p120 catenin family: complex roles in adhesion, signaling and cancer. J Cell Sci 113 (Pt 8), 1319-1334.

Anderson, J.M., Van Itallie, C.M., Peterson, M.D., Stevenson, B.R., Carew, E.A., and Mooseker, M.S. (1989). ZO-1 mRNA and protein expression during tight junction assembly in Caco-2 cells. J Cell Biol 109, 1047-1056.

Anderson, R.H., Webb, S., Brown, N.A., Lamers, W., and Moorman, A. (2003a). Development of the heart: (3) formation of the ventricular outflow tracts, arterial valves, and intrapericardial arterial trunks. Heart 89, 1110-1118.

Anderson, R.H., Webb, S., Brown, N.A., Lamers, W., and Moorman, A. (2003b). Development of the heart: (2) Septation of the atriums and ventricles. Heart 89, 949-958.

Andries, L.J., and Brutsaert, D.L. (1994). Endocardial endothelium in the rat: junctional organization and permeability. Cell Tissue Res 277, 391-400.

Angst, B.D., Marcozzi, C., and Magee, A.I. (2001). The cadherin superfamily: diversity in form and function. J Cell Sci 114, 629-641.

Angus, B., Purvis, J., Stock, D., Westley, B.R., Samson, A.C., Routledge, E.G., Carpenter, F.H., and Horne, C.H. (1987). NCL-5D3: a new monoclonal antibody recognizing low molecular weight cytokeratins effective for immunohistochemistry using fixed paraffin-embedded tissue. J Pathol 153, 377-384.

Anversa, P., Giacomelli, J., and Wiener, J. (1975). Intercellular junctions of rat endocardium. Anat Rec 183, 477-483.

Armstrong, E.J., and Bischoff, J. (2004). Heart valve development: endothelial cell signaling and differentiation. Circ Res 95, 459-470.

Asakura, T., Nakanishi, H., Sakisaka, T., Takahashi, K., Mandai, K., Nishimura, M., Sasaki, T., and Takai, Y. (1999). Similar and differential behaviour between the nectin-afadin-ponsin and cadherin-catenin systems during the formation and disruption of the polarized junctional alignment in epithelial cells. Genes Cells 4, 573-581.

Attardi, L.D., Reczek, E.E., Cosmas, C., Demicco, E.G., McCurrach, M.E., Lowe, S.W., and Jacks, T. (2000). PERP, an apoptosis-associated target of p53, is a novel member of the PMP-22/gas3 family. Genes Dev 14, 704-718.

Awad, M.M., Calkins, H., and Judge, D.P. (2008). Mechanisms of disease: molecular genetics of arrhythmogenic right ventricular dysplasia/cardiomyopathy. Nat Clin Pract Cardiovasc Med 5, 258-267.

Bader, A., Schilling, T., Teebken, O.E., Brandes, G., Herden, T., Steinhoff, G., and Haverich, A. (1998). Tissue engineering of heart valves-human endothelial cell seeding of detergent acellularized porcine valves. Eur J Cardiothorac Surg 14, 279-284.

Bairati, A., and DeBiasi, S. (1981). Presence of a smooth muscle system in aortic valve leaflets. Anat Embryol (Berl) 161, 329-340.

Baluk, P., Fuxe, J., Hashizume, H., Romano, T., Lashnits, E., Butz, S., Vestweber, D., Corada, M., Molendini, C., Dejana, E., and McDonald, D.M. (2007). Functionally specialized junctions between endothelial cells of lymphatic vessels. J Exp Med 204, 2349-2362.

Banerjee, I., Yekkala, K., Borg, T.K., and Baudino, T.A. (2006). Dynamic interactions between myocytes, fibroblasts, and extracellular matrix. Ann N Y Acad Sci 1080, 76-84.

Banerjee, I., Fuseler, J.W., Price, R.L., Borg, T.K., and Baudino, T.A. (2007). Determination of cell types and numbers during cardiac development in the neonatal and adult rat and mouse. Am J Physiol Heart Circ Physiol 293, H1883-1891.

Banno, A., and Ginsberg, M.H. (2008). The ins and outs of integrin signaling. In Cell junctions, S.E. La Flamme, and A.P. Kowalczyk, eds. (Weinheim, Wiley-VCH), pp. 3-23.

Bashey, R.I., Torii, S., and Angrist, A. (1967). Age-related collagen and elastin content of human heart valves. J Gerontol 22, 203-208.

Bass-Zubek, A.E., Godsel, L.M., Delmar, M., and Green, K.J. (2009). Plakophilins: multifunctional scaffolds for adhesion and signaling. Curr Opin Cell Biol 21, 708-716.

Baudino, T.A., Carver, W., Giles, W., and Borg, T.K. (2006). Cardiac fibroblasts: friend or foe? Am J Physiol Heart Circ Physiol 291, H1015-1026.

Baudino, T.A., McFadden, A., Fix, C., Hastings, J., Price, R., and Borg, T.K. (2008). Cell patterning: interaction of cardiac myocytes and fibroblasts in three-dimensional culture. Microsc Microanal 14, 117-125.

Bazzi, H., Getz, A., Mahoney, M.G., Ishida-Yamamoto, A., Langbein, L., Wahl, J.K., 3rd, and Christiano, A.M. (2006). Desmoglein 4 is expressed in highly differentiated keratinocytes and trichocytes in human epidermis and hair follicle. Differentiation 74, 129-140.

Bazzi, H., and Christiano, A.M. (2007). Broken hearts, woolly hair, and tattered skin: when desmosomal adhesion goes awry. Curr Opin Cell Biol 19, 515-520.

Bazzoni, G. (2006). Endothelial tight junctions: permeable barriers of the vessel wall. Thromb Haemost 95, 36-42.

Behrens, J., Birchmeier, W., Goodman, S.L., and Imhof, B.A. (1985). Dissociation of Madin-Darby canine kidney epithelial cells by the monoclonal antibody anti-arc-1: mechanistic aspects and identification of the antigen as a component related to uvomorulin. J Cell Biol 101, 1307-1315.

Behrens, J., and Nelson, W.J. (2004). Cell Adhesion (Berlin, Springer-Verlag), pp. 1-481.

Benton, J.A., Fairbanks, B.D., and Anseth, K.S. (2009). Characterization of valvular interstitial cell function in three dimensional matrix metalloproteinase degradable PEG hydrogels. Biomaterials 30, 6593-6603.

Bernanke, D.H., and Markwald, R.R. (1982). Migratory behavior of cardiac cushion tissue cells in a collagen-lattice culture system. Dev Biol 91, 235-245.

Berndorff, D., Gessner, R., Kreft, B., Schnoy, N., Lajous-Petter, A.M., Loch, N., Reutter, W., Hortsch, M., and Tauber, R. (1994). Liver-intestine cadherin: molecular cloning and characterization of a novel Ca(2+)-dependent cell adhesion molecule expressed in liver and intestine. J Cell Biol 125, 1353-1369.

Bertipaglia, B., Ortolani, F., Petrelli, L., Gerosa, G., Spina, M., Pauletto, P., Casarotto, D., Marchini, M., and Sartore, S. (2003). Cell characterization of porcine aortic valve and decellularized leaflets repopulated with aortic valve interstitial cells: the VESALIO Project (Vitalitate Exornatum Succedaneum Aorticum Labore Ingenioso Obtenibitur). Ann Thorac Surg 75, 1274-1282.

Berx, G., and van Roy, F. (2009). Involvement of members of the cadherin superfamily in cancer. In Cell-cell junctions, W.J. Nelson, and E. Fuchs, eds. (New York, Cold Spring Harbor Laboratory Press), pp. 407-433.

Bhowmick, N.A., Ghiassi, M., Bakin, A., Aakre, M., Lundquist, C.A., Engel, M.E., Arteaga, C.L., and Moses, H.L. (2001). Transforming growth factor-beta1 mediates epithelial to mesenchymal transdifferentiation through a RhoA-dependent mechanism. Mol Biol Cell 12, 27-36.

Birk, D.E., and Trelstad, R.L. (1984). Extracellular compartments in matrix morphogenesis: collagen fibril, bundle, and lamellar formation by corneal fibroblasts. J Cell Biol 99, 2024-2033.

Birk, D.E., and Trelstad, R.L. (1986). Extracellular compartments in tendon morphogenesis: collagen fibril, bundle, and macroaggregate formation. J Cell Biol 103, 231-240.

Bloom, W., and Fawcett, D.W. (1975). Adipose tissue. In A textbook of histology, W. Bloom, and D.W. Fawcett, eds. (Philadelphia, W.B. Saunders Company), pp. 196-208.

Boda-Heggemann, J., Regnier-Vigouroux, A., and Franke, W.W. (2009). Beyond vessels: occurrence and regional clustering of vascular endothelial (VE-)cadherin-containing junctions in non-endothelial cells. Cell Tissue Res 335, 49-65.

Bonné, S., van Hengel, J., Nollet, F., Kools, P., and van Roy, F. (1999). Plakophilin-3, a novel armadillo-like protein present in nuclei and desmosomes of epithelial cells. J Cell Sci 112 (Pt 14), 2265-2276.

Bonné, S., Gilbert, B., Hatzfeld, M., Chen, X., Green, K.J., and van Roy, F. (2003). Defining desmosomal plakophilin-3 interactions. J Cell Biol 161, 403-416.

Borrmann, C.M., Mertens, C., Schmidt, A., Langbein, L., Kuhn, C., and Franke, W.W. (2000). Molecular diversity of plaques of epithelial-adhering junctions. Ann N Y Acad Sci 915, 144-150.

Borrmann, C.M. (2002). Molekulare Charakterisierung der Adhärens-Zellverbindungen des Herzens: Identifizierung einer neuen Art, der Area composita [Molecular characterization of the adherens-type cell junctions in the heart: Identification of a novel kind, the area composita]. (Dissertation Thesis, Heidelberg, Ruprecht Karls University), pp. 1-119.

Borrmann, C.M., Grund, C., Kuhn, C., Hofmann, I., Pieperhoff, S., and Franke, W.W. (2006). The area composita of adhering junctions connecting heart muscle cells of vertebrates. II. Colocalizations of desmosomal and fascia adhaerens molecules in the intercalated disk. Eur J Cell Biol 85, 469-485.

Boukamp, P., Petrussevska, R.T., Breitkreutz, D., Hornung, J., Markham, A., and Fusenig, N.E. (1988). Normal keratinization in a spontaneously immortalized aneuploid human keratinocyte cell line. J Cell Biol 106, 761-771.

Bradfield, P.F., and Imhof, B.A. (2004). Adhesion mechanisms of endothelial cells. In Cell adhesion, J. Behrens, and W.J. Nelson, eds. (Berlin, Springer-Verlag), pp. 405-436.

Bretscher, A. (1986). Purification of the intestinal microvillus cytoskeletal proteins villin, fimbrin, and ezrin. Methods Enzymol 134, 24-37.

Brown, R.D., Ambler, S.K., Mitchell, M.D., and Long, C.S. (2005). The cardiac fibroblast: therapeutic target in myocardial remodeling and failure. Annu Rev Pharmacol Toxicol 45, 657-687.

Brutsaert, D.L., and Andries, L.J. (1992). The endocardial endothelium. Am J Physiol 263, H985-1002.

Bryant, P.J. (1997). Junction genetics. Dev Genet 20, 75-90.

Bussemakers, M.J., van Bokhoven, A., Mees, S.G., Kemler, R., and Schalken, J.A. (1993). Molecular cloning and characterization of the human E-cadherin cDNA. Mol Biol Rep 17, 123-128.

Butcher, J.T., and Nerem, R.M. (2004). Porcine aortic valve interstitial cells in three-dimensional culture: comparison of phenotype with aortic smooth muscle cells. J Heart Valve Dis 13, 478-485; discussion 485-476.

Butcher, J.T., Penrod, A.M., Garcia, A.J., and Nerem, R.M. (2004). Unique morphology and focal adhesion development of valvular endothelial cells in static and fluid flow environments. Arterioscler Thromb Vasc Biol 24, 1429-1434.

Butcher, J.T., Tressel, S., Johnson, T., Turner, D., Sorescu, G., Jo, H., and Nerem, R.M. (2006). Transcriptional profiles of valvular and vascular endothelial cells reveal phenotypic differences: influence of shear stress. Arterioscler Thromb Vasc Biol 26, 69-77.

Butcher, J.T., and Markwald, R.R. (2007). Valvulogenesis: the moving target. Philos Trans R Soc Lond B Biol Sci 362, 1489-1503.

Buxton, R.S., Cowin, P., Franke, W.W., Garrod, D.R., Green, K.J., King, I.A., Koch, P.J., Magee, A.I., Rees, D.A., Stanley, J.R., and Steinberg, M.S. (1993). Nomenclature of the desmosomal cadherins. J Cell Biol 121, 481-483.

Cabral, R.M., Wan, H., Cole, C.L., Abrams, D.J., Kelsell, D.P., and South, A.P. (2010). Identification and characterization of DSPIa, a novel isoform of human desmoplakin. Cell Tissue Res 341, 121-129.

Camelliti, P., Borg, T.K., and Kohl, P. (2005). Structural and functional characterisation of cardiac fibroblasts. Cardiovasc Res 65, 40-51.

Camelliti, P., Green, C.R., and Kohl, P. (2006). Structural and functional coupling of cardiac myocytes and fibroblasts. Adv Cardiol 42, 132-149.

Campbell, R.D., and Campbell, J.H. (1971). Origin and continuity of desmosomes. In Origin and continuity of cell organelles, J. Reinert, and H. Ursprung, eds. (Berlin, Springer Verlag), pp. 261-298.

Canty, E.G., Lu, Y., Meadows, R.S., Shaw, M.K., Holmes, D.F., and Kadler, K.E. (2004). Coalignment of plasma membrane channels and protrusions (fibripositors) specifies the parallelism of tendon. J Cell Biol 165, 553-563.

Canty, E.G., Starborg, T., Lu, Y., Humphries, S.M., Holmes, D.F., Meadows, R.S., Huffman, A., O'Toole, E.T., and Kadler, K.E. (2006). Actin filaments are required for fibripositor-mediated collagen fibril alignment in tendon. J Biol Chem 281, 38592-38598.

Canver, C.C., Gregory, R.D., Cooler, S.D., and Voytovich, M.C. (2000). Association of osteopontin with calcification in human mitral valves. J Cardiovasc Surg (Torino) 41, 171-174.

Carew, E.O., Talman, E.A., Boughner, D.R., and Vesely, I. (1999). Quasi-Linear Viscoelastic theory applied to internal shearing of porcine aortic valve leaflets. J Biomech Eng 121, 386-392.

Carew, E.O., Barber, J.E., and Vesely, I. (2000). Role of preconditioning and recovery time in repeated testing of aortic valve tissues: validation through quasilinear viscoelastic theory. Ann Biomed Eng 28, 1093-1100.

Carmeliet, P., Lampugnani, M.G., Moons, L., Breviario, F., Compernolle, V., Bono, F., Balconi, G., Spagnuolo, R., Oosthuyse, B., Dewerchin, M., Zanetti, A., Angellilo, A., Mattot, V., Nuyens, D., Lutgens, E., Clotman, F., de Ruiter, M.C., Gittenberger-de Groot, A., Poelmann, R., Lupu, F., Herbert, J.M., Collen, D., and Dejana, E. (1999). Targeted deficiency or cytosolic truncation of the VE-cadherin gene in mice impairs VEGF-mediated endothelial survival and angiogenesis. Cell 98, 147-157.

Cattelino, A., Liebner, S., Gallini, R., Zanetti, A., Balconi, G., Corsi, A., Bianco, P., Wolburg, H., Moore, R., Oreda, B., Kemler, R., and Dejana, E. (2003). The conditional inactivation of the beta-catenin gene in endothelial cells causes a defective vascular pattern and increased vascular fragility. J Cell Biol 162, 1111-1122.

Cavallaro, U., Liebner, S., and Dejana, E. (2006). Endothelial cadherins and tumor angiogenesis. Exp Cell Res 312, 659-667.
Cebotari, S., Mertsching, H., Kallenbach, K., Kostin, S., Repin, O., Batrinac, A., Kleczka, C., Ciubotaru, A., and Haverich, A. (2002). Construction of autologous human heart valves based on an acellular allograft matrix. Circulation 106, I63-I68.
Cebotari, S., Lichtenberg, A., Tudorache, I., Hilfiker, A., Mertsching, H., Leyh, R., Breymann, T., Kallenbach, K., Maniuc, L., Batrinac, A., Repin, O., Maliga, O., Ciubotaru, A., and Haverich, A. (2006). Clinical application of tissue engineered human heart valves using autologous progenitor cells. Circulation 114, I132-137.
Chang, C. (1932). On the reaction of the endocardium to the bloodstream in the embryonic heart, with special reference to the endocardial thickenings in the atrioventricular canal and the bulbis cordis. Anat Rec 51, 253-265.
Chen, J.H., Yip, C.Y., Sone, E.D., and Simmons, C.A. (2009). Identification and characterization of aortic valve mesenchymal progenitor cells with robust osteogenic calcification potential. Am J Pathol 174, 1109-1119.
Chen, X., Bonné, S., Hatzfeld, M., van Roy, F., and Green, K.J. (2002). Protein binding and functional characterization of plakophilin 2. Evidence for its diverse roles in desmosomes and beta -catenin signaling. J Biol Chem 277, 10512-10522.
Chester, A.H., and Taylor, P.M. (2007). Molecular and functional characteristics of heart-valve interstitial cells. Philos Trans R Soc Lond B Biol Sci 362, 1437-1443.
Chilton, L., Giles, W.R., and Smith, G.L. (2007). Evidence of intercellular coupling between co-cultured adult rabbit ventricular myocytes and myofibroblasts. J Physiol 583, 225-236.
Claycomb, W.C., Lanson, N.A., Jr., Stallworth, B.S., Egeland, D.B., Delcarpio, J.B., Bahinski, A., and Izzo, N.J., Jr. (1998). HL-1 cells: a cardiac muscle cell line that contracts and retains phenotypic characteristics of the adult cardiomyocyte. Proc Natl Acad Sci U S A 95, 2979-2984.
Cohen, E.D., Tian, Y., and Morrisey, E.E. (2008). Wnt signaling: an essential regulator of cardiovascular differentiation, morphogenesis and progenitor self-renewal. Development 135, 789-798.
Cohen, S.M., Gorbsky, G., and Steinberg, M.S. (1983). Immunochemical characterization of related families of glycoproteins in desmosomes. J Biol Chem 258, 2621-2627.
Cole, W.G., Chan, D., Hickey, A.J., and Wilcken, D.E. (1984). Collagen composition of normal and myxomatous human mitral heart valves. Biochem J 219, 451-460.
Collins, J.E., Legan, P.K., Kenny, T.P., MacGarvie, J., Holton, J.L., and Garrod, D.R. (1991). Cloning and sequence analysis of desmosomal glycoproteins 2 and 3 (desmocollins): cadherin-like desmosomal adhesion molecules with heterogeneous cytoplasmic domains. J Cell Biol 113, 381-391.
Corrado, D., Basso, C., and Thiene, G. (2009). Arrhythmogenic right ventricular cardiomyopathy: an update. Heart 95, 766-773.
Cortesio, C.L., Chan, K.T., and Huttenlocher, A. (2008). Adhesion dynamics in motile cells. In Cell junctions, S.E. La Flamme, and A.P. Kowalczyk, eds. (Weinheim, Wiley-VCH), pp. 71-88.
Cowin, P., and Garrod, D.R. (1983). Antibodies to epithelial desmosomes show wide tissue and species cross-reactivity. Nature 302, 148-150.
Cowin, P., Mattey, D., and Garrod, D. (1984a). Distribution of desmosomal components in the tissues of vertebrates, studied by fluorescent antibody staining. J Cell Sci 66, 119-132.
Cowin, P., Mattey, D., and Garrod, D. (1984b). Identification of desmosomal surface components (desmocollins) and inhibition of desmosome formation by specific Fab'. J Cell Sci 70, 41-60.
Cowin, P., Kapprell, H.P., and Franke, W.W. (1985). The complement of desmosomal plaque proteins in different cell types. J Cell Biol 101, 1442-1454.
Cowin, P., Kapprell, H.P., Franke, W.W., Tamkun, J., and Hynes, R.O. (1986). Plakoglobin: a protein common to different kinds of intercellular adhering junctions. Cell 46, 1063-1073.
Cunningham, B.A., Leutzinger, Y., Gallin, W.J., Sorkin, B.C., and Edelman, G.M. (1984). Linear organization of the liver cell adhesion molecule L-CAM. Proc Natl Acad Sci U S A 81, 5787-5791.
Damsky, C.H., Richa, J., Solter, D., Knudsen, K., and Buck, C.A. (1983). Identification and purification of a cell surface glycoprotein mediating intercellular adhesion in embryonic and adult tissue. Cell 34, 455-466.
Damsky, C.H., Richa, J., Wheelock, M., Damjanov, I., and Buck, C.A. (1985). Characterization of cell-CAM 120/80 and the role of surface membrane adhesion glycoproteins in early events in mouse embryo morphogenesis. In The cell in contact, G.M. Edelman, and J.P. Thiery, eds. (New York, John Wiley and Sons), pp. 233-255.
Dejana, E., Corada, M., and Lampugnani, M.G. (1995). Endothelial cell-to-cell junctions. FASEB J 9, 910-918.
Dejana, E. (1996). Endothelial adherens junctions: implications in the control of vascular permeability and angiogenesis. J Clin Invest 98, 1949-1953.
Dejana, E., Lampugnani, M.G., Martinez-Estrada, O., and Bazzoni, G. (2000). The molecular organization of endothelial junctions and their functional role in vascular morphogenesis and permeability. Int J Dev Biol 44, 743-748.
Dejana, E. (2004). Endothelial cell-cell junctions: happy together. Nat Rev Mol Cell Biol 5, 261-270.
Dejana, E., Simionescu, M., and Wolburg, H. (2009). Endothelial cell biology and pathology. Cell Tissue Res 335, 1-3.
Della Rocca, F., Sartore, S., Guidolin, D., Bertiplaglia, B., Gerosa, G., Casarotto, D., and Pauletto, P. (2000). Cell composition of the human pulmonary valve: a comparative study with the aortic valve: the VESALIO

Project. (Vitalitate Exornatum Succedaneum Aorticum labore Ingegnoso Obtinebitur). Ann Thorac Surg 70, 1594-1600.
Desai, B.V., Harmon, R.M., and Green, K.J. (2009). Desmosomes at a glance. J Cell Sci 122, 4401-4407.
Dohmen, P.M., and Konertz, W. (2009). Tissue-engineered heart valve scaffolds. Ann Thorac Cardiovasc Surg 15, 362-367.
Donalies, M., Cramer, M., Ringwald, M., and Starzinski-Powitz, A. (1991). Expression of M-cadherin, a member of the cadherin multigene family, correlates with differentiation of skeletal muscle cells. Proc Natl Acad Sci U S A 88, 8024-8028.
Dreger, S.A., Taylor, P.M., Allen, S.P., and Yacoub, M.H. (2002). Profile and localization of matrix metalloproteinases (MMPs) and their tissue inhibitors (TIMPs) in human heart valves. J Heart Valve Dis 11, 875-880.
Duguay, D., Foty, R.A., and Steinberg, M.S. (2003). Cadherin-mediated cell adhesion and tissue segregation: qualitative and quantitative determinants. Dev Biol 253, 309-323.
Dunmore-Buyze, J., Boughner, D.R., Macris, N., and Vesely, I. (1995). A comparison of macroscopic lipid content within porcine pulmonary and aortic valves. Implications for bioprosthetic valves. J Thorac Cardiovasc Surg 110, 1756-1761.
Ebata, N., Nodasaka, Y., Sawa, Y., Yamaoka, Y., Makino, S., Totsuka, Y., and Yoshida, S. (2001a). Desmoplakin as a specific marker of lymphatic vessels. Microvasc Res 61, 40-48.
Ebata, N., Sawa, Y., Nodasaka, Y., Yamaoka, Y., Yoshida, S., and Totsuka, Y. (2001b). Immunoelectron microscopic study of PECAM-1 expression on lymphatic endothelium of the human tongue. Tissue Cell 33, 211-218.
Ebnet, K. (2008). Organization of multiprotein complexes at cell-cell junctions. Histochem Cell Biol 130, 1-20.
Edelman, G.M., Hoffman, S., Chuong, C.M., Thiery, J.P., Brackenbury, R., Gallin, W.J., Grumet, M., Greenberg, M.E., Hemperly, J.J., Cohen, C., and Cunningham, B.A. (1983). Structure and modulation of neural cell adhesion molecules in early and late embryogenesis. Cold Spring Harb Symp Quant Biol 48 Pt 2, 515-526.
Edelman, G.M., and Thiery, J.P. (1985). The cell in contact (New York, John Wiley and Sons), pp. 1-507.
Edelman, G.M., Cunningham, B.A., and Thiery, J.P. (1990). Morphoregulatory Molecules (New York, John Wiley and Sons), pp. 1-648.
Eger, A., Stockinger, A., Schaffhauser, B., Beug, H., and Foisner, R. (2000). Epithelial mesenchymal transition by c-Fos estrogen receptor activation involves nuclear translocation of beta-catenin and upregulation of beta-catenin/lymphoid enhancer binding factor-1 transcriptional activity. J Cell Biol 148, 173-188.
Eisenberg, L.M., and Markwald, R.R. (1995). Molecular regulation of atrioventricular valvuloseptal morphogenesis. Circ Res 77, 1-6.
El-Hamamsy, I., Balachandran, K., Yacoub, M.H., Stevens, L.M., Sarathchandra, P., Taylor, P.M., Yoganathan, A.P., and Chester, A.H. (2009). Endothelium-dependent regulation of the mechanical properties of aortic valve cusps. J Am Coll Cardiol 53, 1448-1455.
Elbashir, S.M., Harborth, J., Lendeckel, W., Yalcin, A., Weber, K., and Tuschl, T. (2001). Duplexes of 21-nucleotide RNAs mediate RNA interference in cultured mammalian cells. Nature 411, 494-498.
Evans, R.M. (1994). Intermediate filaments and lipoprotein cholesterol. Trends Cell Biol 4, 149-151.
Eyden, B. (2001). The fibronexus in reactive and tumoral myofibroblasts: further characterisation by electron microscopy. Histol Histopathol 16, 57-70.
Eyden, B., Banerjee, S.S., Shenjere, P., and Fisher, C. (2009). The myofibroblast and its tumours. J Clin Pathol 62, 236-249.
Fabre, S., Reymond, N., Cocchi, F., Menotti, L., Dubreuil, P., Campadelli-Fiume, G., and Lopez, M. (2002). Prominent role of the Ig-like V domain in trans-interactions of nectins. Nectin3 and nectin 4 bind to the predicted C-C'-C"-D beta-strands of the nectin1 V domain. J Biol Chem 277, 27006-27013.
Fahimi, H.D., and Drochmans, P. (1965). Essais de standardisation de la fixation au glutaraldéhyde. I. Purification et détermination de la concentration du glutaraldéhyde. J Microscopie 4, 725.
Farquhar, M.G., and Palade, G.E. (1963). Junctional complexes in various epithelia. J Cell Biol 17, 375-412.
Fayet, C., Bendeck, M.P., and Gotlieb, A.I. (2007). Cardiac valve interstitial cells secrete fibronectin and form fibrillar adhesions in response to injury. Cardiovasc Pathol 16, 203-211.
Ferreri, D.M., and Vincent, P.A. (2008). Signaling to and through the endothelial adherens junction. In Cell junctions, S.E. La Flamme, and A.P. Kowalczyk, eds. (Weinheim Wiley-VCH), pp. 169-195.
Fidler, L.M., Wilson, G.J., Liu, F., Cui, X., Scherer, S.W., Taylor, G.P., and Hamilton, R.M. (2009). Abnormal connexin43 in arrhythmogenic right ventricular cardiomyopathy caused by plakophilin-2 mutations. J Cell Mol Med 13, 4219-4228.
Filion, R.J., and Ellis, C.G. (2003). A finite difference model of O2 transport in aortic valve cusps: importance of intrinsic microcirculation. Am J Physiol Heart Circ Physiol 285, H2099-2104.
Filip, D.A. (1984). Mouse atrio-ventricular valve ultrastructure morphometrical correlations. Morphol Embryol (Bucur) 30, 165-173.
Filip, D.A., Radu, A., and Simionescu, M. (1986). Interstitial cells of the heart valves possess characteristics similar to smooth muscle cells. Circ Res 59, 310-320.
Flameng, W. (2004). A new approach to heart valve tissue engineering. Int J Cardiol 95 Suppl 1, S55-56.
Flanagan, T.C., and Pandit, A. (2003). Living artificial heart valve alternatives: a review. Eur Cell Mater 6, 28-45.
Forbes, M.S., and Sperelakis, N. (1985). Intercalated discs of mammalian heart: a review of structure and function. Tissue Cell 17, 605-648.

Foty, R.A., and Steinberg, M.S. (2005). The differential adhesion hypothesis: a direct evaluation. Dev Biol 278, 255-263.
Fouquet, B., Zimbelmann, R., and Franke, W.W. (1992). Identification of plakoglobin in oocytes and early embryos of Xenopus laevis: maternal expression of a gene encoding a junctional plaque protein. Differentiation 51, 187-194.
Franke, W.W., Schmid, E., Osborn, M., and Weber, K. (1978). Different intermediate-sized filaments distinguished by immunofluorescence microscopy. Proc Natl Acad Sci U S A 75, 5034-5038.
Franke, W.W., Schmid, E., Osborn, M., and Weber, K. (1979a). Intermediate-sized filaments of human endothelial cells. J Cell Biol 81, 570-580.
Franke, W.W., Schmid, E., Winter, S., Osborn, M., and Weber, K. (1979b). Widespread occurrence of intermediate-sized filaments of the vimentin-type in cultured cells from diverse vertebrates. Exp Cell Res 123, 25-46.
Franke, W.W., Schmid, E., Grund, C., Müller, H., Engelbrecht, I., Moll, R., Stadler, J., and Jarasch, E.D. (1981). Antibodies to high molecular weight polypeptides of desmosomes: specific localization of a class of junctional proteins in cells and tissue. Differentiation 20, 217-241.
Franke, W.W., Grund, C., Kuhn, C., Jackson, B.W., and Illmensee, K. (1982a). Formation of cytoskeletal elements during mouse embryogenesis. III. Primary mesenchymal cells and the first appearance of vimentin filaments. Differentiation 23, 43-59.
Franke, W.W., Moll, R., Schiller, D.L., Schmid, E., Kartenbeck, J., and Müller, H. (1982b). Desmoplakins of epithelial and myocardial desmosomes are immunologically and biochemically related. Differentiation 23, 115-127.
Franke, W.W., Moll, R., Müller, H., Schmid, E., Kuhn, C., Krepler, R., Artlieb, U., and Denk, H. (1983a). Immunocytochemical identification of epithelium-derived human tumors with antibodies to desmosomal plaque proteins. Proc Natl Acad Sci U S A 80, 543-547.
Franke, W.W., Müller, H., Mittnacht, S., Kapprell, H.P., and Jorcano, J.L. (1983b). Significance of two desmosome plaque-associated polypeptides of molecular weights 75 000 and 83 000. EMBO J 2, 2211-2215.
Franke, W.W., Cowin, P., Schmelz, M., and Kapprell, H.P. (1987a). The desmosomal plaque and the cytoskeleton. Ciba Found Symp 125, 26-48.
Franke, W.W., Hergt, M., and Grund, C. (1987b). Rearrangement of the vimentin cytoskeleton during adipose conversion: formation of an intermediate filament cage around lipid globules. Cell 49, 131-141.
Franke, W.W., Kapprell, H.P., and Cowin, P. (1987c). Immunolocalization of plakoglobin in endothelial junctions: identification as a special type of Zonulae adhaerentes. Biol Cell 59, 205-218.
Franke, W.W., Cowin, P., Grund, C., Kuhn, C., and Kapprell, H.P. (1988). The endothelial junction: The plaque and its components, In Endothelial cell biology, N. Simionescu, and M. Simionescu, eds. (New York, Plenum Press), pp. 147-166.
Franke, W.W., Goldschmidt, M.D., Zimbelmann, R., Müller, H., Schiller, D.L., and Cowin, P. (1989). Molecular cloning and amino acid sequence of human plakoglobin, the common junctional plaque protein. Proc Natl Acad Sci U S A 86, 4027-4031.
Franke, W.W., Troyanovsky, S.M., Koch, P.J., Troyanovsky, R., Fouquet, B., and Leube, R.E. (1992). Desmosomal proteins: mediators of intercellular coupling and intermediate filament anchorage. Cold Spring Harb Symp Quant Biol 57, 643-652.
Franke, W.W., Stehr, S., Stumpp, S., Kuhn, C., Heid, H., Rackwitz, H.R., Schnölzer, M., Baumann, R., Holzhausen, H.J., and Moll, R. (1996). Specific immunohistochemical detection of cardiac/fetal alpha-actin in human cardiomyocytes and regenerating skeletal muscle cells. Differentiation 60, 245-250.
Franke, W.W., Borrmann, C.M., Grund, C., and Pieperhoff, S. (2006). The area composita of adhering junctions connecting heart muscle cells of vertebrates. I. Molecular definition in intercalated disks of cardiomyocytes by immunoelectron microscopy of desmosomal proteins. Eur J Cell Biol 85, 69-82.
Franke, W.W. (2009). Discovering the molecular components of intercellular junctions - a historical view. In Cell-cell junctions, W.J. Nelson, and E. Fuchs, eds. (New York, Cold Spring Harbor Laboratory Press), pp. 1-34.
Franke, W.W., Rickelt, S., Barth, M., and Pieperhoff, S. (2009). The junctions that don't fit the scheme: special symmetrical cell-cell junctions of their own kind. Cell Tissue Res 338, 1-17.
French, W.J., Creemers, E.E., and Tallquist, M.D. (2008). Platelet-derived growth factor receptors direct vascular development independent of vascular smooth muscle cell function. Mol Cell Biol 28, 5646-5657.
Frohman, M.A., Dush, M.K., and Martin, G.R. (1988). Rapid production of full-length cDNAs from rare transcripts: amplification using a single gene-specific oligonucleotide primer. Proc Natl Acad Sci U S A 85, 8998-9002.
Furthmayr, H., Lankes, W., and Amieva, M. (1992). Moesin, a new cytoskeletal protein and constituent of filopodia: its role in cellular functions. Kidney Int 41, 665-670.
Furuse, M., Hirase, T., Itoh, M., Nagafuchi, A., Yonemura, S., and Tsukita, S. (1993). Occludin: a novel integral membrane protein localizing at tight junctions. J Cell Biol 123, 1777-1788.
Furuse, M., Fujita, K., Hiiragi, T., Fujimoto, K., and Tsukita, S. (1998a). Claudin-1 and -2: novel integral membrane proteins localizing at tight junctions with no sequence similarity to occludin. J Cell Biol 141, 1539-1550.
Furuse, M., Sasaki, H., Fujimoto, K., and Tsukita, S. (1998b). A single gene product, claudin-1 or -2, reconstitutes tight junction strands and recruits occludin in fibroblasts. J Cell Biol 143, 391-401.

Gabbiani, G., Ryan, G.B., and Majne, G. (1971). Presence of modified fibroblasts in granulation tissue and their possible role in wound contraction. Experientia 27, 549-550.
Gabbiani, G. (1996). The cellular derivation and the life span of the myofibroblast. Pathol Res Pract 192, 708-711.
Gallin, W.J., Edelman, G.M., and Cunningham, B.A. (1983). Characterization of L-CAM, a major cell adhesion molecule from embryonic liver cells. Proc Natl Acad Sci U S A 80, 1038-1042.
Gallin, W.J., Sorkin, B.C., Edelman, G.M., and Cunningham, B.A. (1987). Sequence analysis of a cDNA clone encoding the liver cell adhesion molecule, L-CAM. Proc Natl Acad Sci U S A 84, 2808-2812.
Gao, C., Cheng, X., Lam, M., Liu, Y., Liu, Q., Chang, K.S., and Kao, H.Y. (2008). Signal-dependent regulation of transcription by histone deacetylase 7 involves recruitment to promyelocytic leukemia protein nuclear bodies. Mol Biol Cell 19, 3020-3027.
Geiger, B. (1979). A 130K protein from chicken gizzard: its localization at the termini of microfilament bundles in cultured chicken cells. Cell 18, 193-205.
Geiger, B., Tokuyasu, K.T., Dutton, A.H., and Singer, S.J. (1980). Vinculin, an intracellular protein localized at specialized sites where microfilament bundles terminate at cell membranes. Proc Natl Acad Sci U S A 77, 4127-4131.
Geiger, B., Avnur, Z., Volberg, T., and Volk, T. (1985a). Molecular domains of adherens junctions. In The cell in contact, G.M. Edelman, and J.P. Thiery, eds. (New York, John Wiley and Sons), pp. 461-489.
Geiger, B., Volk, T., and Volberg, T. (1985b). Molecular heterogeneity of adherens junctions. J Cell Biol 101, 1523-1531.
Gerdes, J., Schwab, U., Lemke, H., and Stein, H. (1983). Production of a mouse monoclonal antibody reactive with a human nuclear antigen associated with cell proliferation. Int J Cancer 31, 13-20.
Gerull, B., Heuser, A., Wichter, T., Paul, M., Basson, C.T., McDermott, D.A., Lerman, B.B., Markowitz, S.M., Ellinor, P.T., MacRae, C.A., Peters, S., Grossmann, K.S., Drenckhahn, J., Michely, B., Sasse-Klaassen, S., Birchmeier, W., Dietz, R., Breithardt, G., Schulze-Bahr, E., and Thierfelder, L. (2004). Mutations in the desmosomal protein plakophilin-2 are common in arrhythmogenic right ventricular cardiomyopathy. Nat Genet 36, 1162-1164.
Gessner, R., and Tauber, R. (2000). Intestinal cell adhesion molecules. Liver-intestine cadherin. Ann N Y Acad Sci 915, 136-143.
Gimona, M., Vandekerckhove, J., Goethals, M., Herzog, M., Lando, Z., and Small, J.V. (1994). Beta-actin specific monoclonal antibody. Cell Motil Cytoskeleton 27, 108-116.
Girardi, A.J., Weinstein, D., and Moorhead, P.S. (1966). SV40 transformation of human diploid cells. A parallel study of viral and karyologic parameters. Ann Med Exp Biol Fenn 44, 242-254.
Giudice, G.J., Cohen, S.M., Patel, N.H., and Steinberg, M.S. (1984). Immunological comparison of desmosomal components from several bovine tissues. J Cell Biochem 26, 35-45.
Glauert, A.M. (1975). Fixation, dehydration and embedding of biological specimens. (Amsterdam, Elsevier North-Holland Biomedical Press), pp. 1-207.
Godsel, L.M., Getsios, S., Huen, A.C., and Green, K.J. (2004). The molecular composition and function of desmosomes. Handb Exp Pharmacol, 137-193.
Goldner, J. (1938). A modification of the masson trichrome technique for routine laboratory purposes. Am J Pathol 14, 237-243.
Goldsmith, E.C., Hoffman, A., Morales, M.O., Potts, J.D., Price, R.L., McFadden, A., Rice, M., and Borg, T.K. (2004). Organization of fibroblasts in the heart. Dev Dyn 230, 787-794.
Goossens, S., and van Roy, F. (2005). Cadherin-mediated cell-cell adhesion in the testis. Front Biosci 10, 398-419.
Goossens, S., Janssens, B., Bonné, S., De Rycke, R., Braet, F., van Hengel, J., and van Roy, F. (2007). A unique and specific interaction between alphaT-catenin and plakophilin-2 in the area composita, the mixed-type junctional structure of cardiac intercalated discs. J Cell Sci 120, 2126-2136.
Gorbsky, G., and Steinberg, M.S. (1981). Isolation of the intercellular glycoproteins of desmosomes. J Cell Biol 90, 243-248.
Gorbsky, G., Cohen, S.M., Shida, H., Giudice, G.J., and Steinberg, M.S. (1985). Isolation of the non-glycosylated proteins of desmosomes and immunolocalization of a third plaque protein: desmoplakin III. Proc Natl Acad Sci U S A 82, 810-814.
Grande-Allen, K.J., Cochran, R.P., Reinhall, P.G., and Kunzelman, K.S. (2001). Mechanisms of aortic valve incompetence: finite-element modeling of Marfan syndrome. J Thorac Cardiovasc Surg 122, 946-954.
Grandmougin, D., Fayad, G., Moukassa, D., Decoene, C., Abolmaali, K., Bodart, J.C., Limousin, M., and Warembourg, H. (2000). Cardiac valve papillary fibroelastomas: clinical, histological and immunohistochemical studies and a physiopathogenic hypothesis. J Heart Valve Dis 9, 832-841.
Grauss, R.W., Hazekamp, M.G., van Vliet, S., Gittenberger-de Groot, A.C., and DeRuiter, M.C. (2003). Decellularization of rat aortic valve allografts reduces leaflet destruction and extracellular matrix remodeling. J Thorac Cardiovasc Surg 126, 2003-2010.
Green, K.J., Goldman, R.D., and Chisholm, R.L. (1988). Isolation of cDNAs encoding desmosomal plaque proteins: evidence that bovine desmoplakins I and II are derived from two mRNAs and a single gene. Proc Natl Acad Sci U S A 85, 2613-2617.
Green, K.J., Parry, D.A., Steinert, P.M., Virata, M.L., Wagner, R.M., Angst, B.D., and Nilles, L.A. (1990). Structure of the human desmoplakins. Implications for function in the desmosomal plaque. J Biol Chem 265, 2603-2612.

Green, K.J., and Simpson, C.L. (2007). Desmosomes: new perspectives on a classic. J Invest Dermatol 127, 2499-2515.
Gross, L., and Kugel, M.A. (1931). Topographic Anatomy and Histology of the Valves in the Human Heart. Am J Pathol 7, 445-474 447.
Grossmann, K.S., Grund, C., Huelsken, J., Behrend, M., Erdmann, B., Franke, W.W., and Birchmeier, W. (2004). Requirement of plakophilin 2 for heart morphogenesis and cardiac junction formation. J Cell Biol 167, 149-160.
Grotendorst, G.R., Rahmanie, H., and Duncan, M.R. (2004). Combinatorial signaling pathways determine fibroblast proliferation and myofibroblast differentiation. FASEB J 18, 469-479.
Gui, Y.H., Linask, K.K., Khowsathit, P., and Huhta, J.C. (1996). Doppler echocardiography of normal and abnormal embryonic mouse heart. Pediatr Res 40, 633-642.
Gummert, J.F., Funkat, A., Beckmann, A., Schiller, W., Hekmat, K., Ernst, M., and Haverich, A. (2009). Cardiac surgery in Germany during 2008. A report on behalf of the German Society for Thoracic and Cardiovascular Surgery. Thorac Cardiovasc Surg 57, 315-323.
Gwanmesia, P., Ziegler, H., Eurich, R., Barth, M., Kamiya, H., Karck, M., Lichtenberg, A., and Akhyari, P. (2010). Opposite Effects of Transforming Growth Factor-beta1 and Vascular Endothelial Growth Factor on the Degeneration of Aortic Valvular Interstitial Cell Are Modified by the Extracellular Matrix Protein Fibronectin: Implications for Heart Valve Engineering. Tissue Eng Part A 16, 3737-3746.
Halbleib, J.M., and Nelson, W.J. (2006). Cadherins in development: cell adhesion, sorting, and tissue morphogenesis. Genes Dev 20, 3199-3214.
Hämmerling, B., Grund, C., Boda-Heggemann, J., Moll, R., and Franke, W.W. (2006). The complexus adhaerens of mammalian lymphatic endothelia revisited: a junction even more complex than hitherto thought. Cell Tissue Res 324, 55-67.
Hanft, L.M., Rybakova, I.N., Patel, J.R., Rafael-Fortney, J.A., and Ervasti, J.M. (2006). Cytoplasmic gamma-actin contributes to a compensatory remodeling response in dystrophin-deficient muscle. Proc Natl Acad Sci U S A 103, 5385-5390.
Harris, I.S., and Black, B.L. (2010). Development of the endocardium. Pediatr Cardiol 31, 391-399.
Harris, T.J., and Tepass, U. (2010). Adherens junctions: from molecules to morphogenesis. Nat Rev Mol Cell Biol 11, 502-514.
Haskins, J., Gu, L., Wittchen, E.S., Hibbard, J., and Stevenson, B.R. (1998). ZO-3, a novel member of the MAGUK protein family found at the tight junction, interacts with ZO-1 and occludin. J Cell Biol 141, 199-208.
Hatta, K., and Takeichi, M. (1986). Expression of N-cadherin adhesion molecules associated with early morphogenetic events in chick development. Nature 320, 447-449.
Hatta, K., Takagi, S., Fujisawa, H., and Takeichi, M. (1987). Spatial and temporal expression pattern of N-cadherin cell adhesion molecules correlated with morphogenetic processes of chicken embryos. Dev Biol 120, 215-227.
Hatzfeld, M., Kristjansson, G.I., Plessmann, U., and Weber, K. (1994). Band 6 protein, a major constituent of desmosomes from stratified epithelia, is a novel member of the armadillo multigene family. J Cell Sci 107 (Pt 8), 2259-2270.
Hatzfeld, M., and Nachtsheim, C. (1996). Cloning and characterization of a new armadillo family member, p0071, associated with the junctional plaque: evidence for a subfamily of closely related proteins. J Cell Sci 109 (Pt 11), 2767-2778.
Hatzfeld, M. (1999). The armadillo family of structural proteins. Int Rev Cytol 186, 179-224.
Hayat, M.A. (1970). Principles and techniques of electron microscopy (New York, Van Nostrand Reinhold), pp. 1-543.
Hayes, H., Kossmann, E., Wilson, E., Meininger, C., and Zawieja, D. (2003). Development and characterization of endothelial cells from rat microlymphatics. Lymphat Res Biol 1, 101-119.
Heid, H.W., Moll, I., and Franke, W.W. (1988). Patterns of expression of trichocytic and epithelial cytokeratins in mammalian tissues. I. Human and bovine hair follicles. Differentiation 37, 137-157.
Heid, H.W., Schmidt, A., Zimbelmann, R., Schäfer, S., Winter-Simanowski, S., Stumpp, S., Keith, M., Figge, U., Schnölzer, M., and Franke, W.W. (1994). Cell type-specific desmosomal plaque proteins of the plakoglobin family: plakophilin 1 (band 6 protein). Differentiation 58, 113-131.
Heid, H.W., Moll, R., Schwetlick, I., Rackwitz, H.R., and Keenan, T.W. (1998). Adipophilin is a specific marker of lipid accumulation in diverse cell types and diseases. Cell Tissue Res 294, 309-321.
Heimark, R.L., and Schwartz, S.M. (1988). Endothelial morphogenesis. In Endothelial cell biology, N. Simionescu, and M. Simionescu, eds. (New York, Plenum Press), pp. 123-143.
Herren, T., Gerber, P.A., and Duru, F. (2009). Arrhythmogenic right ventricular cardiomyopathy/dysplasia: a not so rare "disease of the desmosome" with multiple clinical presentations. Clin Res Cardiol 98, 141-158.
Herrenknecht, K., Ozawa, M., Eckerskorn, C., Lottspeich, F., Lenter, M., and Kemler, R. (1991). The uvomorulin-anchorage protein alpha catenin is a vinculin homologue. Proc Natl Acad Sci U S A 88, 9156-9160.
Herrmann, H., Fouquet, B., and Franke, W.W. (1989). Expression of intermediate filament proteins during development of Xenopus laevis. I. cDNA clones encoding different forms of vimentin. Development 105, 279-298.
Herrmann, H., Bar, H., Kreplak, L., Strelkov, S.V., and Aebi, U. (2007). Intermediate filaments: from cell architecture to nanomechanics. Nat Rev Mol Cell Biol 8, 562-573.

Herschman, H.R., Levine, L., and De Vellis, J. (1971). Appearance of a brain-specific antigen (S-100 protein) in the developing rat brain. J Neurochem 18, 629-633.
Heuberger, J., and Birchmeier, W. (2009). Interplay of cadherin-mediated cell adhesion and canonical Wnt signaling. In Cell-cell junctions, W.J. Nelson, and E. Fuchs, eds. (New York, Cold Spring Harbor Laboratory Press), pp. 203-226.
Hinton, R.B., and Yutzey, K.E. (2011). Heart valve structure and function in development and disease. Annu Rev Physiol 73, 29-46.
Hinz, B., Dugina, V., Ballestrem, C., Wehrle-Haller, B., and Chaponnier, C. (2003). Alpha-smooth muscle actin is crucial for focal adhesion maturation in myofibroblasts. Mol Biol Cell 14, 2508-2519.
Hinz, B., and Gabbiani, G. (2003). Cell-matrix and cell-cell contacts of myofibroblasts: role in connective tissue remodeling. Thromb Haemost 90, 993-1002.
Hinz, B., Pittet, P., Smith-Clerc, J., Chaponnier, C., and Meister, J.J. (2004). Myofibroblast development is characterized by specific cell-cell adherens junctions. Mol Biol Cell 15, 4310-4320.
Hirano, S., Kimoto, N., Shimoyama, Y., Hirohashi, S., and Takeichi, M. (1992). Identification of a neural alpha-catenin as a key regulator of cadherin function and multicellular organization. Cell 70, 293-301.
Hirschy, A., Schatzmann, F., Ehler, E., and Perriard, J.C. (2006). Establishment of cardiac cytoarchitecture in the developing mouse heart. Dev Biol 289, 430-441.
Hobmayer, B., Rentzsch, F., Kuhn, K., Happel, C.M., von Laue, C.C., Snyder, P., Rothbacher, U., and Holstein, T.W. (2000). WNT signalling molecules act in axis formation in the diploblastic metazoan Hydra. Nature 407, 186-189.
Hobmayer, E., Hatta, M., Fischer, R., Fujisawa, T., Holstein, T.W., and Sugiyama, T. (1996). Identification of a Hydra homologue of the beta-catenin/plakoglobin/armadillo gene family. Gene 172, 155-159.
Hoffmann, I., and Balling, R. (1995). Cloning and expression analysis of a novel mesodermally expressed cadherin. Dev Biol 169, 337-346.
Hofmann, I., Kuhn, C., and Franke, W.W. (2008). Protein p0071, a major plaque protein of non-desmosomal adhering junctions, is a selective cell-type marker. Cell Tissue Res 334, 381-399.
Hofmann, I., Schlechter, T., Kuhn, C., Hergt, M., and Franke, W.W. (2009). Protein p0071 - an armadillo plaque protein that characterizes a specific subtype of adherens junctions. J Cell Sci 122, 21-24.
Hollnagel, A., Grund, C., Franke, W.W., and Arnold, H.H. (2002). The cell adhesion molecule M-cadherin is not essential for muscle development and regeneration. Mol Cell Biol 22, 4760-4770.
Holthöfer, B., Windoffer, R., Troyanovsky, S., and Leube, R.E. (2007). Structure and function of desmosomes. Int Rev Cytol 264, 65-163.
Holton, J.L., Kenny, T.P., Legan, P.K., Collins, J.E., Keen, J.N., Sharma, R., and Garrod, D.R. (1990). Desmosomal glycoproteins 2 and 3 (desmocollins) show N-terminal similarity to calcium-dependent cell-cell adhesion molecules. J Cell Sci 97 (Pt 2), 239-246.
Horiuchi, K., Amizuka, N., Takeshita, S., Takamatsu, H., Katsuura, M., Ozawa, H., Toyama, Y., Bonewald, L.F., and Kudo, A. (1999). Identification and characterization of a novel protein, periostin, with restricted expression to periosteum and periodontal ligament and increased expression by transforming growth factor beta. J Bone Miner Res 14, 1239-1249.
Hort, W., and Horstkotte, D. (2006). Fibroelastoma and Lambl's excrescences: localization, morphology and pathogenesis, differential diagnosis and infection. J Heart Valve Dis 15, 591-593.
Hulpiau, P., and van Roy, F. (2009). Molecular evolution of the cadherin superfamily. Int J Biochem Cell Biol 41, 349-369.
Hurle, J.M., Garcia-Martinez, V., and Sanchez-Quintana, D. (1986). Morphologic characteristics and structure of surface excrescences (Lambl's excrescences) in the normal aortic valve. Am J Cardiol 58, 1223-1227.
Hurle, J.M., Kitten, G.T., Sakai, L.Y., Volpin, D., and Solursh, M. (1994). Elastic extracellular matrix of the embryonic chick heart: an immunohistological study using laser confocal microscopy. Dev Dyn 200, 321-332.
Hurlstone, A.F., Haramis, A.P., Wienholds, E., Begthel, H., Korving, J., Van Eeden, F., Cuppen, E., Zivkovic, D., Plasterk, R.H., and Clevers, H. (2003). The Wnt/beta-catenin pathway regulates cardiac valve formation. Nature 425, 633-637.
Hynes, R.O. (2002). Integrins: bidirectional, allosteric signaling machines. Cell 110, 673-687.
Icardo, J.M., and Colvee, E. (1995). Atrioventricular valves of the mouse: II. Light and transmission electron microscopy. Anat Rec 241, 391-400.
Ihrie, R.A., and Attardi, L.D. (2005). A new Perp in the lineup: linking p63 and desmosomal adhesion. Cell Cycle 4, 873-876.
Ikenouchi, J., Furuse, M., Furuse, K., Sasaki, H., and Tsukita, S. (2005). Tricellulin constitutes a novel barrier at tricellular contacts of epithelial cells. J Cell Biol 171, 939-945.
Imhof, B.A., Vollmers, H.P., Goodman, S.L., and Birchmeier, W. (1983). Cell-cell interaction and polarity of epithelial cells: specific perturbation using a monoclonal antibody. Cell 35, 667-675.
Inoko, A., Itoh, M., Tamura, A., Matsuda, M., Furuse, M., and Tsukita, S. (2003). Expression and distribution of ZO-3, a tight junction MAGUK protein, in mouse tissues. Genes Cells 8, 837-845.
Inuzuka, H., Miyatani, S., and Takeichi, M. (1991). R-cadherin: a novel Ca(2+)-dependent cell-cell adhesion molecule expressed in the retina. Neuron 7, 69-79.
Iop, L., Renier, V., Naso, F., Piccoli, M., Bonetti, A., Gandaglia, A., Pozzobon, M., Paolin, A., Ortolani, F., Marchini, M., Spina, M., De Coppi, P., Sartore, S., and Gerosa, G. (2009). The influence of heart valve leaflet matrix characteristics on the interaction between human mesenchymal stem cells and decellularized scaffolds. Biomaterials 30, 4104-4116.

Itoh, M., Furuse, M., Morita, K., Kubota, K., Saitou, M., and Tsukita, S. (1999). Direct binding of three tight junction-associated MAGUKs, ZO-1, ZO-2, and ZO-3, with the COOH termini of claudins. J Cell Biol 147, 1351-1363.

Janssens, B., Goossens, S., Staes, K., Gilbert, B., van Hengel, J., Colpaert, C., Bruyneel, E., Mareel, M., and van Roy, F. (2001). alphaT-catenin: a novel tissue-specific beta-catenin-binding protein mediating strong cell-cell adhesion. J Cell Sci 114, 3177-3188.

Janssens, B., Mohapatra, B., Vatta, M., Goossens, S., Vanpoucke, G., Kools, P., Montoye, T., van Hengel, J., Bowles, N.E., van Roy, F., and Towbin, J.A. (2003). Assessment of the CTNNA3 gene encoding human alpha T-catenin regarding its involvement in dilated cardiomyopathy. Hum Genet 112, 227-236.

Joseph, L. (1858). Ueber die Ringe und Klappen des menschlichen Herzens. Virchows Arch 14, 244.

Joyce, E.M., Liao, J., Schoen, F.J., Mayer, J.E., Jr., and Sacks, M.S. (2009). Functional collagen fiber architecture of the pulmonary heart valve cusp. Ann Thorac Surg 87, 1240-1249.

Kalluri, R., and Zeisberg, M. (2006). Fibroblasts in cancer. Nat Rev Cancer 6, 392-401.

Kapprell, H.P., Cowin, P., Franke, W.W., Ponstingl, H., and Opferkuch, H.J. (1985). Biochemical characterization of desmosomal proteins isolated from bovine muzzle epidermis: amino acid and carbohydrate composition. Eur J Cell Biol 36, 217-229.

Kapprell, H.P., Cowin, P., and Franke, W.W. (1987). Biochemical characterization of the soluble form of the junctional plaque protein, plakoglobin, from different cell types. Eur J Biochem 166, 505-517.

Kapprell, H.P., Owaribe, K., and Franke, W.W. (1988). Identification of a basic protein of Mr 75,000 as an accessory desmosomal plaque protein in stratified and complex epithelia. J Cell Biol 106, 1679-1691.

Kartenbeck, J., Franke, W.W., Moser, J.G., and Stoffels, U. (1983). Specific attachment of desmin filaments to desmosomal plaques in cardiac myocytes. EMBO J 2, 735-742.

Kartenbeck, J., Schwechheimer, K., Moll, R., and Franke, W.W. (1984). Attachment of vimentin filaments to desmosomal plaques in human meningiomal cells and arachnoidal tissue. J Cell Biol 98, 1072-1081.

Kasimir, M.T., Rieder, E., Seebacher, G., Silberhumer, G., Wolner, E., Weigel, G., and Simon, P. (2003). Comparison of different decellularization procedures of porcine heart valves. Int J Artif Organs 26, 421-427.

Kattman, S.J., Huber, T.L., and Keller, G.M. (2006). Multipotent flk-1+ cardiovascular progenitor cells give rise to the cardiomyocyte, endothelial, and vascular smooth muscle lineages. Dev Cell 11, 723-732.

Kiener, H.P., and Brenner, M.B. (2005). Building the synovium: cadherin-11 mediates fibroblast-like synoviocyte cell-to-cell adhesion. Arthritis Res Ther 7, 49-54.

Kimura, Y., Matsunami, H., Inoue, T., Shimamura, K., Uchida, N., Ueno, T., Miyazaki, T., and Takeichi, M. (1995). Cadherin-11 expressed in association with mesenchymal morphogenesis in the head, somite, and limb bud of early mouse embryos. Dev Biol 169, 347-358.

King, I.A., Arnemann, J., Spurr, N.K., and Buxton, R.S. (1993a). Cloning of the cDNA (DSC1) coding for human type 1 desmocollin and its assignment to chromosome 18. Genomics 18, 185-194.

King, I.A., Tabiowo, A., Purkis, P., Leigh, I., and Magee, A.I. (1993b). Expression of distinct desmocollin isoforms in human epidermis. J Invest Dermatol 100, 373-379.

King, I.A., Sullivan, K.H., Bennett, R., Jr., and Buxton, R.S. (1995). The desmocollins of human foreskin epidermis: identification and chromosomal assignment of a third gene and expression patterns of the three isoforms. J Invest Dermatol 105, 314-321.

King, I.A., Angst, B.D., Hunt, D.M., Kruger, M., Arnemann, J., and Buxton, R.S. (1997). Hierarchical expression of desmosomal cadherins during stratified epithelial morphogenesis in the mouse. Differentiation 62, 83-96.

King, N., Hittinger, C.T., and Carroll, S.B. (2003). Evolution of key cell signaling and adhesion protein families predates animal origins. Science 301, 361-363.

Kinsella, M.G., and Fitzharris, T.P. (1980). Origin of cushion tissue in the developing chick heart: cinematographic recordings of in situ formation. Science 207, 1359-1360.

Kleinman, H.K., and Martin, G.R. (2005). Matrigel: basement membrane matrix with biological activity. Semin Cancer Biol 15, 378-386.

Klewer, S.E., Krob, S.L., Kolker, S.J., and Kitten, G.T. (1998). Expression of type VI collagen in the developing mouse heart. Dev Dyn 211, 248-255.

Klymkowsky, M.W. (1999). Plakophilin, armadillo repeats, and nuclear localization. Microsc Res Tech 45, 43-54.

Knight, R.L., Wilcox, H.E., Korossis, S.A., Fisher, J., and Ingham, E. (2008). The use of acellular matrices for the tissue engineering of cardiac valves. Proc Inst Mech Eng H 222, 129-143.

Koch, P.J., Goldschmidt, M.D., Walsh, M.J., Zimbelmann, R., and Franke, W.W. (1991a). Complete amino acid sequence of the epidermal desmoglein precursor polypeptide and identification of a second type of desmoglein gene. Eur J Cell Biol 55, 200-208.

Koch, P.J., Goldschmidt, M.D., Walsh, M.J., Zimbelmann, R., Schmelz, M., and Franke, W.W. (1991b). Amino acid sequence of bovine muzzle epithelial desmocollin derived from cloned cDNA: a novel subtype of desmosomal cadherins. Differentiation 47, 29-36.

Koch, P.J., Goldschmidt, M.D., Zimbelmann, R., Troyanovsky, R., and Franke, W.W. (1992). Complexity and expression patterns of the desmosomal cadherins. Proc Natl Acad Sci U S A 89, 353-357.

Koch, P.J., and Franke, W.W. (1994). Desmosomal cadherins: another growing multigene family of adhesion molecules. Curr Opin Cell Biol 6, 682-687.

Konopka, G., Tekiela, J., Iverson, M., Wells, C., and Duncan, S.A. (2007). Junctional adhesion molecule-A is critical for the formation of pseudocanaliculi and modulates E-cadherin expression in hepatic cells. J Biol Chem 282, 28137-28148.

Köser, J. (1999). In vivo Rekonstitution von Desmosomen: Funktionelle Charakterisierung desmosomaler Komponenten. (Dissertation Thesis, Heidelberg, Ruprecht Karls University), pp. 1-146.

Köser, J., Troyanovsky, S.M., Grund, C., and Franke, W.W. (2003). De novo formation of desmosomes in cultured cells upon transfection of genes encoding specific desmosomal components. Exp Cell Res 285, 114-130.

Koster, J., Borradori, L., and Sonnenberg, A. (2004). Hemidesmosomes: Molecular characterization and their importance. In Cell adhesion, J. Behrens, and W.J. Nelson, eds. (Berlin, Springer-Verlag), pp. 243-280.

Kostrewa, D., Brockhaus, M., D'Arcy, A., Dale, G.E., Nelboeck, P., Schmid, G., Mueller, F., Bazzoni, G., Dejana, E., Bartfai, T., Winkler, F.K., and Hennig, M. (2001). X-ray structure of junctional adhesion molecule: structural basis for homophilic adhesion via a novel dimerization motif. EMBO J 20, 4391-4398.

Krohne, G., and Benavente, R. (1986). The nuclear lamins. A multigene family of proteins in evolution and differentiation. Exp Cell Res 162, 1-10.

Krug, E.L., Runyan, R.B., and Markwald, R.R. (1985). Protein extracts from early embryonic hearts initiate cardiac endothelial cytodifferentiation. Dev Biol 112, 414-426.

Kühnel, W. (1965). Elektronische Untersuchungen an den Herzklappen [Electron microscopic investigation of the heart valves]. Experientia 21, 535-536.

Kundu, S.T., Gosavi, P., Khapare, N., Patel, R., Hosing, A.S., Maru, G.B., Ingle, A., Decaprio, J.A., and Dalal, S.N. (2008). Plakophilin3 downregulation leads to a decrease in cell adhesion and promotes metastasis. Int J Cancer 123, 2303-2314.

Kuruc, N., and Franke, W.W. (1988). Transient coexpression of desmin and cytokeratins 8 and 18 in developing myocardial cells of some vertebrate species. Differentiation 38, 177-193.

Kurzen, H., Moll, I., Moll, R., Schäfer, S., Simics, E., Amagai, M., Wheelock, M.J., and Franke, W.W. (1998). Compositionally different desmosomes in the various compartments of the human hair follicle. Differentiation 63, 295-304.

Kyhse-Andersen, J. (1984). Electroblotting of multiple gels: a simple apparatus without buffer tank for rapid transfer of proteins from polyacrylamide to nitrocellulose. J Biochem Biophys Methods 10, 203-209.

La Flamme, S.E., and Kowalczyk, A.P. (2008). Cell Junctions (Weinheim, Wiley-VCH), pp. 1-301.

La Flamme, S.E., Shi, F., and Sottile, J. (2008). Integrin trafficking. In Cell junctions, S.E. La Flamme, and A.P. Kowalczyk, eds. (Weinheim, Wiley-VCH), pp. 89-107.

Laemmli, U.K. (1970). Cleavage of structural proteins during the assembly of the head of bacteriophage T4. Nature 227, 680-685.

Lampugnani, M.G., Corada, M., Caveda, L., Breviario, F., Ayalon, O., Geiger, B., and Dejana, E. (1995). The molecular organization of endothelial cell to cell junctions: differential association of plakoglobin, beta-catenin, and alpha-catenin with vascular endothelial cadherin (VE-cadherin). J Cell Biol 129, 203-217.

Lampugnani, M.G., and Dejana, E. (1997). Interendothelial junctions: structure, signalling and functional roles. Curr Opin Cell Biol 9, 674-682.

Langbein, L., Grund, C., Kuhn, C., Prätzel, S., Kartenbeck, J., Brandner, J.M., Moll, I., and Franke, W.W. (2002). Tight junctions and compositionally related junctional structures in mammalian stratified epithelia and cell cultures derived therefrom. Eur J Cell Biol 81, 419-435.

Langbein, L., Pape, U.F., Grund, C., Kuhn, C., Prätzel, S., Moll, I., Moll, R., and Franke, W.W. (2003). Tight junction-related structures in the absence of a lumen: occludin, claudins and tight junction plaque proteins in densely packed cell formations of stratified epithelia and squamous cell carcinomas. Eur J Cell Biol 82, 385-400.

Latif, N., Sarathchandra, P., Taylor, P.M., Antoniw, J., and Yacoub, M.H. (2005). Molecules mediating cell-ECM and cell-cell communication in human heart valves. Cell Biochem Biophys 43, 275-287.

Latif, N., Sarathchandra, P., Taylor, P.M., Antoniw, J., Brand, N., and Yacoub, M.H. (2006). Characterization of molecules mediating cell-cell communication in human cardiac valve interstitial cells. Cell Biochem Biophys 45, 255-264.

Lendahl, U., Zimmerman, L.B., and McKay, R.D. (1990). CNS stem cells express a new class of intermediate filament protein. Cell 60, 585-595.

Lester, W.M., and Gotlieb, A.I. (1988). In vitro repair of the wounded porcine mitral valve. Circ Res 62, 833-845.

Lester, W.M., Damji, A.A., Tanaka, M., and Gedeon, I. (1992). Bovine mitral valve organ culture: role of interstitial cells in repair of valvular injury. J Mol Cell Cardiol 24, 43-53.

Lester, W.M., Damji, A.A., Gedeon, I., and Tanaka, M. (1993). Interstitial cells from the atrial and ventricular sides of the bovine mitral valve respond differently to denuding endocardial injury. In Vitro Cell Dev Biol 29A, 41-50.

Leube, R.E., Langbein, L., and Kartenbeck, J. (2003). Differenzierungsmarker in der Gewebe- und Tumordiagnostik: Molekulare Komponenten der Intermediärfilamente und ihrer Verankerungsstrukturen in Epithelien. In Onkologie, W.J. Zeller, and H. zur Hausen, eds. (Landsberg/Lech, ecomed), pp. 1-31.

Li, J., and Radice, G.L. (2010). A new perspective on intercalated disc organization: implications for heart disease. Dermatol Res Pract 2010, 207835.

Lieber, J.G., and Evans, R.M. (1996). Disruption of the vimentin intermediate filament system during adipose conversion of 3T3-L1 cells inhibits lipid droplet accumulation. J Cell Sci 109 (Pt 13), 3047-3058.

Linask, K.K., and Lash, J.W. (1993). Early heart development: dynamics of endocardial cell sorting suggests a common origin with cardiomyocytes. Dev Dyn 196, 62-69.
Lincoln, J., Alfieri, C.M., and Yutzey, K.E. (2004). Development of heart valve leaflets and supporting apparatus in chicken and mouse embryos. Dev Dyn 230, 239-250.
Lincoln, J., Lange, A.W., and Yutzey, K.E. (2006). Hearts and bones: shared regulatory mechanisms in heart valve, cartilage, tendon, and bone development. Dev Biol 294, 292-302.
Liu, A.C., and Gotlieb, A.I. (2007). Characterization of cell motility in single heart valve interstitial cells in vitro. Histol Histopathol 22, 873-882.
Liu, A.C., Joag, V.R., and Gotlieb, A.I. (2007). The emerging role of valve interstitial cell phenotypes in regulating heart valve pathobiology. Am J Pathol 171, 1407-1418.
Lopez, M., Cocchi, F., Menotti, L., Avitabile, E., Dubreuil, P., and Campadelli-Fiume, G. (2000). Nectin2alpha (PRR2alpha or HveB) and nectin2delta are low-efficiency mediators for entry of herpes simplex virus mutants carrying the Leu25Pro substitution in glycoprotein D. J Virol 74, 1267-1274.
Lough, J., and Sugi, Y. (2000). Endoderm and heart development. Dev Dyn 217, 327-342.
Lu, Q., Paredes, M., Medina, M., Zhou, J., Cavallo, R., Peifer, M., Orecchio, L., and Kosik, K.S. (1999). delta-catenin, an adhesive junction-associated protein which promotes cell scattering. J Cell Biol 144, 519-532.
Luo, Y., and Radice, G.L. (2005). N-cadherin acts upstream of VE-cadherin in controlling vascular morphogenesis. J Cell Biol 169, 29-34.
Lupu, F., and Simionescu, M. (1985). Organization of the intercellular junctions in the endothelium of cardiac valves. J Submicrosc Cytol 17, 119-132.
Madri, J.A., Pratt, B.M., and Yannariello-Brown, J. (1988). Endothelial cell-extracellular matrix interactions: matrix as a modulator of cell function. In Endothelial cell biology, N. Simionescu, and M. Simionescu, eds. (New York, Plenum Press), pp. 167-188.
Magin, T.M., Bader, B.L., Freudenmann, M., and Franke, W.W. (1990). De novo formation of cytokeratin filaments in calf lens cells and cytoplasts after transfection with cDNAs or microinjection with mRNAs encoding human cytokeratins. Eur J Cell Biol 53, 333-348.
Majno, G. (1979). The story of the myofibroblasts. Am J Surg Pathol 3, 535-542.
Manasek, F.J. (1970). Sulfated extracellular matrix production in the embryonic heart and adjacent tissues. J Exp Zool 174, 415-439.
Manasek, F.J., Reid, M., Vinson, W., Seyer, J., and Johnson, R. (1973). Glycosaminoglycan synthesis by the early embryonic chick heart. Dev Biol 35, 332-348.
Mandai, K., Nakanishi, H., Satoh, A., Obaishi, H., Wada, M., Nishioka, H., Itoh, M., Mizoguchi, A., Aoki, T., Fujimoto, T., Matsuda, Y., Tsukita, S., and Takai, Y. (1997). Afadin: A novel actin filament-binding protein with one PDZ domain localized at cadherin-based cell-to-cell adherens junction. J Cell Biol 139, 517-528.
Mandai, K., Nakanishi, H., Satoh, A., Takahashi, K., Satoh, K., Nishioka, H., Mizoguchi, A., and Takai, Y. (1999). Ponsin/SH3P12: an l-afadin- and vinculin-binding protein localized at cell-cell and cell-matrix adherens junctions. J Cell Biol 144, 1001-1017.
Marcus, F.I., Nava, A., and Thiene, G. (2007). Arrhythmogenic RV Cardiomyopathy/Dysplasia (Heidelberg, Springer-Verlag), pp. 1-217.
Mariner, D.J., Sirotkin, H., Daniel, J.M., Lindman, B.R., Mernaugh, R.L., Patten, A.K., Thoreson, M.A., and Reynolds, A.B. (1999). Production and characterization of monoclonal antibodies to ARVCF. Hybridoma 18, 343-349.
Mariner, D.J., Wang, J., and Reynolds, A.B. (2000). ARVCF localizes to the nucleus and adherens junction and is mutually exclusive with p120(ctn) in E-cadherin complexes. J Cell Sci 113 (Pt 8), 1481-1490.
Markwald, R.R., Fitzharris, T.P., and Manasek, F.J. (1977). Structural development of endocardial cushions. Am J Anat 148, 85-119.
Markwald, R.R., Norris, R.A., Moreno-Rodriguez, R., and Levine, R.A. (2010). Developmental basis of adult cardiovascular diseases: valvular heart diseases. Ann N Y Acad Sci 1188, 177-183.
Masson, P. (1929). Some histological methods; trichrome stainings and their preliminary techniques. J Tech Methods 12, 75-90.
Matter, K., and Balda, M.S. (2003). Signalling to and from tight junctions. Nat Rev Mol Cell Biol 4, 225-236.
McAllister, H.A., and Fenoglio, J.J., Jr. (1978). Tumors of the cardiovascular system. In Atlas of tumor pathology, W.H. Hartmann, and W.R. Cowan, eds. (Washington, D.C., Armed Forces Institute of Pathology), pp. 1-20.
McColl, B.W., Rothwell, N.J., and Allan, S.M. (2008). Systemic inflammation alters the kinetics of cerebrovascular tight junction disruption after experimental stroke in mice. J Neurosci 28, 9451-9462.
McCrea, P.D., Turck, C.W., and Gumbiner, B. (1991). A homolog of the armadillo protein in Drosophila (plakoglobin) associated with E-cadherin. Science 254, 1359-1361.
McCrea, P.D., Gu, D., and Balda, M.S. (2009). Junctional music that the nucleus hears: Cell-cell contact signaling and the modulation of gene activity. In Cell-cell junctions, W.J. Nelson, and E. Fuchs, eds. (New York, Cold Spring Harbor Laboratory Press), pp. 265-293.
McNutt, N.S., and Fawcett, D.W. (1969). The ultrastructure of the cat myocardium. II. Atrial muscle. J Cell Biol 42, 46-67.
McNutt, N.S. (1970). Ultrastructure of intercellular junctions in adult and developing cardiac muscle. Am J Cardiol 25, 169-183.
Mendelson, K., and Schoen, F.J. (2006). Heart valve tissue engineering: concepts, approaches, progress, and challenges. Ann Biomed Eng 34, 1799-1819.

Meng, W., and Takeichi, M. (2009). Adherens junction: molecular architecture and regulation. In Cell-cell junctions, W.J. Nelson, and E. Fuchs, eds. (New York, Cold Spring Harbor Laboratory Press), pp. 49-61.
Merryman, W.D., Youn, I., Lukoff, H.D., Krueger, P.M., Guilak, F., Hopkins, R.A., and Sacks, M.S. (2006). Correlation between heart valve interstitial cell stiffness and transvalvular pressure: implications for collagen biosynthesis. Am J Physiol Heart Circ Physiol 290, H224-231.
Mertens, C., Kuhn, C., and Franke, W.W. (1996). Plakophilins 2a and 2b: constitutive proteins of dual location in the karyoplasm and the desmosomal plaque. J Cell Biol 135, 1009-1025.
Mertens, C., Kuhn, C., Moll, R., Schwetlick, I., and Franke, W.W. (1999). Desmosomal plakophilin 2 as a differentiation marker in normal and malignant tissues. Differentiation 64, 277-290.
Mertens, C., Hofmann, I., Wang, Z., Teichmann, M., Sepehri Chong, S., Schnölzer, M., and Franke, W.W. (2001). Nuclear particles containing RNA polymerase III complexes associated with the junctional plaque protein plakophilin 2. Proc Natl Acad Sci U S A 98, 7795-7800.
Messier, R.H., Jr., Bass, B.L., Aly, H.M., Jones, J.L., Domkowski, P.W., Wallace, R.B., and Hopkins, R.A. (1994). Dual structural and functional phenotypes of the porcine aortic valve interstitial population: characteristics of the leaflet myofibroblast. J Surg Res 57, 1-21.
Mikawa, T. (1999). Cardiac lineages. In Heart development, R.P. Harvey, and N. Rosenthal, eds. (San Diego, Academic Press), pp. 19-33.
Misfeld, M., and Sievers, H.H. (2007). Heart valve macro- and microstructure. Philos Trans R Soc Lond B Biol Sci 362, 1421-1436.
Misfeldt, A.M., Boyle, S.C., Tompkins, K.L., Bautch, V.L., Labosky, P.A., and Baldwin, H.S. (2009). Endocardial cells are a distinct endothelial lineage derived from Flk1+ multipotent cardiovascular progenitors. Dev Biol 333, 78-89.
Mitomo, Y., Nakao, K., and Angrist, A. (1969). The fine structure of the heart valves in the chicken. I. Mitral valve. Am J Anat 125, 147-167.
Mjaatvedt, C.H., Lepera, R.C., and Markwald, R.R. (1987). Myocardial specificity for initiating endothelial-mesenchymal cell transition in embryonic chick heart correlates with a particulate distribution of fibronectin. Dev Biol 119, 59-67.
Mjaatvedt, C.H., Yamamura, H., Wessels, A., Ramsdell, A., Turner, D., and Markwald, R.R. (1999). Mechanisms of segmentation, septation, and remodeling of the tubular heart: Endocardial cushion fate and cardiac looping. In Heart development, R.P. Harvey, and N. Rosenthal, eds. (San Diego, Academic Press), pp. 159-177.
Mohler, E.R., 3rd, Chawla, M.K., Chang, A.W., Vyavahare, N., Levy, R.J., Graham, L., and Gannon, F.H. (1999). Identification and characterization of calcifying valve cells from human and canine aortic valves. J Heart Valve Dis 8, 254-260.
Moll, R., Franke, W.W., Schiller, D.L., Geiger, B., and Krepler, R. (1982a). The catalog of human cytokeratins: patterns of expression in normal epithelia, tumors and cultured cells. Cell 31, 11-24.
Moll, R., Franke, W.W., Volc-Platzer, B., and Krepler, R. (1982b). Different keratin polypeptides in epidermis and other epithelia of human skin: a specific cytokeratin of molecular weight 46,000 in epithelia of the pilosebaceous tract and basal cell epitheliomas. J Cell Biol 95, 285-295.
Moll, R., Holzhausen, H.J., Mennel, H.D., Kuhn, C., Baumann, R., Taege, C., and Franke, W.W. (2006). The cardiac isoform of alpha-actin in regenerating and atrophic skeletal muscle, myopathies and rhabdomyomatous tumors: an immunohistochemical study using monoclonal antibodies. Virchows Arch 449, 175-191.
Moll, R., Sievers, E., Hämmerling, B., Schmidt, A., Barth, M., Kuhn, C., Grund, C., Hofmann, I., and Franke, W.W. (2009). Endothelial and virgultar cell formations in the mammalian lymph node sinus: endothelial differentiation morphotypes characterized by a special kind of junction (complexus adhaerens). Cell Tissue Res 335, 109-141.
Mönckeberg, J.G. (1904). Der normale histologische Bau und die Sklerose der Aortenklappen. Virchows Arch 176, 472-514.
Moorman, A., Webb, S., Brown, N.A., Lamers, W., and Anderson, R.H. (2003). Development of the heart: (1) formation of the cardiac chambers and arterial trunks. Heart 89, 806-814.
Morita, K., Furuse, M., Fujimoto, K., and Tsukita, S. (1999a). Claudin multigene family encoding four-transmembrane domain protein components of tight junction strands. Proc Natl Acad Sci U S A 96, 511-516.
Morita, K., Sasaki, H., Fujimoto, K., Furuse, M., and Tsukita, S. (1999b). Claudin-11/OSP-based tight junctions of myelin sheaths in brain and Sertoli cells in testis. J Cell Biol 145, 579-588.
Mulholland, D.L., and Gotlieb, A.I. (1996). Cell biology of valvular interstitial cells. Can J Cardiol 12, 231-236.
Müller, H., and Franke, W.W. (1983). Biochemical and immunological characterization of desmoplakins I and II, the major polypeptides of the desmosomal plaque. J Mol Biol 163, 647-671.
Nagafuchi, A., Takeichi, M., and Tsukita, S. (1991). The 102 kd cadherin-associated protein: similarity to vinculin and posttranscriptional regulation of expression. Cell 65, 849-857.
Navarro, P., Ruco, L., and Dejana, E. (1998). Differential localization of VE- and N-cadherins in human endothelial cells: VE-cadherin competes with N-cadherin for junctional localization. J Cell Biol 140, 1475-1484.
Nelson, W.J., and Nusse, R. (2004). Convergence of Wnt, beta-catenin, and cadherin pathways. Science 303, 1483-1487.
Nelson, W.J., and Fuchs, E. (2010). Cell-cell junctions (New York, Cold Spring Harbor Laboratory Press), pp. 1-443.

Nichols, S.A., Dirks, W., Pearse, J.S., and King, N. (2006). Early evolution of animal cell signaling and adhesion genes. Proc Natl Acad Sci U S A 103, 12451-12456.
Niessen, C.M. (2007). Tight junctions/adherens junctions: basic structure and function. J Invest Dermatol 127, 2525-2532.
Norris, R.A., Moreno-Rodriguez, R.A., Sugi, Y., Hoffman, S., Amos, J., Hart, M.M., Potts, J.D., Goodwin, R.L., and Markwald, R.R. (2008). Periostin regulates atrioventricular valve maturation. Dev Biol 316, 200-213.
Nose, A., and Takeichi, M. (1986). A novel cadherin cell adhesion molecule: its expression patterns associated with implantation and organogenesis of mouse embryos. J Cell Biol 103, 2649-2658.
Nose, A., Nagafuchi, A., and Takeichi, M. (1987). Isolation of placental cadherin cDNA: identification of a novel gene family of cell-cell adhesion molecules. EMBO J 6, 3655-3661.
Nuber, U.A., Schäfer, S., Schmidt, A., Koch, P.J., and Franke, W.W. (1995). The widespread human desmocollin Dsc2 and tissue-specific patterns of synthesis of various desmocollin subtypes. Eur J Cell Biol 66, 69-74.
Nuber, U.A., Schäfer, S., Stehr, S., Rackwitz, H.R., and Franke, W.W. (1996). Patterns of desmocollin synthesis in human epithelia: immunolocalization of desmocollins 1 and 3 in special epithelia and in cultured cells. Eur J Cell Biol 71, 1-13.
Nürnberger, J., Bacallao, R.L., and Phillips, C.L. (2002). Inversin forms a complex with catenins and N-cadherin in polarized epithelial cells. Mol Biol Cell 13, 3096-3106.
Okazaki, M., Takeshita, S., Kawai, S., Kikuno, R., Tsujimura, A., Kudo, A., and Amann, E. (1994). Molecular cloning and characterization of OB-cadherin, a new member of cadherin family expressed in osteoblasts. J Biol Chem 269, 12092-12098.
Oldberg, A., Franzen, A., and Heinegard, D. (1986). Cloning and sequence analysis of rat bone sialoprotein (osteopontin) cDNA reveals an Arg-Gly-Asp cell-binding sequence. Proc Natl Acad Sci U S A 83, 8819-8823.
Osborn, M., Ludwig-Festl, M., Weber, K., Bignami, A., Dahl, D., and Bayreuther, K. (1981). Expression of glial and vimentin type intermediate filaments in cultures derived from human glial material. Differentiation 19, 161-167.
Owaribe, K., Kartenbeck, J., Stumpp, S., Magin, T.M., Krieg, T., Diaz, L.A., and Franke, W.W. (1990). The hemidesmosomal plaque. I. Characterization of a major constituent protein as a differentiation marker for certain forms of epithelia. Differentiation 45, 207-220.
Owaribe, K., Nishizawa, Y., and Franke, W.W. (1991). Isolation and characterization of hemidesmosomes from bovine corneal epithelial cells. Exp Cell Res 192, 622-630.
Oxford, E.M., Musa, H., Maass, K., Coombs, W., Taffet, S.M., and Delmar, M. (2007). Connexin43 remodeling caused by inhibition of plakophilin-2 expression in cardiac cells. Circ Res 101, 703-711.
Ozawa, M., Baribault, H., and Kemler, R. (1989). The cytoplasmic domain of the cell adhesion molecule uvomorulin associates with three independent proteins structurally related in different species. EMBO J 8, 1711-1717.
Ozawa, M., Hoschutzky, H., Herrenknecht, K., and Kemler, R. (1990a). A possible new adhesive site in the cell-adhesion molecule uvomorulin. Mech Dev 33, 49-56.
Ozawa, M., Ringwald, M., and Kemler, R. (1990b). Uvomorulin-catenin complex formation is regulated by a specific domain in the cytoplasmic region of the cell adhesion molecule. Proc Natl Acad Sci U S A 87, 4246-4250.
Paffenholz, R., and Franke, W.W. (1997). Identification and localization of a neurally expressed member of the plakoglobin/armadillo multigene family. Differentiation 61, 293-304.
Paffenholz, R., Kuhn, C., Grund, C., Stehr, S., and Franke, W.W. (1999). The arm-repeat protein NPRAP (neurojungin) is a constituent of the plaques of the outer limiting zone in the retina, defining a novel type of adhering junction. Exp Cell Res 250, 452-464.
Palade, G.E. (1988). The microvascular endothelium revisited. In Endothelial cell biology, N. Simionescu, and M. Simionescu, eds. (New York, Plenum Press), pp. 3-22.
Parrish, E.P., Garrod, D.R., Mattey, D.L., Hand, L., Steart, P.V., and Weller, R.O. (1986). Mouse antisera specific for desmosomal adhesion molecules of suprabasal skin cells, meninges, and meningioma. Proc Natl Acad Sci U S A 83, 2657-2661.
Parrish, E.P., Marston, J.E., Mattey, D.L., Measures, H.R., Venning, R., and Garrod, D.R. (1990). Size heterogeneity, phosphorylation and transmembrane organisation of desmosomal glycoproteins 2 and 3 (desmocollins) in MDCK cells. J Cell Sci 96 (Pt 2), 239-248.
Patten, B.M., Kramer, T.C., and Barry, A. (1948). Valvular action in the embryonic chick heart by localized apposition of endocardial masses. Anat Rec 102, 299-311.
Pedrotty, D.M., Klinger, R.Y., Badie, N., Hinds, S., Kardashian, A., and Bursac, N. (2008). Structural coupling of cardiomyocytes and noncardiomyocytes: quantitative comparisons using a novel micropatterned cell pair assay. Am J Physiol Heart Circ Physiol 295, H390-400.
Peifer, M., and Wieschaus, E. (1990). The segment polarity gene armadillo encodes a functionally modular protein that is the Drosophila homolog of human plakoglobin. Cell 63, 1167-1176.
Peifer, M., McCrea, P.D., Green, K.J., Wieschaus, E., and Gumbiner, B.M. (1992). The vertebrate adhesive junction proteins beta-catenin and plakoglobin and the Drosophila segment polarity gene armadillo form a multigene family with similar properties. J Cell Biol 118, 681-691.
Peifer, M., Pai, L.M., and Casey, M. (1994). Phosphorylation of the Drosophila adherens junction protein Armadillo: roles for wingless signal and zeste-white 3 kinase. Dev Biol 166, 543-556.

Perez-Moreno, M., Jamora, C., and Fuchs, E. (2003). Sticky business: orchestrating cellular signals at adherens junctions. Cell 112, 535-548.
Perriard, J.C., Hirschy, A., and Ehler, E. (2003). Dilated cardiomyopathy: a disease of the intercalated disc? Trends Cardiovasc Med 13, 30-38.
Person, A.D., Garriock, R.J., Krieg, P.A., Runyan, R.B., and Klewer, S.E. (2005a). Frzb modulates Wnt-9a-mediated beta-catenin signaling during avian atrioventricular cardiac cushion development. Dev Biol 278, 35-48.
Person, A.D., Klewer, S.E., and Runyan, R.B. (2005b). Cell biology of cardiac cushion development. Int Rev Cytol 243, 287-335.
Pfeiffer, F., Kumar, V., Butz, S., Vestweber, D., Imhof, B.A., Stein, J.V., and Engelhardt, B. (2008). Distinct molecular composition of blood and lymphatic vascular endothelial cell junctions establishes specific functional barriers within the peripheral lymph node. Eur J Immunol 38, 2142-2155.
Pho, M., Lee, W., Watt, D.R., Laschinger, C., Simmons, C.A., and McCulloch, C.A. (2008). Cofilin is a marker of myofibroblast differentiation in cells from porcine aortic cardiac valves. Am J Physiol Heart Circ Physiol 294, H1767-1778.
Pieperhoff, S., and Franke, W.W. (2007). The area composita of adhering junctions connecting heart muscle cells of vertebrates - IV: coalescence and amalgamation of desmosomal and adhaerens junction components - late processes in mammalian heart development. Eur J Cell Biol 86, 377-391.
Pieperhoff, S., and Franke, W.W. (2008). The area composita of adhering junctions connecting heart muscle cells of vertebrates. VI. Different precursor structures in non-mammalian species. Eur J Cell Biol 87, 413-430.
Pieperhoff, S., Schumacher, H., and Franke, W.W. (2008). The area composita of adhering junctions connecting heart muscle cells of vertebrates. V. The importance of plakophilin-2 demonstrated by small interference RNA-mediated knockdown in cultured rat cardiomyocytes. Eur J Cell Biol 87, 399-411.
Pieperhoff, S., Barth, M., Rickelt, S., and Franke, W.W. (2010). Desmosomal molecules in and out of adhering junctions: normal and diseased States of epidermal, cardiac and mesenchymally derived cells. Dermatol Res Pract 2010, 139167.
Pieperhoff, S., Heid, H., Claycomb, W.C., Zimbelmann, R., Kuhn, C., Winter-Simanowski, S., Kuhn, C., Frey, N., and Franke, W.W. (2011). The plaque protein myozap defines novel major types of cardiovascular adhering junctions. Submitted.
Pokutta, S., Drees, F., Takai, Y., Nelson, W.J., and Weis, W.I. (2002). Biochemical and structural definition of the l-afadin- and actin-binding sites of alpha-catenin. J Biol Chem 277, 18868-18874.
Posner, B.I., and Laporte, S.A. (2010). Cellular signalling: Peptide hormones and growth factors. Prog Brain Res 181, 1-16.
Powell, D.W., Mifflin, R.C., Valentich, J.D., Crowe, S.E., Saada, J.I., and West, A.B. (1999). Myofibroblasts. I. Paracrine cells important in health and disease. Am J Physiol 277, C1-9.
Rabkin-Aikawa, E., Farber, M., Aikawa, M., and Schoen, F.J. (2004). Dynamic and reversible changes of interstitial cell phenotype during remodeling of cardiac valves. J Heart Valve Dis 13, 841-847.
Rabkin, E., and Schoen, F.J. (2002). Cardiovascular tissue engineering. Cardiovasc Pathol 11, 305-317.
Rahner, C., Mitic, L.L., and Anderson, J.M. (2001). Heterogeneity in expression and subcellular localization of claudins 2, 3, 4, and 5 in the rat liver, pancreas, and gut. Gastroenterology 120, 411-422.
Ranscht, B., and Dours-Zimmermann, M.T. (1991). T-cadherin, a novel cadherin cell adhesion molecule in the nervous system lacks the conserved cytoplasmic region. Neuron 7, 391-402.
Reynolds, A.B., Daniel, J., McCrea, P.D., Wheelock, M.J., Wu, J., and Zhang, Z. (1994). Identification of a new catenin: the tyrosine kinase substrate p120cas associates with E-cadherin complexes. Mol Cell Biol 14, 8333-8342.
Reynolds, A.B., Daniel, J.M., Mo, Y.Y., Wu, J., and Zhang, Z. (1996a). The novel catenin p120cas binds classical cadherins and induces an unusual morphological phenotype in NIH3T3 fibroblasts. Exp Cell Res 225, 328-337.
Reynolds, A.B., Jenkins, N.A., Gilbert, D.J., Copeland, N.G., Shapiro, D.N., Wu, J., and Daniel, J.M. (1996b). The gene encoding p120cas, a novel catenin, localizes on human chromosome 11q11 (CTNND) and mouse chromosome 2 (Catns). Genomics 31, 127-129.
Reynolds, E.S. (1963). The use of lead citrate at high pH as an electron-opaque stain in electron microscopy. . J Cell Biol 17, 208-212.
Richardson, S.H., Starborg, T., Lu, Y., Humphries, S.M., Meadows, R.S., and Kadler, K.E. (2007). Tendon development requires regulation of cell condensation and cell shape via cadherin-11-mediated cell-cell junctions. Mol Cell Biol 27, 6218-6228.
Rickelt, S., Franke, W.W., Dörflinger, Y., Goerdt, S., Brandner, J.M., and Peitsch, W.K. (2008). Subtypes of melanocytes and melanoma cells distinguished by their intercellular contacts: heterotypic adherens junctions, adhesive associations, and dispersed desmoglein 2 glycoproteins. Cell Tissue Res 334, 401-422.
Rickelt, S., Winter-Simanowski, S., Noffz, E., Kuhn, C., and Franke, W.W. (2009). Upregulation of plakophilin-2 and its acquisition to adherens junctions identifies a novel molecular ensemble of cell-cell-attachment characteristic for transformed mesenchymal cells. Int J Cancer 125, 2036-2048.
Rickelt, S. (2010). The molecular and cell biological characterization of cell-cell junctions in mesenchymally derived cells and tissues (Dissertation Thesis, Heidelberg, Ruprecht Karls University), pp. 1-65.

Rickelt, S., Rizzo, S., Dörflinger, Y., Zentgraf, H., Basso, C., Gerosa, G., Thiene, G., Moll, R., and Franke, W.W. (2010). A novel kind of tumor type-characteristic junction: plakophilin-2 as a major protein of adherens junctions in cardiac myxomata. Mod Pathol 23, 1429-1437.

Rimm, D.L., Kebriaei, P., and Morrow, J.S. (1994). Molecular cloning reveals alternative splice forms of human alpha(E)-catenin. Biochem Biophys Res Commun 203, 1691-1699.

Rimm, D.L., Koslov, E.R., Kebriaei, P., Cianci, C.D., and Morrow, J.S. (1995). Alpha 1(E)-catenin is an actin-binding and -bundling protein mediating the attachment of F-actin to the membrane adhesion complex. Proc Natl Acad Sci U S A 92, 8813-8817.

Ringwald, M., Schuh, R., Vestweber, D., Eistetter, H., Lottspeich, F., Engel, J., Dölz, R., Jähnig, F., Epplen, J., Mayer, S., Müller, C., and Kemler, R. (1987). The structure of cell adhesion molecule uvomorulin. Insights into the molecular mechanism of Ca2+-dependent cell adhesion. EMBO J 6, 3647-3653.

Ritter, S.A., Gross, L., and Kugel, M.A. (1928). Blood vessels in the valves of normal human hearts: From a study of 700 human hearts. Am Heart J 3, 433-446.

Rose, O., Grund, C., Reinhardt, S., Starzinski-Powitz, A., and Franke, W.W. (1995). Contactus adherens, a special type of plaque-bearing adhering junction containing M-cadherin, in the granule cell layer of the cerebellar glomerulus. Proc Natl Acad Sci U S A 92, 6022-6026.

Rubin, M.A., Snell, J.A., Tazelaar, H.D., Lack, E.E., Austenfeld, J.L., and Azumi, N. (1995). Cardiac papillary fibroelastoma: an immunohistochemical investigation and unusual clinical manifestations. Mod Pathol 8, 402-407.

Runyan, R.B., and Markwald, R.R. (1983). Invasion of mesenchyme into three-dimensional collagen gels: a regional and temporal analysis of interaction in embryonic heart tissue. Dev Biol 95, 108-114.

Sabatini, D.D., Bensch, K., and Barrnett, R.J. (1963). Cytochemistry and electron microscopy. The preservation of cellular ultrastructure and enzymatic activity by aldehyde fixation. J Cell Biol 17, 19-58.

Saffitz, J.E. (2009). Arrhythmogenic cardiomyopathy and abnormalities of cell-to-cell coupling. Heart Rhythm 6, S62-65.

Sakai, L.Y., Keene, D.R., Morris, N.P., and Burgeson, R.E. (1986). Type VII collagen is a major structural component of anchoring fibrils. J Cell Biol 103, 1577-1586.

Salomon, D., Ayalon, O., Patel-King, R., Hynes, R.O., and Geiger, B. (1992). Extrajunctional distribution of N-cadherin in cultured human endothelial cells. J Cell Sci 102 (Pt 1), 7-17.

Santini, M.P. (2005). mIGF-1 regulates heart physiology and induces complete regeneration of infarcted myocardial tissue (Dissertation Thesis, Heidelberg, Ruprecht Karls University), pp. 1-131.

Sato, P.Y., Musa, H., Coombs, W., Guerrero-Serna, G., Patino, G.A., Taffet, S.M., Isom, L.L., and Delmar, M. (2009). Loss of plakophilin-2 expression leads to decreased sodium current and slower conduction velocity in cultured cardiac myocytes. Circ Res 105, 523-526.

Schäfer, S., Troyanovsky, S.M., Heid, H.W., Eshkind, L.G., Koch, P.J., and Franke, W.W. (1993). Cytoskeletal architecture and epithelial differentiation: molecular determinants of cell interaction and cytoskeletal filament anchorage. C R Acad Sci III 316, 1316-1323.

Schäfer, S., Koch, P.J., and Franke, W.W. (1994). Identification of the ubiquitous human desmoglein, Dsg2, and the expression catalogue of the desmoglein subfamily of desmosomal cadherins. Exp Cell Res 211, 391-399.

Schäfer, S., Stumpp, S., and Franke, W.W. (1996). Immunological identification and characterization of the desmosomal cadherin Dsg2 in coupled and uncoupled epithelial cells and in human tissues. Differentiation 60, 99-108.

Schenke-Layland, K., Riemann, I., Opitz, F., Konig, K., Halbhuber, K.J., and Stock, U.A. (2004). Comparative study of cellular and extracellular matrix composition of native and tissue engineered heart valves. Matrix Biol 23, 113-125.

Schlüter, H., Moll, I., Wolburg, H., and Franke, W.W. (2007). The different structures containing tight junction proteins in epidermal and other stratified epithelial cells, including squamous cell metaplasia. Eur J Cell Biol 86, 645-655.

Schmelz, M., Duden, R., Cowin, P., and Franke, W.W. (1986a). A constitutive transmembrane glycoprotein of Mr 165,000 (desmoglein) in epidermal and non-epidermal desmosomes. I. Biochemical identification of the polypeptide. Eur J Cell Biol 42, 177-183.

Schmelz, M., Duden, R., Cowin, P., and Franke, W.W. (1986b). A constitutive transmembrane glycoprotein of Mr 165,000 (desmoglein) in epidermal and non-epidermal desmosomes. II. Immunolocalization and microinjection studies. Eur J Cell Biol 42, 184-199.

Schmelz, M., Moll, R., and Franke, W.W. (1990). A new type of intercellular junction: desmosomal proteins in the extended junctions of certain endothelial cells of the lymphatic system. Cell Biol Int Rep 14, 54.

Schmelz, M., and Franke, W.W. (1993). Complexus adhaerentes, a new group of desmoplakin-containing junctions in endothelial cells: the syndesmos connecting retothelial cells of lymph nodes. Eur J Cell Biol 61, 274-289.

Schmelz, M., Moll, R., Kuhn, C., and Franke, W.W. (1994). Complexus adhaerentes, a new group of desmoplakin-containing junctions in endothelial cells: II. Different types of lymphatic vessels. Differentiation 57, 97-117.

Schmidt, A., Heid, H.W., Schäfer, S., Nuber, U.A., Zimbelmann, R., and Franke, W.W. (1994). Desmosomes and cytoskeletal architecture in epithelial differentiation: cell type-specific plaque components and intermediate filament anchorage. Eur J Cell Biol 65, 229-245.

Schmidt, A., Langbein, L., Rode, M., Prätzel, S., Zimbelmann, R., and Franke, W.W. (1997). Plakophilins 1a and 1b: widespread nuclear proteins recruited in specific epithelial cells as desmosomal plaque components. Cell Tissue Res 290, 481-499.
Schmidt, A., Langbein, L., Prätzel, S., Rode, M., Rackwitz, H.R., and Franke, W.W. (1999). Plakophilin 3--a novel cell-type-specific desmosomal plaque protein. Differentiation 64, 291-306.
Schmidt, A., and Koch, P.J. (2007). Desmosomes: just cell adhesion or is there more? Cell Adh Migr 1, 28-32.
Schmidt, A., and Koch, P.J. (2008). Desmosomes in development and disease. In Cell junctions, S.E. La Flamme, and A.P. Kowalczyk, eds. (Weinheim, Wiley-VCH), pp. 235-249.
Schmidt, D., and Hoerstrup, S.P. (2005). Tissue engineered heart valves based on human cells. Swiss med wkly 135, 618-623.
Schmitt, C.J., Franke, W.W., Goerdt, S., Falkowska-Hansen, B., Rickelt, S., and Peitsch, W.K. (2007). Homo- and heterotypic cell contacts in malignant melanoma cells and desmoglein 2 as a novel solitary surface glycoprotein. J Invest Dermatol 127, 2191-2206.
Schulze, C., and Firth, J.A. (1993). Immunohistochemical localization of adherens junction components in blood-brain barrier microvessels of the rat. J Cell Sci 104 (Pt 3), 773-782.
Schürch, W., Seemayer, T.A., and Gabbiani, G. (1998). The myofibroblast: a quarter century after its discovery. Am J Surg Pathol 22, 141-147.
Schwarz, M.A., Owaribe, K., Kartenbeck, J., and Franke, W.W. (1990). Desmosomes and hemidesmosomes: constitutive molecular components. Annu Rev Cell Biol 6, 461-491.
Schweitzer, S.C., and Evans, R.M. (1998). Vimentin and lipid metabolism. Subcell Biochem 31, 437-462.
Scott, M.J., and Vesely, I. (1996). Morphology of porcine aortic valve cusp elastin. J Heart Valve Dis 5, 464-471.
Seeger, T.S., Frank, D., Rohr, C., Will, R., Just, S., Grund, C., Lyon, R., Luedde, M., Koegl, M., Sheikh, F., Rottbauer, W., Franke, W.W., Katus, H.A., Olson, E.N., and Frey, N. (2010). Myozap, a novel intercalated disc protein, activates serum response factor-dependent signaling and is required to maintain cardiac function in vivo. Circ Res 106, 880-890.
Sen-Chowdhry, S., Morgan, R.D., Chambers, J.C., and McKenna, W.J. (2010). Arrhythmogenic cardiomyopathy: etiology, diagnosis, and treatment. Annu Rev Med 61, 233-253.
Shi, S.R., Key, M.E., and Kalra, K.L. (1991). Antigen retrieval in formalin-fixed, paraffin-embedded tissues: an enhancement method for immunohistochemical staining based on microwave oven heating of tissue sections. J Histochem Cytochem 39, 741-748.
Shibamoto, S., Hayakawa, M., Takeuchi, K., Hori, T., Miyazawa, K., Kitamura, N., Johnson, K.R., Wheelock, M.J., Matsuyoshi, N., Takeichi, M., and Ito, F. (1995). Association of p120, a tyrosine kinase substrate, with E-cadherin/catenin complexes. J Cell Biol 128, 949-957.
Simonneau, L., Kitagawa, M., Suzuki, S., and Thiery, J.P. (1995). Cadherin 11 expression marks the mesenchymal phenotype: towards new functions for cadherins? Cell Adhes Commun 3, 115-130.
Sirotkin, H., Morrow, B., Saint-Jore, B., Puech, A., Das Gupta, R., Patanjali, S.R., Skoultchi, A., Weissman, S.M., and Kucherlapati, R. (1997a). Identification, characterization, and precise mapping of a human gene encoding a novel membrane-spanning protein from the 22q11 region deleted in velo-cardio-facial syndrome. Genomics 42, 245-251.
Sirotkin, H., O'Donnell, H., DasGupta, R., Halford, S., St Jore, B., Puech, A., Parimoo, S., Morrow, B., Skoultchi, A., Weissman, S.M., Scambler, P., and Kucherlapati, R. (1997b). Identification of a new human catenin gene family member (ARVCF) from the region deleted in velo-cardio-facial syndrome. Genomics 41, 75-83.
Skalli, O., Ropraz, P., Trzeciak, A., Benzonana, G., Gillessen, D., and Gabbiani, G. (1986). A monoclonal antibody against alpha-smooth muscle actin: a new probe for smooth muscle differentiation. J Cell Biol 103, 2787-2796.
Snarr, B.S., Kern, C.B., and Wessels, A. (2008). Origin and fate of cardiac mesenchyme. Dev Dyn 237, 2804-2819.
Snider, P., Hinton, R.B., Moreno-Rodriguez, R.A., Wang, J., Rogers, R., Lindsley, A., Li, F., Ingram, D.A., Menick, D., Field, L., Firulli, A.B., Molkentin, J.D., Markwald, R., and Conway, S.J. (2008). Periostin is required for maturation and extracellular matrix stabilization of noncardiomyocyte lineages of the heart. Circ Res 102, 752-760.
Snider, P., Standley, K.N., Wang, J., Azhar, M., Doetschman, T., and Conway, S.J. (2009). Origin of cardiac fibroblasts and the role of periostin. Circ Res 105, 934-947.
Snipstad, K., Fenton, C.G., Kjaeve, J., Cui, G., Anderssen, E., and Paulssen, R.H. (2010). New specific molecular targets for radio-chemotherapy of rectal cancer. Mol Oncol 4, 52-64.
Sohaskey, M.L., Yu, J., Diaz, M.A., Plaas, A.H., and Harland, R.M. (2008). JAWS coordinates chondrogenesis and synovial joint positioning. Development 135, 2215-2220.
Souders, C.A., Bowers, S.L., and Baudino, T.A. (2009). Cardiac fibroblast: the renaissance cell. Circ Res 105, 1164-1176.
Soule, H.D., Vazguez, J., Long, A., Albert, S., and Brennan, M. (1973). A human cell line from a pleural effusion derived from a breast carcinoma. J Natl Cancer Inst 51, 1409-1416.
Stacker, S.A., Achen, M.G., Jussila, L., Baldwin, M.E., and Alitalo, K. (2002). Lymphangiogenesis and cancer metastasis. Nat Rev Cancer 2, 573-583.
Staehelin, L.A. (1974). Structure and function of intercellular junctions. Int Rev Cytol 39, 191-283.
Steinberg, M. (1958). On the chemical bonds between animal cells. A mechanism for type-specific association. Am Nat 92, 65-81.

Steinberg, M.S., Shida, H., Giudice, G.J., Shida, M., Patel, N.H., and Blaschuk, O.W. (1987). On the molecular organization, diversity and functions of desmosomal proteins. Ciba Found Symp 125, 3-25.
Stevenson, B.R., Siliciano, J.D., Mooseker, M.S., and Goodenough, D.A. (1986). Identification of ZO-1: a high molecular weight polypeptide associated with the tight junction (zonula occludens) in a variety of epithelia. J Cell Biol 103, 755-766.
Straub, B.K., Boda, J., Kuhn, C., Schnölzer, M., Korf, U., Kempf, T., Spring, H., Hatzfeld, M., and Franke, W.W. (2003). A novel cell-cell junction system: the cortex adhaerens mosaic of lens fiber cells. J Cell Sci 116, 4985-4995.
Tachibana, K., Nakanishi, H., Mandai, K., Ozaki, K., Ikeda, W., Yamamoto, Y., Nagafuchi, A., Tsukita, S., and Takai, Y. (2000). Two cell adhesion molecules, nectin and cadherin, interact through their cytoplasmic domain-associated proteins. J Cell Biol 150, 1161-1176.
Takai, Y., Ikeda, W., Ogita, H., and Rikitake, Y. (2008). The immunoglobulin-like cell adhesion molecule nectin and its associated protein afadin. Annu Rev Cell Dev Biol 24, 309-342.
Takeichi, M. (1977). Functional correlation between cell adhesive properties and some cell surface proteins. J Cell Biol 75, 464-474.
Takeichi, M. (1995). Morphogenetic roles of classic cadherins. Curr Opin Cell Biol 7, 619-627.
Tao, Y.S., Edwards, R.A., Tubb, B., Wang, S., Bryan, J., and McCrea, P.D. (1996). beta-Catenin associates with the actin-bundling protein fascin in a noncadherin complex. J Cell Biol 134, 1271-1281.
Taylor, P.M., Allen, S.P., and Yacoub, M.H. (2000). Phenotypic and functional characterization of interstitial cells from human heart valves, pericardium and skin. J Heart Valve Dis 9, 150-158.
Taylor, P.M., Allen, S.P., Dreger, S.A., and Yacoub, M.H. (2002). Human cardiac valve interstitial cells in collagen sponge: a biological three-dimensional matrix for tissue engineering. J Heart Valve Dis 11, 298-306; discussion 306-297.
Taylor, P.M., Batten, P., Brand, N.J., Thomas, P.S., and Yacoub, M.H. (2003). The cardiac valve interstitial cell. Int J Biochem Cell Biol 35, 113-118.
Todaro, G.J., Green, H., and Swift, M.R. (1966). Susceptibility of human diploid fibroblast strains to transformation by SV40 virus. Science 153, 1252-1254.
Todaro, G.J. (1968). Variable susceptibility of human cell strains to SV40 transformation. Natl Cancer Inst Monogr 29, 271-275.
Tohyama, T., Lee, V.M., Rorke, L.B., Marvin, M., McKay, R.D., and Trojanowski, J.Q. (1993). Monoclonal antibodies to a rat nestin fusion protein recognize a 220-kDa polypeptide in subsets of fetal and adult human central nervous system neurons and in primitive neuroectodermal tumor cells. Am J Pathol 143, 258-268.
Topp, W.C. (1981). Normal rat cell lines deficient in nuclear thymidine kinase. Virology 113, 408-411.
Torii, S., Bashey, R.I., and Nakao, K. (1965). Acid mucopolysaccharide composition of human-heart valve. Biochim Biophys Acta 101, 285-291.
Trinh, L.A., and Stainier, D.Y. (2004). Cardiac development. Methods Cell Biol 76, 455-473.
Troyanovsky, S. (2005). Cadherin dimers in cell-cell adhesion. Eur J Cell Biol 84, 225-233.
Troyanovsky, S.M., Eshkind, L.G., Troyanovsky, R.B., Leube, R.E., and Franke, W.W. (1993). Contributions of cytoplasmic domains of desmosomal cadherins to desmosome assembly and intermediate filament anchorage. Cell 72, 561-574.
Troyanovsky, S.M., Troyanovsky, R.B., Eshkind, L.G., Krutovskikh, V.A., Leube, R.E., and Franke, W.W. (1994). Identification of the plakoglobin-binding domain in desmoglein and its role in plaque assembly and intermediate filament anchorage. J Cell Biol 127, 151-160.
Tsukita, S., and Furuse, M. (1998). Overcoming barriers in the study of tight junction functions: from occludin to claudin. Genes Cells 3, 569-573.
Tsukita, S., Furuse, M., and Itoh, M. (2001). Multifunctional strands in tight junctions. Nat Rev Mol Cell Biol 2, 285-293.
Tumbarello, D.A., and Turner, C.E. (2008). The paxillin family and tissue remodeling In Cell junctions, S.E. La Flamme, and A.P. Kowalczyk, eds. (Weinheim, Wiley-VCH), pp. 47-69.
Turner, C.E., Glenney, J.R., Jr., and Burridge, K. (1990). Paxillin: a new vinculin-binding protein present in focal adhesions. J Cell Biol 111, 1059-1068.
Tuschl, T., and Borkhardt, A. (2002). Small interfering RNAs: a revolutionary tool for the analysis of gene function and gene therapy. Mol Interv 2, 158-167.
Tzahor, E. (2007). Wnt/beta-catenin signaling and cardiogenesis: timing does matter. Dev Cell 13, 10-13.
Uchida, N., Shimamura, K., Miyatani, S., Copeland, N.G., Gilbert, D.J., Jenkins, N.A., and Takeichi, M. (1994). Mouse alpha N-catenin: two isoforms, specific expression in the nervous system, and chromosomal localization of the gene. Dev Biol 163, 75-85.
Uyeda, C.T., Eng, L.F., and Bignami, A. (1972). Immunological study of the glial fibrillary acidic protein. Brain Res 37, 81-89.
Valente, M., Basso, C., Thiene, G., Bressan, M., Stritoni, P., Cocco, P., and Fasoli, G. (1992). Fibroelastic papilloma: a not-so-benign cardiac tumor. Cardiovasc Pathol 1, 161-166.
Valiron, O., Chevrier, V., Usson, Y., Breviario, F., Job, D., and Dejana, E. (1996). Desmoplakin expression and organization at human umbilical vein endothelial cell-to-cell junctions. J Cell Sci 109 (Pt 8), 2141-2149.
Van der Loop, F.T., Schaart, G., Langmann, H., Ramaekers, F.C., and Viebahn, C. (1995). Rearrangement of intercellular junctions and cytoskeletal proteins during rabbit myocardium development. Eur J Cell Biol 68, 62-69.

Van Muijen, G.N., Ruiter, D.J., and Warnaar, S.O. (1987). Coexpression of intermediate filament polypeptides in human fetal and adult tissues. Lab Invest 57, 359-369.
Vesely, I., Boughner, D.R., and Leeson-Dietrich, J. (1995). Bioprosthetic valve tissue viscoelasticity: implications on accelerated pulse duplicator testing. Ann Thorac Surg 60, S379-382; discussion S383.
Vesely, I. (1998). The role of elastin in aortic valve mechanics. J Biomech 31, 115-123.
Vesely, I. (2005). Heart valve tissue engineering. Circ Res 97, 743-755.
Vestweber, D., and Kemler, R. (1984). Rabbit antiserum against a purified surface glycoprotein decompacts mouse preimplantation embryos and reacts with specific adult tissues. Exp Cell Res 152, 169-178.
Vestweber, D., and Kemler, R. (1985). Identification of a putative cell adhesion domain of uvomorulin. EMBO J 4, 3393-3398.
Virata, M.L., Wagner, R.M., Parry, D.A., and Green, K.J. (1992). Molecular structure of the human desmoplakin I and II amino terminus. Proc Natl Acad Sci U S A 89, 544-548.
Von Overbeck, J., Stahli, C., Gudat, F., Carmann, H., Lautenschlager, C., Durmuller, U., Takacs, B., Miggiano, V., Staehelin, T., and Heitz, P.U. (1985). Immunohistochemical characterization of an anti-epithelial monoclonal antibody (mAB lu-5). Virchows Arch A Pathol Anat Histopathol 407, 1-12.
Wagner, R.C. (1988). Ultrastructural studies of capillary endothelium: Compartmental tracing, high-voltage electron microscopy, and cryofixation. In Endothelial cell biology, N. Simionescu, and M. Simionescu, eds. (New York, Plenum Press), pp. 23-47.
Walker, G.A., Guerrero, I.A., and Leinwand, L.A. (2001). Myofibroblasts: molecular crossdressers. Curr Top Dev Biol 51, 91-107.
Walter, B., Schlechter, T., Hergt, M., Berger, I., and Hofmann, I. (2008). Differential expression pattern of protein ARVCF in nephron segments of human and mouse kidney. Histochem Cell Biol 130, 943-956.
Weind, K.L., Ellis, C.G., and Boughner, D.R. (2000). The aortic valve blood supply. J Heart Valve Dis 9, 1-7; discussion 7-8.
Weind, K.L., Boughner, D.R., Rigutto, L., and Ellis, C.G. (2001). Oxygen diffusion and consumption of aortic valve cusps. Am J Physiol Heart Circ Physiol 281, H2604-2611.
Weind, K.L., Ellis, C.G., and Boughner, D.R. (2002). Aortic valve cusp vessel density: relationship with tissue thickness. J Thorac Cardiovasc Surg 123, 333-340.
Witcher, L.L., Collins, R., Puttagunta, S., Mechanic, S.E., Munson, M., Gumbiner, B., and Cowin, P. (1996). Desmosomal cadherin binding domains of plakoglobin. J Biol Chem 271, 10904-10909.
Witsch, E., Sela, M., and Yarden, Y. (2010). Roles for growth factors in cancer progression. Physiology (Bethesda) 25, 85-101.
Wood, J.N., and Anderton, B.H. (1981). Monoclonal antibodies to mammalian neurofilaments. Biosci Rep 1, 263-268.
Wrenn, D.S., Griffin, G.L., Senior, R.M., and Mecham, R.P. (1986). Characterization of biologically active domains on elastin: identification of a monoclonal antibody to a cell recognition site. Biochemistry 25, 5172-5176.
Wuchter, P., Boda-Heggemann, J., Straub, B.K., Grund, C., Kuhn, C., Krause, U., Seckinger, A., Peitsch, W.K., Spring, H., Ho, A.D., and Franke, W.W. (2007). Processus and recessus adhaerentes: giant adherens cell junction systems connect and attract human mesenchymal stem cells. Cell Tissue Res 328, 499-514.
Yacoub, M.H., Kilner, P.J., Birks, E.J., and Misfeld, M. (1999). The aortic outflow and root: a tale of dynamism and crosstalk. Ann Thorac Surg 68, S37-43.
Yoganathan, A.P., He, Z., and Casey Jones, S. (2004). Fluid mechanics of heart valves. Annu Rev Biomed Eng 6, 331-362.
Yoo, Y., and Guan, J.-L. (2008). Integrin signaling through focal adhesion kinase. In Cell junctions, S.E. La Flamme, and A.P. Kowalczyk, eds. (Weinheim, Wiley-VCH), pp. 25-46.
Yoshida-Noro, C., Suzuki, N., and Takeichi, M. (1984). Molecular nature of the calcium-dependent cell-cell adhesion system in mouse teratocarcinoma and embryonic cells studied with a monoclonal antibody. Dev Biol 101, 19-27.
Yoshida, C., and Takeichi, M. (1982). Teratocarcinoma cell adhesion: identification of a cell-surface protein involved in calcium-dependent cell aggregation. Cell 28, 217-224.
Yue, X., Li, X., Nguyen, H.T., Chin, D.R., Sullivan, D.E., and Lasky, J.A. (2008). Transforming growth factor-beta1 induces heparan sulfate 6-O-endosulfatase 1 expression in vitro and in vivo. J Biol Chem 283, 20397-20407.
Zacks, S., Rosenthal, A., Granton, B., Havenith, M., Opas, M., and Gotlieb, A.I. (1991). Characterization of Cobblestone mitral valve interstitial cells. Arch Pathol Lab Med 115, 774-779.
Zamir, E., and Geiger, B. (2001). Molecular complexity and dynamics of cell-matrix adhesions. J Cell Sci 114, 3583-3590.
Zuckerman, J.E., Herschman, H.R., and Levine, L. (1970). Appearance of a brain specific antigen (the S-100 protein) during human foetal development. J Neurochem 17, 247-251.

Acknowledgements

I would like to thank my supervisor and mentor, Prof. emer. Dr. Werner W. Franke, for his guidance, support and enthusiasm.

I also thank the other members of my thesis committee, Prof. Dr. Thomas W. Holstein (Department of Molecular Evolution and Genomics, Institute of Zoology, University of Heidelberg), Prof. Dr. Jürgen Kleinschmidt (Division of Tumor Virology, German Cancer Research Center, Heidelberg) and Prof. Dr. Stephan Frings (Department of Molecular Physiology, Institute of Zoology, University of Heidelberg).

Special thanks go to the members of the former A010 group and the present Helmholtz Group for Cell Biology for their kind and patient introduction into several techniques. For continuous friendly support and the good atmosphere – not only in the lab – I would like to thank Stefanie Winter-Simanowski and Ralf Zimbelmann, Edeltraut Noffz, Heiderose Schumacher, Cilly Kuhn and Christine Grund. For proofreading and scientific as well as non-scientific discussions I want to thank Dr. Hans Heid.

I would also like to thank Dr. Steffen Rickelt, Dr. Sebastian Pieperhoff, Yvette Dörflinger, the “Boukamp girls” and Karsten, the “Mannheim Group” and of course Malte, for their amity and many nice evenings, vanilla-cappuccino-breaks and pizza-sessions. Anna, let me thank you for taking care of me during the last years.

Finally, I would like to thank Prof. Dr. Artur Lichtenberg and Dr. Payam Akhyari (Department of Cardiovascular Surgery, University Hospital Düsseldorf) for the good cooperation and for kindly providing me with human and ovine heart valve tissue. Furthermore I thank Prof. Dr. Heiner Niemann (Institute of Farm Animal Genetics, Friedrich-Loeffler-Institute Mariensee, Neustadt am Rübenberge) for fetal porcine tissues, Prof. Dr. Roland Moll (Institue of Pathology, University Hospital Giessen and Marburg) and Prof Dr. Ingrid Moll (Dermatology and Venereology Department and Clinic, University Medical Center Hamburg-Eppendorf, Hamburg) for human tissues, Prof. emer. Dr. Waldemar Hort for the fibroelastoma samples (Institue of Pathology, University Hospital Düsseldorf), Dr. Beate Straub (Institue of Pathology, University Hospital Heidelberg) for embedding reams of samples and the members of the Light and Electron Microscopy Core Facility (DKFZ, Heidelberg).

Above all, I thank my family for the loving encouragement and for always being there for me.
Payam, kheily khoobe ke toro daram.

Declaration

Herewith I, Mareike Barth, declare that this thesis and the work presented in it are the result of my own original research. Any help I received during the preparation of this thesis has been acknowledged.

Heidelberg,

Mareike Barth